

**D. Y. LEE  
NOVEMBER**

**FINAL REPORT HR 142  
ISU — ERI — AMES — 71101**

# **ABSORPTIVE AGGREGATES IN ASPHALT PAVING MIXTURES**

**Submitted to:**

**Iowa State Highway Commission**

**Project 780-S**

**ENGINEERING  
RESEARCH**  
**ENGINEERING  
RESEARCH**  
**ENGINEERING  
RESEARCH**  
**ENGINEERING  
RESEARCH**  
**ENGINEERING  
RESEARCH**

**FINAL REPORT**  
**HR 142**  
**ABSORPTIVE AGGREGATES IN**  
**ASPHALT PAVING MIXTURES**

Dah-Yinn Lee

December 1971

Submitted to the  
Iowa State Highway Commission

The opinions, findings, and conclusions  
expressed in this publication are those  
of the author, and not necessarily those  
of the Iowa State Highway Commission

*Project 780-S*  
*ISU-ERI-AMES-71101*

**ENGINEERING    RESEARCH    INSTITUTE**  
**IOWA STATE UNIVERSITY                    AMES**

1. Report No. ISU-ERI-AMES-71101	2. Government Accession No.	3. Recipient's Catalog No.	
4. Title and Subtitle ABSORPTIVE AGGREGATES IN ASPHALT PAVING MIXTURES		5. Report Date November 1971	
		6. Performing Organization Code	
7. Author(s) D. Y. Lee		8. Performing Organization Report No. ISU-ERI-AMES-71101	
9. Performing Organization Name and Address Iowa State University Engineering Research Institute Ames, Iowa 50010		10. Work Unit No.	
		11. Contract or Grant No. HR-142	
12. Sponsoring Agency Name and Address  Iowa State Highway Commission Ames, Iowa 50010		13. Type of Report and Period Covered Final Report 1969-1971	
		14. Sponsoring Agency Code	
15. Supplementary Notes The opinions, findings, and conclusions expressed in this publication are those of the author and not necessarily those of the Iowa State Highway Commission.			
16. Abstract  In this study, the asphalt absorption of six Iowa limestones were investigated. It was found that the most important factors that determined the nature, amount, and rate of asphalt absorption are porosity and pore-size distribution of the aggregate, viscosity of the asphalt, and time. Methods needed to determine the realistic maximum and minimum asphalt absorption by aggregates are recommended. Simple methods of asphalt absorption were developed. Since the most important factor that determines the accuracy of asphalt absorption is the bulk specific gravity of aggregates and since the current ASTM method is not adequate in this respect, several new methods were developed. Preliminary treatment studies for the purpose of upgrading absorptive aggregates were conducted using close to 40 chemicals. The improvements of some of these treatments on the mixture properties were demonstrated.			
17. Key Words absorption, asphalt, aggregate, porosity, chemical treatments, bulk specific gravity		18. Distribution Statement This document approved for public sale and release; distribution unlimited.	
19. Security Classif. (of this report) Unclassified	20. Security Classif. (of this page) Unclassified	21. No. of Pages 177	22. Price

## CONTENTS

	<u>Page</u>
EXECUTIVE SUMMARY	iii
FIGURES	iv
TABLES	ix
INTRODUCTION	xii
AGGREGATE STUDIES	1
Aggregates Studied	1
Porosity	8
Evaluation of Bulk Specific Gravity	36
ABSORPTION STUDIES	41
Methods and Procedures	41
Water Absorption	45
Kerosene and Oil Absorption	57
Dye Absorption	62
Asphalt Absorption	68
Correlation	94
Field Study of Asphalt Absorption	108
TREATMENT STUDIES	111
Summary	111
Approach	111
Material and Procedure	113
Results	122
Asphalt Concrete Mixtures	134
Conclusions	155
SUMMARY AND CONCLUSIONS	166
RECOMMENDATIONS	169

	<u>Page</u>
ACKNOWLEDGMENTS	
REFERENCES	171
TECHNICAL APPENDIX	
Appendix A. Theses and Publications Resulting from HR-127 and HR-142	A-1
Appendix B. Summary of Materials Studied as Possible Agents for Absorptive Aggregate Treatments	B-1
Appendix C. Determination of Bulk Specific Gravity of Aggregates	C-1
Mercury Pycnometer Method	C-1
Chemical Indicator Methods	C-3
Appendix D. Determination of Asphalt Absorption	D-1
Immersion Method	D-1
Bulk Impregnated Specific Gravity of Aggregates	D-2
Modified Rice Method	D-3

## EXECUTIVE SUMMARY

Recent studies have shown that aggregates are potentially in short supply over about one-third of the US; southern Iowa is included in these areas. Among the most effective approaches to the alleviation of the aggregate shortage problems are: (a) better utilization of locally available aggregates, (b) expanded use of marginal materials (including better materials evaluation and specifications), and (c) the benefaction of otherwise unsuitable materials. These have been the ultimate goals of this project, with respect to absorptive aggregates.

In this study, the asphalt absorption of six Iowa limestones were investigated. It was found that the most important factors that determined the nature, amount, and rate of asphalt absorption are porosity and pore-size distribution of the aggregate, viscosity of the asphalt, and time. Methods needed to determine the realistic maximum and minimum asphalt absorption by aggregates are recommended. Simple methods of asphalt absorption were developed. Since the most important factor that determines the accuracy of asphalt absorption is the bulk specific gravity of aggregates and since the current ASTM method is not adequate in this respect, several new methods were developed. Preliminary treatment studies for the purpose of upgrading absorptive aggregates were conducted using close to 40 chemicals. The improvements of some of these treatments on the mixture properties were demonstrated.

In order for the information generated by this research to be used by the highway engineer to judge the suitability of aggregates and to upgrade the unsuitable or marginal aggregates with respect to asphalt absorption, further research areas have been recommended.

## FIGURES

	<u>Page</u>
Fig. 1. Project HR-142 aggregate quarry locations	2
Fig. 2. Diagram of rock pores	8
Fig. 3. Cumulative porosity distribution, Menlo	16
Fig. 4. Cumulative porosity distribution, Pints	16
Fig. 5. Cumulative porosity distribution, Alden	17
Fig. 6. Cumulative porosity distribution, Linwood	17
Fig. 7. Cumulative porosity distribution, Cook	18
Fig. 8. Cumulative porosity distribution, Keota	18
Fig. 9. Percent of pore volume distribution, Menlo	19
Fig. 10. Percent of pore volume distribution, Pints	19
Fig. 11. Percent of pore volume distribution, Alden	20
Fig. 12. Percent of pore volume distribution, Linwood	20
Fig. 13. Percent of pore volume distribution, Cook	21
Fig. 14. Percent of pore volume distribution, Keota	21
Fig. 15. Non-normalized pore size distribution, Menlo	22
Fig. 16. Non-normalized pore size distribution, Pints	22
Fig. 17. Non-normalized pore size distribution, Alden	23
Fig. 18. Non-normalized pore size distribution, Linwood	23
Fig. 19. Non-normalized pore size distribution, Cook	24
Fig. 20. Non-normalized pore size distribution, Keota	24
Fig. 21. Hysteresis in mercury porosity, Menlo	25
Fig. 22. Hysteresis in mercury porosity, Pints	25
Fig. 23. Hysteresis in mercury porosity, Alden	30
Fig. 24. Hysteresis in mercury porosity, Linwood	30

	<u>Page</u>
Fig. 25. Hysteresis in mercury porosity, Cook	31
Fig. 26. Hysteresis in mercury porosity, Keota	31
Fig. 27a. Time-water absorption curves of cores, Alden	47
Fig. 27b. Time-water absorption curve of cores, Cook	47
Fig. 27c. Time-water absorption curve of cores, Keota I	47
Fig. 27d. Time-water absorption curve of cores, Keota II	48
Fig. 27e. Time-water absorption curve of cores, Linwood	48
Fig. 27f. Time-water absorption curve of cores, Menlo	49
Fig. 27g. Time-water absorption curve of cores, Pints	49
Fig. 27h. Time-water absorption curve of cores, X (Alden II)	49
Fig. 28a. Time-weight in water curves of cores, A, C, and M limestones	50
Fig. 28b. Time-weight in water curves of cores, Pints	50
Fig. 28c. Time-weight in water curves of cores, K 1, L and X (A II)	51
Fig. 28d. Time-weight in water curves of cores, Keota II	51
Fig. 28e. Time-weight in water curves of + 3/8 in fractions, A, C, and P	52
Fig. 28f. Time-weight in water curves of + 3/8 in fractions, K II and L	52
Fig. 28g. Time-weight in water curves of + 3/8 in fractions, K I, M and X	53
Fig. 29. Relations between oil absorption and oil viscosity, + No. 4 fractions	61
Fig. 30. Relations between oil absorption and soaking time, + No. 4 fractions	62
Fig. 31. Asphalt absorption - BISG method vs immersion method	72
Fig. 32a. Asphalt absorption vs time of immersion and time of absorption, cores, Alden	76



	<u>Page</u>
Fig. 32b. Asphalt absorption vs time of immersion and time of absorption, cores, Cook	76
Fig. 32c. Asphalt absorption vs time of immersion and time of absorption, cores, Keota I	77
Fig. 32d. Asphalt absorption vs time of immersion and time of absorption, cores, Keota II	77
Fig. 32e. Asphalt absorption vs time of immersion and time of absorption, cores, Linwood	78
Fig. 32f. Asphalt absorption vs time of immersion and time of absorption, cores, Menlo	78
Fig. 32g. Asphalt absorption vs time of immersion and time of absorption, cores, Pints	79
Fig. 32h. Asphalt absorption vs time of immersion and time of absorption, cores, X	79
Fig. 33. Asphalt absorption vs aggregate type	82
Fig. 34. Effects of immersion temperature on absorption, Pints	82
Fig. 35. Effects of asphalt type on absorption, Pints	83
Fig. 36a. Effects of immersion time on absorption, Alden	83
Fig. 36b. Effects of immersion time on absorption, Cook	84
Fig. 36c. Effects of immersion time on absorption, Keota I	84
Fig. 36d. Effects of immersion time on absorption, Keota II	85
Fig. 36e. Effects of immersion time on absorption, Linwood	85
Fig. 36f. Effects of immersion time on absorption, Menlo	86
Fig. 36g. Effects of immersion time on absorption, Pints	86
Fig. 37. Alden, 60 min immersion in A.C. 668 at 300 °F, 136X	87
Fig. 38. Cook, 5 min immersion in A.C. 668 at 300 °F, 136X	87
Fig. 39. Keota II, 1 min immersion in A.C. 668 at 300 °F, 136X	88
Fig. 40. Menlo, 60 min immersion in A.C. 668 at 300 °F, 136X	88
Fig. 41. Pints, 60 min immersion in A.C. 1425 at 300 °F, 136X	89

	<u>Page</u>
Fig. 42a. SEM, unimpregnated Keota II, 1000X	89
Fig. 42b. SEM, unimpregnated Keota II, 3000X	90
Fig. 42c. SEM, asphalt impregnated Keota II, 1000X	90
Fig. 42d. SEM, asphalt impregnated Keota II, 3000X	91
Fig. 43a. Asphalt absorption vs time of absorption and time of immersion, + No. 4 fractions	92
Fig. 43b. Asphalt absorption vs time of absorption and time of immersion, + No. 4 fractions, Pints	92
Fig. 43c. Asphalt absorption vs time of absorption and time of immersion, + No. 4 fraction, Keota II	93
Fig. 44. Cumulative porosity distribution (Menlo vs Pints cores)	104
Fig. 45. Hysteresis in mercury porosimetry (Menlo vs Pints cores)	104
Fig. 46. Asphalt absorption vs time	110
Fig. 47. Monomer loading vs time for Cook cylinders	119
Fig. 48. Monomer loading vs time for Menlo cylinders	119
Fig. 49. Curing curves for aniline furfural treatments	123
Fig. 50. Effects of curing temperature on water absorption	123
Fig. 51. Water absorption of Cook aggregate vs percent aniline furfural treatment	124
Fig. 52. Water absorption of Menlo aggregate vs percent aniline furfural treatment	124
Fig. 53. Absorption of 85-100 penetration asphalt by graded crushed aggregates vs aniline furfural treatment	128
Fig. 54. Absorption of 120-150 penetration asphalt by graded crushed aggregates vs aniline furfural treatment	128
Fig. 55. Water absorption vs percent Armac T treatment	129
Fig. 56. Test property curves for mixes containing Cook aggregate and agricultural lime by the Marshall method	135

	<u>Page</u>
Fig. 57. Test property curves for mixes containing Menlo aggregate and agricultural lime by the Marshall method	136
Fig. 58. Test property curves for mixes containing aniline furfural treated Cook aggregate and agricultural lime by the Marshall method	138
Fig. 59. Test property curves for mixes containing aniline furfural treated Menlo aggregate and agricultural lime by the Marshall method	139
Fig. 60. Test property curve for mixes containing Armac T treated Cook aggregate and agricultural lime by the Marshall method	140
Fig. 61. Test property curves for mixes containing Armac T treated Menlo aggregate and agricultural lime by the Marshall method	141
Fig. 62. Water absorption of sulfur treated limestones	142
Fig. 63. Time-absorptive curves for treated and untreated Cook limestone	145
Fig. 64. Time-absorptive curves for treated and untreated Pints limestone	146
Fig. 65. Time-absorptive curves for treated and untreated Linwood limestone	147
Fig. 66. Time-absorptive curves for treated and untreated X (Alden II) limestone	148
Fig. 67. Time-absorptive curves for treated and untreated Menlo limestone	149
Fig. 68. Time-absorptive curves for treated and untreated Alden limestone	150
Fig. 69. Time-absorptive curves for treated and untreated Keota I limestone	151
Fig. 70. Time-absorptive curves for treated and untreated Keota II limestone	152

## TABLES

	<u>Page</u>
Table 1. Limestone aggregates studied	2
Table 2. Chemical composition of rocks	4
Table 3. Effective porosity of aggregates studied	5
Table 4. Properties of asphalt studied	7
Table 5. Bulk specific gravity, water absorption, and porosity of rock cores	15
Table 6. Porosity in different pore size ranges	15
Table 7. Linear correlation coefficients between main pore properties	26
Table 8. Relation between mercury intrusion porosity and porosity in other size ranges	27
Table 9. Percent mercury retained on depressurization	32
Table 10. Bulk specific gravity and water absorption of quarry crushed aggregate and cores	43
Table 11. Bulk specific gravity and water absorption of laboratory crushed block samples	54
Table 12a. Water absorption of cores, ASTM vs graphical	55
Table 12b. Water absorption of laboratory crushed and #4, ASTM vs graphical	55
Table 13. Results of CKE, QC vs LC	59
Table 14. Results of oil absorption, QC vs LC	59
Table 15. Oil absorption vs time and temperature	60
Table 16. Asphalt absorption by photometer method	65
Table 17a. Dye absorption by photometer method, methylene blue	66
Table 17b. Dye absorption by photometer method, Safranin T	67
Table 18. Rankings of absorption by photometer method	68
Table 19. Asphalt absorption by rock cores	69

	<u>Page</u>
Table 20. Asphalt absorption by cores	95
Table 21. Asphalt absorption by #4 laboratory crushed aggregates	97
Table 22. Correlation between water absorption of 3/8 in to No. 4 sieve fraction (x) and other absorption properties (y)	98
Table 23. Correlation between water absorption of cores (x) and other absorption properties (y)	99
Table 24. Correlation coefficients for pore properties vs asphalt absorption	100
Table 25. Correlation coefficients for non-normalized pore sizes	101
Table 26. Micron values of $r_{10}$ radii	102
Table 27. Relations between asphalt absorption and 0.7-0.05 $\mu$ porosity	103
Table 28. Correlation between asphalt absorption by photo-colorimeter method (x) and other absorption properties (y)	106
Table 29. Linear correlation coefficients (r) between asphalt absorption by immersion	107
Table 30. Gradation of 1968 surface	110
Table 31. Potential materials for aggregate treatments	114
Table 32. Chemical treatments, Grading A	116
Table 33. Physical constants of aniline	116
Table 34. Physical constants of furfural	117
Table 35. Physical constants of methyl methacrylate	117
Table 36. Chemical treatment, Grading B (sulfur series)	118
Table 37. Series C aggregate treatment	122
Table 38. Specific gravity, water absorption, water permeable pores of graded crushed aggregates treated with aniline furfural	125

	<u>Page</u>
Table 39. Heat stability of graded crushed aggregates treated with aniline furfural	125
Table 40. Asphalt absorption (percent by weight) of graded crushed aggregates treated with aniline furfural	126
Table 41. Specific gravity and water absorption of 1/2 in. cores treated with aniline furfural	127
Table 42. Specific gravity, water absorption and permeable pores of Armac T treated crushed aggregates	127
Table 43. Heat stability of graded crushed aggregates treated with Armac T	130
Table 44. Asphalt absorption (percent by weight) of graded crushed aggregates treated with Armac T	130
Table 45. Specific gravity and absorption of 1/2 in. cores treated with Armac T	132
Table 46. Specific gravity and absorption of cores impregnated with monomer	132
Table 47. Specific gravity and absorption of graded crushed aggregates treated with monomer	133
Table 48. Asphalt absorption of bituminous mixes by Rice method	142
Table 49. Water absorption of sulfur treated limestones	143
Table 50. Asphalt absorption of sulfur treated limestones	153
Table 51. Asphalt absorption of sulfur treated limestone - series C and D	154
Table 52. Absorption of chemically treated aggregate, Alden	158
Table 53. Absorption of chemically treated aggregates, Cook	159
Table 54. Absorption of chemically treated aggregates, Keota I	160
Table 55. Absorption of chemically treated aggregates, Keota II	161
Table 56. Absorption of chemically treated aggregates, Linwood	162
Table 57. Absorption of chemically treated aggregates, Menlo	163
Table 58. Absorption of chemically treated aggregates, Pints	164
Table 59. Absorption of chemically treated aggregates, X-Quarry	165

## INTRODUCTION

A long-range comprehensive research project entitled "Absorptive Aggregates in Asphalt Paving Mixtures," was initiated in 1966 on evaluation and use of absorptive aggregates for asphalt paving mixtures.

The overall objectives of the study are:

- To evaluate existing methods and develop new methods for determining the absorption of asphalt by road aggregates by both quantitative and qualitative methods.
- To correlate basic chemical and physical properties with the absorption characteristics of aggregates with respect to asphalt, and to identify parameters that are indicative of the absorptive characteristics of aggregates.
- To evaluate the effects of asphalt absorption by aggregate on asphalt, aggregate, and the asphalt mixtures.
- To establish criteria and tests for identifying, classifying, and specifying aggregates used in asphalt mixtures with respect to asphalt absorption.
- To develop methods and remedies for utilizing absorptive aggregates in asphalt paving mixtures economically without sacrificing durability and stability of the mixture.

Project HR-127 (1966-1967) was designed to study the first two phases of the overall objectives and, to a limited extent, the third objective. Project HR-142 (1968-1970) was initiated to study the third, fourth, and fifth objectives. This report summarizes the work accomplished in HR-142.

This report is intended to be a detailed summary of the research performed in HR-142. Whenever possible, the work accomplished will be summarized and all pertinent data will be included, especially for the part since HR-142 Progress Report No. 1, (January 1970). For further details, reference to the various theses and publications and previous reports will be made (Appendix A). For clarity, some reference will be made to work performed in HR-127.

The subject matter is organized and presented in the following areas:

- Aggregate studies
- Absorption studies
- Treatment studies
- Summary and conclusions
- Recommendations



## AGGREGATE STUDIES

### Aggregates Studied

Six limestone aggregates were studied from quarries selected by Iowa State Highway Commission engineers. The sources and designations of the aggregates are given in Table 1. The locations of the quarries are shown in Fig. 1.

Four of the aggregates (Menlo quarry, Adair Co.; Linwood quarry, Scott Co.; Cook quarry, Story Co.; and Keota quarry, Washington Co.) were also studied in HR-127. Limestones from Alden quarry, Hardin County, and Pints quarry, Black Hawk County, are included because of their known service performance records as concrete aggregates. In addition to crushed aggregates from 3/8 — 1 in. size, two "block stones" were obtained from all six quarries for preparation of geometrically symmetrical rock cylinders.

Chemical compositions of rocks, both quarry-crushed fractions and laboratory-cored block samples, were determined by the EDTA method.<sup>1</sup> Classification of aggregates was based on Pettijohn's system of classifying carbonate rocks.<sup>2</sup>

Aggregate from Alden is a white-to-cream limestone (97% calcite) with dense, medium-to-coarse-grained texture of rounded white fragments cemented with cream (possibly clastic origin). There are significant differences among quarry-crushed Keota aggregates and two block samples. Quarry Keota and block sample No. 2 (KII) were tan-to-buff, very porous, and fine-grained with some vugs and fractures, and were classified as calcitic dolemites to dolomitic limestones. Keota block sample No. 1 (KI), on the other hand, was a white-to-light grey, dense, medium-textured magnesium limestone (92% calcite). The Cook quarry aggregate is a dolomitic limestone, tan-to-buff,

Table 1. Limestone aggregates studied

#	County	Quarry	Size, in.	Beds or ledges	Geological formation
1-S 1-L	Adair	Menlo	3/8	3-6-Argentine	Missourian series Pennsylvania system
2	Blackhawk	Pints	3/4	Rapid	Cedar Valley formation, Devonian system
3-S 3-L	Hardin	Alden	3/8	-	Gilmore City formation, Mississippian age
4	Scott	Linwood	1/2	Davenport	Devonian system
5-S 5-L	Story	Cook	3/8	-	St. Louis formation, Mississippian series
6	Washington	Keota	1	Beds 14 - 22	Osage series, Mississippian age

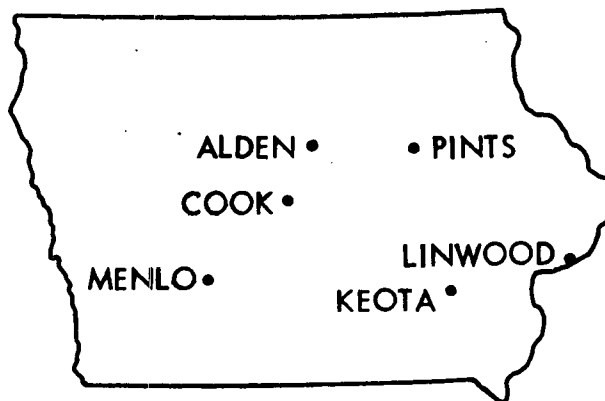


Fig. 1. Project HR-142 aggregate quarry locations

dense, fine-grained, some fractures lined with secondary carbonate. Aggregates from Linwood quarry are magnesium limestone to limestone, mottled grey-to-tan; dense, lithographic, small ( $\approx 1$  mm) inclusions of coarse-grained carbonate and some fractures filled with secondary carbonate, some vugs not filled with secondary minerals. Menlo aggregates are magnesium limestones and are tan to grey, dense, lithographic, but with inclusions (up to 1 cm along longest axis) of coarse-grained calcite (may be fossil replacement). The Pints aggregate is an argillaceous calcitic dolomite (46 - 49% calcite) with scattered chert nodules, grey color and dense, fine-grained, fairly uniform texture. The dolomite has a dirty appearance caused by numerous tiny inclusions.

Chemical compositions of rocks studied are given in Table 2. Bulk specific gravity and effective porosity of coarse fractions and core samples are given in Table 3.

The crushed aggregates were separated by 3/8 in., #4, and #100 sieves, washed and oven dried at  $110^{\circ}\text{C}$  for 24 hr before any tests were conducted.

Various fractions were designated as follows:

- A - Retained on 3/8 in. sieve
- B - Passing 3/8 in. and retained on #4 sieve
- C - Passing #4 sieve and retained on #100 sieve
- D - Passing #100 sieve
- D1 - Passing #100 sieve and retained on #200 sieve

In certain phases of the present study, such as the pore characteristics of the aggregate and time-absorption studies, it was decided to use rock cores (1/2 and 1 in. diameters) drilled from stone blocks received from the respective quarries. This was done to have consistent and comparable results

Table 2. Chemical Composition of Rocks

Code	Quarry	Size, in.	% $\text{CaCO}_3$	% $\text{MgCO}_3$	% Insoluble	Total
Crushed Aggregate						
1LA	Menlo	3/8	94.64	1.18	3.16	98.98
1LB	Menlo	#4-3/8	92.12	1.50	3.95	97.57
1SB	Menlo	#4-3/8	90.43	1.18	4.83	96.44
2A	Pints	3/8 +	47.55	31.74	16.34	95.63
2B	Pints	#4-3/8	46.16	33.98	17.23	97.37
3LA	Alden	3/8 +	98.05	0.46	0.41	98.92
3LB	Alden	#4-3/8	97.65	0.70	0.86	99.21
3SB	Alden	#4-3/8	97.00	1.41	0.43	99.34
4A	Linwood	3/8 +	97.16	0.00	1.42	93.58
4B	Linwood	#4-3/8	95.13	1.00	2.58	98.71
5LA	Cook	3/8 +	58.66	32.22	6.39	97.27
5LB	Cook	#4-3/8	54.45	35.05	7.58	97.08
5SB	Cook	#4-3/8	54.58	35.63	6.54	96.75
6A	Keota	3/8 +	42.16	39.04	24.15	105.35
6B	Keota	#4-3/8	48.15	38.23	12.69	99.07
Block Sample						
1	Menlo	—	94.45	.60	2.97	99.02
2	Pints	—	49.24	34.01	15.20	98.45
3	Alden	—	97.01	0.36	1.21	98.22
4	Linwood	—	95.41	1.13	2.19	98.73
5	Cook	—	56.57	33.87	8.08	98.52
6	Keota	—	96.62	0.19	2.15	98.98
	KI		91.99	5.76	3.84	101.59
	KII		52.96	43.69	4.87	101.52
	X (A2)		98.03	3.50	0.46	101.99

Table 3. Effective porosity of aggregates studied

Quarry	Aggregate #	Bulk Specific gravity (ATM)	Effective porosity, %		
			24 hr soaked	Vacuum saturation	Mercury penetration
Menlo	1-S-B	2.567	4.95	4.90	1.94
	1-L-A	2.613	3.08	3.84	1.95
	1-L-B	2.603	3.64	4.22	1.02
	Core	2.637	2.37	—	0.98
Pints	2-A	2.348	15.40	16.91	11.84
	2-B	2.333	17.06	17.80	11.81
	Core	2.271	16.40	—	16.88
Alden	3-S-B	2.475	7.35	8.44	8.24
	3-L-A	2.517	4.88	7.10	6.46
	3-L-B	2.508	5.80	7.55	6.33
	Core	2.510	4.32	—	9.60
Linwood	4-A	2.613	3.72	4.26	2.78
	4-B	2.582	4.29	4.47	2.30
	Core	2.636	2.37	—	0.90
Cook	5-S-B	2.397	14.33	17.74	10.66
	5-L-A	2.426	10.33	13.73	11.54
	5-L-B	2.408	13.00	14.04	11.42
	Core	2.465	9.56	—	17.44
Keota	6-A	2.326	12.98	16.47	10.50
	6-B	2.303	12.68	19.19	14.77
	Core	2.489	7.77	—	4.66

in studying pore characteristics and asphalt absorption, and for the following reasons:

- Aggregates obtained from stone crushers have variable characteristics both in composition and texture and cannot be depended upon for delicate treatment of analysis of pore characteristics. Rock cores being from one stone block are more likely to be homogeneous and uniform, and correlation between absorption and pore characteristics can be more realistic.
- Rock cores or cylinders allow uniform drying of surface for saturated surface dry condition in ASTM test (C-127-59) for determination of bulk specific gravity and thus give reproducible results to be used in immersion method and bulk-impregnated specific gravity methods for calculating asphalt absorption.
- Due to the same surface texture of drilled cores, mercury porosimetry and absorption results are comparable.
- Chances of inclusion of air bubbles in asphalt are considerably reduced by adding cores one by one, which utilizes bulk-impregnated specific gravity.
- In case of immersion tests, the draining of asphalt from rock cores is more uniform than aggregates with varying surface texture and shapes.

It may be mentioned that cores were drilled out so as to have their longitudinal axis at right angles to the natural bedding planes to keep uniformity.

Hereinafter, the cores shall be referred to in this study by the name of the quarry from which the stone blocks were received.

Two asphalt cements have been included in major phases of this study. The properties of the two asphalts studied are shown in Table 4. The 85-100 pen asphalt will be referred to as 142-1, 142-A or No. 668S and the 120-150 pen asphalt will be referred to as either 142-2 or 142-B. Both asphalt cements were obtained from American Oil Company, Sugar Creek, Missouri.

Table 4. Properties of asphalt studied

#	Property	Asphalt	
		A (142-1)	B (142-2)
1	Penetration 77/100/5	92	127
2	Sp. Gr. 77/77	1.008	1.024
3	Flash point, °F	600	605
4	Fire point, °F	670	665
5	Softening point, R&B, °F	120	118
6	Viscosity at 140°F, poises	1144	727
7	Viscosity at 77°F, poises	$3.96 \times 10^6$	$1.58 \times 10^6$
8	Thin film oven test		
	% loss	0.10	0.08
	Penetration of residue	54	72
	% retained penetration	57	53
9	Soluble in C Cl <sub>4</sub>	99.84%	99.83%
10	Ductility at 77°F, cm	130+	130+
11	Spot test	Negative	Negative
12	Percent asphaltenes	17.94	16.93

### Porosity

The importance of pore size and pore size distribution has been realized and studied extensively in the case of concrete aggregates. However, there has been no published data on the study of the pore-size characteristics of asphalt aggregates and their relationship to the absorption other than that by Lee.<sup>3</sup>

The pores in a system may or may not be interconnected. Flow of interstitial fluid is possible only if at least part of the pore space is interconnected. The interconnected part of the pore system is called the effective pore space of the porous medium.

The diagram of two pores is shown in Fig. 2.

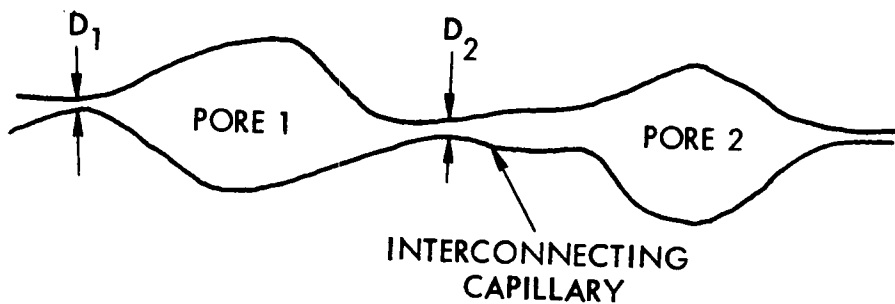


Fig. 2. Diagram of rock pores

The pores in rock are pictured as irregularly-shaped cavities connected by capillaries that have varying shapes and diameters.<sup>4</sup> The smallest entrance diameter to a pore is used as the measure of the size of that pore.

According to Scheidegger,<sup>5</sup> the only unambiguous pore size should be the largest sphere that can be put into the space containing the point in question.



Generally determined pore characteristics are:

- Porosity. A distinction is frequently made between total porosity and the part that is interconnected, which is usually called the effective porosity. In general, any part of the pore space of an aggregate piece that is completely isolated from the exterior is not of concern in the question of asphalt absorption, since other conditions such as density and strength are obviously affected as much by the isolated as by the effective porosity.
- Pore size and pore size distribution. The pore size in terms of radius or diameter of pore (assumed cylindrical in shape, generally) is measured. The frequency of each pore size is also measured to ascertain pore size distribution.
- Specific surface. Another well-defined geometrical quantity of a porous medium is its specific internal area, called specific surface.

Probably the most common method used in casual investigation of aggregate porosity is to measure the absorption and assume the volume of water absorbed equals the pore volume, that is, to assume complete saturation. The ASTM test for specific gravity and absorption of coarse aggregate (C 127) is the method for absorption of coarse aggregates and is straightforward except for the question of surface drying. The surface moisture must be dried from the wet aggregate without removing any water from the pores, either by evaporation or by capillary attraction into the cloth used. The result may be termed water permeable or 24 hr soaked porosity. Dinkle<sup>4</sup> obtained vacuum saturated porosity and reported good correlation between saturated porosity, 24 hr soaked porosity, and mercury intrusion porosity. The main point with respect to the absorption method as a

measurement of porosity is that one hardly ever gets complete saturation.<sup>6</sup>

Washburn and Bunting<sup>7</sup> employed the gas expansion method based on Boyle's law to determine porosity. Isolated voids will be counted as solids and thus the method measures effective porosity if the sample is not powdered. Beeson<sup>8</sup> modified the apparatus and most of the commercially available equipment is based on this principle.

Porosity can be determined visually on a polished or thin section of aggregate by measuring void area (pore space) microscopically by various camera-lucida or photomicrographic methods. Sweet<sup>9</sup> has used such optical methods on aggregates.

Dolch<sup>10</sup> determined the effective porosity of limestone aggregates with the McLeod gauge porosimeter developed by Washburn and Bunting.<sup>11</sup> The method gives a value for the effective void volume by causing the head to be lowered on a dry sample while it is immersed in mercury. The air in voids expands and leaves the sample and is then measured volumetrically at atmospheric pressure. If the bulk volume of the sample is obtained by the use of shaped pieces, porosity can be calculated.

#### Pore Size and Specific Surface of the Solids

Parameters of the porous aggregates can be determined by methods described earlier for porosity determination, such as microscopic methods.

One of the most effective and frequently used methods of determining the specific surface of a solid is the sorption method. Brunauer, Emmett and Teller<sup>12</sup> advanced the BET theory for obtaining specific surfaces from sorption isotherms. Surface adsorption has also been used indirectly to obtain a curve for pore size distribution. Other methods for determining pore size and specific surface are small angle x-ray scattering, heat of immersion, rate of dissolution, ionic adsorption, and radioactive and

electrical methods,<sup>13,14</sup> but these have been little used.

The method most frequently used is that of injection of mercury into the pore system.<sup>15</sup> This method has been adopted in the present study. Washburn<sup>16</sup> was the first to suggest the use of pressed mercury in determining the pore-size distribution of porous solids assuming a model based on a system of circular capillaries.

The relation developed by him may be stated in the following form

$$pr = - 2\sigma \cos \theta$$

where  $p$  is the pressure applied,  $r$  is the pore radius,  $\sigma$  is the surface tension of mercury, and  $\theta$  is the contact angle of the mercury with respect to the solids.

Ritter and Drake<sup>17</sup> put Washburn's conception to practical use and developed the apparatus measuring the penetration of mercury into pores down to 200 Å in diameter at 10,000 psi covering the so-called macropore range. The apparatus generally referred to as mercury porosimeter has been described by Purcell.<sup>18</sup>

Subsequently, Drake<sup>19</sup> utilized a high pressure mercury porosimeter and made measurements up to 60,000 psi to measure pore radii down to 20 Å. As a result, the mercury penetration method can, in principle, be used for practically the whole range of pores of importance in research work. The method was applied successfully to concrete aggregates by Hiltrop and Lemish.<sup>20</sup>

#### Testing Procedure

Water permeable or 24-hr soaked porosity. The water permeable porosity was computed by multiplying the percent water absorption by the bulk specific gravity where both were determined on 1/2 in. diameter rock cores from the

standard 24 hr soaked procedure as in the ASTM C-127-59 test.

Effective porosity or mercury intrusion porosity. Effective porosity is a measure of the permeable or interconnected pores in a rock. It was determined with mercury capillary apparatus or mercury porosimeter apparatus. The effective pore volume was the volume of mercury injected into the rock core at pressure 2000 psi. The bulk volume was that occupied by the rock surrounded by mercury at a pressure of 5 psi. In other words, the effective porosity as defined in this study is the ratio of the interconnected permeable pores in the pore entry radius range, from 21.32-0.05  $\mu$ , to the total bulk volume of particle including pores, expressed as a percentage.

Pore size and pore size distribution. The pore size and its distribution was determined with mercury porosimeter apparatus manufactured and distributed by the Ruska Instrument Corporation, Houston, Texas, under license of the Shell Development Company. The apparatus and procedure have been described in detail elsewhere.<sup>3,20</sup>

The data of the cumulative volume of pores or volume of mercury absorbed at various applied pressures or corresponding pore radii can be treated in various ways; results of the study were:

Data obtained from non-normalized pore size distribution curve. This curve represents the frequency of occurrence of one particular pore size. The curve indicates at what size (say  $r$ ) the greatest number of pores occur. Ritter and Drake<sup>17</sup> derived the equation for a non-normalized distribution curve

$$D(r) = \frac{P}{r} \times \frac{d(V_o - V)}{dp}$$

where

$D(r)$  = distribution function

$p$  = applied pressure, psi

$r$  = pore entry radius, microns

$(V_o - V)$  = volume of mercury injected from zero to pressure  $p$ ,  
cc/g

$\frac{d(V_o - V)}{dp}$  = slope of  $(V_o - V)$  vs pressure determined from pressure-  
pore volume curve

All the terms on the right side of this equation are known or determinable. Values of the derivation are readily obtained by graphical differentiation. Plotting  $D(r)$  against  $r$  gives the distribution curve. Hiltrop and Lemish<sup>20</sup> also derived an equation for a normalized distribution curve in which the area under the curve was equated to unity.

Porosity distribution curve. Curves of cumulative porosity vs pore radius were plotted for all rock cores. The cumulative porosity is the cumulative pore volume divided by total bulk volume of a particle.

Percent of pore volume distribution curve. Curves of pore volume expressed as a percent of total pore volume for each aggregate were plotted as a function of pore radius.

Percent porosity in various pore radius range. The porosity for pores between certain radii is the ratio of the pore volume in these sizes to the total bulk volume of an aggregate including pores, expressed as a percentage. These porosities were determined for the following pore radius ranges (in microns): 21-11, 21-5, 21-2, 21-1, 11-1, 5-1, 1-0.5, 1-0.1, 1-0.05, 0.1-0.05, and 0.7-0.05.

Hysteresis in the mercury porosimetry. When the pressure is systematically released in the mercury-porosimeter, the depressurization curve does not

follow the original pressurization curve and some of the mercury is retained in the sample even on complete removal of pressure. The phenomenon was also observed by Ritter and Drake,<sup>17</sup> who attributed the action to the so-called "ink bottle" shape of the pores. Curves illustrating hysteresis have been obtained for all rock cores.

#### Pore properties of rock cores

Water permeable or 24 hr soaked porosity. Results of water permeable or 24 hr soaked porosity, bulk specific gravity and water absorption as determined from ASTM C-127-59 test for 1/2 in. rock cores are given in Table 5.

Effective porosity or mercury-intrusion porosity. This covers the pore entry radius from 21.32-0.05  $\mu$ . The results are given in Table 6.

Pore size and pore size distribution. Plots were made from the data of the cumulative volume of pores or volume of mercury absorbed at various applied pressures or corresponding pore radii. From these the following graphs were drawn after necessary computations:

Porosity distribution curves. Curves of cumulative porosity (%) vs pore radius for rock cores are given in Figs. 3 - 8. The cumulative porosity is the cumulative pore volume divided by total bulk volume of a particle.

Percent of pore volume distribution curves. Curves of cumulative pore volume expressed as a percent of total pore volume of core vs pore radius are given in Figs. 9 - 14.

Non-normalized pore size distribution curves. These curves representing the frequency of occurrence of one particular pore size, as mentioned earlier, are given in Figs. 15 - 20.

Table 5. Bulk specific gravity, water absorption, and porosity of rock cores

Cores	Bulk specific gravity	Water absorption, %	24 hr soaked porosity
Menlo	2.637	0.90	2.37
Pints	2.271	7.22	16.40
Alden	2.510	1.72	4.32
Linwood	2.636	0.90	2.37
Cook	2.565	2.16	5.54
Keota	2.489	3.12	7.77

Table 6. Porosity in different pore size ranges

Pore size range, $\mu$	Quarry					
	Menlo	Pints	Alden	Linwood	Cook	Keota
21 - 11	0.17	0.12	0.10	0.13	0.17	0.71
21 - 5	0.26	0.18	0.28	0.24	0.25	1.52
21 - 2	0.36	0.32	0.50	0.32	1.10	2.29
21 - 1	0.43	2.30	1.12	0.36	7.00	2.68
11 - 1	0.26	2.18	1.02	0.23	6.83	1.97
5 - 1	0.17	2.12	0.84	0.12	6.75	1.16
1 - 6.5	0.08	6.20	5.28	0.08	5.30	0.22
1 - 0.1	0.45	12.90	8.29	0.51	10.00	0.97
1 - 0.05	0.55	14.65	8.48	0.54	10.40	1.98
0.1 - 0.05	0.10	1.75	0.19	0.03	0.40	1.01
0.7 - 0.05	0.52	10.45	5.80	0.49	7.20	1.86
21 - 0.05 <sup>a</sup>	0.98	16.88	9.60	0.90	17.44	4.66

<sup>a</sup>Mercury intrusion porosity

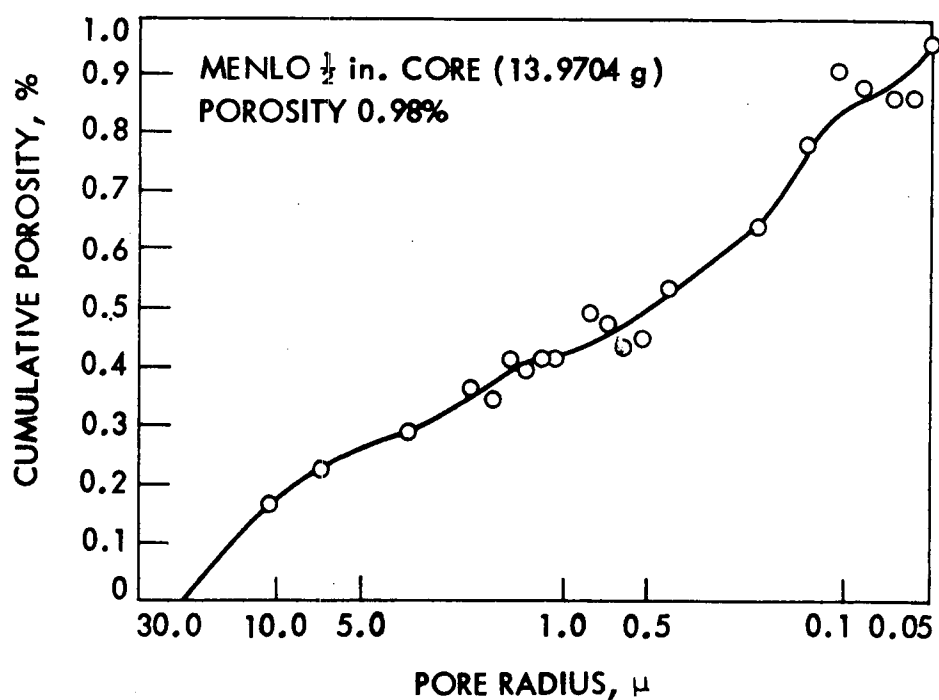


Fig. 3. Cumulative porosity distribution, Menlo

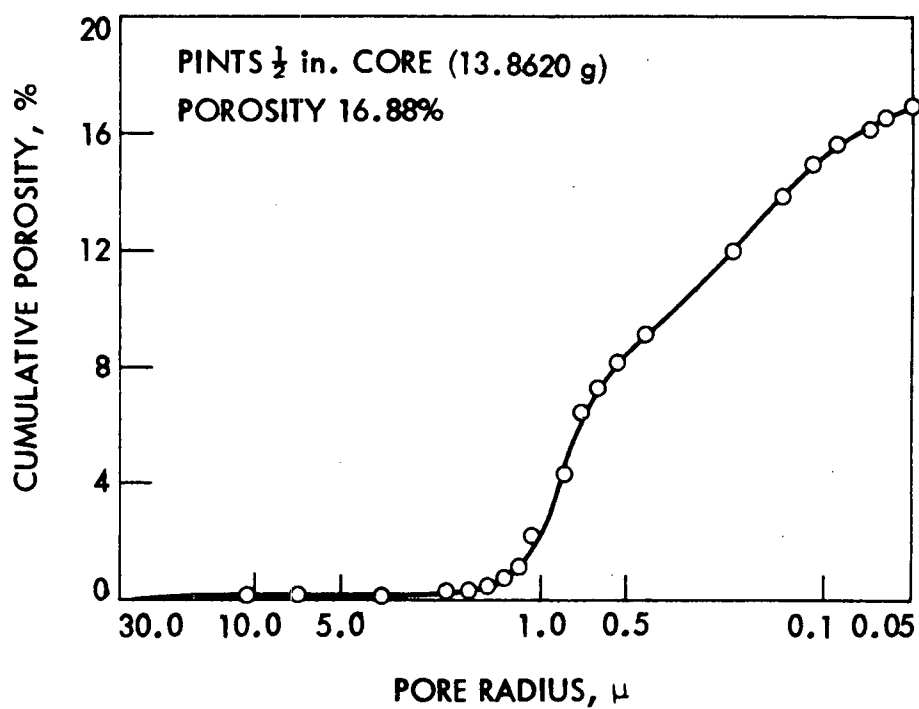


Fig. 4. Cumulative porosity distribution, Pints



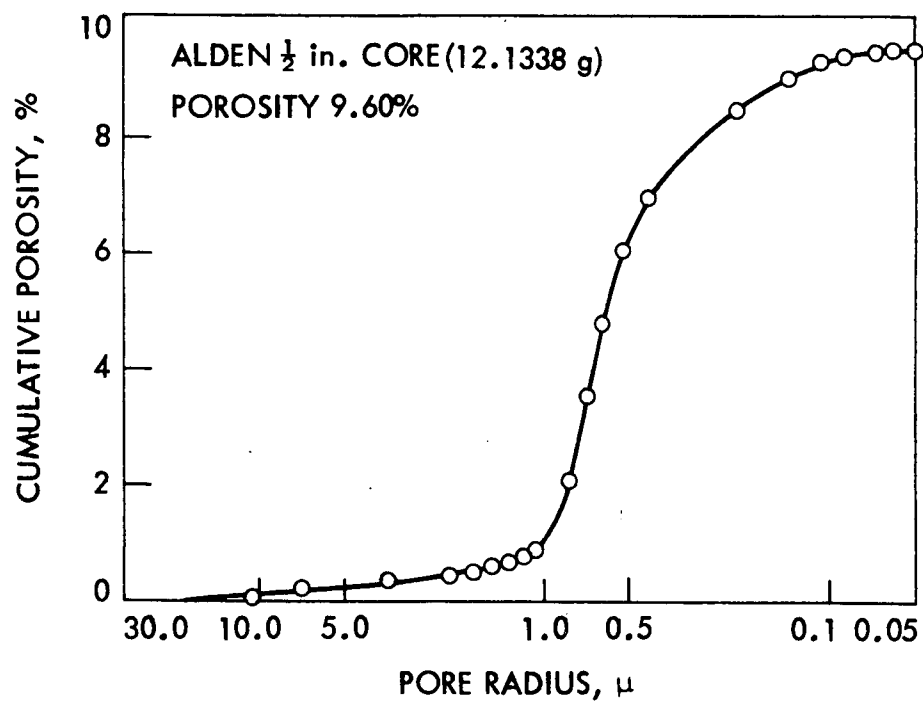


Fig. 5. Cumulative porosity distribution, Alden

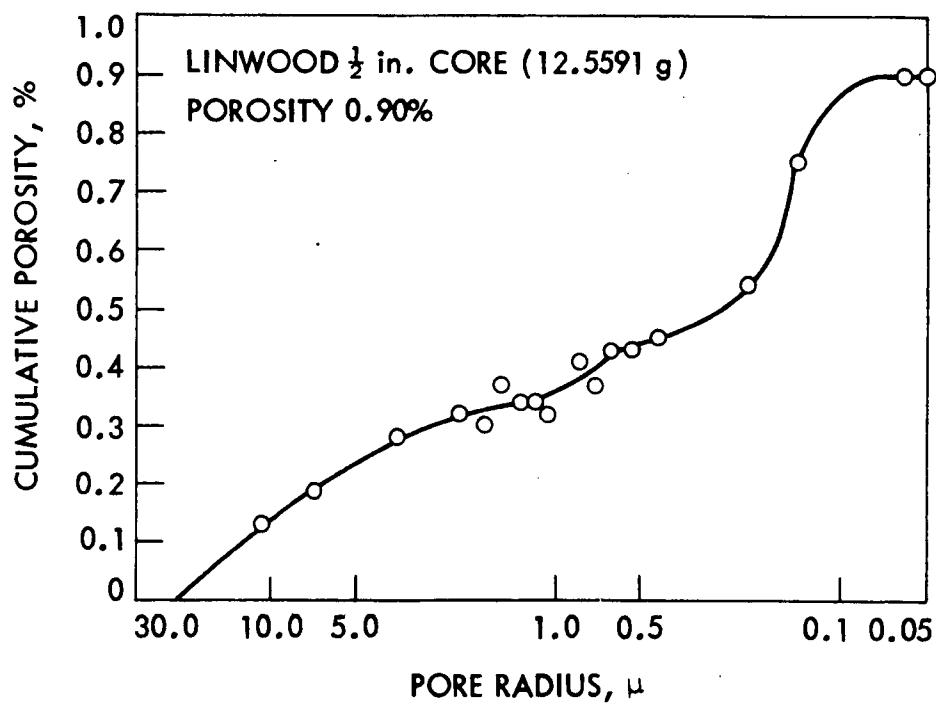


Fig. 6. Cumulative porosity distribution, Linwood

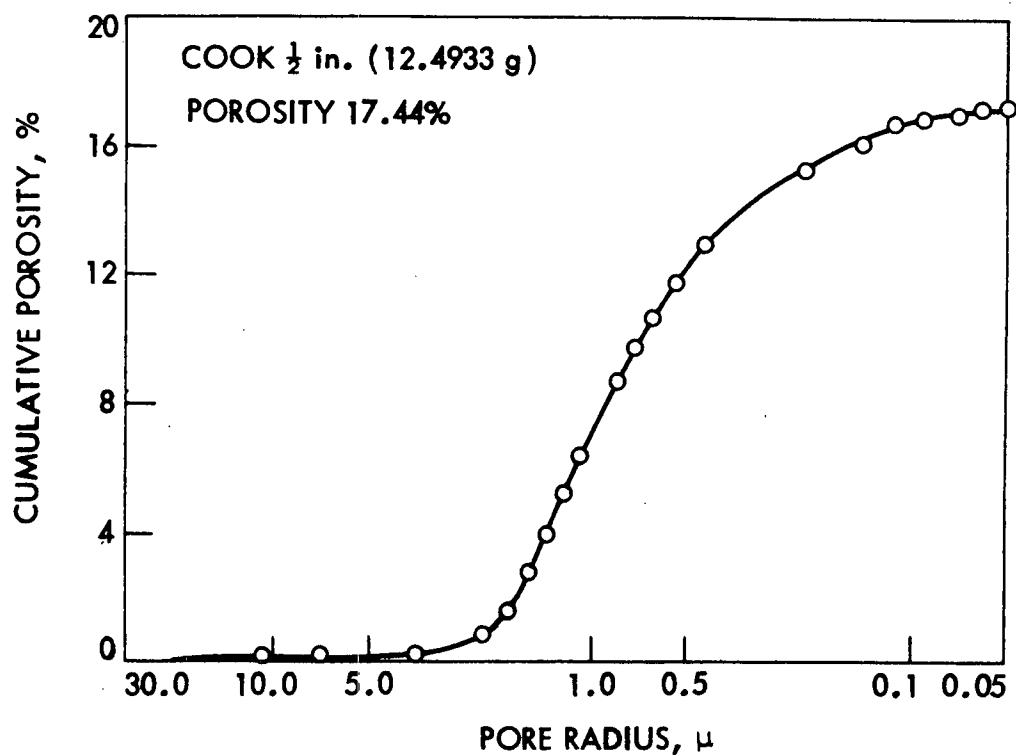


Fig. 7. Cumulative porosity distribution, Cook

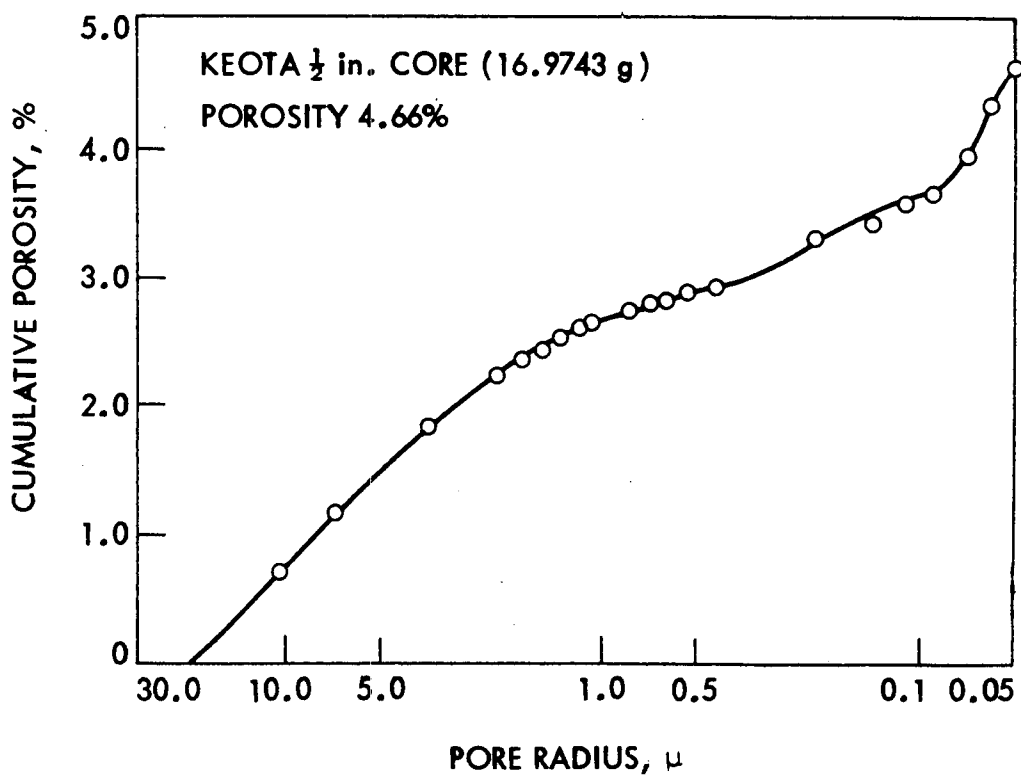


Fig. 8. Cumulative porosity distribution, Keota

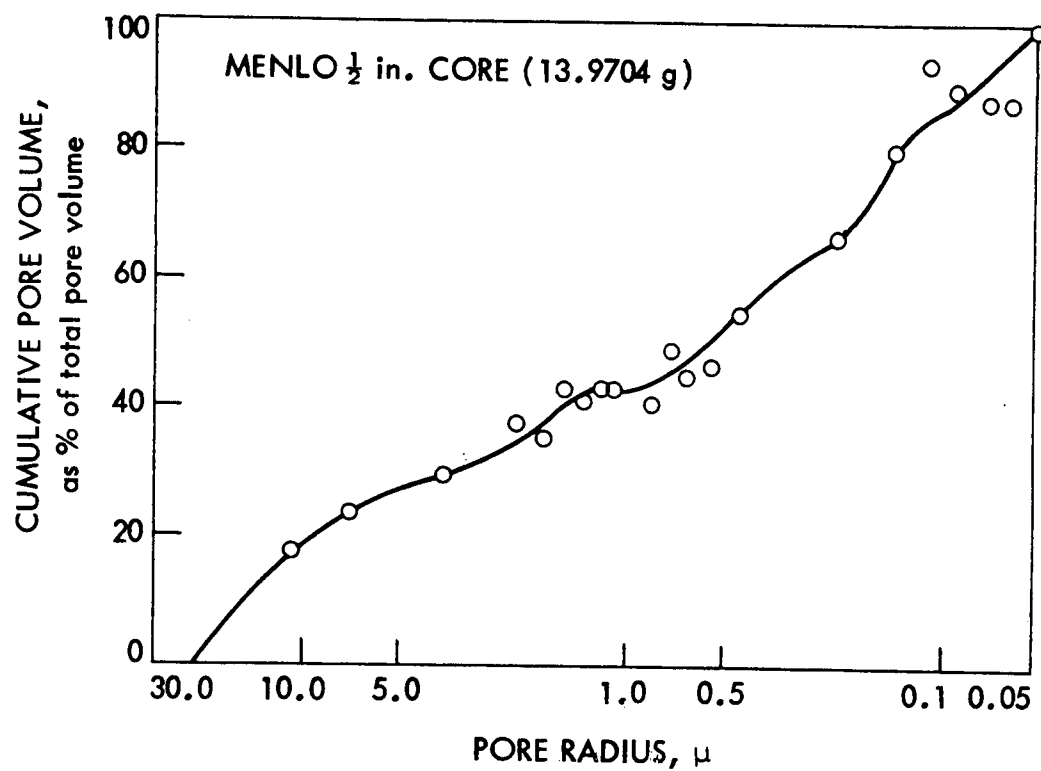


Fig. 9. Percent of pore volume distribution, Menlo

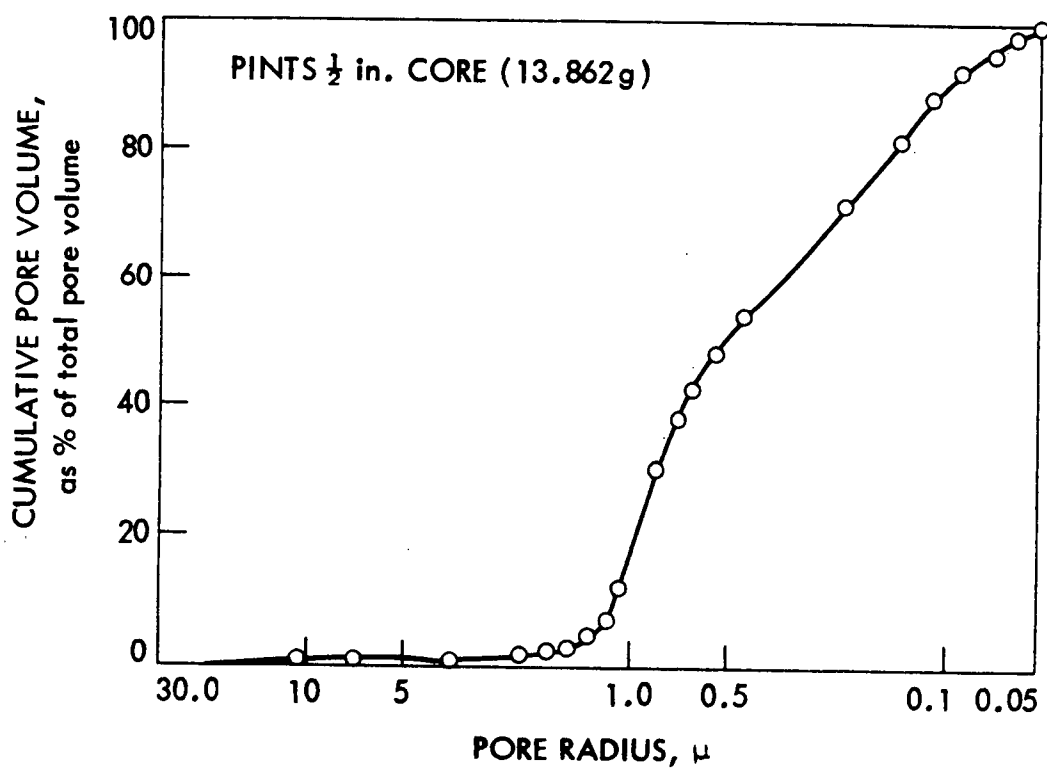


Fig. 10. Percent of pore volume distribution, Pints

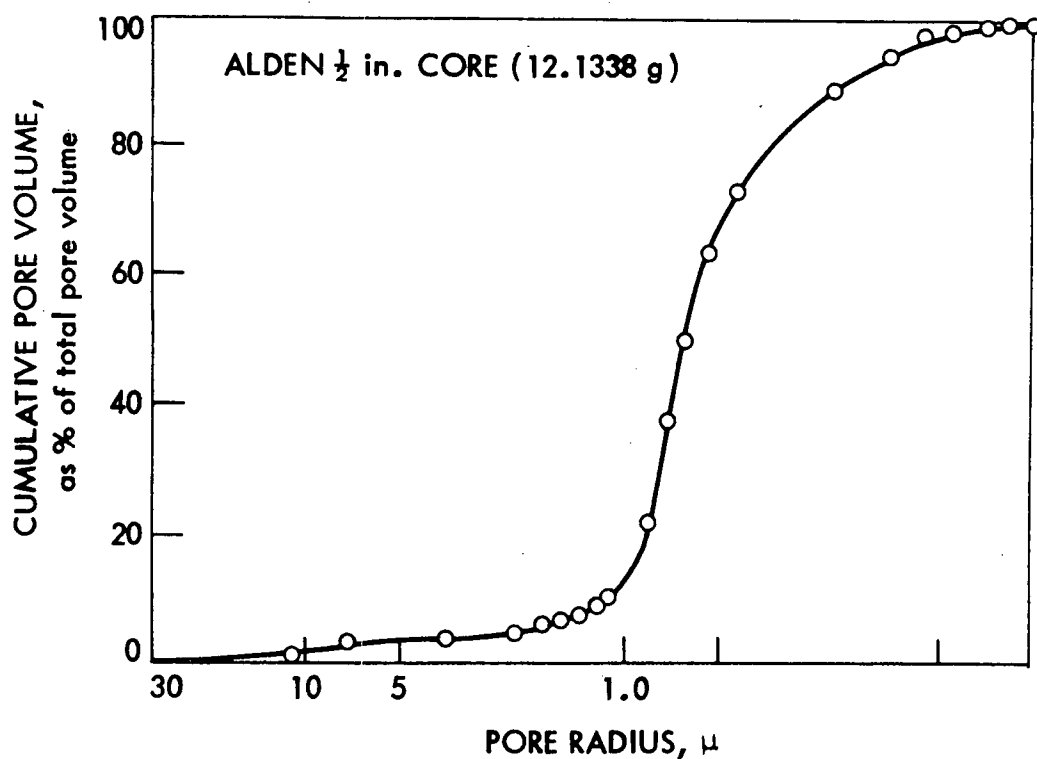


Fig. 11. Percent of pore volume distribution, Alden

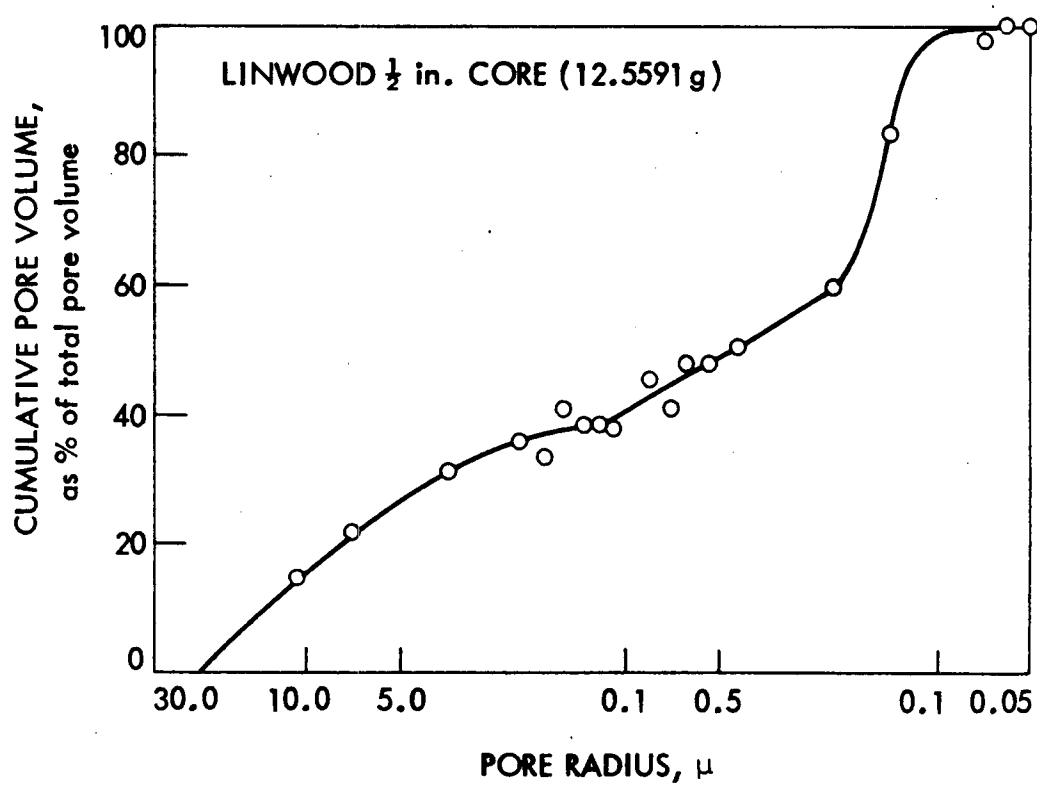


Fig. 12. Percent of pore volume distribution, Linwood

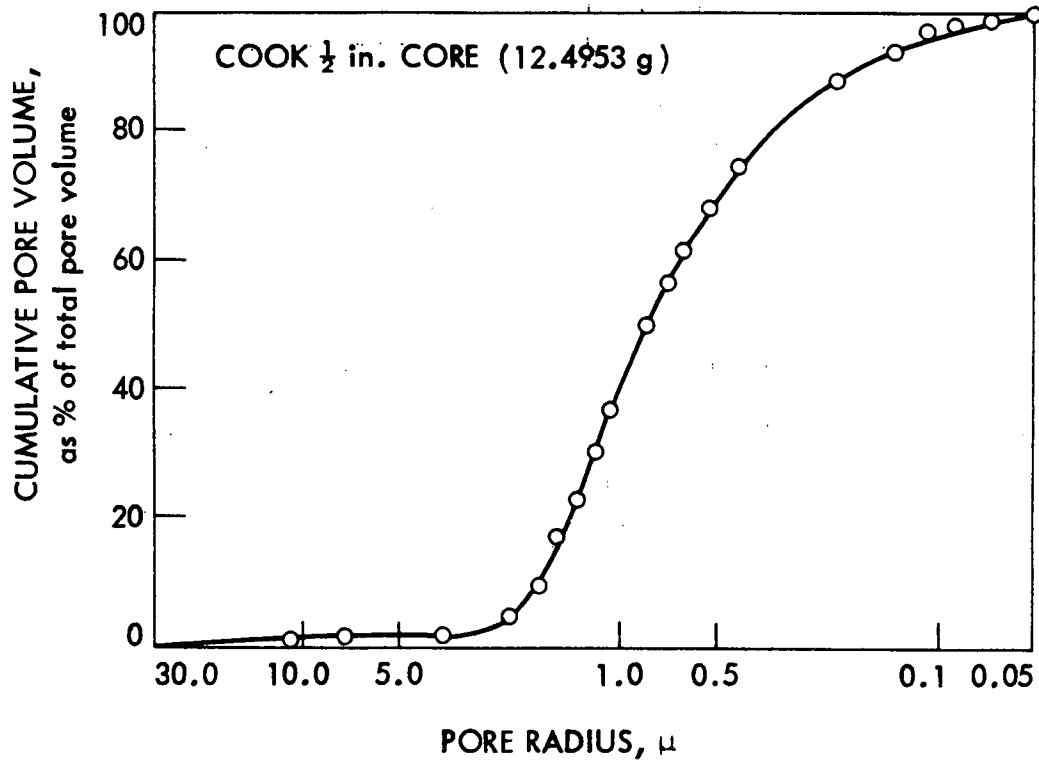


Fig. 13. Percent of pore volume distribution, Cook

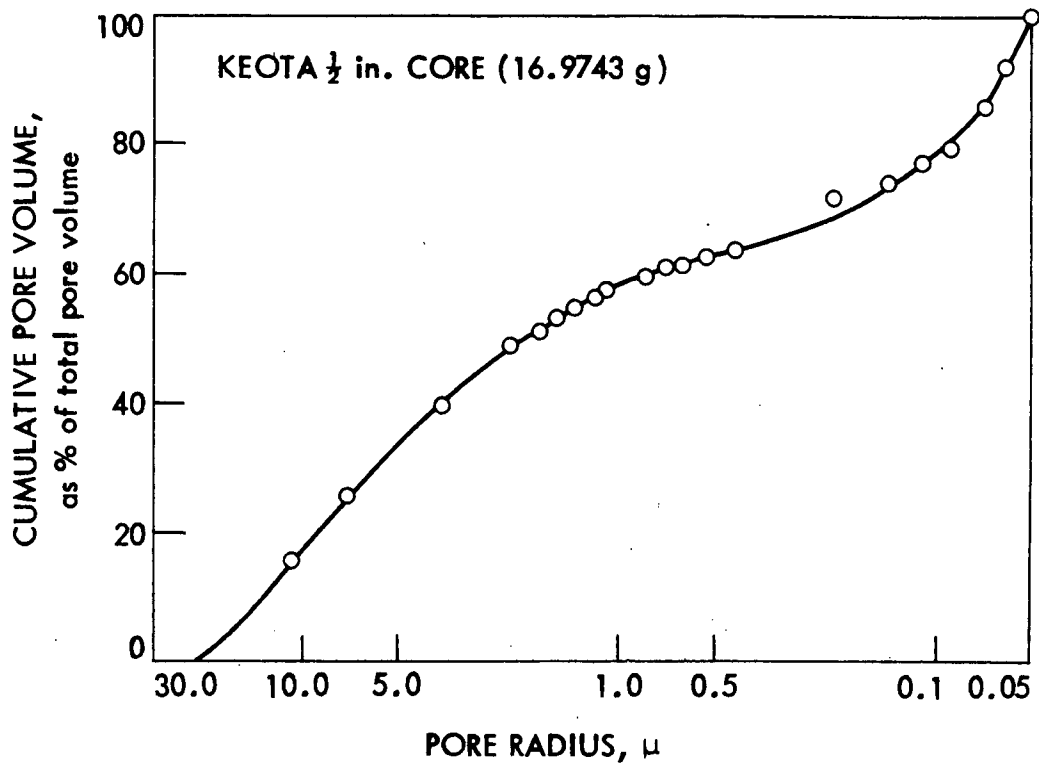


Fig. 14. Percent of pore volume distribution, Keota

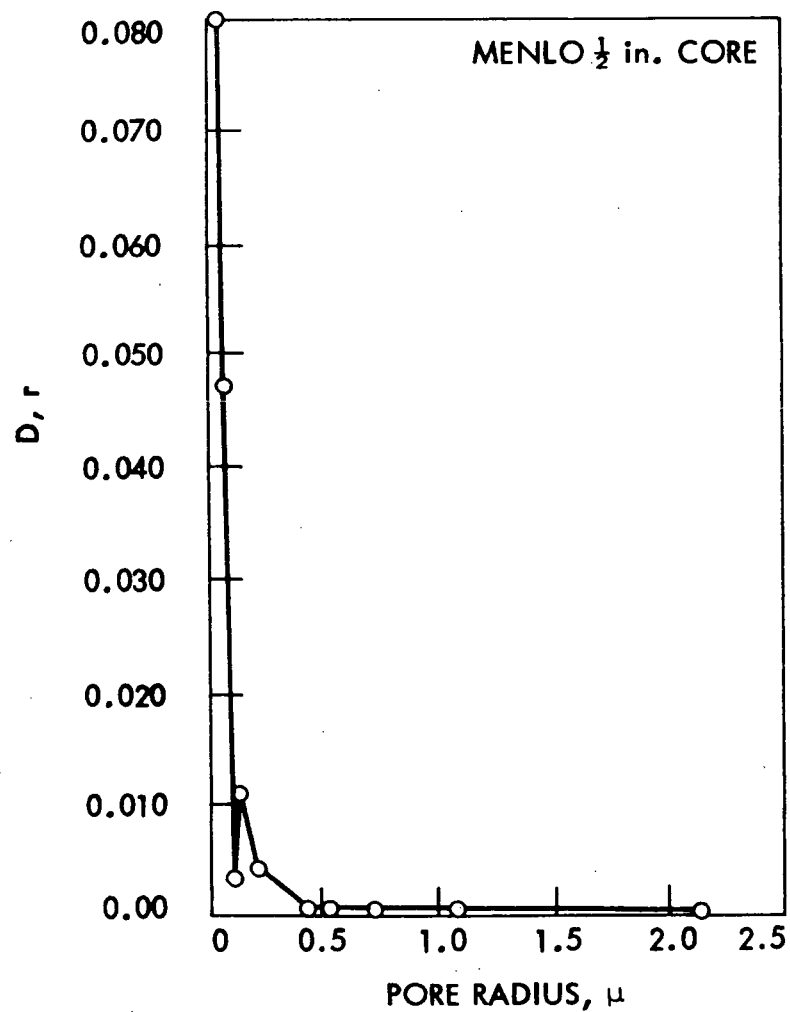


Fig. 15. Non-normalized pore size distribution, Menlo

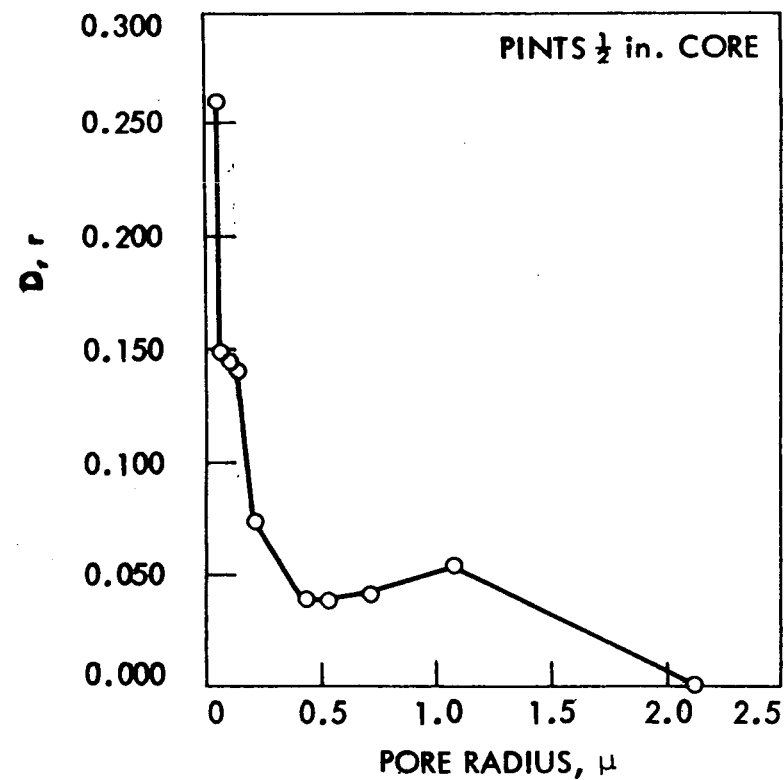


Fig. 16. Non-normalized pore size distribution, Pints

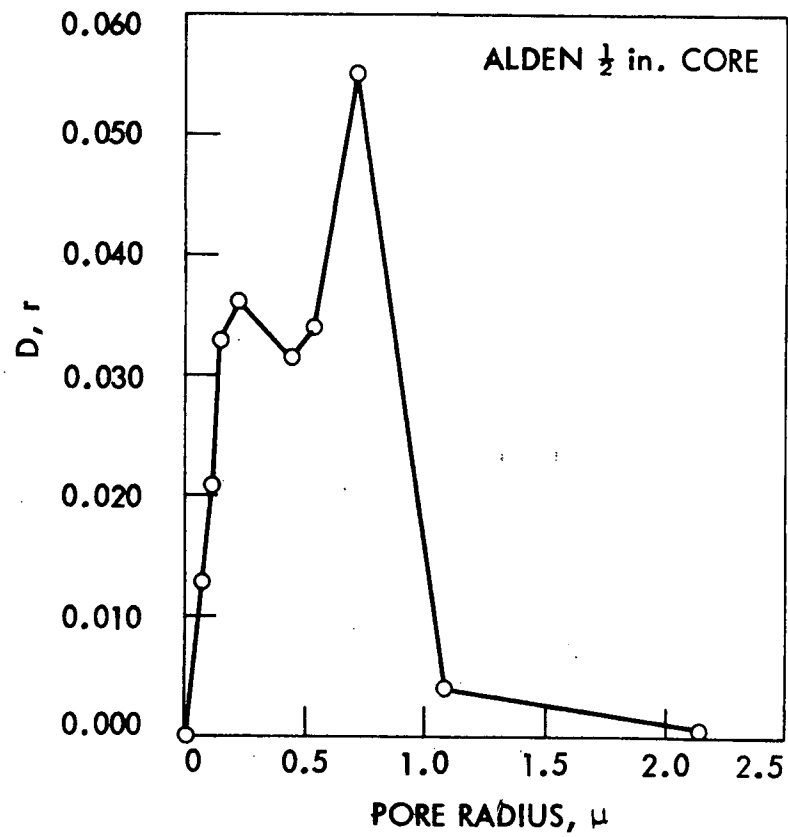


Fig. 17. Non-normalized pore size distribution, Alden

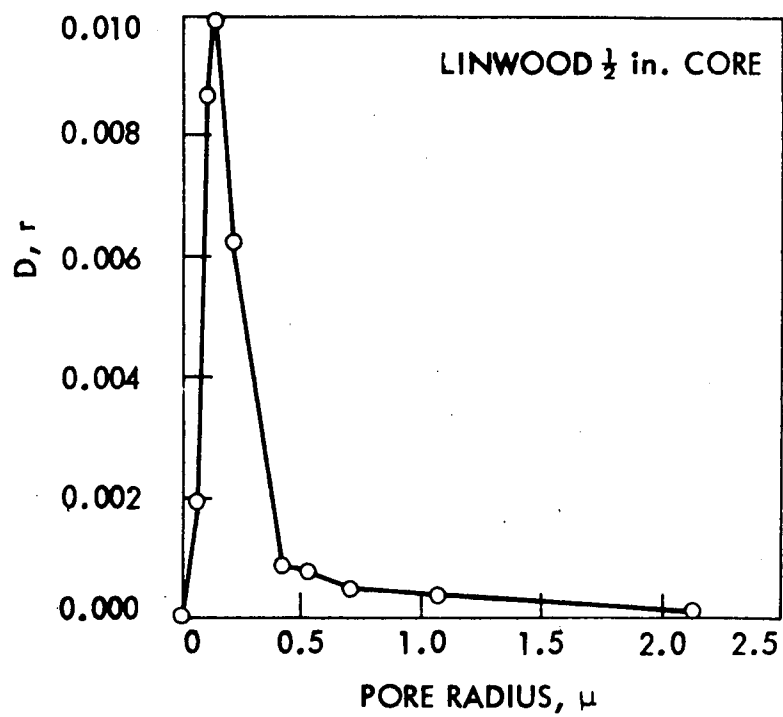


Fig. 18. Non-normalized pore size distribution, Linwood

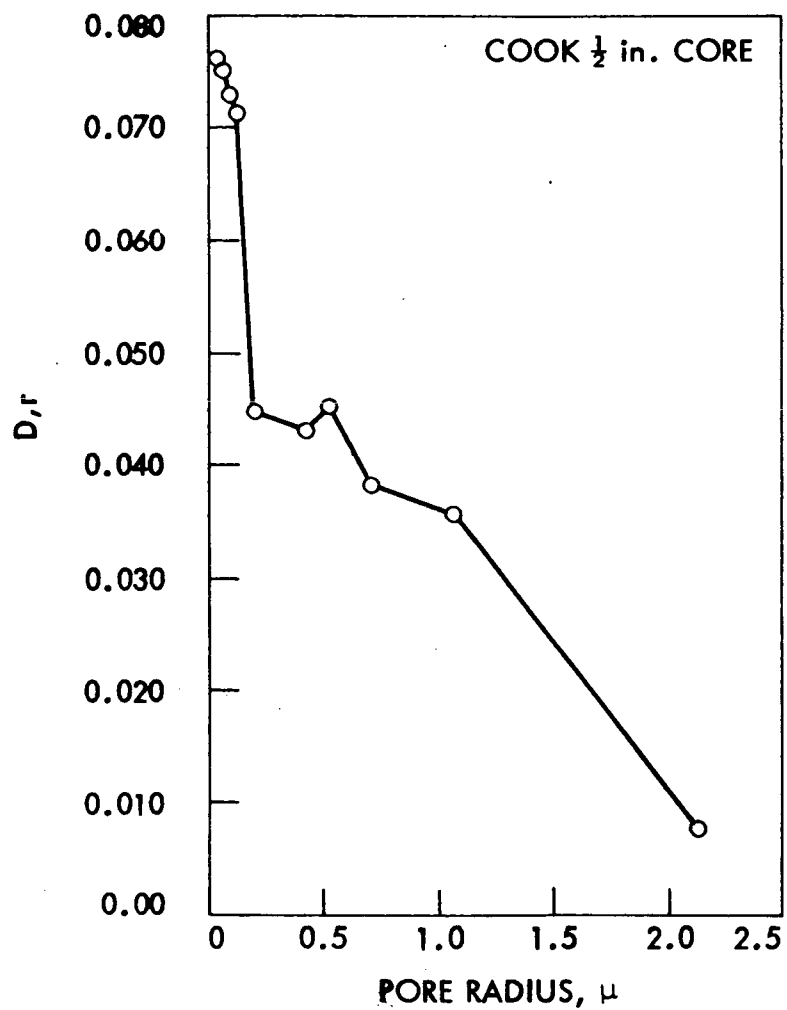


Fig. 19. Non-normalized pore size distribution, Cook

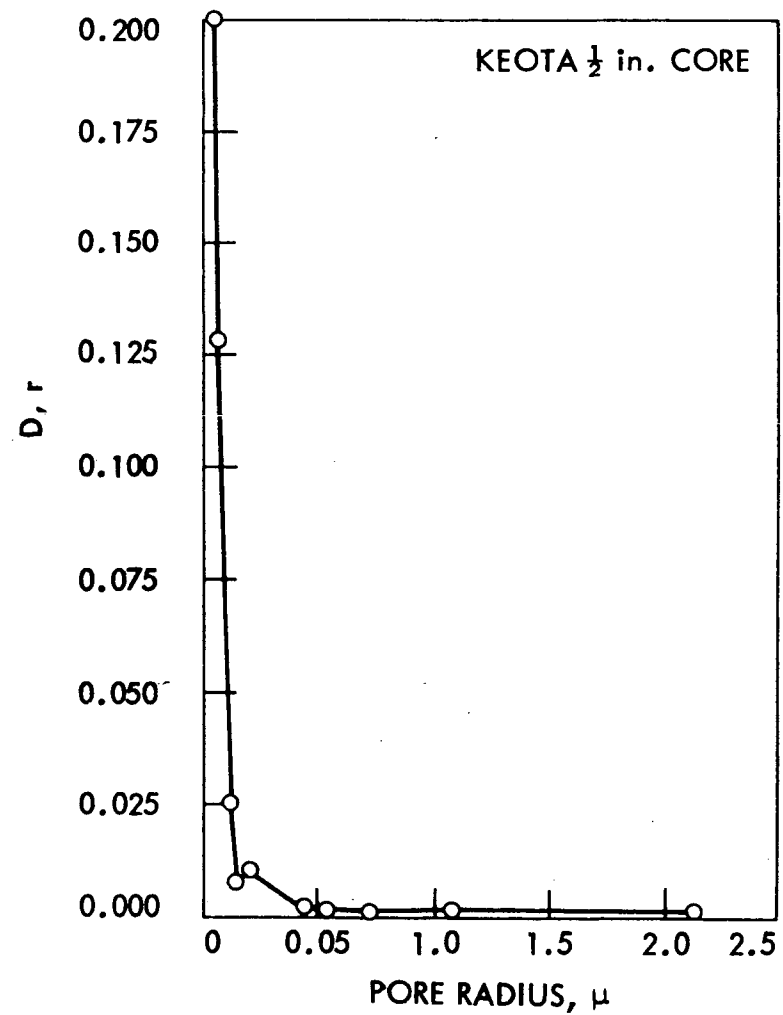


Fig. 20. Non-normalized pore size distribution, Keota



Percent porosity in various pore radius range. The porosity between certain radii, the ratio of the pore volume in these sizes to the total bulk volume of an aggregate including pores, expressed as a percentage, was determined for the following pore radius ranges (in microns): 21-11, 21-5, 21-2, 21-1, 11-1, 5-1, 1-0.5, 1-0.1, 1-0.05, 0.1-0.05 and 0.7-0.05.

The last range included in the study was based on six non-normalized pore size distribution curves which had the range from 0.05 to 0.7 for the most frequently occurring pore radius.

The above-mentioned porosities are included in Table 6.

Statistical analysis results. Out of the various pore size ranges, important ranges indicated later were selected. Linear correlation coefficients between these main pore properties were determined in order to study how they vary with each other. The computed correlation coefficients have been recorded in Table 7.

Pore size ranges in Table 7 were selected on the basis of their correlation with asphalt absorption. Those with poor or no correlation were not included. However, an inverse correlation exists between intrusion porosity and porosity in all pore size ranges (Table 8).

It appears mercury intrusion porosity is mainly dependent upon the porosities in the following ranges, (in microns) 0.7-0.05, 1-0.05, 1-0.1 and 1-0.5; the porosity in 5-1, 11-1, 21-2, and 0.1-0.05 ranges have fair correlations with mercury intrusion porosity and show a general trend.

Based on the determination of 24 hr soaked porosity and mercury intrusion porosity, the following plots have been made which show good correlations:

24 hr soaked porosity vs mercury intrusion. Correlation coefficient is 0.7093. Menlo and Linwood cores behave almost alike. Cook and Alden cores

Table 7. Linear correlation coefficients between main pore properties

Property	24 hr soaked porosity	Mercury intrusion porosity	0.7-0.05 $\mu$ porosity	0.1-0.05 $\mu$ porosity	1-0.05 $\mu$ porosity	1-0.1 $\mu$ porosity	1-0.5 $\mu$ porosity
24 hr soaked porosity	1						
Mercury intrusion porosity	0.7093						
0.7 - 0.05 $\mu$ porosity	0.7716	0.9553	1				
0.1 - 0.05 $\mu$ porosity	0.9782	0.5510	0.6510	1			
1 - 0.05 $\mu$ porosity	0.7405	0.9548	0.9987	0.6128	1		
1 - 0.1 $\mu$ porosity	0.6733	0.7084	0.9894	0.5341	0.9953	1	
1 - 0.5 $\mu$ porosity	0.5664	0.9275	0.9566	0.4188	0.9687	0.9854	1

Table 8. Relation between mercury intrusion porosity and porosity in other size ranges

#	Pore size range, $\mu$	Correlation coefficient	Equation for regression line <sup>a</sup>
1	0.7 - 0.05	0.9553 <sup>b</sup>	$Y = 0.0101 + 0.5204 X$
2	1 - 0.05	0.9548 <sup>b</sup>	$Y = 0.7580 X - 0.2747$
3	1 - 0.1	0.9547 <sup>b</sup>	$Y = 0.7084 X - 0.4376$
4	1 - 0.5	0.9275 <sup>b</sup>	$Y = 0.3732 X - 0.2786$
5	5 - 1	0.7823	
6	11 - 1	0.7610	
7	21 - 1	0.7315	
8	0.1 - 0.05	0.5510	
9	21 - 5	-0.2717	
10	21 - 11	-0.2534	
11	21 - 2	-0.0145	

<sup>a</sup>X = mercury intrusion porosity  
Y = porosity in respective pore size range

<sup>b</sup>Significant at 5% level

tend to absorb less water, while Keota and Pints cores absorb more water as compared to mercury intrusion.

Mercury intrusion porosity vs 0.7-0.05  $\mu$  range porosity. Since values of pore radius  $r$  corresponding to maximum value of  $D(r)$  in the non-normalized pore size distribution curves (Figs. 15-20) range from 0.05-0.7  $\mu$ , this range was correlated with mercury intrusion porosity. The correlation is excellent, correlation coefficient being 0.9553. The equation for regression line is  $Y = 0.0101 + 0.5204 X$

where

X = mercury intrusion porosity, %, and

Y = 0.7 - 0.05  $\mu$  porosity

Table 7 also indicates that mercury intrusion porosity has the highest correlation with porosity in this range. In other words, in the cores studied, mercury intrusion porosity is mainly dependent on this range of porosity. This is also confirmed by the excellent correlations between porosity of 1-0.05 and 1-0.1; 1-0.05 and 1-0.5; and 1-0.1 and 1-0.5 pore size ranges (in microns). It seems porosity in the 1-0.05 range is the controlling factor for total mercury intrusion, while the 0.1-0.05 range is for water absorption, as the correlation coefficient between 0.1-0.05 range porosity and water absorption is 0.9782.

Hysteresis in the mercury porosimetry. Curves illustrating the phenomenon of hysteresis have been plotted in Figs. 21 - 26 with the log pore radius (micron) as the abscissa and mercury penetration volume (cc/g) as the ordinate, based on mercury intrusion experiments.

If the pores are cylindrical with uniform diameter or V-shaped, the points of penetration and retraction of mercury in the pressure-penetration curve will fall on the same line, provided the advancing and receding contact angles are also equal. If they do not, it is practically certain that the pore system deviates from this simple picture. Pores with narrow throat, the so-called ink-bottle pores, would not be expected to empty when the pressure is released and thus shall be responsible for hysteresis. The occurrence can be accounted for as follows: the start of the penetration is determined by the radius of curvature of a mercury surface that can just penetrate into a narrow passage to an interstice. The start of the retraction, however, is determined by the radius of curvature of the mercury surface formed by the interfering mercury surfaces inside the interstice; this surface has a different radius of curvature than the one formed during penetration.

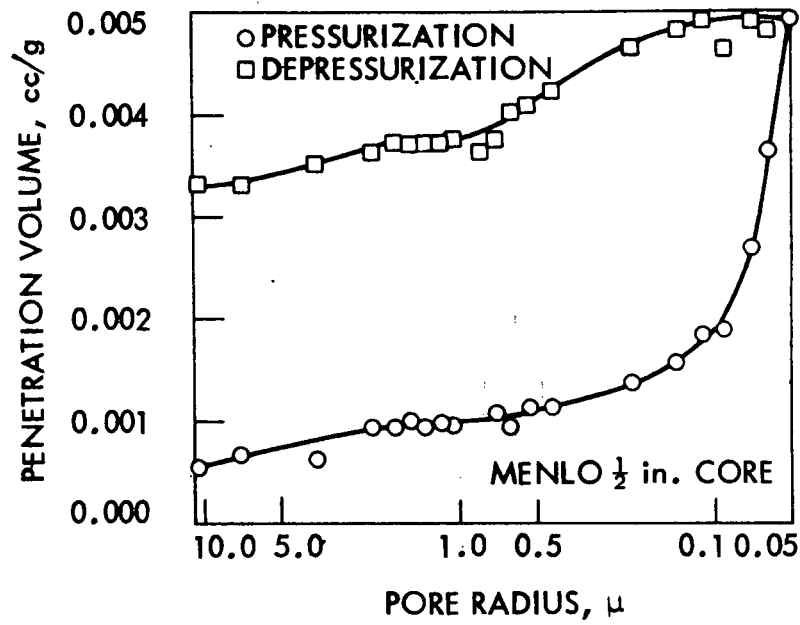


Fig. 21. Hysteresis in mercury porosity, Menlo

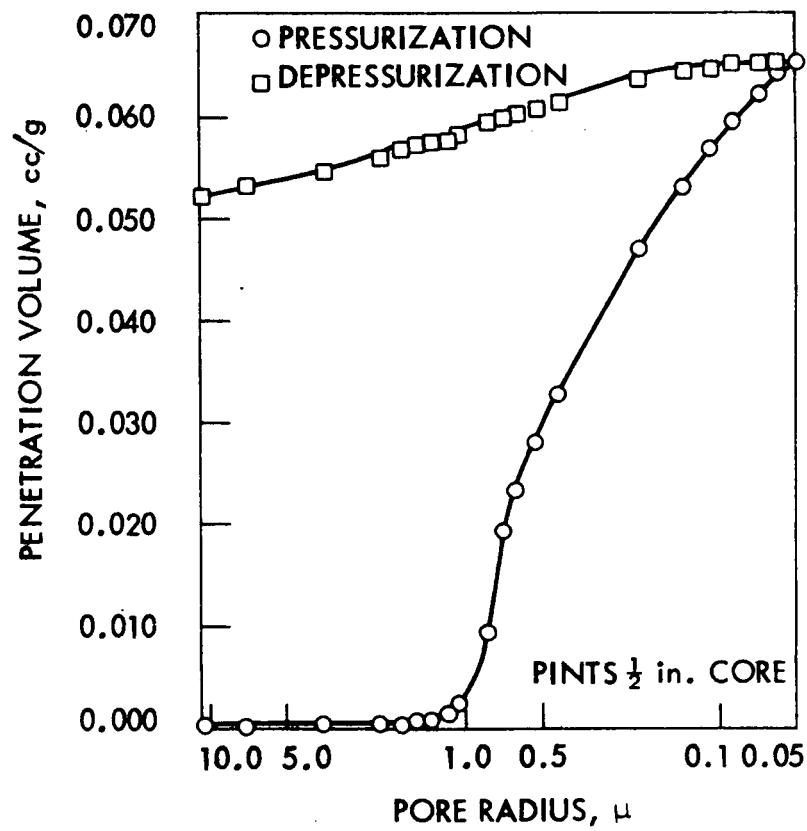


Fig. 22. Hysteresis in mercury porosity, Pints

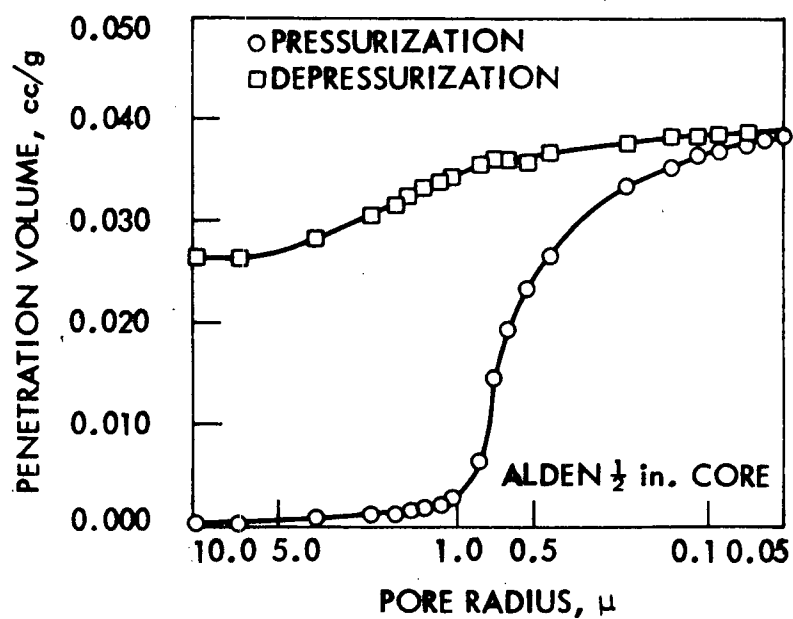


Fig. 23. Hysteresis in mercury porosity, Alden

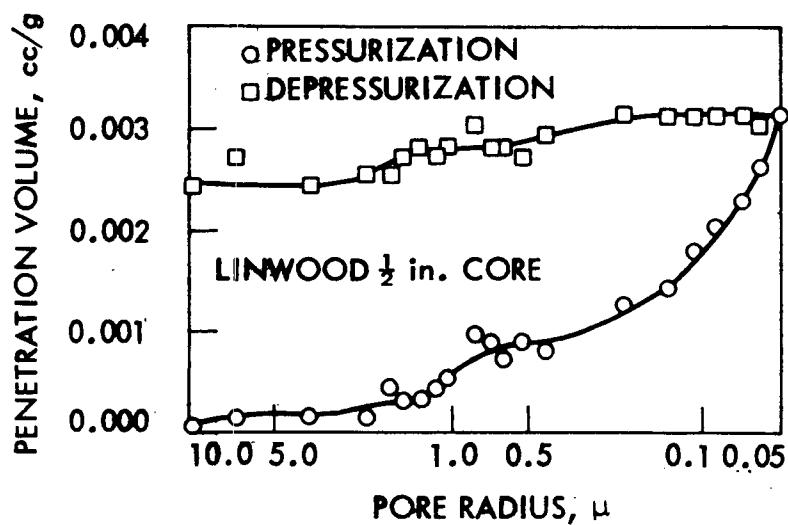


Fig. 24. Hysteresis in mercury porosity, Linwood

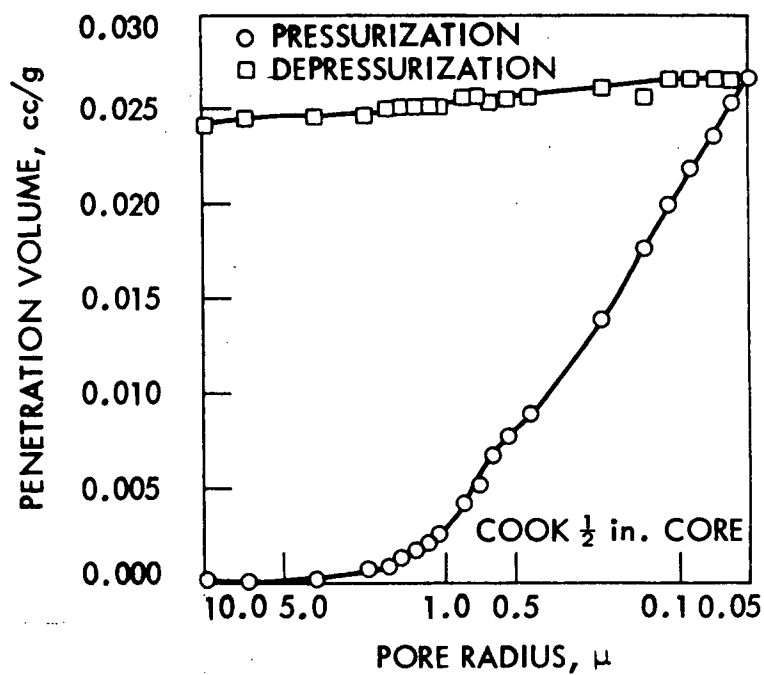


Fig. 25. Hysteresis in mercury porosity, Cook

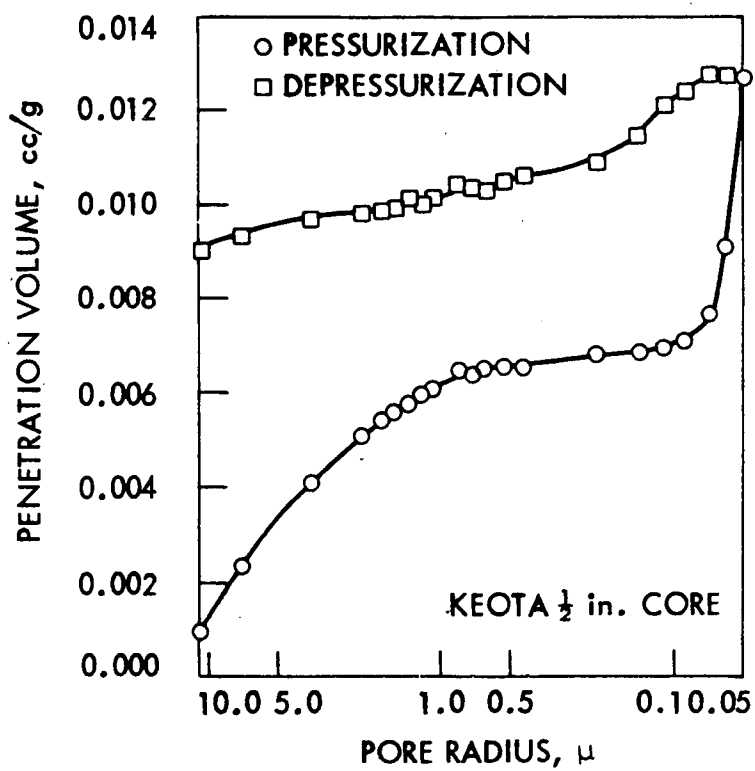


Fig. 26. Hysteresis in mercury porosity, Keota

Examining Figs. 21 - 26, it is evident that all rock cores retain a large percentage of mercury when the pressure is released for 2000 psi - 10 psi. Percentages of mercury retained on depressurizing to 10 psi are shown in Table 9.

Table 9. Percent mercury retained on depressurization

Core	Mercury retained, %
Menlo	63.77
Pints	79.85
Alden	69.33
Linwood	80.56
Cook	90.54
Keota	68.18

#### Interpretation of Porosity Data

Menlo core. The porosity distribution curve indicates a uniform upward trend with more steepness in the latter part. Mercury intrusion porosity above 1  $\mu$  pore size is 0.43 while less than that size is 0.55. The pore size most frequent and having maximum value is 0.05  $\mu$ . Since 24 hr soaked porosity (2.37) is more than mercury intrusion porosity (0.98), it seems rock structure is made of capillaries finer than 0.05  $\mu$  which could absorb more water whereas mercury could not penetrate at 2000 psi. Thus, this core is expected to absorb less bitumen.

Hysteresis (Fig. 21) shows pore throats are predominantly between 0.2 and 0.05  $\mu$  in radius since this is where the mercury entered. The major dimensions of the interior cavities, on the other hand, are between 0.15 and 0.8  $\mu$  in radius because these are the sizes indicated by the receding mercury. Non-normalized pore size distribution curve



(Fig. 15) indicates  $0.05 \mu$  as the most frequent pore size with  $0.15 \mu$  following it as second peak for the range  $0.1 \mu$  and above.

Pints core. The porosity distribution curve (Fig. 4) reveals that most of the porosity is below  $1 \mu$  pore size (14.65 out of total 16.88%) of which  $1-0.1 \mu$  range has 12.9%. Since water absorption and mercury intrusion are almost equal, the rock may not have many fine capillaries less than  $0.05 \mu$  radius. Non-normalized pore size distribution shows  $0.05 \mu$  radius most frequent with  $1.1 \mu$  following it as second peak in the curve (Fig. 16) for the range  $0.5 \mu$  and above. Hysteresis (Fig. 22) shows pore throats are predominantly between  $1.1 - 0.05 \mu$  in radius while interior cavities are of varying size more than  $0.1 \mu$  in radius evenly dispersed throughout. It has been observed in this study that rock cores having no major defined dimensions for the interior cavities, as shown by the depressurization curve, retain more mercury after releasing pressure from 2000 - 10 psi. A possible explanation could be that interconnected cavities of uniformly decreasing dimensions opening successively into each other. After the mercury porosimetry, the shining mercury could be observed visually in the Pints core. It retained a substantial percentage of mercury (79.85%) at the end of the test.

Higher mercury intrusion porosity indicates that the Pints core is likely to absorb more bitumen also.

Alden core. The porosity distribution curve (Fig. 5) reveals

<u>Range</u>	<u>Porosity</u>
$21 - 1 \mu$	1.12%
$1 - 0.05 \mu$	8.48%

Thus the core contains more pores having diameter less than  $1 \mu$  (most of the pores are  $1-0.1 \mu$  range as in the case of Pints, comprising 8.29 out of 8.48%). Since water absorption is much less than mercury

intrusion, it seems there are few fine capillaries and also the internal structure might have been disrupted by mercury intrusion to some extent. Such instances have been noted by Dinkle also.<sup>4</sup> As the mercury penetrates the soft stone, it breaks through the pore walls of some pores that originally had no entrance capillaries into them; these pores were completely sealed off by their pore walls. As a result, the mercury intrusion method measures the volume of these once-sealed pores. Alden was observed to be quite soft in drilling operations. The other reason could be chemisorption of mercury, especially in fine pores. Non-normalized pore size distribution curve (Fig. 17) indicates  $0.71 \mu$  as peak pore radius (having maximum pore volume) with  $0.21 \mu$  as the next higher peak. Hysteresis (Fig. 23) shows that predominant pore throats range from  $1-0.05 \mu$ , while most internal cavities have a radius of  $1-3 \mu$ .

Due to greater dimension of the internal cavities, it is expected Alden may absorb much bitumen also.

Linwood core. Referring to the porosity distribution curves, the porosities are:

<u>Range</u>	<u>Porosity</u>
21 - $1 \mu$	0.36%
1 - $0.05 \mu$	0.54%

The porosity is uniformly distributed from  $21-0.2 \mu$ ; it is maximum in the range of  $0.1-0.2 \mu$  (Fig. 6). Since 24 hr soaked porosity is higher than mercury intrusion porosity, it seems the rock core has more fine capillaries having radius less than  $0.05 \mu$ . Non-normalized curve indicates  $0.14 \mu$  as the most frequently occurring pore radius. Pore throats range from  $1.3-0.7 \mu$  and  $0.4-0.05 \mu$  (Fig. 24), whereas internal cavities range in

dimensions (radius) from 1.5-2  $\mu$  and 0.25-0.45, but their extent is not so much as observed in the Alden core.

Though the pore radius having maximum pore volume (0.14  $\mu$ ) is greater than four other cores, the total porosity (both water-soaked and mercury-intrusion) of Linwood core is the least among six cores. Thus it is expected that the Linwood core will absorb less asphalt.

Cook core. The porosity distribution curve (Fig. 7) indicates porosity in the 21-2  $\mu$  range as 1.10% while it goes up and is 16.34% in the 2.0-0.05  $\mu$  range. Water absorption is far less than the mercury intrusion. It seems that mercury has very much disrupted the internal structure by breaking through the pore walls into isolated interstices or cavities. The striking constance of the volume of mercury retained (Fig. 25), despite the fact that pore volumes, and hence surface areas, were of widely differing extent, constitutes strong evidence that chemisorption is insignificant and the retention is a result of ink-bottle pore shapes. The constance of retention, moreover, indicates that ink-bottling occurs primarily in the coarse pores. Cook core retained 90.54% of mercury after depressurizing to 10 psi. The pore radius having maximum pore volume is 0.05  $\mu$  as seen in non-normalized pore size distribution curve (Fig. 19).

Keota core. The pore size distribution curve (Fig. 8) indicates:

<u>Range</u>	<u>Porosity</u>
21 - 1 $\mu$	2.68%
1 - 0.1 $\mu$	0.97%
0.1 - 0.05 $\mu$	1.01%

Mercury intrusion porosity is 4.66% while 24 hr saturated porosity is 7.77% which can imply that Keota core has more fine capillaries of radius less than 0.05  $\mu$ , which can absorb water readily.

The non-normalized pore size distribution curve (Fig. 20) shows  $0.05 \mu$  as the pore radius having maximum pore volume.

In the hysteresis (Fig. 36) the predominant pore throat radii seem to range from  $10 - 0.7 \mu$ , and  $0.1 - 0.05 \mu$ . The internal cavities have  $0.07 - 0.2 \mu$  radius in general.

Due to narrowness of the most frequently occurring cavities and moderate mercury intrusion porosity, it is likely the Keota cores will absorb moderate amounts of asphalt among the cores studied.

The relationship between absorptions determined by various methods and between pore characteristics and absorption have been reported<sup>3,22</sup> elsewhere and will be discussed under "Absorption Studies."

#### Evaluation of Bulk Specific Gravity

Accurate determination of bulk specific gravity of the aggregate is of paramount importance in a number of engineering design applications.

Percent voids is generally used as one of the criteria for the design of bituminous paving mixtures. The exact determination of bulk specific gravity of the various constituents of the paving mixture is a necessary part of the design procedure for determination of void properties of bituminous mixtures. It is also used to estimate percent of asphalt absorption by aggregate, which is the major consideration of projects HR-127 and HR-142. In the design and control of portland cement concrete, bulk specific gravity is used in design calculation of concrete mixtures by the absolute volume concept.

Bulk specific gravity can be defined as the ratio of the weight in air of a given volume of a permeable material (including both permeable and

impermeable voids normal to the material) at a stated temperature to the weight in air of an equal volume of distilled water at a stated temperature. The bulk specific gravity of an aggregate as defined by the ASTM equals the oven-dry weight of the aggregate (A) divided by the sum of the aggregate volume (Vs), the volume of the permeable voids (Vp) and the impermeable voids (Vi), and the unit weight of water ( $\gamma_w$ )

$$\text{bulk specific gravity} = \frac{A}{(V_s + V_p + V_i)\gamma_w}$$

or

$$= \frac{A}{B - C}$$

where B is the saturated surface-dry weight of the material in air, and C is the weight of saturated material in water. Those voids that cannot be filled with water after a 24 hr soaking are referred to as impermeable voids. Voids that can be filled with water after a 24 hr soaking are referred to as permeable.

ASTM Standards C-127 and C-128 outline methods for determining absorption and bulk specific gravity of aggregates. These standards call for immersion of material in water for 24 hr, followed by drying until the surface-dry state is attained. Coarse aggregates are rolled in an absorbent cloth until all visible water films are gone. Some operators judge this condition by observing the shine contributed by water film while others judge by observing a slight color change in the aggregate.

Fine aggregates are spread on a pan and exposed to a gentle current of warm air until a free flowing condition is reached. The aggregate is then lightly tamped into a conical mold. If the cone stands when the mold is

removed, the fine aggregate is assumed to carry moisture on its surface and it is dried further. When the cone just begins to slump upon removal of the cone, it is assumed to be in a saturated surface-dry state.

For natural, well graded fine aggregates, the saturated surface-dry condition is usually reproducible. However, the end point is more erratic for crushed fine aggregates because the angularity of the particles does not permit a definite slump condition as do the rounded surfaces of natural sands. Besides this, the higher percentage of material passing the #100 sieve also poses a problem in achieving slump condition.

Various attempts have been made in the past to pinpoint the saturated surface-dry condition of the aggregates to improve the reproducibility of the bulk specific gravity test results. These include Howard's glass jar method<sup>23,24</sup> Martin's wet and dry bulb temperature method,<sup>25</sup> Saxer's absorption time curve procedure<sup>26</sup> and Hughes' and Bahramian's saturated air drying method.<sup>27</sup> However, the various modifications either offer little improvement or are too elaborate to be practical in the field or average laboratory.

During the first year of Project HR-142, a special study was conducted to develop new, simple, and more reproducible methods to determine the bulk specific gravity or the saturated surface-dry condition for granular materials. As a result, a new chemical indicator method was developed to determine the saturated surface-dry condition, and a glass mercury pycnometer was designed to determine bulk specific gravity of aggregates larger than the #100 sieve size. Preliminary work on the mercury pycnometer is described in Appendix C.

In the chemical indicator study, the bulk specific gravity of crushed aggregates and cylindrical rock cores from the six HR-142 limestone quarries,

one crushed trap rock, and one synthetic aggregate (Synopal) from Denmark, was determined by five methods. The methods are standard ASTM, geometrical measurement, mercury displacement, and two chemical indicator methods (cobalt chloride and fluorescein di-sodium salt) developed at the Iowa State University Bituminous Research Laboratory. The chemical methods are described in Appendix B. The detailed work on the chemical indicator method is reported elsewhere.<sup>28</sup> The general conclusions of the study were:

- The ASTM standard tests underestimate the bulk specific gravity of aggregates, as these tests measure adsorption as well as absorption of particles. Results obtained in determining bulk specific gravity by other methods such as the mercury displacement method, the geometrical mensuration method, and the chemical methods appear to confirm this statement.
- Experiments on rock cores indicate that the mercury displacement method gives realistic values between those obtained from the ASTM standard method and the geometrical mensuration method. Further investigations are needed in order to have a properly specified pressure at which measurements of volume displaced by mercury should be taken for consistent results with all aggregates.
- Chemical methods eliminate the human element to a great extent in observing the saturated surface-dry condition of the aggregates since color change is quite apparent.
- Attainment of saturated surface-dry condition by the chemical method is not affected by the surface character, particle shape, or gradation of the particles.
- Results of chemical methods agree well with those obtained from the mercury displacement method.

- On the basis of the data in this study and the relative cost of each chemical method, the cobalt chloride method appears to be the more preferable of the two chemical methods investigated. However, fluorescein di-sodium salt is better suited when dealing with dark-colored aggregates.
- Data in this limited study seem to indicate that most duplicate determinations check within 0.01 reliability in the case of the chemical method as compared to 0.02 reliability specified in the ASTM standard test.
- Additional work is needed in order to establish the reproducibility of the chemical indicator methods.

A third method for determination of bulk specific gravity and water absorption was developed during absorption-time studies. The procedure and results of this method will be discussed in the next section.



## ABSORPTION STUDIES

Methods and Procedures

Many investigators have attempted to evaluate aggregate absorption with kerosene and have applied suitable corrections for the amount of asphalt absorbed by aggregates in mixture design. Hveem<sup>29</sup> devised the Centrifuge Kerosene Equivalent test (CKE) in 1942. The CKE measures the quantity of kerosene absorbed by 100 g of aggregate under specified conditions of soaking and centrifuging, shown to be a function of the surface area and absorptive capacity of the aggregate, and has been used as a part of the design of bituminous mixtures by Hveem's method. Lohn<sup>21</sup> adopted similar procedure with some modifications in soaking and centrifuging time and was able to correlate bitumen absorption of an aggregate with kerosene absorption. Donaldson et al.<sup>30</sup> proposed modifying the Hveem CKE method by increasing soaking time to 30 min and by testing a non-absorptive aggregate of the same gradation as the aggregate in question for purposes of comparison. Since kerosene has wetting properties similar to asphalt, it has been believed to be a better representative absorption agent than water.<sup>31</sup> Oils have also been used by some investigators<sup>29,32</sup> to evaluate the absorptive capacity of coarse aggregates.

In 1942, Goshorn and Williams<sup>33</sup> developed an immersion method in which the coarse aggregate is immersed in a tarred wire basket in asphalt at 275°F for 3 hr. The basket is removed from the asphalt and suspended in an oven for 10 min to drain off excess asphalt. The basket with coated aggregate is cooled to room temperature and weighed in air and in water at 77°F. The percent asphalt absorbed is calculated by the procedure described by Goshorn and Williams, based on straightforward volume-weight relationships of aggregate,

asphalt and effective volume of coated aggregate.

Since the aggregate is in contact with an unlimited supply of asphalt at relatively low viscosity for extended periods of time, the absorption is much higher than would be expected in a bituminous mixture. However, the values can definitely be taken as the absorptive potentials of aggregates used for bituminous mixtures.<sup>30</sup> Accuracy of this test is limited by homogeneity of the aggregate and accuracy of the bulk specific gravity and

Rice<sup>34</sup> proposed a procedure to determine the maximum specific gravity of the mixture by using volumetric flasks. The absorption of asphalt by aggregate in a mixture can be calculated if the maximum specific gravity of the mixture (after Rice's method), the asphalt content, and the bulk specific gravity of the aggregate used in the mixture are known.

One serious limitation of this method is that aggregate particles must be thoroughly coated; failure to do this may give erratic data because of possible water absorption during saturation. However, in this method, results can be obtained from actual mixtures.

The US Corps of Engineers<sup>35</sup> developed and used bulk-impregnated specific gravity in the design and control of bituminous paving mixtures. The bulk-impregnated specific gravity ( $G_{bi}$ ) can be defined as the ratio of the weight in air of a given volume of a permeable aggregate (including solids, impermeable pores, and pores normally permeable to water but which are variably permeable to bitumen) at a stated temperature ( $77^{\circ}\text{F}$ ) to the weight of an equal volume of water ( $V_t$ ) minus the weight of the volume of bitumen ( $V_b$ ) absorbed by pores permeable to it. In the CGS system, the bulk-impregnated specific gravity,  $G_{bi}$ , is the ratio of the weight of the aggregate to the volume of the aggregate including solids, impermeable internal pores, and bitumen impermeable pores.

Table 10. Bulk specific gravity and water absorption of quarry-crushed aggregate and cores

Quarry	Aggregate #	Bulk specific gravity (ATM)	Water absorption, %
Menlo	1-S-B	2.567	1.93
	1-L-A	2.613	1.18
	1-L-B	2.603	1.40
	Core	2.637	0.90
Pints	2-A	2.348	6.56
	2-B	2.348	7.31
	Core	2.271	7.22
Alden	3-S-B	2.475	2.97
	3-L-A	2.517	1.94
	3-L-B	2.508	2.31
	Core	2.510	1.72
Linwood	4-A	2.613	1.42
	4-B	2.582	1.66
	Core	2.636	0.90
Cook	5-S-B	2.397	5.98
	5-L-A	2.426	4.26
	5-L-B	2.408	5.40
	Core	2.465	3.88
Keota	6-A	2.326	5.58
	6-B	2.303	7.51
	Core	2.489	3.12

Thus, when an aggregate absorbs no bitumen, its bulk-impregnated specific gravity,  $G_{bi}$ , equals bulk specific gravity,  $G_b$ ; on the other hand, if absorbed bitumen is equal to water absorption, its  $G_{bi}$  is equal to the apparent specific gravity,  $G_a$ . Therefore,  $G_a = G_{bi} - G_b$ . Thus, bulk-impregnated specific gravity is a function of the ratio of bitumen to water absorption, which varies widely but follows a definite pattern with different types of aggregate. This is suitable for general use with all aggregates used in bituminous mixtures and is particularly suited for use with porous aggregates.

McLeod<sup>36</sup> has recommended the use of this method to determine the maximum, or upper limit, absorption for aggregate. Lee<sup>37</sup> compared the data with those obtained by other methods and concluded that these absorption values were by no means the absolute maximum absorption values for a particular aggregate, but can be looked upon as the "realistic" maximum absorption values aggregates will have in bituminous mixtures.

Absorption capacity of aggregates can also be determined by colorimetric analysis with photometer, using either asphalt solution or dye solution and calibration curves.<sup>37</sup>

In this investigation, aggregate absorption has been evaluated with respect to water, CKE and oil, asphalt (Rice method, bulk-impregnated specific gravity method, and immersion method), and dyes (photometer method). Factors studied included asphalt type, aggregate type, temperature, and time.

In the following sections, the results of these studies will be presented. The techniques and methods used will be briefly described. Detailed procedures will be referred to specific references or given in Appendix D.

### Water Absorption

Several series of bulk specific gravity and water absorption tests were conducted on fractioned quarry crushed, cores and laboratory crushed block samples at various stages of this investigation. Because of the inherent unhomogeneity of the material (even among cores from block samples) and the weaknesses of the standard specific gravity and water absorption tests, the results of different series of tests were not always comparable. Table 10 represents the results of specific gravity and absorption of quarry crushed, laboratory separated coarse fractions, and 1/2 in. rock cores from one of the two block samples for each quarry during early stages of this project. Table 11 gives the results of specific gravity and water absorption of laboratory crushed and separated aggregates made during the latter part of this investigation. Most calculations used in asphalt absorption reported in this section and chemical treatment studies reported later were based on values from this table (or weighed average for graded aggregates). Values in Table 10 were used for correlation studies.

In order to investigate the nature and rate of water absorption by aggregates, two series of time-absorption studies were made. One series was made on 1 in. core samples and the other series was made on laboratory crushed 3/8 in. to #4 sieve fractions. In these tests, oven-dried samples (about 100-120 g) were weighed on a single-pan, direct reading analytical balance with special attachment in air and water (at 25°C) after immersion time of 1/2, 1, 3, 5, 10, 20, 30, 60 min and 2, 4, 8, 12, 24 hr (some to 96 hr). At the end of the last weighing in water, samples were surface-dried and weighed in air. Apparent and bulk specific gravities and water absorption were calculated and tabulated in Table 12a for rock cores and in

Table 12b for crushed 3/8 in. samples. Time-absorption curves of core sample are shown in Figs. 27a to 27b. Weight in water vs time curves of these core samples were plotted in Figs. 28a to 28d. Similar plots for +~~7~~4 sieve fractions.

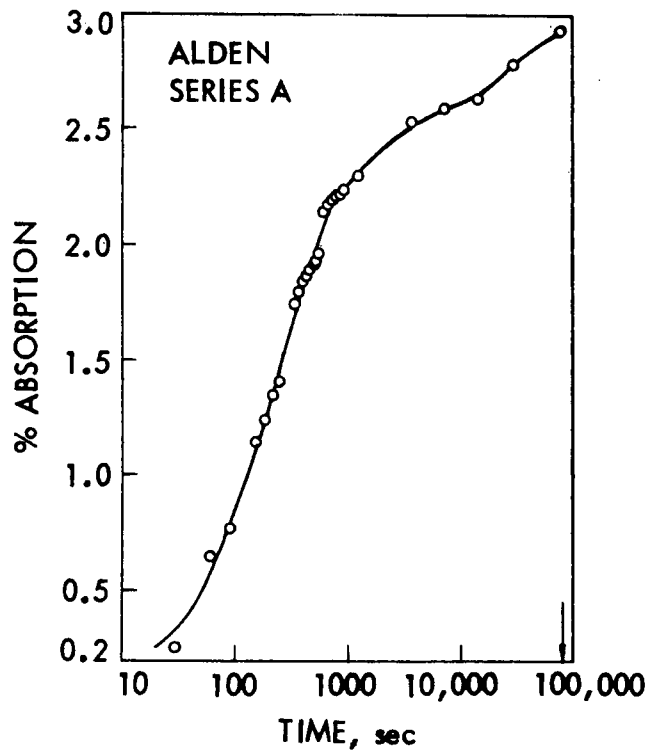


Fig. 27a. Time-water absorption curves of cores, Alden

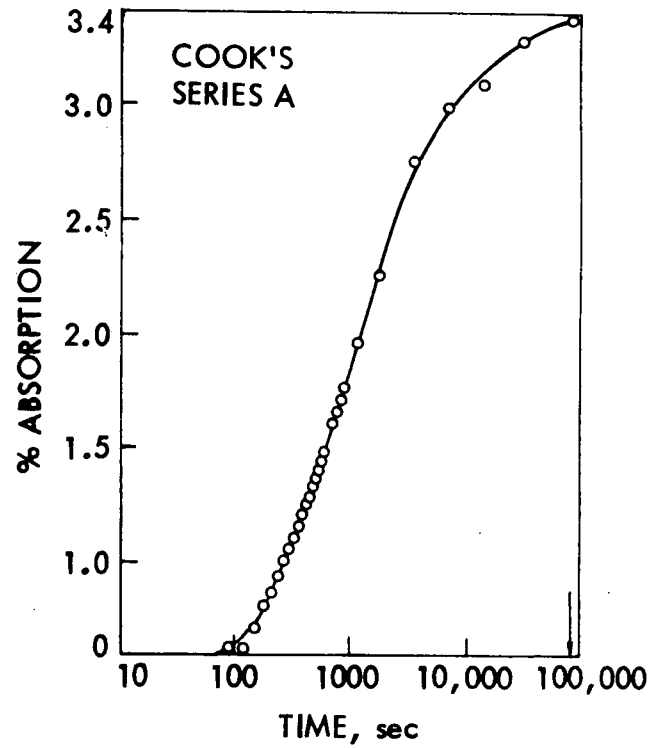


Fig. 27b. Time-water absorption curve of cores, Cook

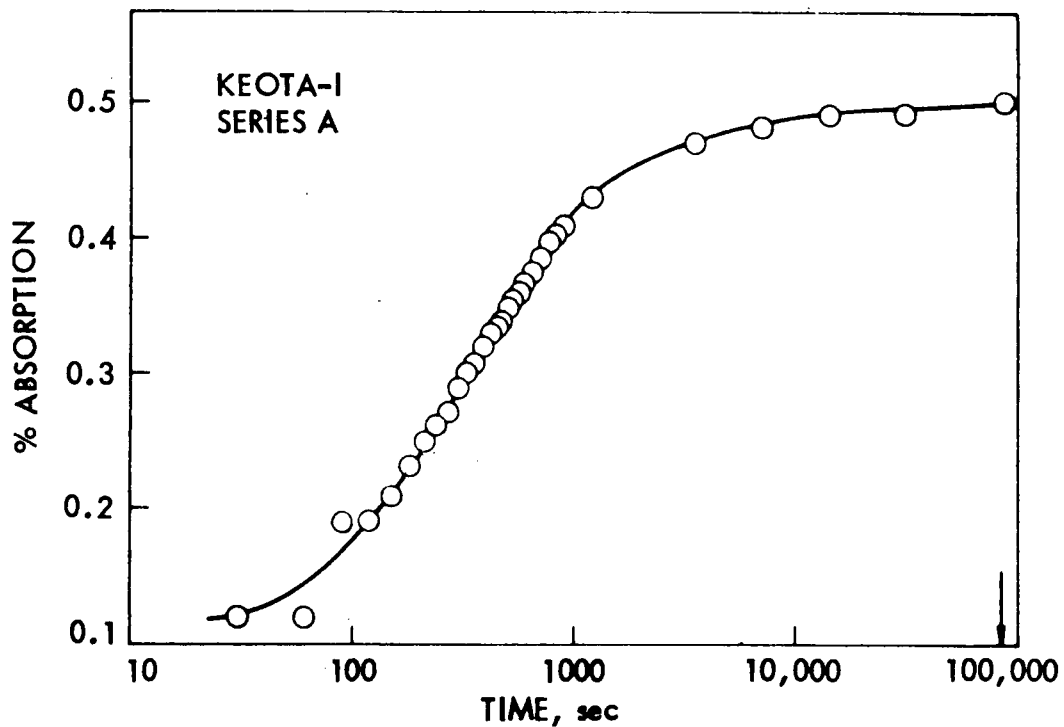


Fig. 27c. Time-water absorption curve of cores, Keota I

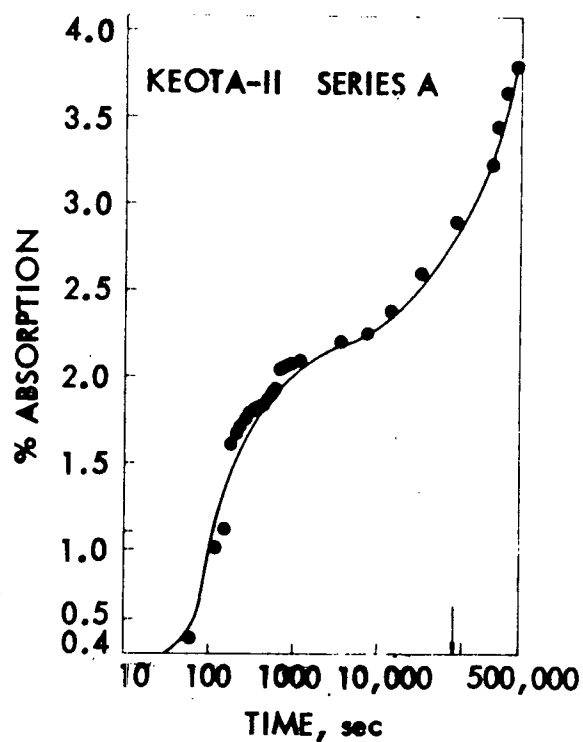


Fig. 27d. Time-water absorption curve of cores, Keota II

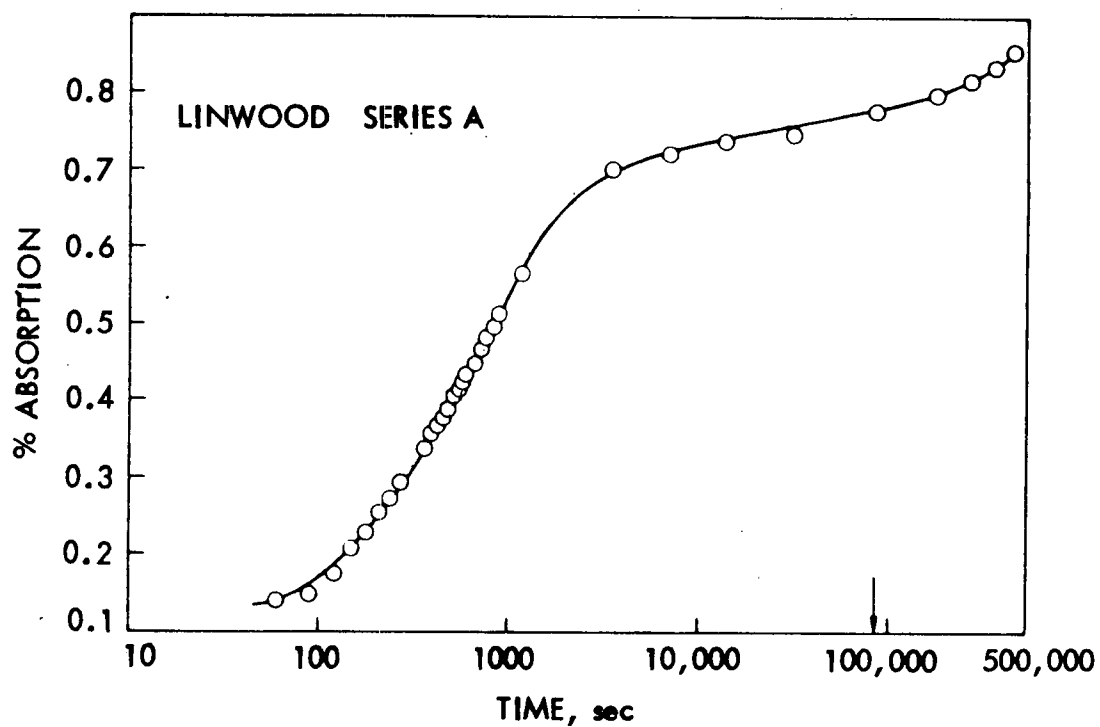


Fig. 27e. Time-water absorption curve of cores, Linwood



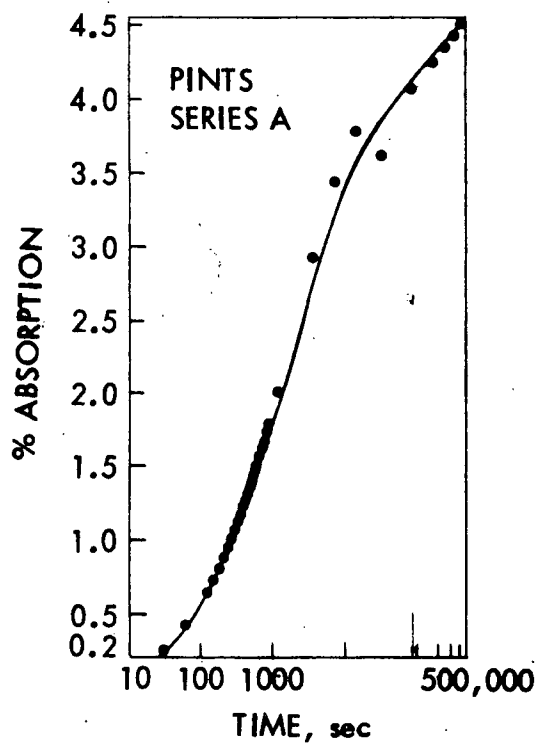


Fig. 27f. Time-water absorption curve of cores, Menlo

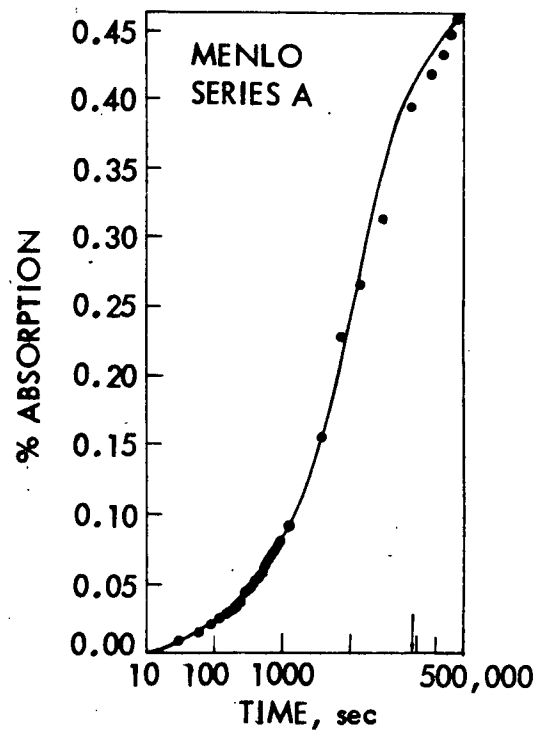


Fig. 27g. Time-water absorption curve of cores, Pints

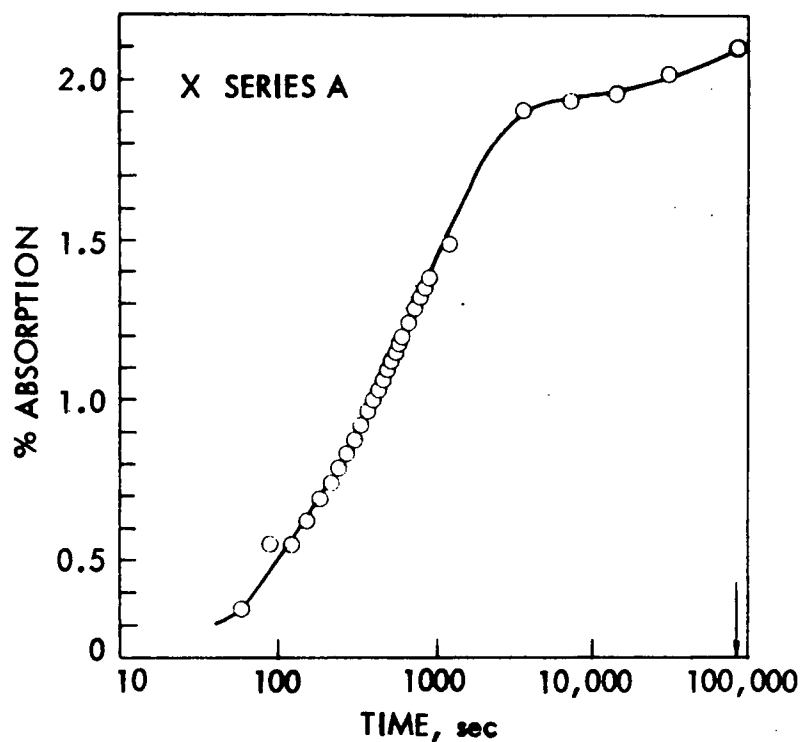


Fig. 27h. Time-water absorption curve of cores, X (Alden II)

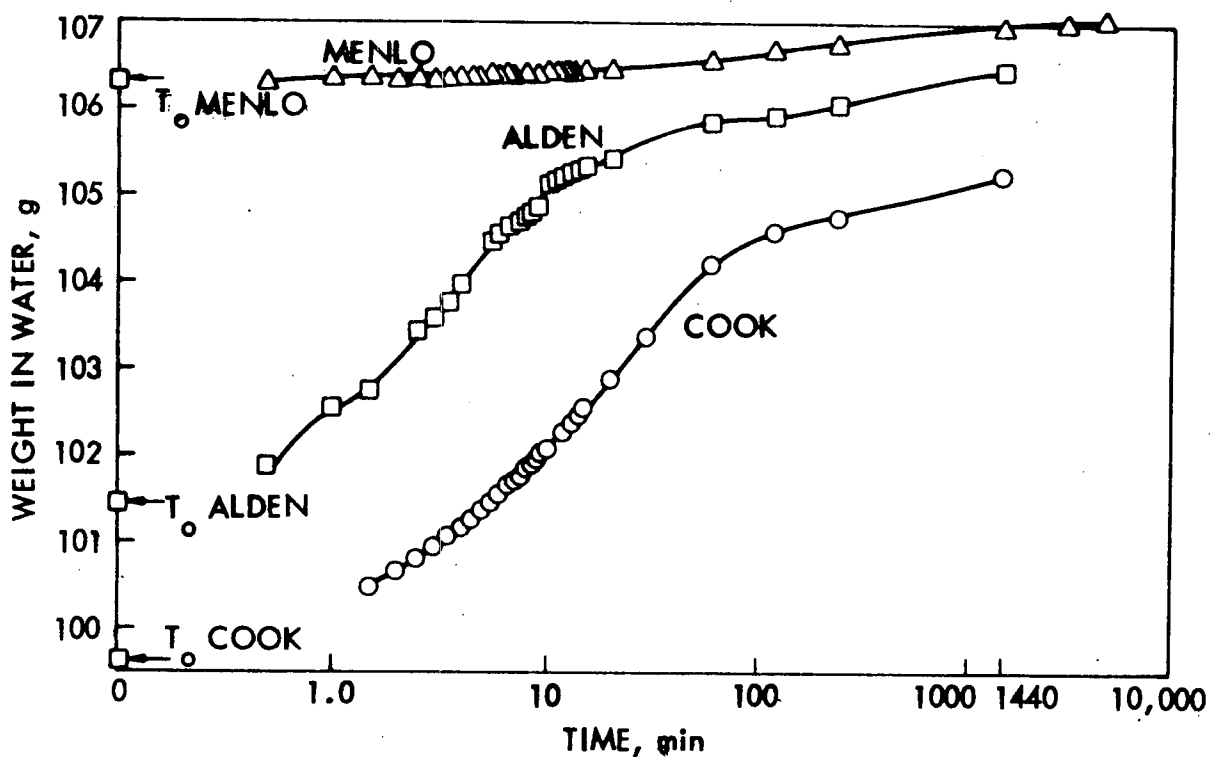


Fig. 28a. Time-weight in water curves of cores, A, C, and M limestones

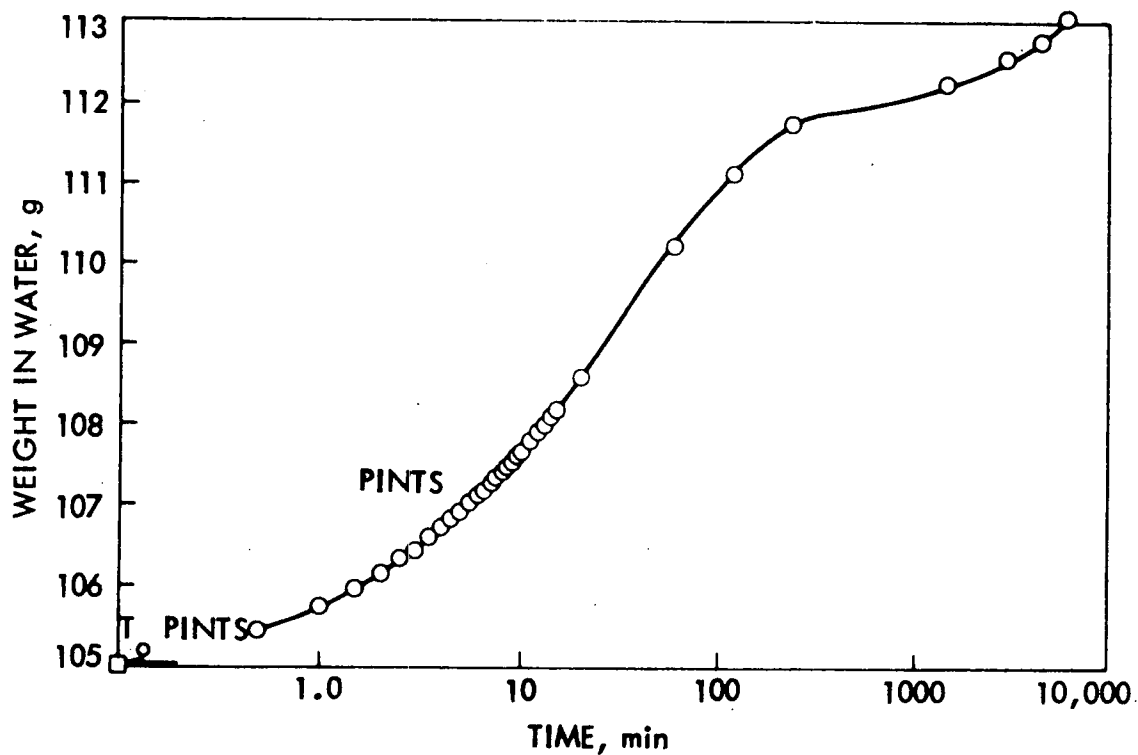


Fig. 28b. Time-weight in water curves of cores, Pints

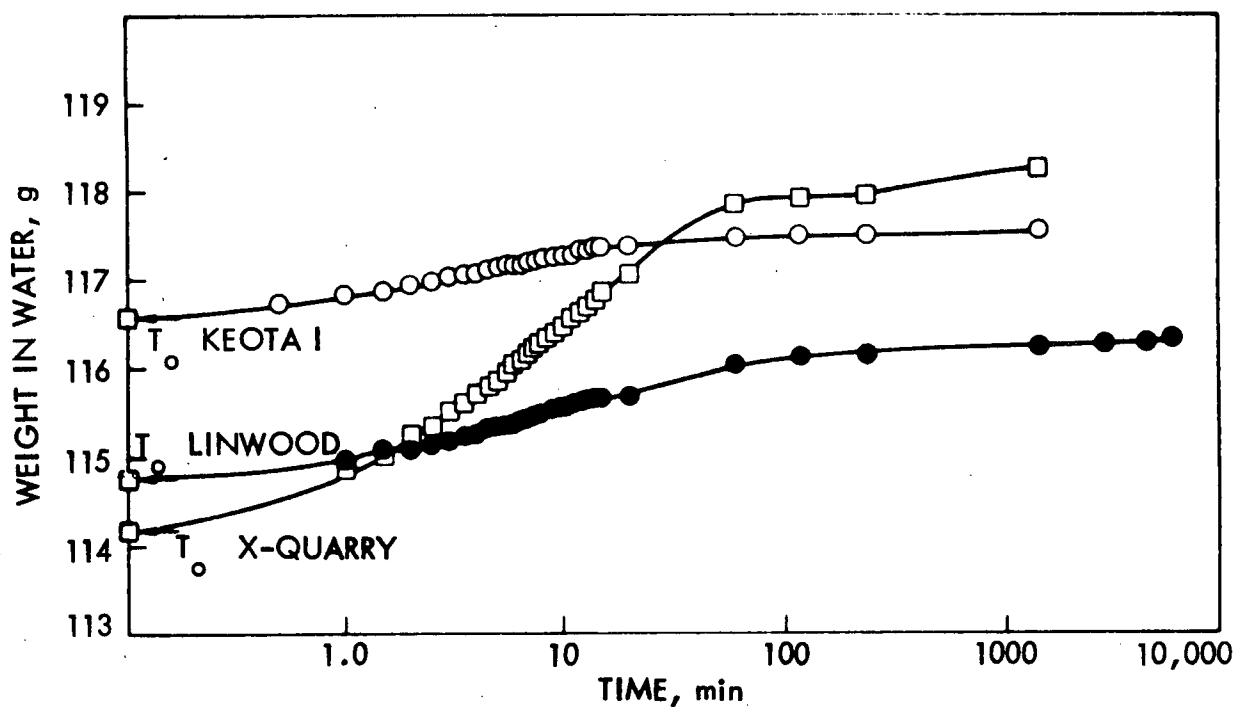


Fig. 28c. Time-weight in water curves of cores, K 1, L and X (A II)

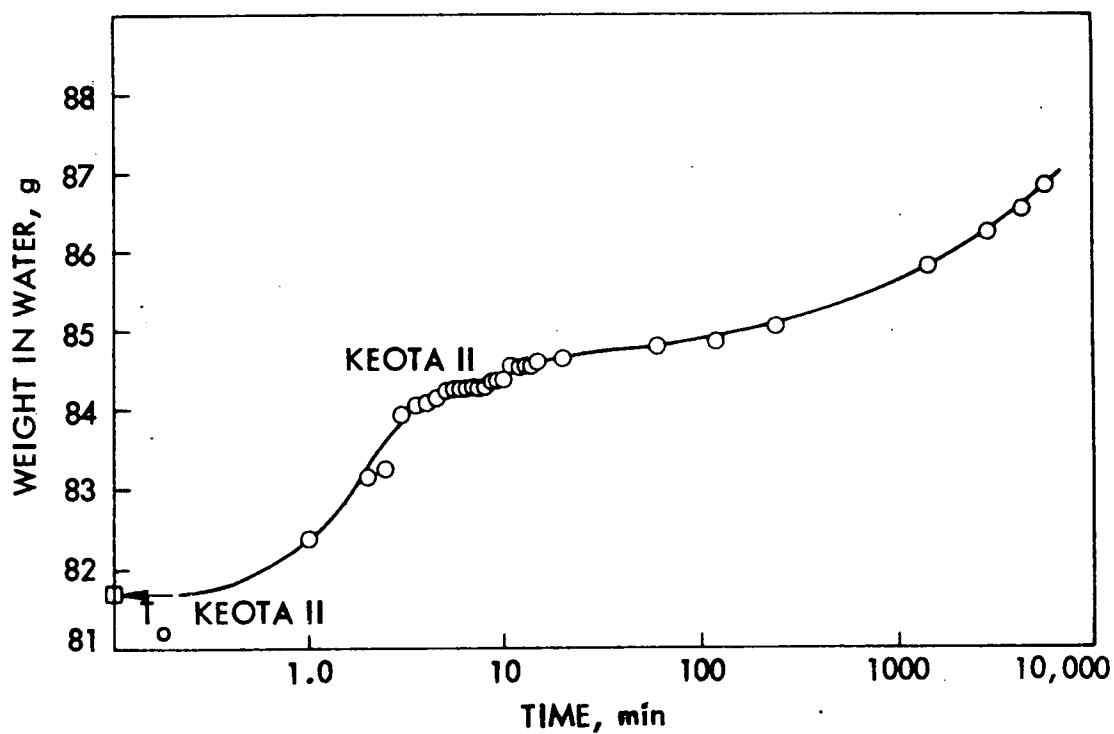


Fig. 28d. Time-weight in water curves of cores, Keota II

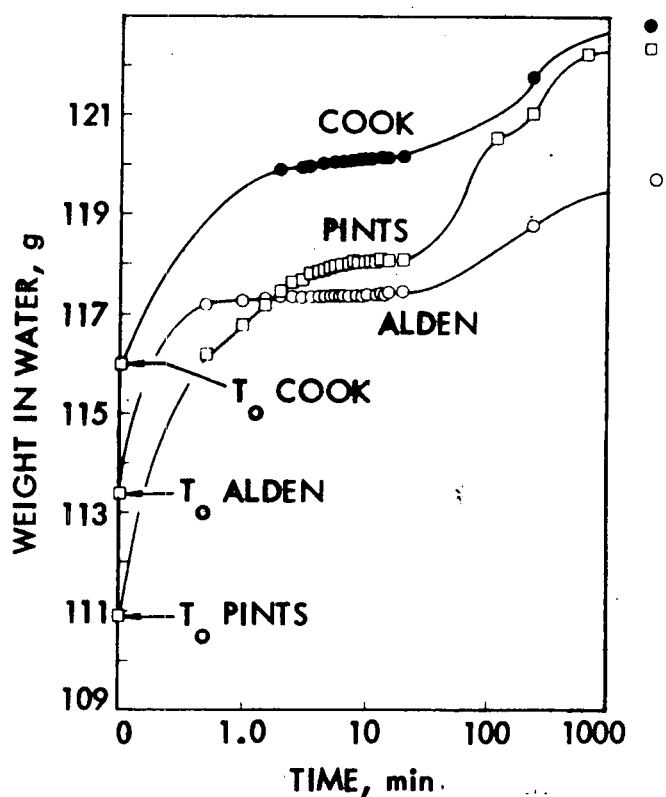


Fig. 28e. Time-weight in water curves of + 3/8 in fractions, A, C, and P

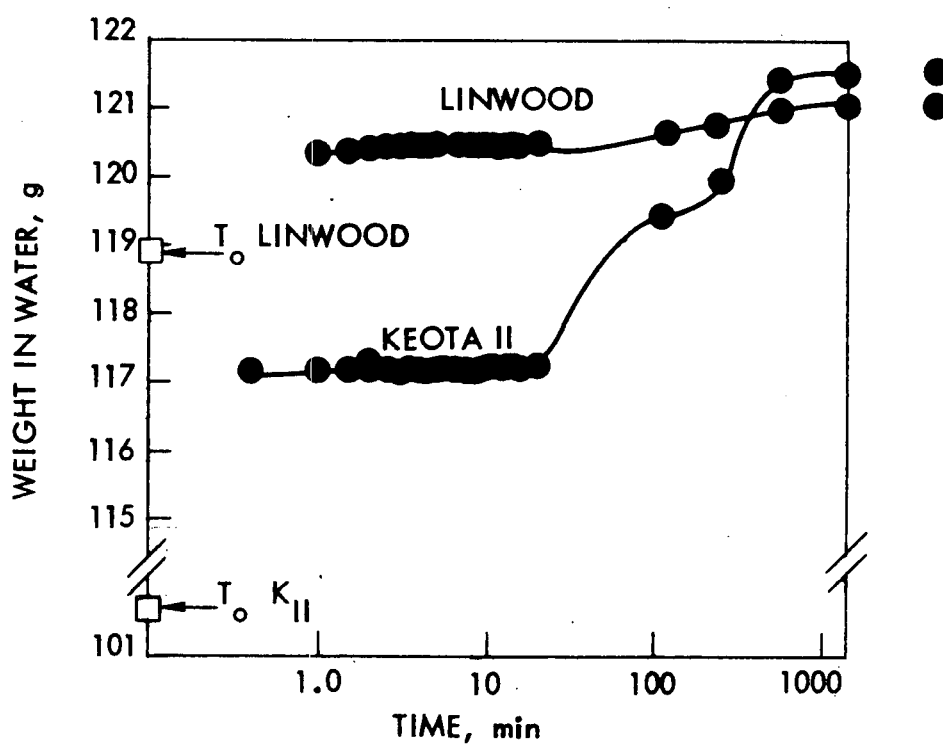


Fig. 28f. Time-weight in water curves of + 3/8 in fractions, K II and L

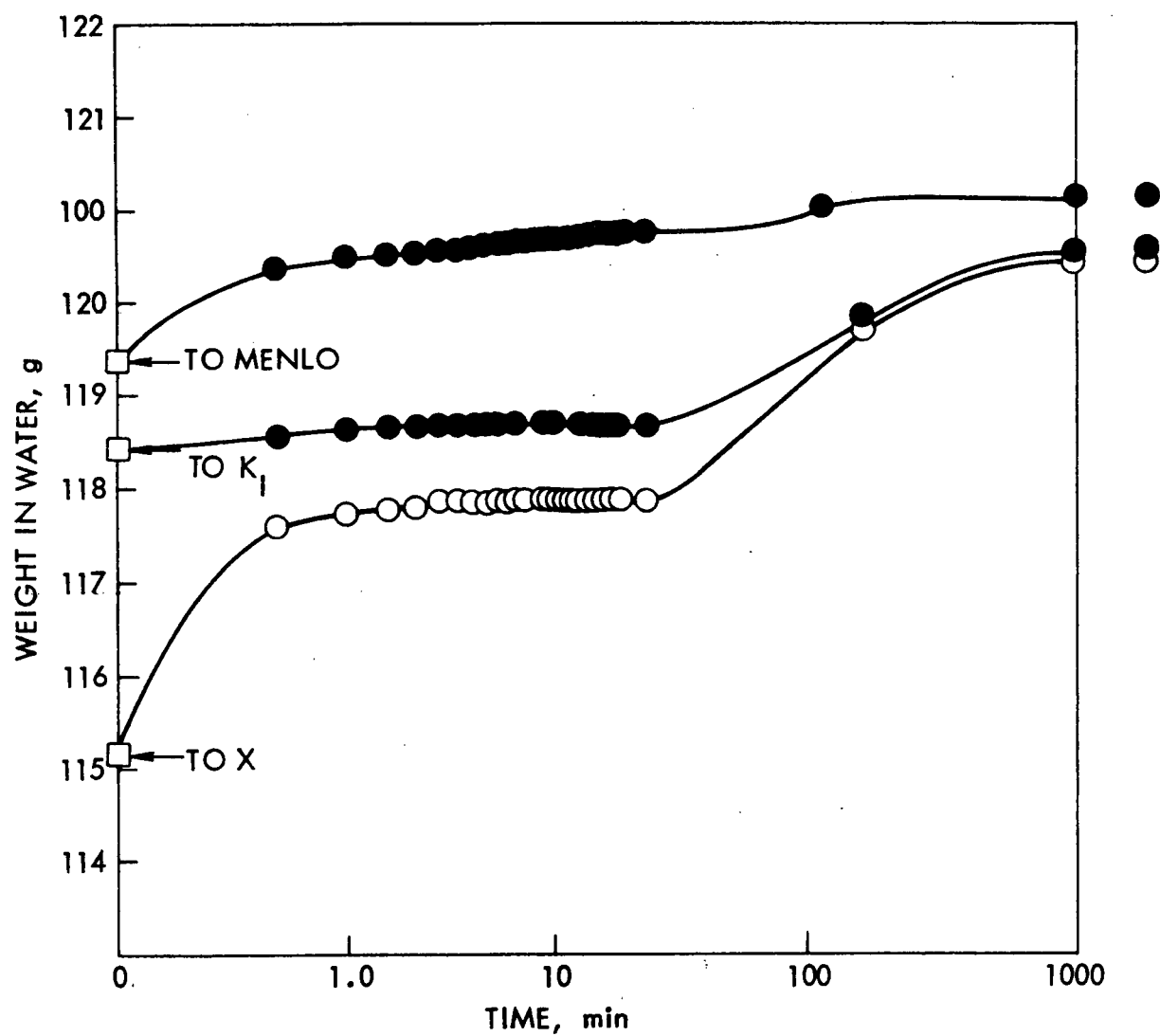


Fig. 28g. Time-weight in water curves of + 3/8 in fractions, K I, M and X

Table 11. Bulk specific gravity and absorption of crushed block

Size fraction	Alden	Cook	Keota I	Keota II	Linwood	Menlo	Pints	X-Quarry
<u>Bulk specific gravity (ASTM)</u>								
1/2	2.439	2.457	2.305	1.984	2.6081	2.617	2.320	2.430
3/8	2.433	2.456	2.405	1.985	2.611	2.620	2.320	2.426
4	2.404	2.449	2.493	1.990	2.599	2.618	2.297	2.415
8	2.383	2.368	2.479	1.996	2.575	2.585	2.237	2.344
8 → 100	2.546	2.556	2.619	2.430	2.620	2.586	2.620	2.548
<u>Water Absorption, %</u>								
1/2	2.71	3.99	6.12	12.60	1.17	0.84	6.44	3.10
3/8	2.92	4.19	5.51	13.00	1.24	0.94	6.80	3.28
4	3.64	4.83	3.52	13.80	1.49	1.35	7.57	3.70
8	4.58	6.86	3.56	14.73	1.98	1.87	9.39	5.55
8 → 100	1.69	3.49	1.36	4.33	1.47	1.70	2.78	2.02

Table 12a. Water absorption of cores

	<u>Specific gravity<sup>a</sup></u>		<u>Absorption, %</u>	
	Ga	Gb	ASTM	Graphical <sup>c</sup>
Cook	2.708	2.450	3.88	3.38
Alden	2.576	2.447	2.78	2.90
KI	2.689	2.652	0.51	0.50
Pints	2.713	2.398	4.83	4.07
Linwood	2.787	2.589	0.81	0.78
KII	2.704	1.973	11.85	2.92
Menlo	2.701	2.638	0.46	0.39

<sup>a</sup>Ga = Apparent specific gravity

Gb = Bulk specific gravity

<sup>b</sup>Correlation coefficient (r) = 0.6183

Table 12b. Water absorption of crushed block samples<sup>a</sup>

	<u>Specific gravity<sup>b</sup></u>		<u>Absorption, %</u>	
	Ga	Gb	ASTM	Graphical <sup>c</sup>
Cook	4.72	2.19	2.769	2.449
Alden	2.91	1.78	2.641	2.443
KI	1.64	1.57	2.695	2.405
X	3.26	2.17	2.646	2.426
Pints	6.89	4.67	2.773	2.275
Linwood	1.45	0.61	2.697	2.596
KII	13.77	3.05	2.741	1.990
Menlo	1.05	0.55	2.704	2.620

<sup>a</sup>3/8" to #4 sieve

<sup>b</sup>Ga = Apparent specific Gravity

Gb = Bulk specific Gravity

<sup>c</sup>Correlation Coef. (r) = 0.6768

Some interesting and perhaps significant observations can be made from these curves:

- Only one out of eight limestones (Keota 1) reached equilibrium saturation at 24 hr (1440 min or 86,400 sec) which is the basis for ASTM specific gravity and absorption determinations. Two other core samples (Menlo and Linwood) can be considered having reached saturation due to insignificant amount of change and low total absorption. All the other cores (especially highly absorptive Keota II and Pints) continued to increase absorption beyond 24 hr.
- When plotted on a semi-logarithmic scale, the first part of the time-absorption curves all take shapes of an "S". Depending on pore-size distribution, the steep portion of the curve occurs somewhere between 100-10,000 sec.
- For certain aggregates, there is a second rapid increase in absorption with respect to time (Keota II and Pints) beyond 100,000 sec immersion.
- From the weight-in-water vs time plot (Figs. 28), one can determine specific gravity and absorption following ASTM definitions and equations for coarse aggregates, if oven dry weight of the sample (A) is known, and if the weight of the sample in water at time zero (Co) can be accurately extrapolated. The equations for specific gravity and absorption will be

$$\text{Apparent specific gravity (Ga)} = \frac{A}{A - C}$$

$$\text{Bulk specific gravity (Gb)} = \frac{A}{A - Co}$$

$$\text{Absorption, \%} = \frac{C - Co}{A} \times 100$$



where

A = oven-dry weight of sample in air, g

C = water of sample in water after 24 hr immersion, g

Co = water of sample in water at zero time, gm

(from weight-in-water vs time plot)

Bulk specific gravity and absorption can be determined this way without trying to achieve the saturated-surface dry condition of the aggregate, of which, for certain material, the reproducibility can be very poor. The difficulty of this method is, of course, the accurate determination of Co. This difficulty can be overcome with more sophisticated electronic digit print-out balances such as Mettler PE series balance, with a BE control unit which can be hooked up to a printer, paper tape punch, a card punch or a recorder, or an Ainsworth digimetric weighing system Model 30D or 30DT with Model DP-6 data printer.

Absorption of cores and 3/8 in. laboratory crushed samples were determined by this method. The results, together with those of the ASTM method, are given in Table 12. The results were reasonably close for core samples, but very poor for crushed and highly absorptive samples (Keota II). The discrepancies were mainly from Co extrapolation and entrapped air in crushed aggregate samples; both sources of error can be reduced by further refinement of instrument and procedure.

#### Kerosene and Oil Absorption

In this investigation, a modified CKE method<sup>38,39,40</sup> was used to determine both the specific surface and the kerosene absorption of aggregates. The revised method provides a procedure for predetermining the asphalt content

of a bituminous mixture by obtaining independently the surface area and absorption of a composite aggregate sample. This method involves first determining the specific surface (sq ft/lb) of the aggregate by wetting with kerosene (without soaking) and determining the absorption by soaking in kerosene for ten minutes. Centrifuge conditions for both determinations are 2 min @ 400 g. The standard California method<sup>38</sup> was followed for oil absorption by aggregates.

Both CKE and oil absorption were determined for several times at various stages of this investigation by different individuals on fractioned samples. The repeatability of these tests (especially CKE) were very poor. Slight variation in the interpretation of the procedure will result in large discrepancies. In addition, there was some difficulty in getting even reasonably close results on minus No. 100 sieve fractions. This could be the contributing factor in the poor correlation between kerosen-asphalt and oil-asphalt absorption reported by another investigation.<sup>37</sup> Results of one of such CKE determinations are given in Tables 13 and 14.

Limited studies on time-absorption and viscosity-absorption relationships were conducted. The results of these are given in Table 15 and plotted in Figs. 29 and 30. The ratios of oil absorption between Pints and Menlo aggregates at 5 cP (300°F) was 2.7, whereas at 82 cP (68°F), it was 2.0; the absorption ratio at 5 min absorption was 2.0, and at 1440 min, absorption was 2.7.

Table 13. Results of CKE (HR-142)

Quarry	Sample <sup>a</sup>	Quarry crushed (QC) <sup>b</sup>		Lab crushed (LC) <sup>c</sup>	
		Surface area (sq ft/lb)	Absorption (g/100 g)	Surface area (sq ft/lb)	Absorption (g/100 g)
Menlo	1-S-C	40.3	0.26	34.9	0.16
	1-S-D1	292.3	6.06	233.5	5.39
Pints	2-L-C	98.2	0.62	87.6	0.71
	2-L-D1	192.7	9.20	184.6	8.91
Alden	3-L-C	57.0	0.15	54.4	0.23
	3-L-D1	125.3	5.01	129.0	5.08
Linwood	4-L-C	35.0	0.32	36.0	0.20
	4-L-D1	264.5	5.43	244.0	4.34
Cook	5-S-C	79.5	0.72	68.0	0.73
	5-S-D1	236.6	7.19	173.3	6.88
Keota	6-L-C	52.8	0.19	63.0	0.24
	6-L-D1	179.0	2.40	201.0	3.09

<sup>a</sup>Size fraction designations:  
 A: -3/4 in. - +3/8 in.  
 B: -3/8 in. - +1/4  
 C: -1/4 - +100  
 D: -100  
 D1: -100 - +200

<sup>b</sup>Duplicate samples

<sup>c</sup>Correlation coefficient  $r$  between QC and LC = 0.8864, significant at 5% level

Table 14. Results of oil absorption (HR-142)

Quarry	Sample <sup>a</sup>	Quarry crushed (QC) <sup>b</sup>	Lab crushed (LC) <sup>c</sup>
		g/100 g	g/100 g
Menlo	1-L-B	2.68	2.63
Pints	2-L-B	4.97	4.71
Alden	3-L-B	3.07	4.02
Linwood	4-L-B	3.21	3.24
Cook	5-L-B	5.90	5.65
Keota	6-L-B	5.96	6.07

<sup>a</sup>Size designations:  
 A: -3/4 in. - +3/8 in.  
 A1: +1/2 in. (-3/4 in. - +1/2 in.)  
 A2: +3/8 in. (-1/2 in. - +3/8 in.)  
 B: +1/4 (-3/8 in. - +1/4)

<sup>b</sup>Average of duplicate determinations  
<sup>c</sup>Correlation coefficient  $r$  between  
 QC and LC = 0.9551, significant  
 at 1% level

Table 15. Oil absorption vs time and temperature

Aggregate <sup>a</sup>	Oil temp., °F <sup>b</sup>	Soaking time, min	Oil absorption, % <sup>c</sup>
A	68	5	5.19
C	68	5	4.63
KI	68	5	3.30
KII	68	5	12.50
L	68	5	2.96
M	68	5	2.81
P	68	5	5.63
X	68	5	4.65
A	300	5	4.63
C	300	5	4.55
KI	300	5	5.32
KII	300	5	17.52
L	300	5	2.93
M	300	5	2.55
P	300	5	6.90
X	300	5	4.66
M	68	10	3.02
		60	3.58
		240	3.03
		1440	3.16
P	68	10	6.07
		60	7.39
		240	8.16
		1440	8.67

<sup>a</sup>Laboratory crushed, passing 3/8 in., retained on #4

<sup>b</sup>SAE #10

<sup>c</sup>Duplicate determinations

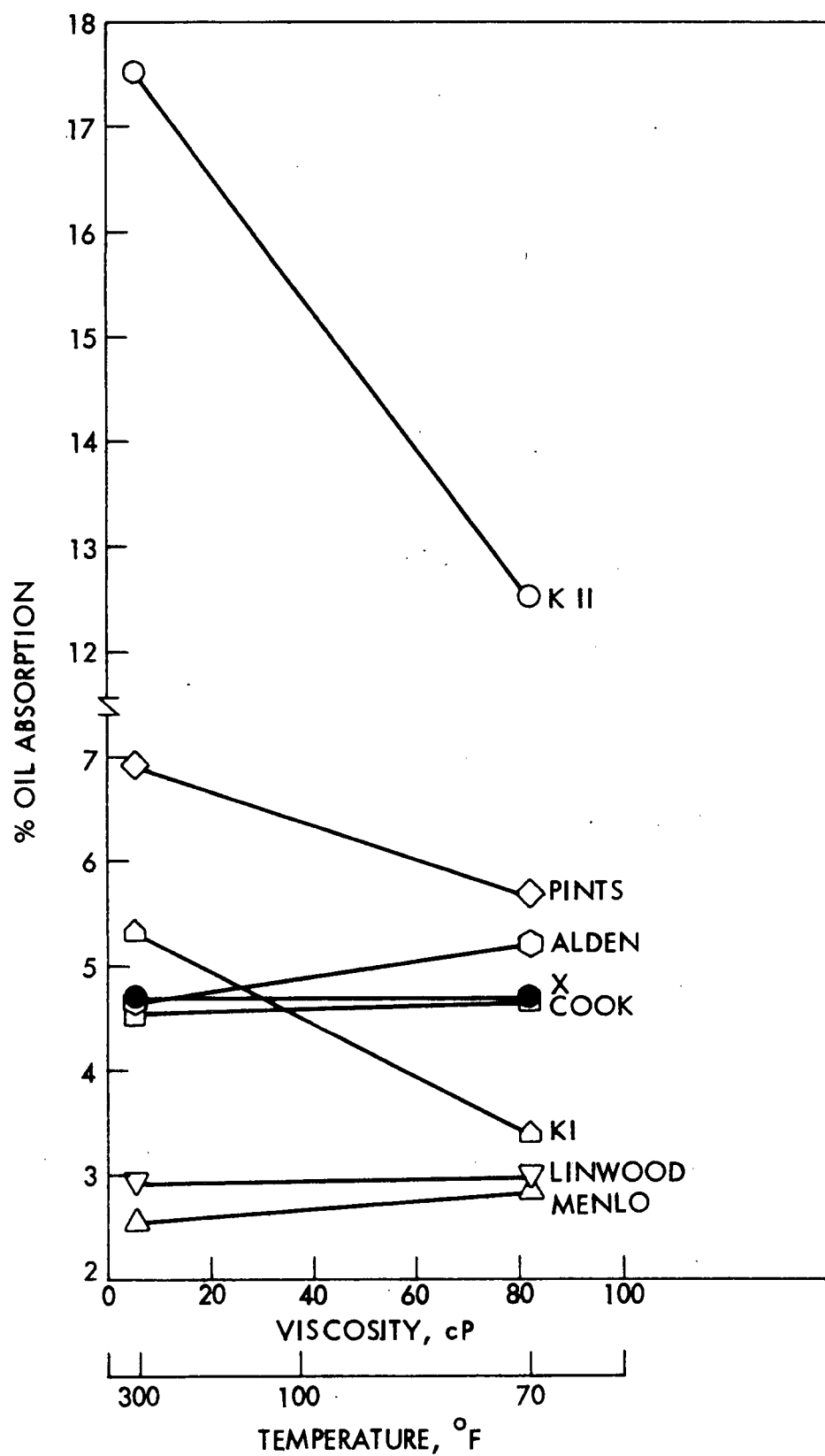


Fig. 29. Relations between oil absorption and oil viscosity, + #4 fractions

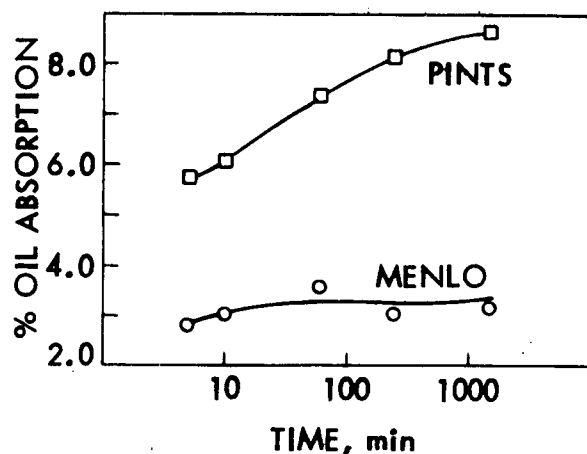


Fig. 30. Relations between oil absorption and soaking time, + #4 fractions

#### Dye Absorption

The use of photo-colorimeter in measurement of aggregate absorption capacity was first suggested by Lee.<sup>37</sup>

The basic principle in colorimetry is that the amount of light absorbed by a given species in solution is proportional to the intensity of the incident light and to the concentration of the absorbing species in the path of the light beam.

For a specific substance, a given wavelength, and a constant length of the light path through the sample (standard sample cell), the ratio between the intensity,  $P$ , of a beam of monochromatic light transmitted through a solution and the intensity of the beam,  $P_o$ , transmitted through the solvent is a function of the concentration of the solution,  $c$ . This relationship, the Lambert-Beer law, can be expressed

$$\text{Log} = \frac{P_o}{P} = kc$$

or

$$\text{Log} = \frac{1}{P/P_o} = kc$$

where  $\log P_o/P$  is defined as the absorbance of the sample and  $P/P_o$ , the transmittance of the sample. For substances that follow this law, it is obvious that the absorbance or the logarithms of the reciprocals of the transmittance is a linear function of concentration  $c$ . The Nefluoro-Photometer used in this investigation was calibrated to read directly the logarithmic value  $\log \frac{1}{P/P_o} \times 100$ .

When a specific amount of aggregate is shaken and soaked in a specific amount of asphalt solution of known concentration, the reduction in asphalt concentration due to absorption of the asphalt by the aggregate results in a change in the light transmittance of the solution. The concentration change, thus the asphalt absorbed or adsorbed, can be easily and quantitatively determined by the colorimetric analysis with a concentration-log absorption calibration curve.

Factors involved in this experiment include: (a) solvent, (b) optimum asphalt concentration, (c) filter combination, and (d) method of removing aggregate from solution for colorimetric or light transmittance determination.

In this investigation the following procedure was used: A stock solution of 1.000 g asphalt in 1 liter trichloroethylene was prepared and the light transmittance concentration calibration curve was determined. Oven-dry aggregates (100 g) were weighed into Erlenmeyer flasks. Two hundred milliliters of 1 g/liter asphalt stock solution were added to the aggregates. The flasks and contents were shaken for 3 min, allowed to set for 30 min and shaken for another minute and set for 30 min. About 100 ml of the solution was drawn from the flask and centrifuged, in a pear-shaped flask, for 30 min at 400 g. About 20 ml of solution was carefully drawn from the top of the settled aggregate with a syringe and transferred into a 1-in. cell.

Transmittance was determined using a 650 filter. (A cutoff filter was also used to pass only those wavelengths above 430 m $\mu$ .) Concentration was determined from the calibrated curves. Reduction in concentration (or increase in light transmission) was considered as loss of asphalt due to absorption or adsorption by aggregate and was expressed in mg per 100 g of aggregate. Alternative methods of filtering the solution through a filter paper, asbestos filter or through a Buchner filter funnel were also investigated. There was no difference in light transmission found for asphalt solutions. However, there were difficulties in getting repeatable results when dye solutions were used (see next section). Therefore, a uniform centrifuge method was used for both methods.

Results of asphalt absorption by photo-colorimetric method are given in Table 16.

Relative absorption capacity of aggregate by photometer method was also determined using dye solutions. Two dyes were selected: methylene blue and safranin T. Except for optimum concentrations and filter combinations, the procedures for dye absorption by photometer method was essentially the same as that for asphalt absorption. In addition, time-absorption relations were also studied. The results of these two series of study are given in Tables 17. Qualitative comparison of absorption by the three photometer method in terms of absorptivity rankings are given in Table 18. The results of the photometer method of dye solution, especially methylene blue, are excellent. Correlation between absorption by this method and other absorption methods will be discussed later. Certain conclusions resulting from a previous study<sup>37</sup> have been confirmed during this investigation: (a) the photo-colorimeter definitely can be used to evaluate the absorptive properties of aggregate, (b) the method is simple



Table 16. Asphalt absorption by photometer method<sup>a,b</sup>

Date	Source	Wt. of aggregate, g <sup>c</sup>	Log-abs. <sup>d</sup>	Stock Conc. mg/l	Abs. of Asphalt mg/l	Abs. of Asphalt (mg/100 g of aggr.)
3-4-71	Alden	100.04	102.5	1153.4	288.4	57.68
3-4-71	Cook	100.01	63.0	1153.4	638.4	127.68
3-5-71	Keota I	100.00	82.0	1045.8	360.8	72.16
3-5-71	Keota II	100.00	34.5	1045.8	785.8	157.16
3-5-71	Linwood	100.04	100.0	1045.8	200.8	40.16
3-4-71	Menlo	100.02	111.5	1053.4	106.4	21.28
3-5-71	Pints	100.02	13.2	1045.8	975.8	195.16
3-5-71	x(Alden II)	100.02	90.5	1045.8	286.8	57.36

<sup>a</sup>A.C. 124-2; solvent = trichloroethylene

<sup>b</sup>Filters: Center 650  
Right 430+  
Left Diffuser

<sup>c</sup>Laboratory crushed, passing 3/8 in., retained on #4

<sup>d</sup>Average of three samples

Table 17a. Dye absorption by photometer<sup>a</sup> (methylene blue)

Source	Wt. of <sup>b</sup> Aggr., g	Stock Conc. (g/l)	1 hr		24 hrs	
			Log-abs. <sup>c</sup>	Abs of Dye (g/100 g aggr.)	Log-Abs. <sup>c</sup>	Abs. of Dye (g/100 g aggr.)
Alden	100.04	0.25043	113.0	0.0110	81.0	0.0220
Cook	100.03	0.25043	92.0	0.0182	22.4	0.0416
Keota I	100.02	0.25043	122.0	0.0080	85.8	0.0204
Keota II	100.02	0.25043	85.5	0.0204	8.5	0.0464
Linwood	100.04	0.25043	129.0	0.0060	109.0	0.0126
Menlo	100.02	0.25043	116.0	0.0100	86.0	0.0202
Pints	100.06	0.25043	43.0	0.0348	9.2	0.0460
x(Alden II)	100.04	0.25043	125.0	0.0072	85.0	0.0206

<sup>a</sup>Filters: Center 425  
Right 430+  
Left Diffuser

<sup>b</sup>Laboratory crushed, passing 3/8 in., retained on #4

<sup>c</sup>Average of three samples

Table 17b. Dye absorption by photometer (Safranine T)<sup>a</sup>

Source	Wt. of Aggr., g <sup>c</sup>	Stock Conc. (g/l)	1 hr		24 hr	
			Log-abs. <sup>d</sup>	Abs. of Dye (g/100 g aggr.)	Log-Abs. <sup>d</sup>	Abs. of Dye (g/100 g aggr.)
Alden	100.01	4.0002	126.0	0.0280	98.0	0.2460
Cook	100.03	4.0000	125.0	0.0360	72.0	0.4440
Keota I	100.03	4.0019	119.0	0.0823	109.5	0.1563
Keota II	100.02	4.0000	120.0	0.0740	82.0	0.3720
Linwood	100.01	4.0014	97.0	0.2522	88.0	0.3262
Menlo <sup>b</sup>	100.00	4.0000	113.0	0.1300	83.0	0.3640
Pints	100.01	4.0019	88.0	0.3262	61.5	0.5103
x(Alden II)	100.02	4.0002	122.5	0.0560	95.0	0.2700

<sup>a</sup>Filters: Center 650  
Right 430+  
Left Diffuser

<sup>b</sup>Passing #4, retained on #8

<sup>c</sup>Passing 3/8 in., retained on #4

<sup>d</sup>Average of three samples

Table 18. Rankings of absorption by photometer method

Rank <sup>a</sup>	<u>Safranine T</u>		<u>Methylene Blue</u>		<u>Asphalt</u>
	1 hr	24 hr	1 hr	24 hr	1 hr
1	A	KI	L	L	M
2	C	A	X	M	L
3	X	X	KI	KI	X
4	KII	L	M	X	A
5	KI	M	A	A	KI
6	M	KII	C	C	C
7	L	C	KII	P	KII
8	P	P	P	KII	P

<sup>a</sup>Increasing absorptivity

and rapid; the instrument is standard, inexpensive and readily available; and (c) the method can be applied to evaluate single-sized aggregates, graded aggregates, as well as mineral fillers. No currently available methods provide the means to evaluate the absorptive characteristics of fillers.

#### Asphalt Absorption

Several series of asphalt absorption tests were conducted during the course of this investigation. Variables investigated included:

- Type and size of aggregate: Six major types, eight subtypes (laboratory crushed), rock cores, fractioned as well as graded.
- Absorption methods: Immersion method, bulk-impregnated specific gravity and Rice specific gravity method.
- Asphalt type: from 91-127 pen.

- Temperature: 220-300°F.
- Time factor: Extensive time-absorption curves were established for core samples, crushed 3/8 in. to #4 sieve fractions and graded aggregates up to 100 days.

Four major series of asphalt absorption studies were carried out in HR-142, each with different emphases:

#### Series A

The major purpose of this series of tests was to determine the influence of asphalt type, aggregate type, method of measurement and pore characteristics on asphalt absorption.<sup>22</sup> Rock cores from six major limestones and two asphalt cements (91 and 127 pen) were studied by immersion and bulk-impregnated specific gravity (Corps of Engineers) methods.

The immersion method used is essentially that developed by Goshorn and Williams<sup>33</sup> for coarse aggregates, with the exception that the rock cores (about 250 g) were immersed in asphalt at 300°F (instead of 275°F) for 1 hr only (instead of a total of 3 hr) and without cooling the sample to room temperature and reheating it to 275°F before removing the cores from the asphalt. It is felt that by this modification, the time required to complete the test can be greatly reduced, the conditions more nearly approach the field operation of hot mix, and the absorption should be more indicative of the maximum or potential absorptive capacity of an aggregate. A detailed procedure is described in Appendix D.

The procedure used in determining the bulk-impregnated specific gravity (G<sub>bi</sub>) is essentially that described by Ricketts et al.<sup>38</sup> except that 250 g of rock cores were used. For detailed procedure and calculation of asphalt absorption, see Appendix D.

The results of absorption tests are summarized in Table 19. Each value represents the average of two determinations.

Table 19. Asphalt absorbed by rock cores, wt %

Rock core	<u>BISG method</u>		<u>Immersion method</u>	
	Asphalt A	Asphalt B	Asphalt A	Asphalt B
Menlo	0.30	0.30	0.59	0.59
Pints	2.01	2.27	2.11	2.47
Alden	0.91	1.08	1.20	1.31
Linwood	0.30	0.33	0.44	0.28
Cook	0.40	0.70	0.45	0.83
Keota	0.41	0.69	0.52	0.98

Absorption by bulk-impregnated specific gravity method. The percent absorption varied from a low of 0.30 for Menlo cores to a high of 2.01 for Pints cores, using Asphalt A. Correlation of results of absorption for asphalts of different penetrations (A and B) were made. The correlation coefficient is 0.9861, which is excellent. The equation of the regression line is

$$Y = 0.1111 + 1.07 X$$

where

Y = percent asphalt absorption (Asphalt B), and

X = percent asphalt absorption (Asphalt A).

The regression line suggests, as was found in HR-127,<sup>37</sup> the absorption of higher penetration Asphalt B is somewhat higher than Asphalt A.

Asphalt absorption by immersion method. The percent absorption varied from 0.44% for Linwood cores to 2.11% for Pints cores, using Asphalt A. The correlation between absorption of two asphalts is very good, correlation coefficient being 0.9504. The equation for regression line is

$$Y = 0.0993 + 1.0912 X$$

where

Y = percent asphalt absorption using Asphalt B, and

X = percent asphalt absorption using Asphalt A.

Again, the regression line indicates a slightly higher absorption for softer or lower viscosity asphalt.

Comparison of two methods. It shall be observed in Table 19 that the absorption values from the immersion method are higher than those by BISG method. Figure 31 shows the plot of percent absorption, by BISG method vs same by the immersion method. The correlation is excellent for both A and B asphalts used, correlation coefficients being 0.9883 and 0.9862, respectively. Equations for the regression line are:

Asphalt A,  $Y = 0.1788 + 0.9785 X$  and

Asphalt B,  $Y = 0.1523 + 1.0332 X$

where

Y = percent asphalt absorption by immersion method, and

X = percent asphalt absorption by BISG method.

In Fig. 31, regression lines resulted from HR-127<sup>37</sup> with quarry crushed fractioned aggregates of considerably different nature were also plotted. Despite the differences in two sets of materials, the regression lines are surprisingly consistent.

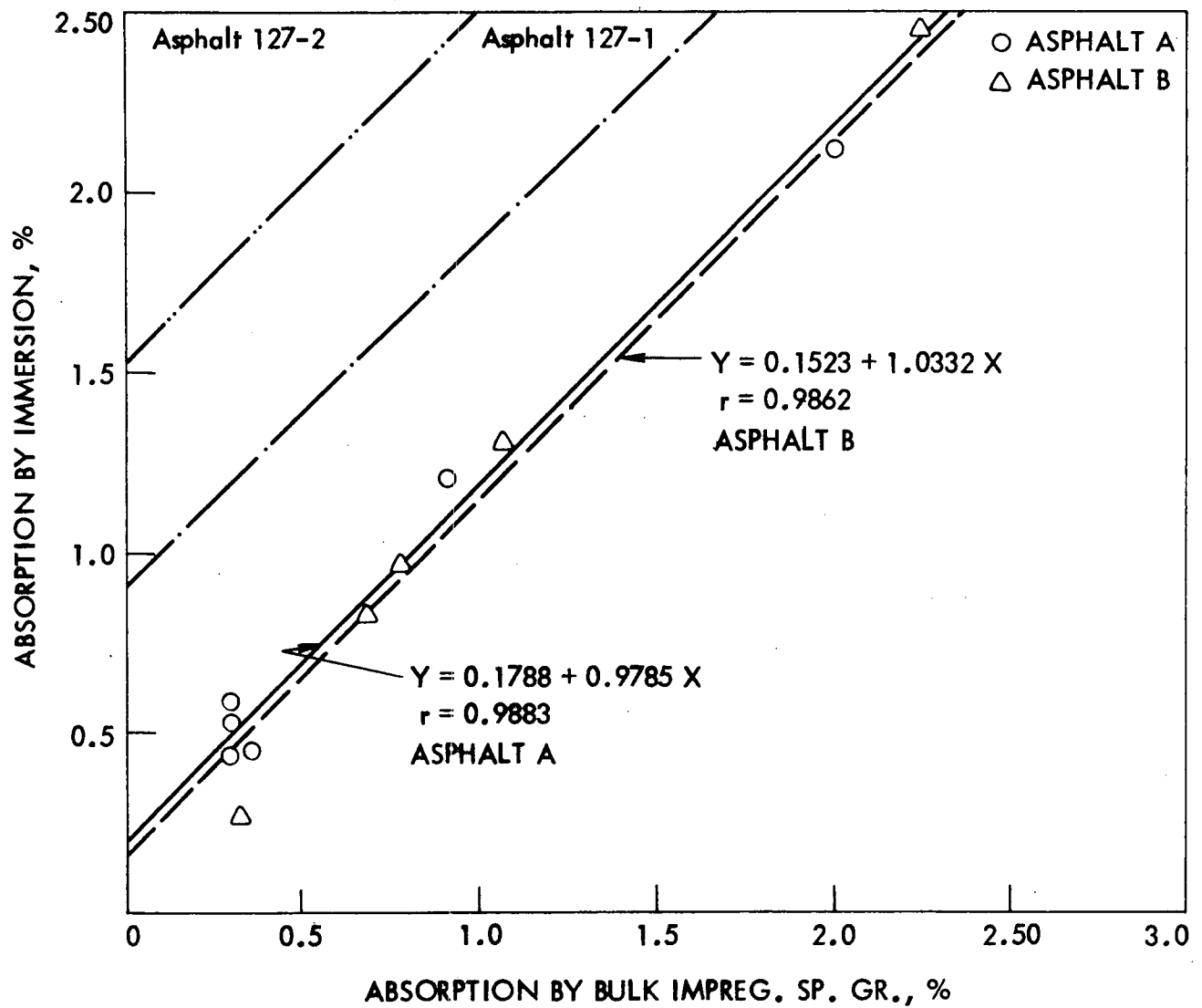


Fig. 31. Asphalt absorption - BISG method vs immersion method



McLeod<sup>36</sup> considered the absorption values obtained by the BISG method to represent the maximum or upper limit of bitumen absorption. But, from this study, as well as results from HR-127, it is evident that the immersion method gives still higher values which can be taken as the absorptive potentials of aggregates in question. The values obtained from the BISG method can be considered as "realistic" maximum value, which can occur during mixing, hauling, spreading and cooling of the paving mixture, and in service under traffic.

Accuracy of both the absorption tests is generally limited by homogeneity of the aggregate and accuracy of the bulk specific gravity and water absorption. But in this study, use of rock cores drilled out from a single block sample has practically eliminated the first discrepancy. The determination of bulk specific gravity by the ASTM C-127 test gave excellent reproducible results in case of rock cores, as the saturated surface dry condition could be achieved uniformly by rolling the cores on cloth. The results can be considered to be consistent as far as these limitations are concerned.

It should be mentioned that the results of absorption tests performed on uniform size rock cores (1/2 in. dia) with smooth round surfaces are considerably lower than that from crushed aggregates obtained from the same rocks since the surface capacity is comprised of the surface area, varying with gradation and the roughness of the aggregates in addition to the effective porosity.

#### Series B

This series of absorption tests were conducted in conjunction with aggregate treatment tests (discussed later). The major purposes of this

series of tests were to establish the absorption-time curves of eight laboratory crushed and graded limestones and to evaluate the effectiveness of sulfur treatments on these aggregates. The asphalt absorption was determined by the modified Rice method (Appendix D) and absorption of treated and untreated aggregates were determined from one day up to 135 days. The results of these mixtures are given in Table 43 and plotted on a semi-log scale in Figs. 63 - 70. The following were observed:

- All absorption-time (A-t) curves approach an exponential relationship, and can be represented by

$$t = ae^{bA}$$

where

a and b are constants.

- Major absorption occurs during first 10-30 days and the absorption levels off after about three months.
- The ratios between 100 day absorption and one day absorption varied from 1.15-3.15, actual absorption increase varied from 0.7-1.2%. Regression analysis was made between absorption at one day and at 100 days. The equation for line of regression is

$$y = 0.923 + 1.034 x$$

where

y = 100 day absorption, %

x = 1 day absorption, %

Correlation coefficient is 0.998 which is significant at the 1% level.

- Asphalt absorption varied from a low of 0.5% for Linwood limestone to a high of 7.7% for Keota II. Absorption value is most significantly affected by bulk specific gravity value of the aggregate.
- Even though quantitative data are lacking, it is reasonable to assume that many flexible pavements can fail (crack) through delayed absorption by aggregate and loss of effective binder in the paving mixture.

### Series C

This series of asphalt absorption tests were conducted on rock cores by immersion method to evaluate absorption as affected by aggregate type, asphalt viscosity (asphalt penetration and temperature), immersion time, and absorption time.

Fifty-six immersion tests were conducted with absorption determined at the end of 2 hr, 24 hr, and 2 weeks. Bulk specific gravity of cores was determined by the standard ASTM method. Asphalt cements of either 91 or 127 pen were heated in 1000 ml beakers to either 300°F or 220°F. Three to five cores used for bulk specific gravity test were heated to asphalt temperatures and suspended (in a wire basket) in asphalts for 1/2, 1, 2, 30, 60, and 120 min, respectively. Baskets with cores were removed from asphalt at the end of the immersion or soaking period and suspended in an oven at 275°F for 10-15 min or until the excess asphalt had drained off. The cores were cooled to room temperature and weighed in air on an analytical balance with a special attachment. Cores (with baskets) were weighed in water at 77°F at the end of 2, 24, 48, 72 hrs and at the end of 1 and 2 weeks. Asphalt absorption for each set of cores was calculated from the procedure outlined in Appendix D. Results of the 56 tests are presented in Table 20 and are shown in Figs. 32.

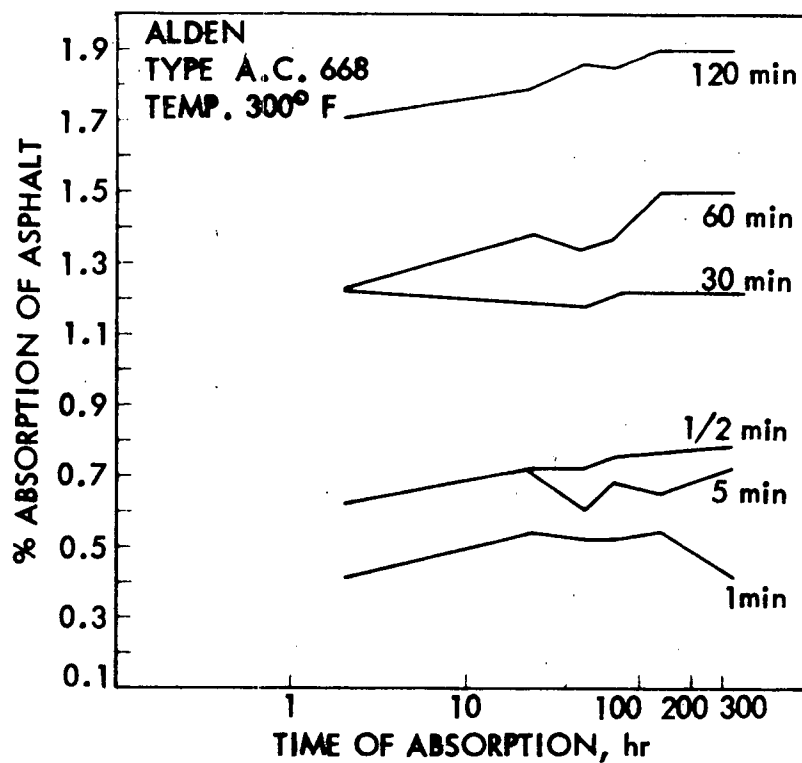


Fig. 32a. Asphalt absorption vs time of immersion and time of absorption, cores, Alden

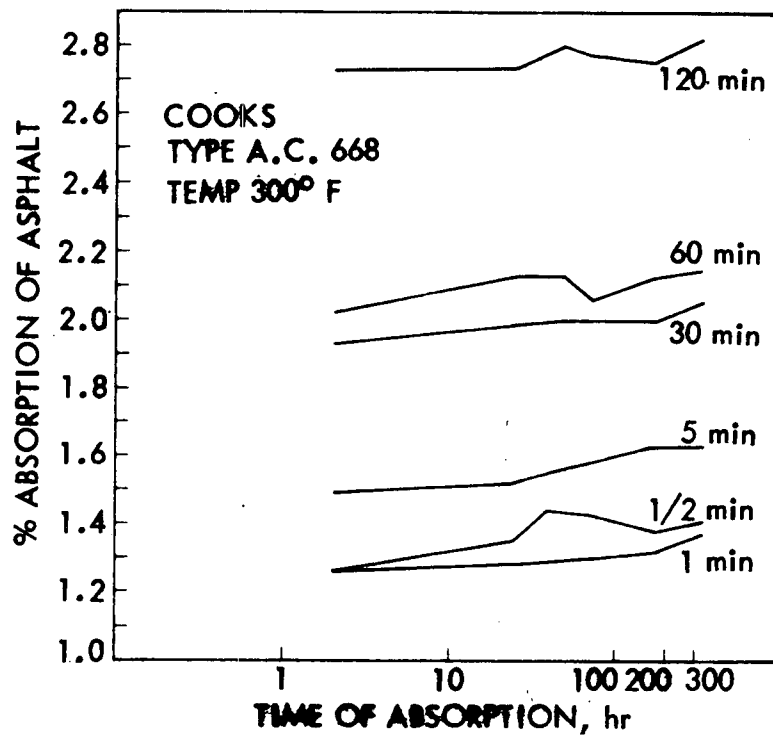


Fig. 32b. Asphalt absorption vs time of immersion and time of absorption, cores, Cook

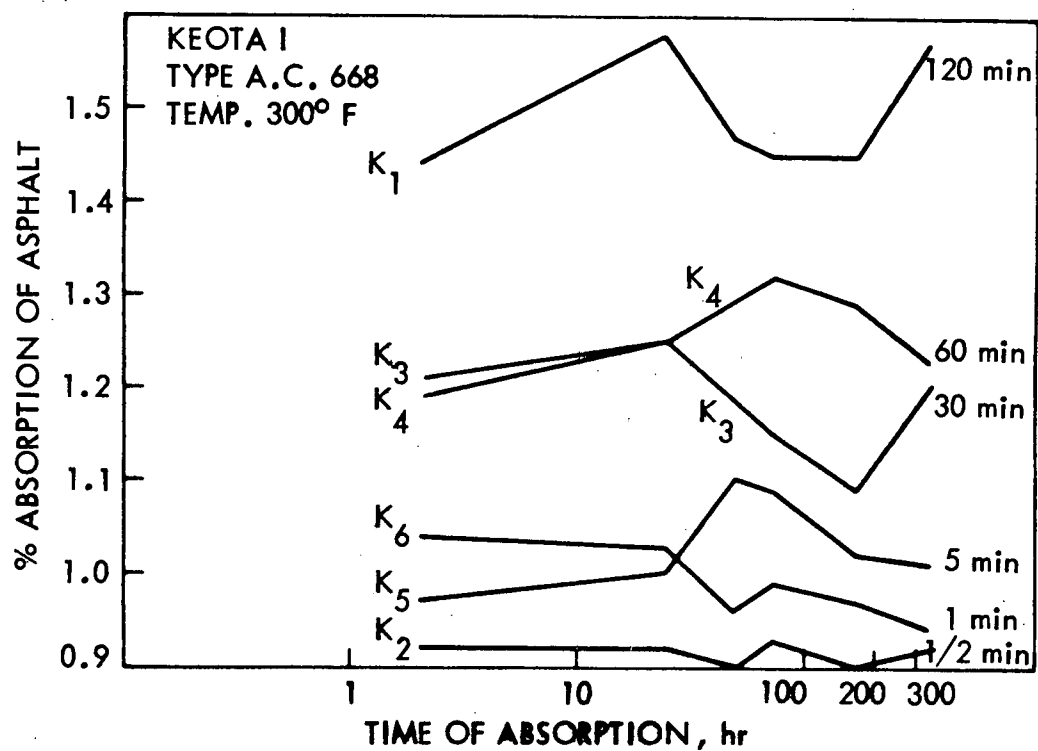


Fig. 32c. Asphalt absorption vs time of immersion and time of absorption, cores, Keota I

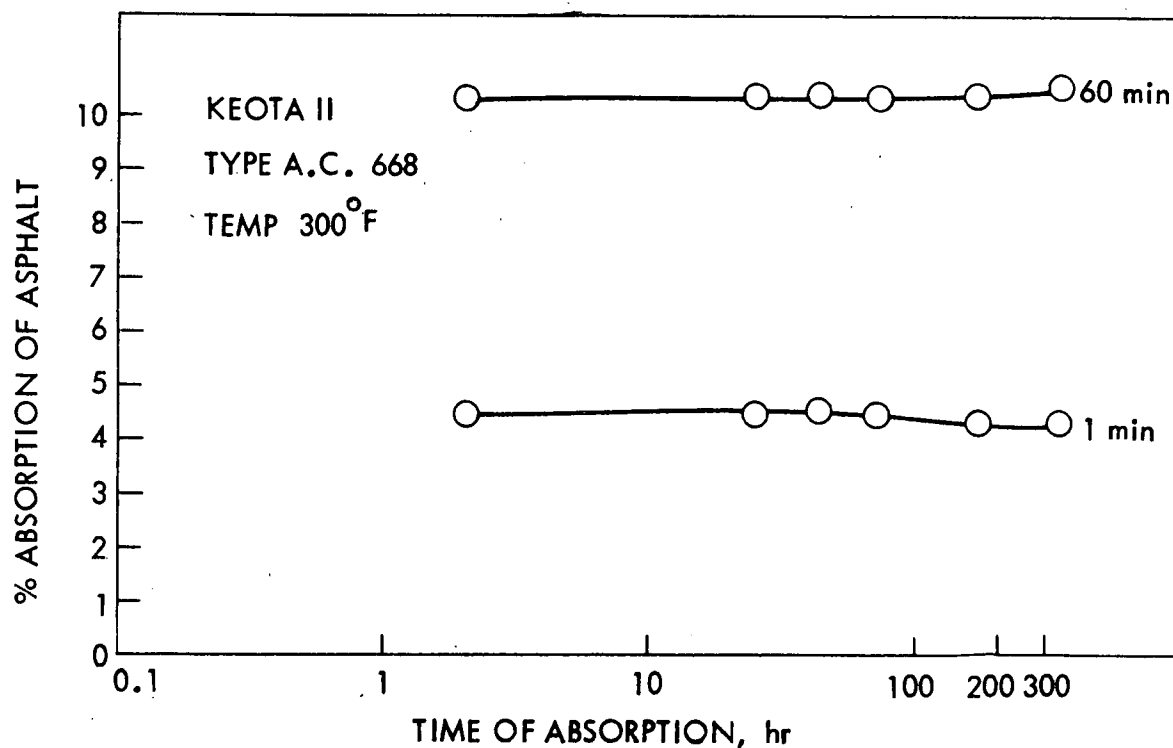


Fig. 32d. Asphalt absorption vs time of immersion and time of absorption, cores, Keota II

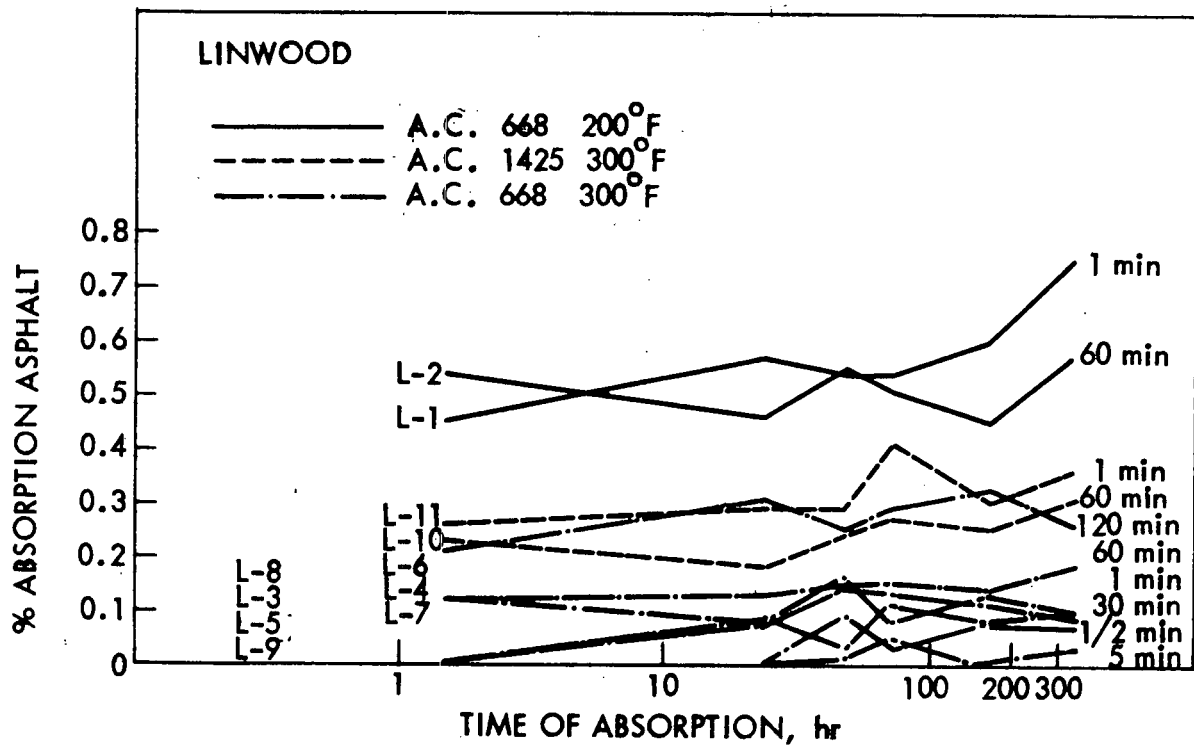


Fig. 32e. Asphalt absorption vs time of immersion and time of absorption, cores, Linwood

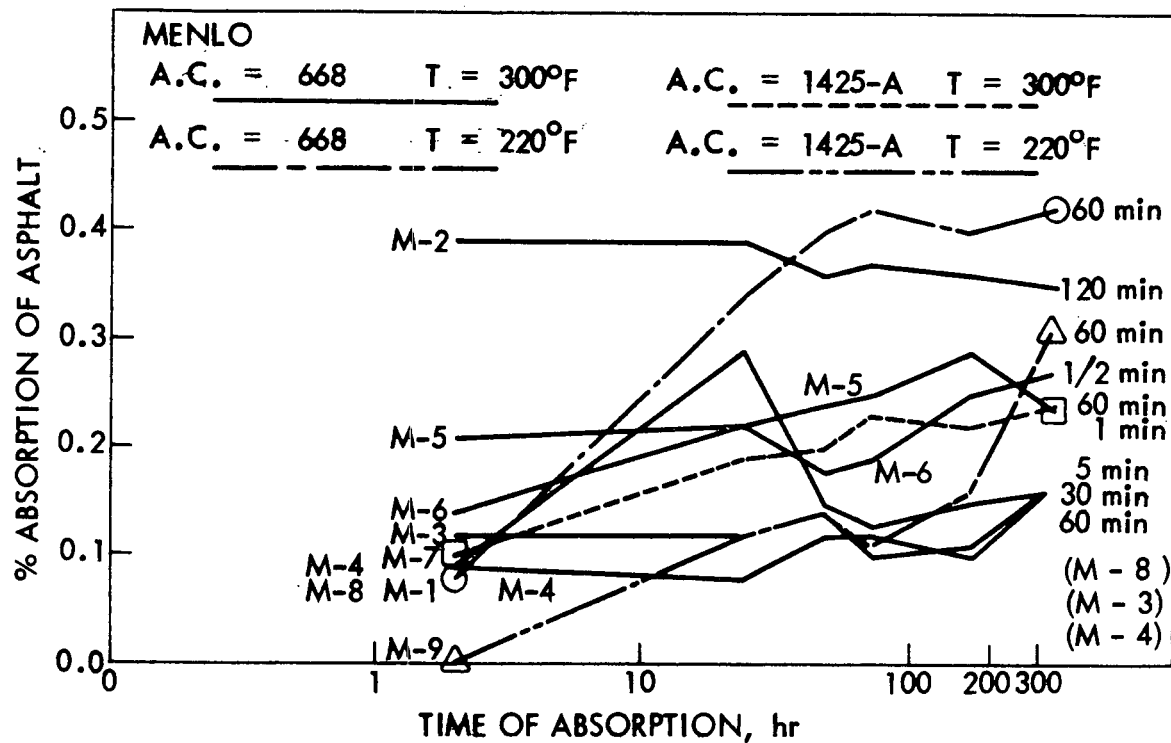


Fig. 32f. Asphalt absorption vs time of immersion and time of absorption, cores, Menlo

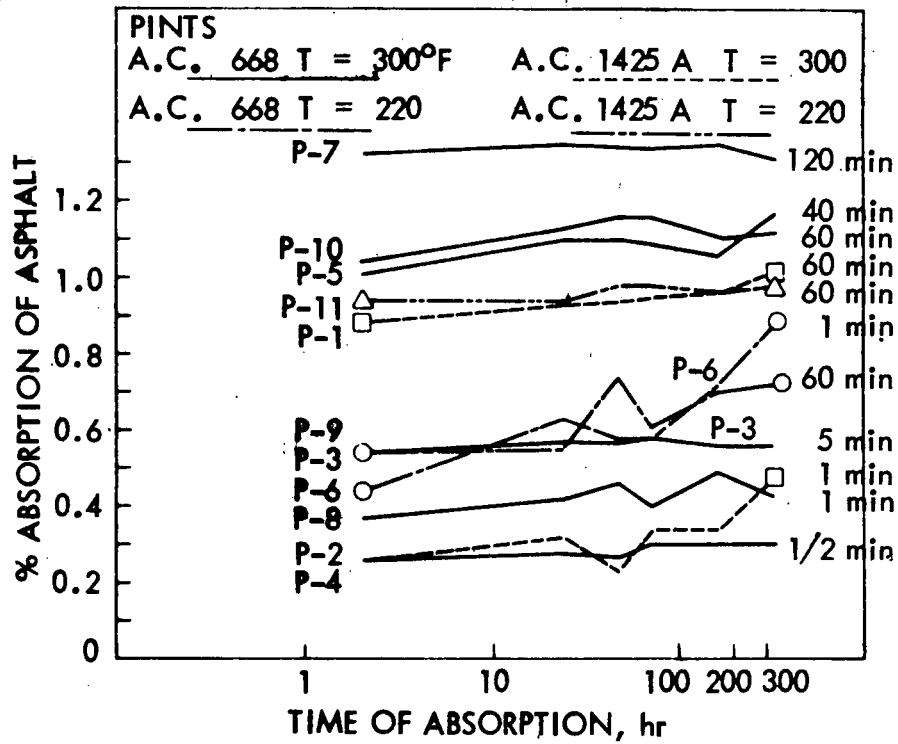


Fig. 32g. Asphalt absorption vs time of immersion and time of absorption, cores, Pints

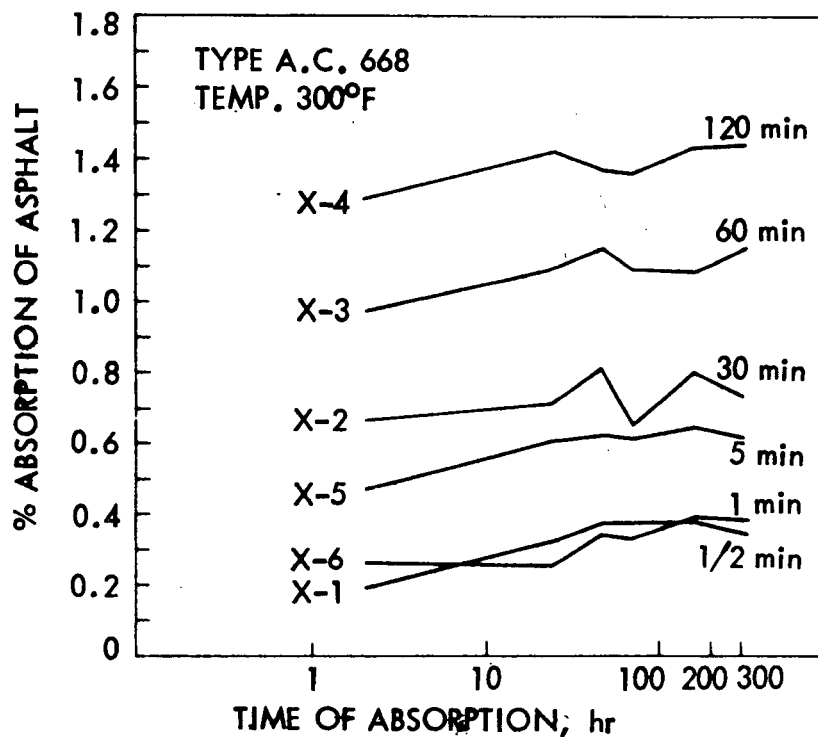


Fig. 32h. Asphalt absorption time of immersion and time of absorption, cores, X

The following were observed:

- There is a general trend of increased absorption with increasing immersion time. However, when immersion time is below 5 min the effect is insignificant. The largest increase seemed to occur between 5-30 min.

Though not completely brought out by this series of tests, the data seemed to support conclusions drawn in HR-127, i.e.:

(a) absorption increased with increasing immersion time but at a decreasing rate and may reach a maximum in 20-60 hr when the aggregate is completely saturated; maximum absorption is limited by the total porosity of the particular aggregate, and (b) most of the absorption occurred in the first few minutes when the asphalt was in contact with the aggregate.

- There is increased absorption with time after immersion. This effect is less significant for long immersion time and highly absorptive aggregates such as Keota II and Pints.
- The effects of temperature and asphalt penetration were not obvious.
- It was thought that, with cored block samples, material heterogeneous heneity effects could be practically eliminated. However, this was not so. Large differences were discovered between cores from the two block samples from Keota and Pints. Core samples from Pints block #1 (used in Series A) had immersion absorption of 2.1-2.5%, whereas core samples from Pints #2 used in this series had an average immersion absorption of 1.0-1.1%. Consequently, in correlation studies, care will be taken that



only data from materials of same blocks or batches of aggregates will be correlated.

In order to visually examine the effects of concern on asphalt absorption by immersion, photographs of sectioned and polished cores tested in this series were taken. Figure 33 shows absorption differences by aggregate type. Figure 34 shows effects of asphalt temperature. Figure 35 shows effects of asphalt type. Figure 36 shows effect of immersion time on the seven major block samples. Figures 37-41 show the photomicrographs of some of these cores, all magnified 136 times. Scanning electron micrographs of asphalt impregnated and non-impregnated Keota II core samples are shown in Figs. 42.

#### Series D

This series of absorption tests (22 samples) were similar to Series C, except that only laboratory crushed limestones passing 3/8 in. and retained on #4 sieve fractions were used. Immersion time was limited to 1 and 60 min. The results of these are presented in Table 21 and plotted in Figs. 43. Observations made on cored samples in Series C are generally true for crushed samples except that absorption was much higher and effect of immersion time, temperature, and asphalt type were more pronounced.

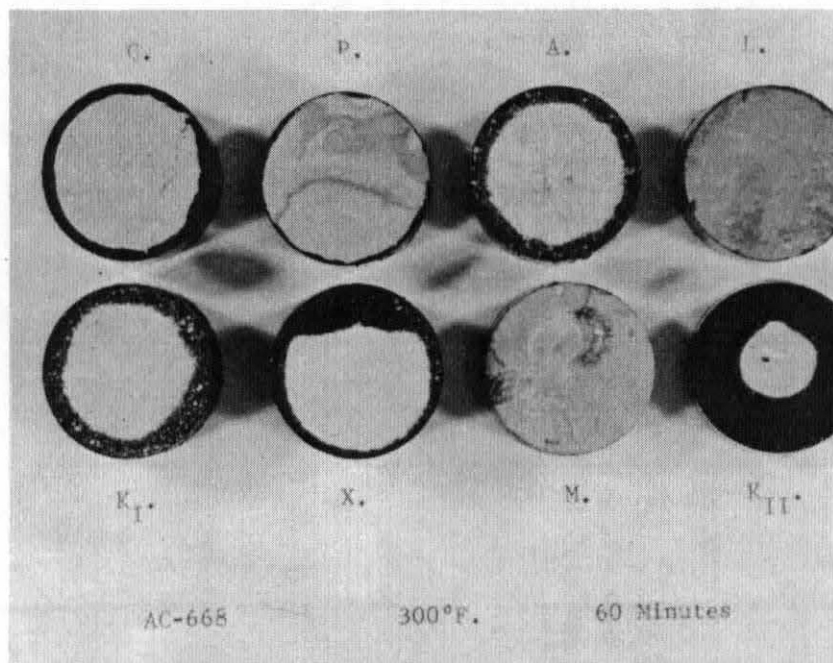


Fig. 33. Asphalt absorption vs aggregate type.

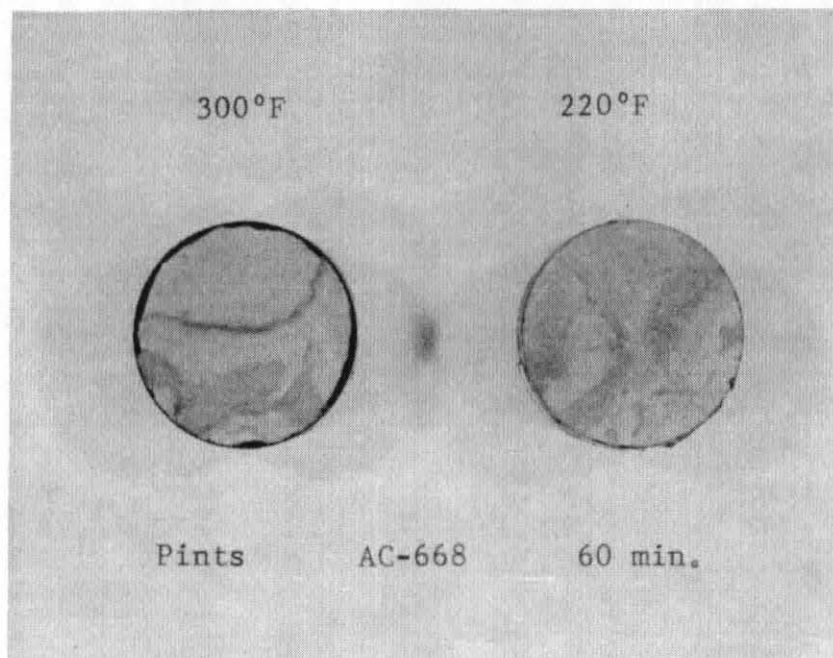


Fig. 34. Effects of immersion temperature on absorption, Pints.

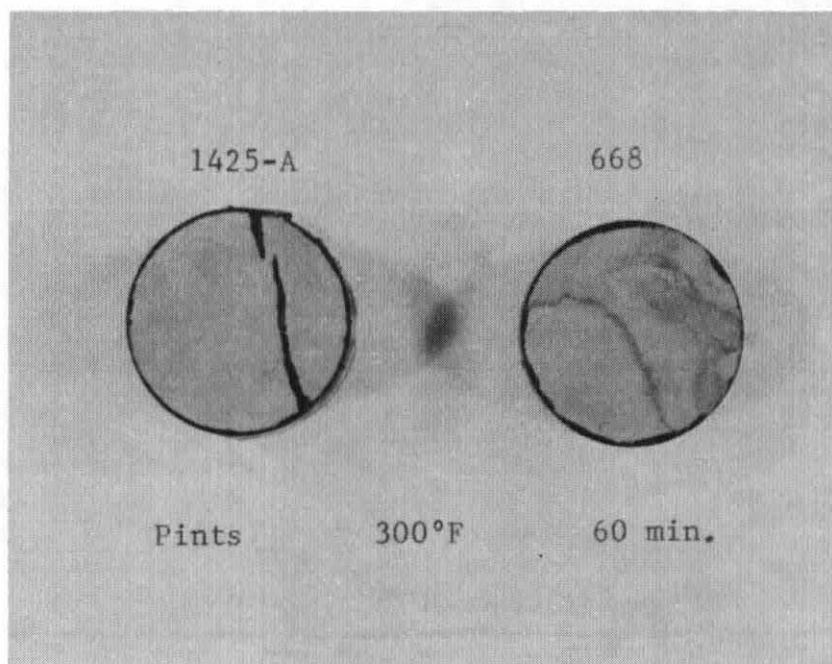


Fig. 35. Effects of asphalt type on absorption,

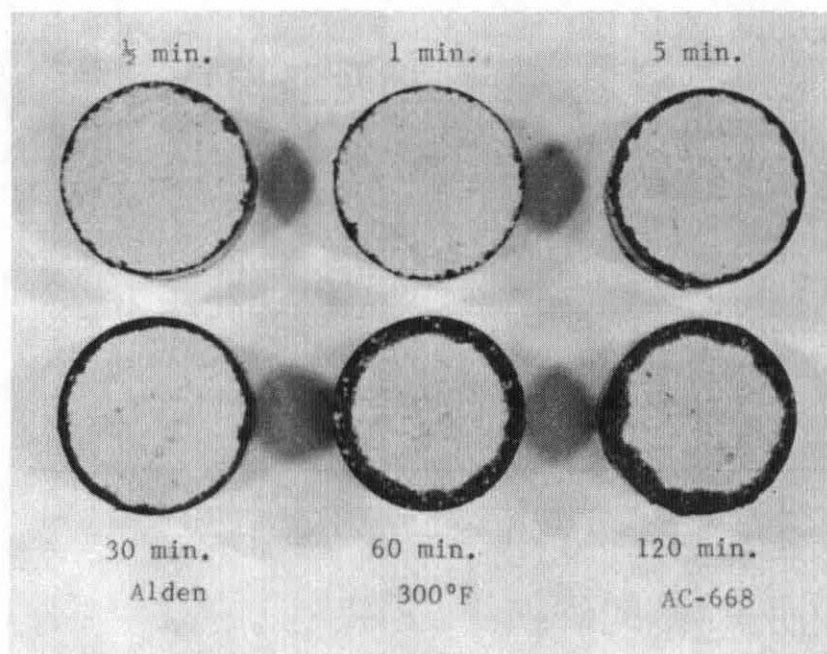


Fig. 36a. Effects of immersion time on absorption, Alden.

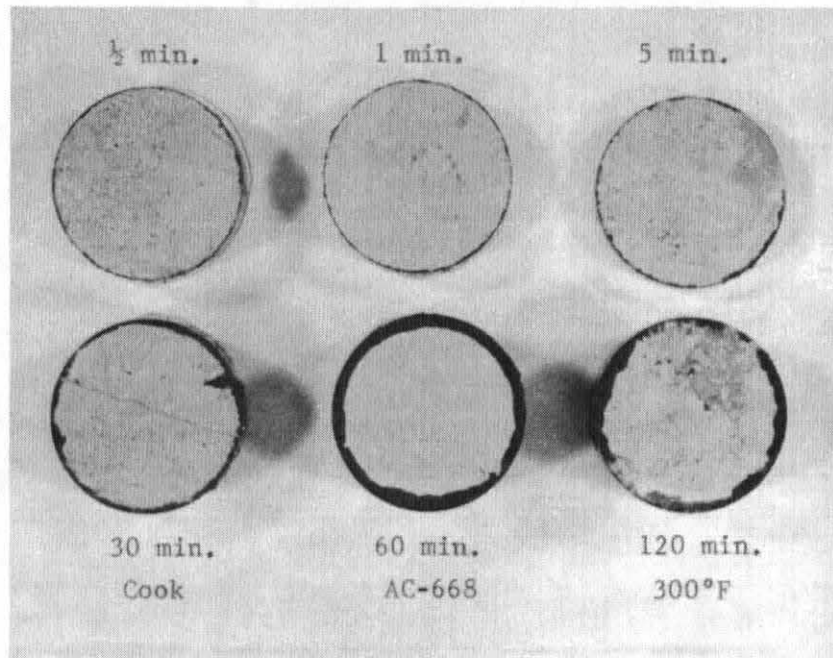


Fig. 36b. Effects of immersion time on absorption, Cook.

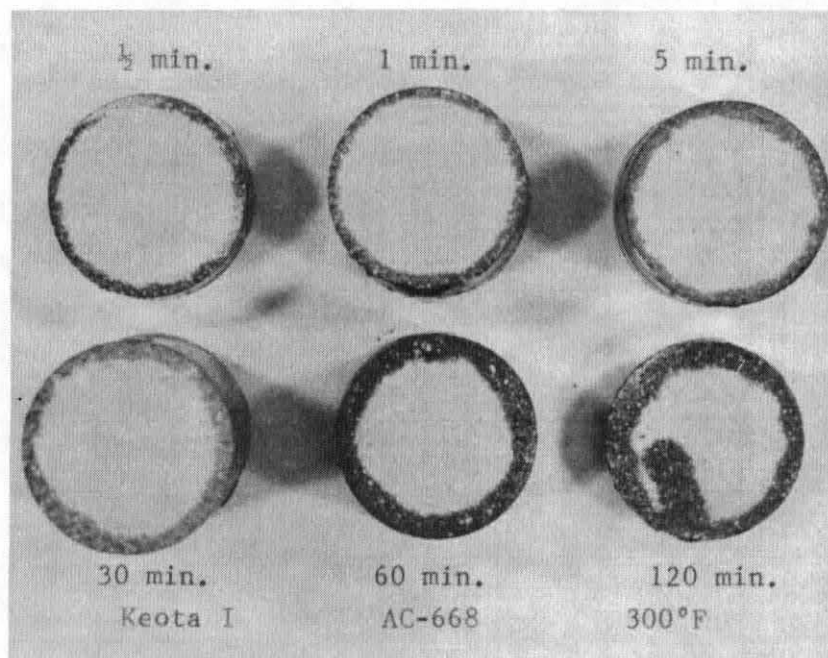


Fig. 36c. Effects of immersion time on absorption, Keota I.

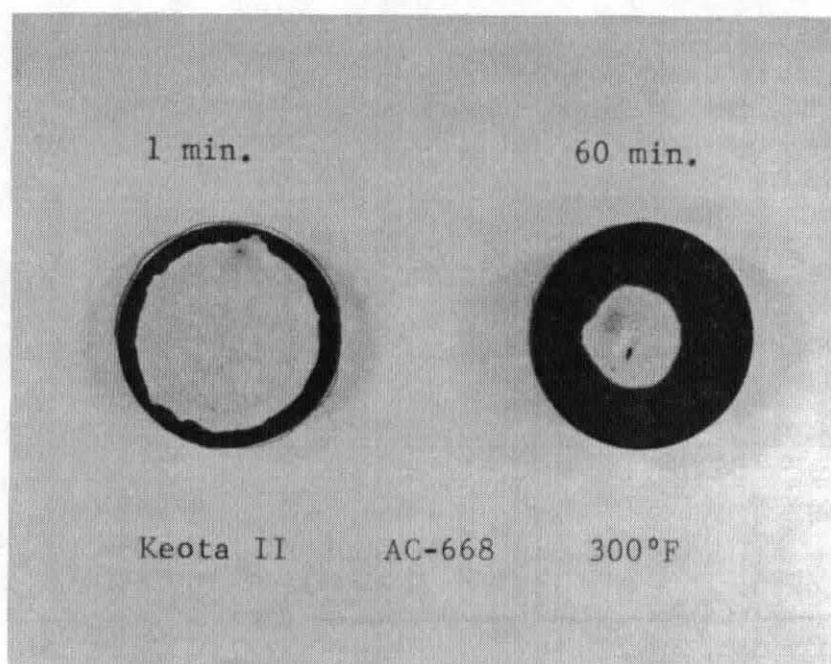


Fig. 36d. Effects of immersion time on absorption, Keota II.

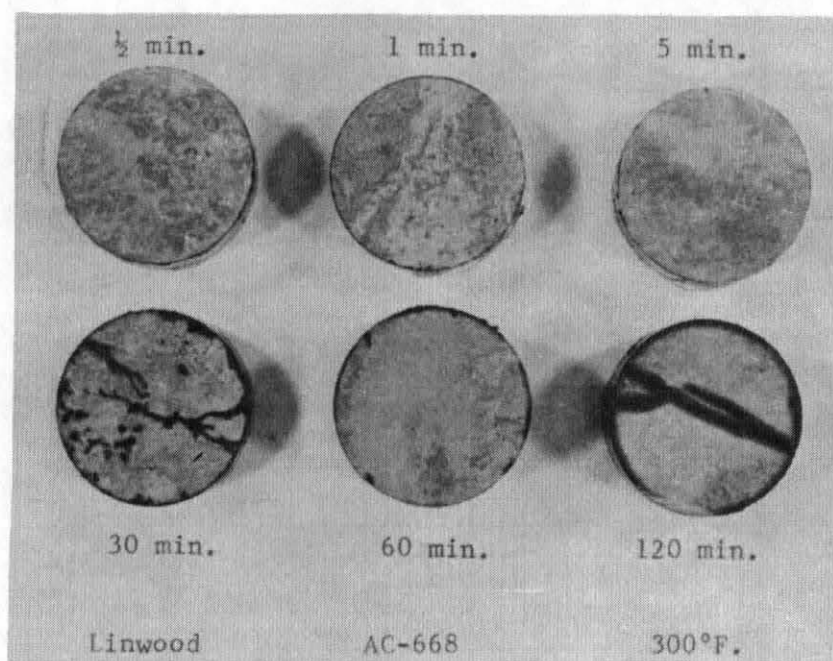


Fig. 36e. Effects of immersion time on absorption, Linwood.



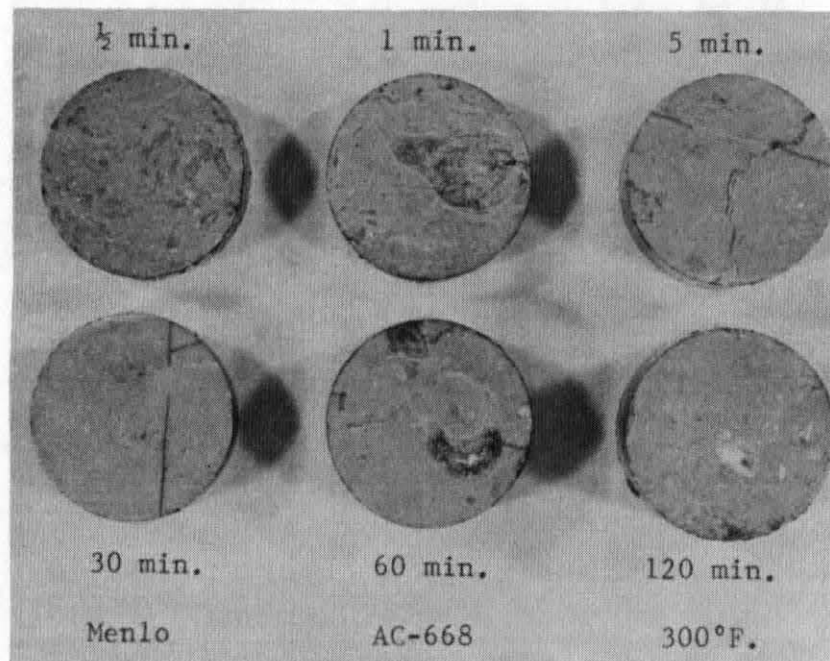


Fig. 36f. Effects of immersion time on absorption, Menlo.

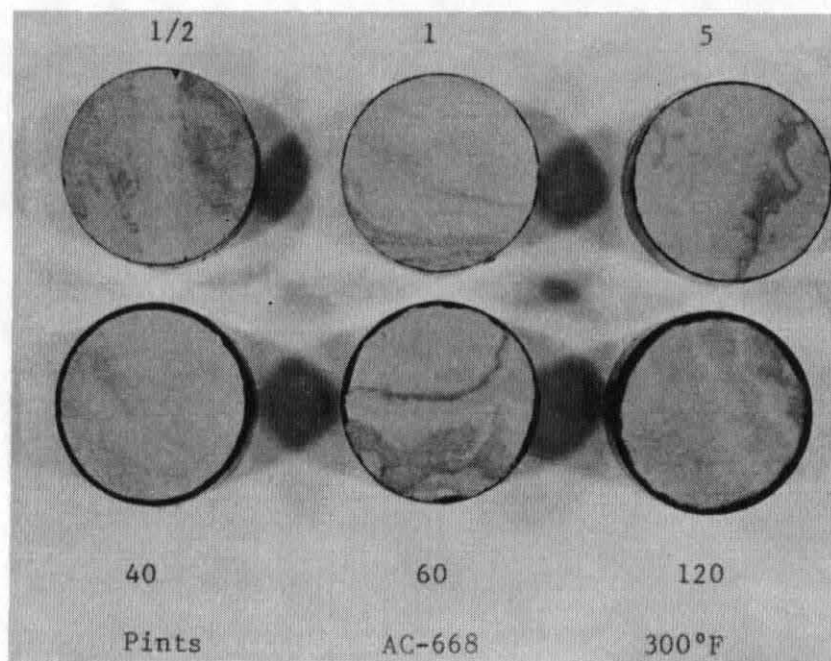


Fig. 36g. Effects of immersion time on absorption, Pints.



Fig. 37. Alden, 60 min immersion in A.C. 668 at 300°F, 136X.

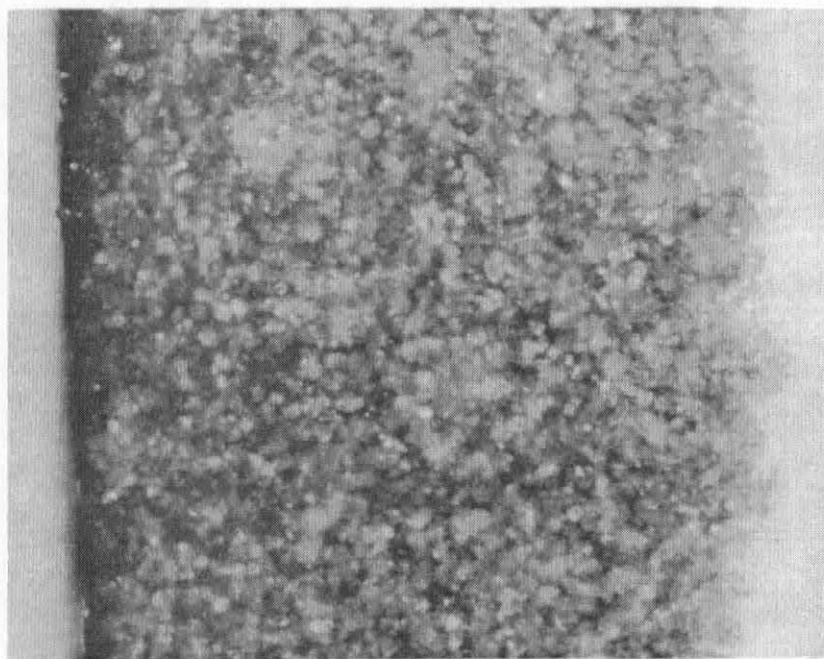


Fig. 38. Cook, 5 min immersion in A.C. 668 at 300°F, 136X.

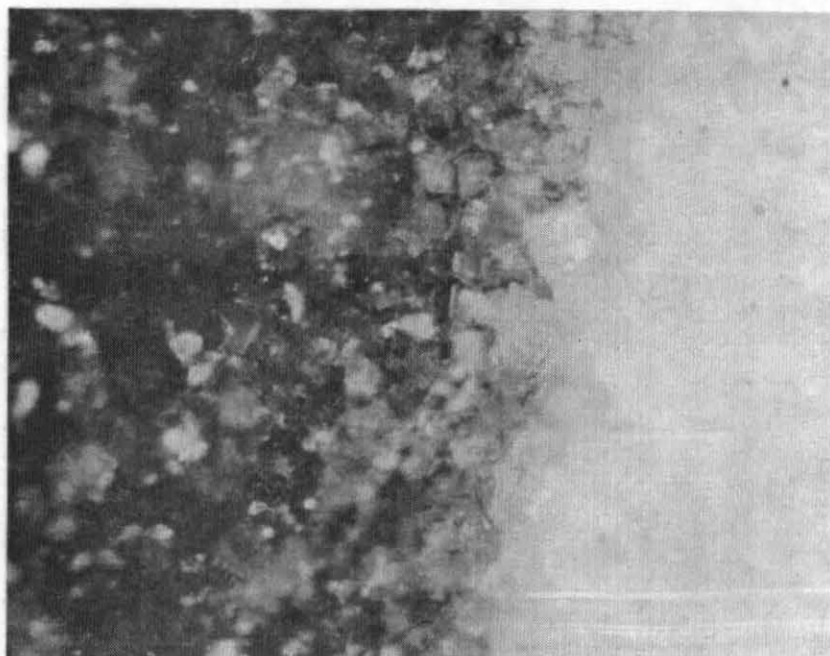


Fig. 39. Keota II, 1 min immersion in A.C. 668 at 300°F, 136X.

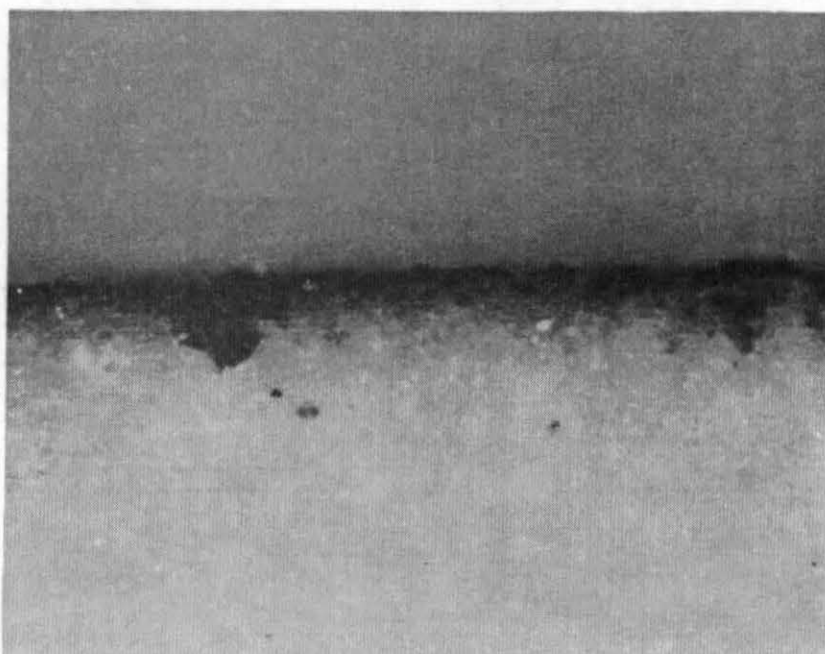


Fig. 40. Menlo, 60 min immersion in A.C. 668 at 300°F, 136X.



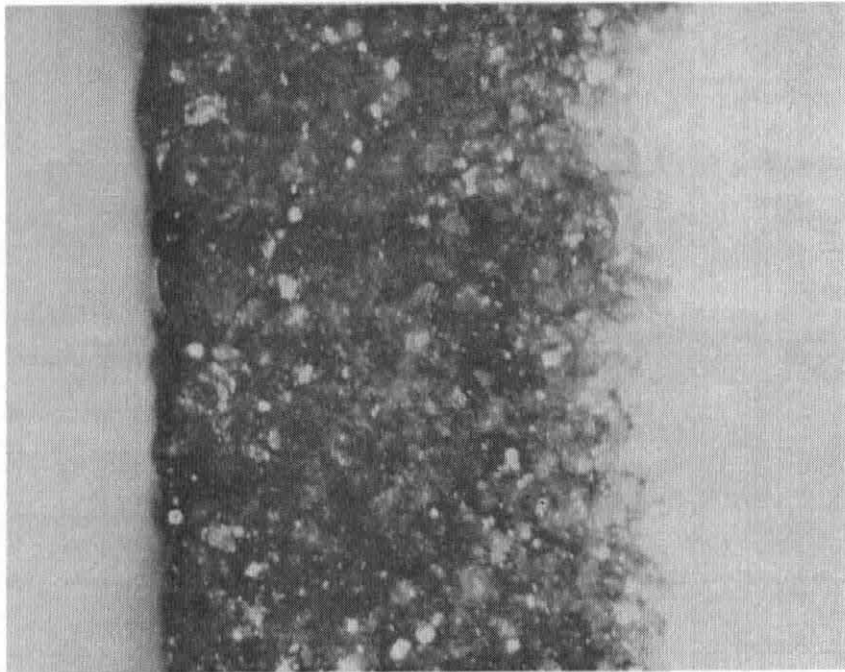


Fig. 41. Pints, 60 min immersion in A.C. 1425 at 300°F, 136X.



Fig. 42a. SEM, unimpregnated Keota II, 1000X.

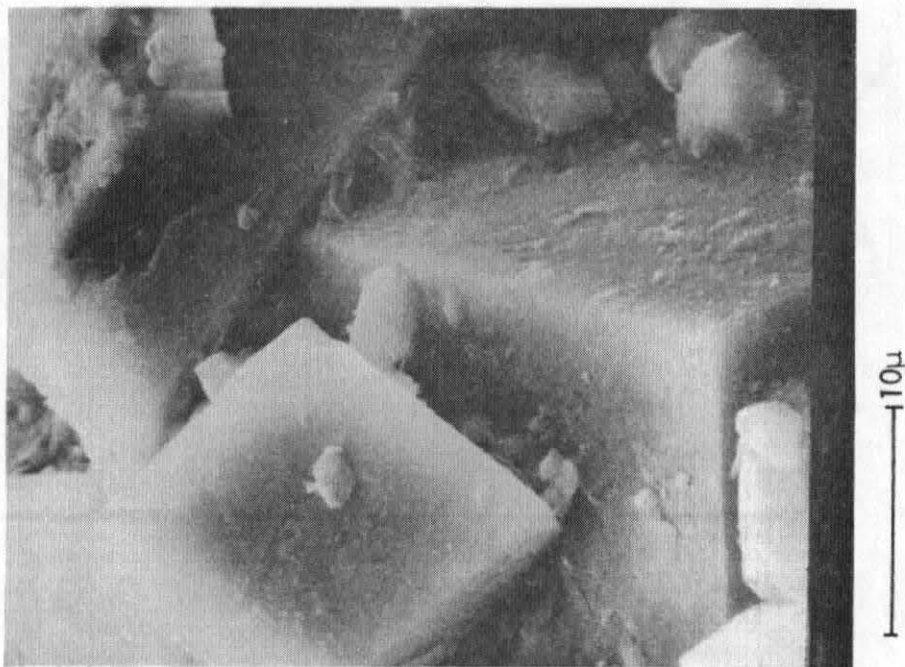


Fig. 42b. SEM, unimpregnated Keota II, 3000X.

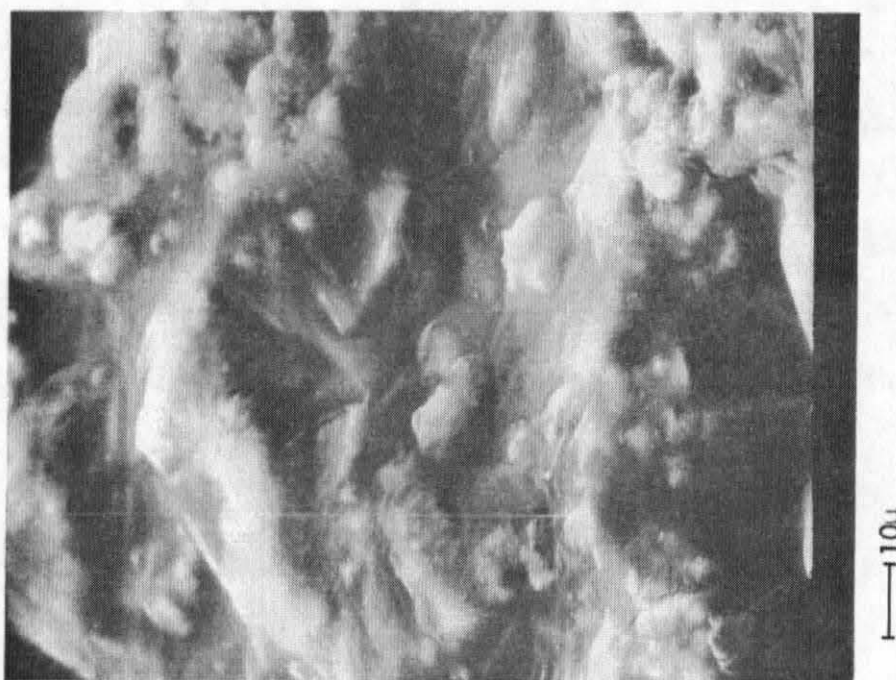


Fig. 42c. SEM, asphalt impregnated Keota II, 1000X.



Fig. 42d. SEM, asphalt impregnated Keota II, 3000X.

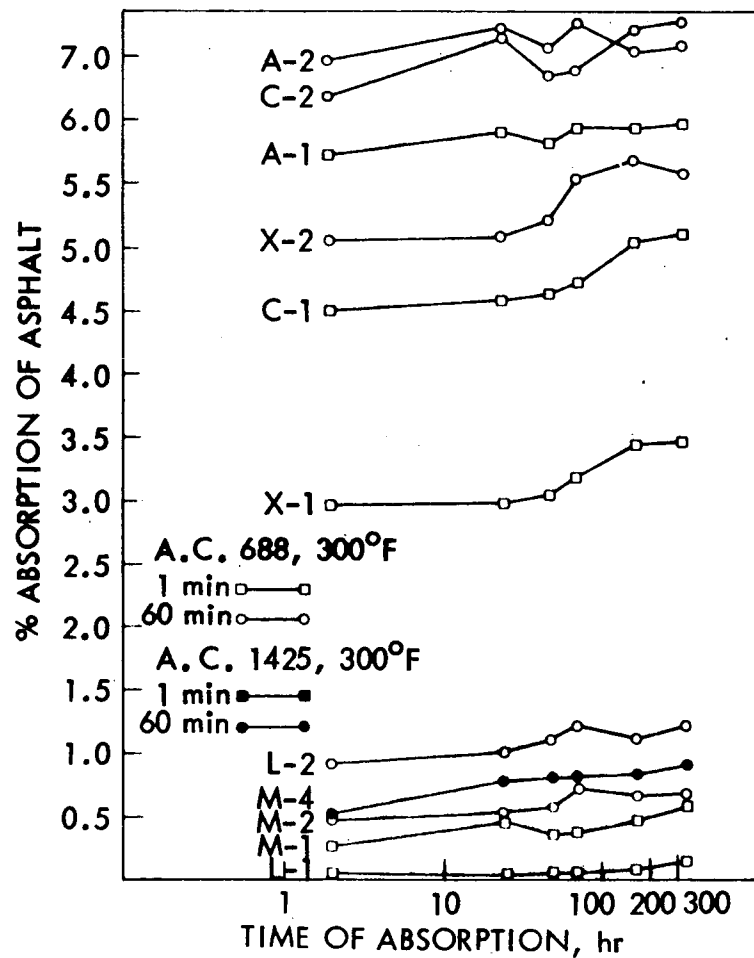


Fig. 43a. Asphalt absorption vs time of absorption and time of immersion, + No. 4 fractions

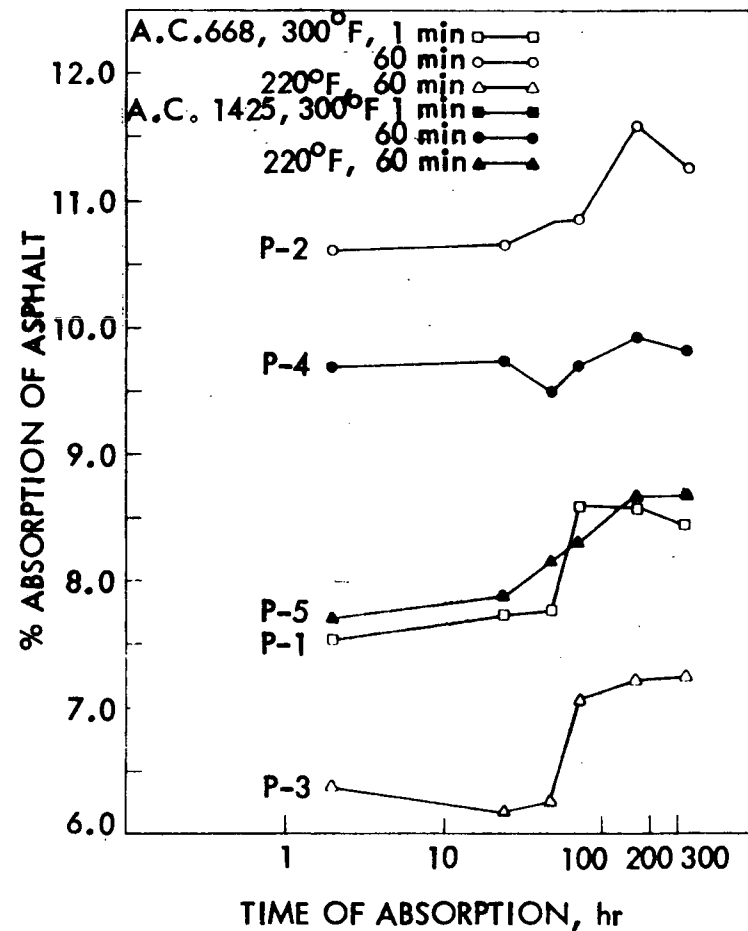


Fig. 43b. Asphalt absorption vs time of absorption and time of immersion, + No. 4 fractions, Pints

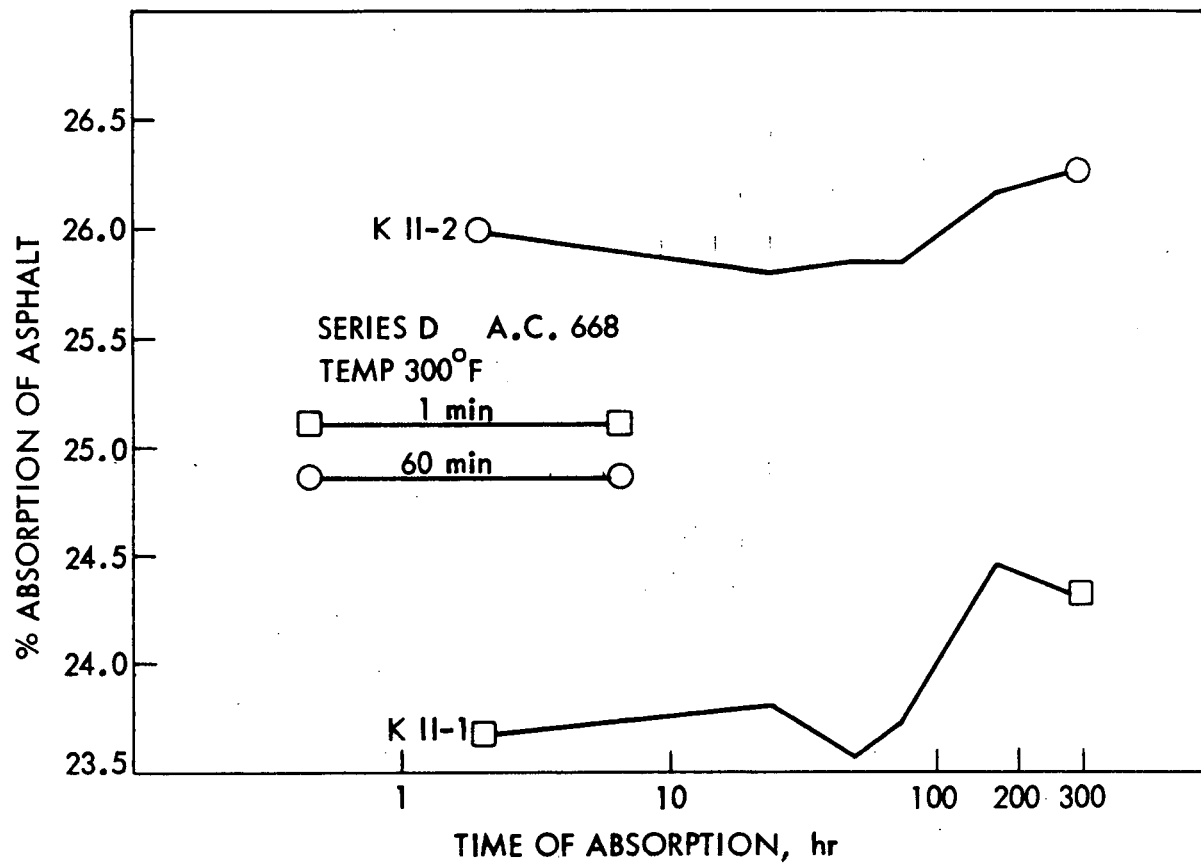


Fig. 43c. Asphalt absorption vs time of absorption and time of immersion, + No. 4 fractions, Keota II

### Correlations

#### Water absorption and asphalt absorption.

Efforts have been made in the past<sup>32,37,39</sup> to correlate water absorption of aggregates to asphalt absorption since the former is a relatively very simple standard test. In this study, the linear correlation coefficients for core samples (Series A) ranged from 0.8398 - 0.9341, as compared to 0.874 - 0.956 found in HR-127.<sup>37</sup> Correlation coefficients between water absorption (Table 12) and asphalt absorptions (Tables 20 and 21) are given in Tables 22 and 23.

Experience has shown that the water absorption is not a reliable test for predicting asphalt absorption due to noted exceptions. Bitumen-water absorption ratios have been reported ranging from 1-100%. Aggregates have been reported to show higher bitumen absorption than water absorption in rare cases.<sup>39</sup> Differences in absorptions in case of different liquids are expected since penetration of a liquid into aggregate pores (absorption) is basically a capillary phenomenon influenced not only by pore size but also the surface tension and contact angle of the liquid. However, water absorption indicates the potential of asphalt absorption. Aggregates having high water absorption are likely to absorb more asphalt than those having low water absorption.

#### Porosity and asphalt absorption.

Extensive statistical analyses were undertaken to find the pore size range and other porosity characteristics which may have some correlation with asphalt absorption. Absorption and porosity data for core samples (Series A) were used to eliminate material error. Correlation coefficients are given in Table 24.

Table 20. Asphalt absorption by cores

Quarry	A.C. <sup>a</sup>	Temp., °F	Time immersed, min	% Absorption		
				2 hr	24 hr	2 wks
Pints	668	300	1/2	0.26	0.28	0.30
Pints	668	300	1	0.37	0.42	0.43
Pints	668	300	5	0.54	0.57	0.56
Pints	668	300	40	1.01	1.10	1.17
Pints	668	300	60	1.04	1.13	1.12
Pints	668	300	120	1.32	1.35	1.31
Pints	668	220	1	0.44	0.63	0.88
Pints	668	220	60	0.54	0.55	0.72
Pints	1425	220	1	0.26	0.32	0.48
Pints	1425	220	60	0.88	0.93	1.02
Pints	1425	300	60	0.94	0.94	.98
Alden	668	300	1/2	0.62	0.72	.78
Alden	668	300	1	0.41	0.54	.42
Alden	668	300	5	—	0.70	.72
Alden	668	300	30	1.21	1.19	1.21
Alden	668	300	60	1.23	1.38	1.50
Alden	668	300	120	1.71	1.79	1.90
Linwood	668	300	1/2	0.00	0.00	.07
Linwood	668	300	1	0.00	0.09	.10
Linwood	668	300	5	0.00	0.00	.03
Linwood	668	300	30	0.12	0.07	.09
Linwood	668	300	60	0.00	0.08	.10
Linwood	668	300	120	0.21	0.31	.26
Linwood	668	220	1	0.45	0.57	.75
Linwood	668	220	60	0.54	0.46	.57
Linwood	1425	300	1	0.26	0.29	.36
Linwood	1425	300	60	0.23	0.18	.30
Keota I	668	300	1	1.04	1.03	.94
Keota I	668	300	1/2	0.92	0.92	.92
Keota I	668	300	30	1.21	1.25	1.20
Keota I	668	300	60	1.19	1.25	1.23
Keota I	668	300	5	0.97	1.00	1.01
Keota I	668	300	120	1.44	1.58	1.57
X-Quarry	668	300	1/2	0.19	0.32	0.34
X-Quarry	668	300	1	0.47	0.60	0.61
X-Quarry	668	300	5	0.26	0.25	0.38
X-Quarry	668	300	30	0.65	0.71	0.73
X-Quarry	668	300	60	0.97	1.09	1.15
X-Quarry	668	300	120	1.28	1.42	1.44

Table 20. Con't.

Quarry	A.C. <sup>a</sup>	Temp, °F	Time Immersed, min	% Absorption		
				2 hr	24 hr	2 wk
Cook	668	300	1/2	1.26	1.35	1.41
Cook	668	300	60	2.02	2.13	2.15
Cook	668	300	1	1.26	1.28	1.37
Cook	668	300	30	1.93	1.99	2.06
Cook	668	300	5	1.49	1.52	1.63
Cook	668	300	120	2.73	2.74	2.83
Menlo	668	300	1/2	0.14	0.22	0.27
Menlo	668	300	1	0.21	0.22	0.24
Menlo	668	300	5	0.09	0.20	0.26
Menlo	668	300	30	0.12	0.12	0.16
Menlo	668	300	60	0.09	0.08	0.16
Menlo	668	300	120	0.39	0.39	0.35
Menlo	668	220	60	0.08	0.34	0.42
Menlo	1425	220	60	0.00	0.12	0.31
Menlo	1425	300	60	0.10	0.19	0.24
Keota II	668	300	1	4.45	4.44	4.31
Keota II	668	300	60	10.28	10.33	10.47

<sup>a</sup>A.C. 668: 91 pen.

A.C. 1425:125 pen.



Table 21. Asphalt absorption of #4 lab. crushed aggregate

Quarry	A.C.	Temp., °F	Time immersed, min	Absorption, %		
				2 hr	24 hr	2 wk
Cook	668	300	1	4.50	4.57	5.09
Cook	668	300	60	6.18	6.66	6.76
Alden	668	300	1	5.71	5.89	5.95
Alden	668	300	60	6.47	6.72	6.58
Keota I	668	300	60	0.16	0.31	0.52
Keota I	668	300	1	0.00	0.02	0.17
X-Quarry	668	300	1	2.98	2.98	3.44
X-Quarry	668	300	60	5.06	5.07	5.55
Pints	668	300	1	7.54	7.72	8.43
Pints	668	300	60	10.60	10.64	11.26
Linwood	668	300	1	0.12	0.04	0.16
Linwood	668	300	60	0.92	1.00	1.21
Keota II	668	300	1	23.66	23.80	24.31
Keota II	668	300	60	25.98	25.80	26.26
Menlo	668	300	1	0.26	0.48	0.57
Menlo	668	300	60	0.48	0.53	0.67
Pints	668	220	60	6.36	6.16	7.23
Menlo	668	220	60	0.00	0.00	0.00
Pints	1425	300	60	9.69	9.73	9.82
Menlo	1425	300	60	0.55	0.77	0.90
Pints	1425	220	60	7.70	7.86	8.66
Menlo	1425	220	60	0.00	0.00	0.04

Table 22. Correlation between water absorption of 3/8 in. - #4 sieve fractions (x) and other absorption properties (y)

#	Property	Correlation coefficient (r) <sup>a</sup>	Equation
1	water absorption of cores	0.993	$y = -0.499 + 0.882x$
2	water absorption of +3/8 in. fractions	0.997	$y = 0.185 + 1.047x$
3	asphalt absorption of cores 1 min immersion, 2 hr absorption	0.969	$y = -0.242 + 0.341x$
4	asphalt absorption of cores 1 min immersion, 24 hr absorption	0.975	$y = -0.171 + 0.336x$
5	asphalt absorption of cores 1 min immersion, 2 wk absorption	0.975	$y = -0.167 + 0.329x$
6	asphalt absorption of cores 60 min immersion, 2 hr absorption	0.977	$y = -1.098 + 0.774x$
7	asphalt absorption of cores 60 min immersion, 24 hr absorption	0.978	$y = -1.018 + 0.774x$
8	asphalt absorption of cores 60 min immersion, 2 wk absorption	0.977	$y = -0.993 + 0.780x$
9	asphalt absorption of cores & #4 1 min immersion, 2 hr absorption	0.977	$y = -2.460 + 1.806x$
10	asphalt absorption of cores & #4 1 min immersion, 24 hr absorption	0.976	$y = -2.403 + 1.814x$
11	asphalt absorption of cores & #4 1 min immersion, 2 wk absorption	0.981	$y = -2.250 + 1.853x$
12	asphalt absorption of cores & #4 60 min immersion, 2 hr absorption	0.988	$y = -1.868 + 1.984x$
13	asphalt absorption of cores & #4 60 min immersion, 24 hr absorption	0.988	$y = -1.662 + 1.962x$
14	asphalt absorption of cores & #4 60 min immersion, 2 wk absorption	0.991	$y = -1.540 + 1.993x$

<sup>a</sup>significant at 1% level

Table 23. Correlation between water absorption of rock cores (x) and other absorption properties (y)

#	Property (y)	Correlation coefficient (r) <sup>a</sup>	Equation
1	asphalt absorption, + #4 1 min immersion, 2 hr absorption	0.990	$y = -1.401 + 2.054x$
2	asphalt absorption, + #4 1 min immersion, 24 hr absorption	0.989	$y = -1.326 + 2.062x$
3	asphalt absorption, + #4 1 min immersion, 2 wk absorption	0.992	$y = -1.169 + 2.104x$
4	asphalt absorption, + #4 60 min immersion, 2 hr absorption	0.995	$y = -0.833 + 2.254x$
5	asphalt absorption, + #4, 60 min immersion, 24 hr absorption	0.996	$y = -0.622 + 2.230x$
6	asphalt absorption, + #4, 60 min immersion, 2 wk absorption	0.996	$y = -0.511 + 2.262x$
7	asphalt absorption of cores, 1 min immersion, 2 hr absorption	0.946	$y = 0.074 + 0.368x$
8	asphalt absorption of cores, 1 min immersion, 24 hr absorption	0.950	$y = 0.125 + 0.364x$
9	asphalt absorption of cores, 1 min immersion, 2 wk absorption	0.950	$y = 0.123 + 0.356x$
10	asphalt absorption of cores, 60 min immersion, 2 hr absorption	0.977	$y = -0.551 + 0.865x$
11	asphalt absorption of cores, 60 min immersion, 24 hr absorption	0.979	$y = -0.480 + 0.866x$
12	asphalt absorption of cores,	0.979	$y = -0.460 + 0.874x$

<sup>a</sup>significant at 1% level

Table 24. Correlation coefficients for pore properties vs asphalt absorption

Properties	Value of correlation coefficients (r)			
	Asphalt absorption (BISG), %		Asphalt absorption (Immersion), %	
	Asphalt A	Asphalt B	Asphalt A	Asphalt B
<u>Porosity range, <math>\mu</math></u>				
21-11	-0.2902	-0.1970	-0.3361	-0.1172
21-5	-0.2738	-0.1831	-0.3099	-0.1040
21-2	-0.3233	-0.1903	-0.3903	-0.1163
21-1	-0.0294	0.1100	-0.1380	0.1038
11-1	-0.0020	0.1296	-0.1056	0.1157
5-1	0.0278	0.1471	-0.0722	0.1246
1-0.5	0.7063	0.7563	0.6806	0.7314
1-0.1	0.7663	0.8170 <sup>b</sup>	0.7247	0.7872
1-0.05	0.8063	0.8594 <sup>b</sup>	0.7595	0.8331 <sup>b</sup>
0.1-0.05	0.7925	0.8429 <sup>b</sup>	0.7226	0.8566 <sup>b</sup>
0.7-0.05	0.8208 <sup>b</sup>	0.8760 <sup>b</sup>	0.7708	0.8518 <sup>b</sup>
21-0.05 <sup>a</sup>	0.6248	0.7136	0.5516	0.6907
<u>Other Properties</u>				
24-hr soaked porosity	0.8884 <sup>b</sup>	0.9274 <sup>b</sup>	0.8238 <sup>b</sup>	0.9235 <sup>b</sup>
Bulk sp. gr. of cores	-0.9358 <sup>b</sup>	-0.9711 <sup>b</sup>	-0.8939 <sup>b</sup>	-0.9750 <sup>b</sup>
Water absorption (%)	0.9014 <sup>b</sup>	0.9341 <sup>b</sup>	0.8398 <sup>b</sup>	0.9280 <sup>b</sup>
Percent mercury retained at 10 psi	0.1400	0.2055	0.0217	0.0852

<sup>a</sup>Total effective porosity<sup>b</sup>Significant at 5% level

It can be noted that the correlation is poor in 21-11, 21-5, 21-2, 21-1, 11-1 and 5-1  $\mu$  pore size ranges. For the rest of the pore size ranges, the correlation coefficients in decreasing order are given in Table 25.

Table 25. Correlation coefficients for non-normalized pore sizes

Porosity range, $\mu$	Range of correlation coefficients
0.7 - 0.05	0.8760 - 0.7708
1 - 0.05	0.8594 - 0.7595
0.1 - 0.05	0.8566 - 0.7226
1 - 0.1	0.8170 - 0.7247
1 - 0.5	0.7563 - 0.6806
21 - 0.05	0.7136 - 0.5517
(mercury intrusion porosity)	

The range 0.7-0.05  $\mu$  was included in Table 25 since non-normalized pore size distribution curves for all six rock cores indicated a range from 0.05-0.71  $\mu$  for the peak pore radius (most frequent pore radius). The porosity in this range as determined by mercury porosimeter has excellent correlations with asphalt absorption. This is closely followed by the porosity in 1-0.05  $\mu$  range which is almost the same range for practical purposes. Correlation coefficient between porosities in these two ranges is 0.9987 (Table 7), which confirms this.

These ranges are then followed by the ranged 0.1-0.05 and 1-0.1  $\mu$  which obviously add up to make 1-0.05  $\mu$  range. Since the porosity in 0.7-0.05  $\mu$  range has correlation coefficient of 0.9894 and 0.6510 with porosities in ranges 1-0.1 and 0.1-0.05  $\mu$  respectively, it seems it is mainly dependent upon the porosity of the former range.

Effective porosity or mercury intrusion porosity (21-0.05  $\mu$  range) has correlation coefficients ranging from 0.7136 — 0.5517 with asphalt absorption. However, effective porosity does indicate the general trend of asphalt absorption.

An attempt was made earlier to make use of percent of pore volume distribution curves to correlate the values of pore radius ( $r$ ) corresponding to a specified percent of pore volume with the asphalt absorption. For example, in case of Menlo core, 90% of pore volume had pores of radii smaller than 15  $\mu$  ( $r_{10}$ ). All percentages of pore volume were tried, but only  $r_{10}$  gives some indication of the general trend of absorption. The results are shown in Table 26.

Table 26. Value of  $r_{10}$  radii

Quarry	Value of $r_{10}$ , $\mu$
Menlo	15
Pints	1.1
Alden	1.1
Linwood	3
Cook	1.8
Keota	13.0

It seems that different pore size ranges control the absorption of different liquids depending upon their viscosities, surface tension, contact angles with solids, etc. Observation of correlation coefficients between major pore properties (Table 7) will reveal that

0.1-0.05  $\mu$  porosity has the best correlation ( $r = 0.9782$ ) with 24-hr soaked porosity out of porosities in various ranges and hence may be regarded as the main controlling pore size range for water absorption as far as limestone rock cores in this study are concerned; while porosity in the 0.7-0.05  $\mu$  range has the best correlation with both effective porosity ( $r = 0.9009$ ) and asphalt absorption ( $r = 0.8760$  to  $0.7708$ ) out of various pore size ranges. As expected, water having good wettability has lower range of 0.1-0.05  $\mu$

compared to asphalt having higher range of 0.7-0.05  $\mu$  as the main controlling range.

The equations for regression lines for the linear correlations with 0.7-0.05  $\mu$  range discussed above are presented in Table 27.

Table 27. Relations between asphalt absorption and 0.7-0.05  $\mu$  porosity

Absorption method	Asphalt type	Equation for regression line <sup>a</sup>
BISG	A	$Y = 0.1294 + 0.135X$
	B	$Y = 0.1977 + 0.1563X$
Immersion	A	$Y = 0.3640 + 0.1255X$
	B	$Y = 0.3362 + 0.1593X$

<sup>a</sup>X = percent porosity in 0.7-0.05  $\mu$  range, and Y = percent asphalt absorption.

In all cases, correlations are better in case of Asphalt B having higher penetration than Asphalt A. Also, absorption values obtained from BISG method have better correlation with the porosity in the above pore size ranges than those obtained from immersion test.

The following conclusions can be drawn from these pore size and absorption correlations:

- Pore size distribution has direct effect on asphalt absorption.

To visualize this, Fig. 44 has been drawn to combine cumulative pore size distribution of Menlo and Pints cores on same scale.

Considerable difference in asphalt absorption between these two types of rock cores is reflected by the significant variation between the two curves. This is also evident in Fig. 45, which

combines hysteresis in mercury porosimetry of Menlo and Pints cores.

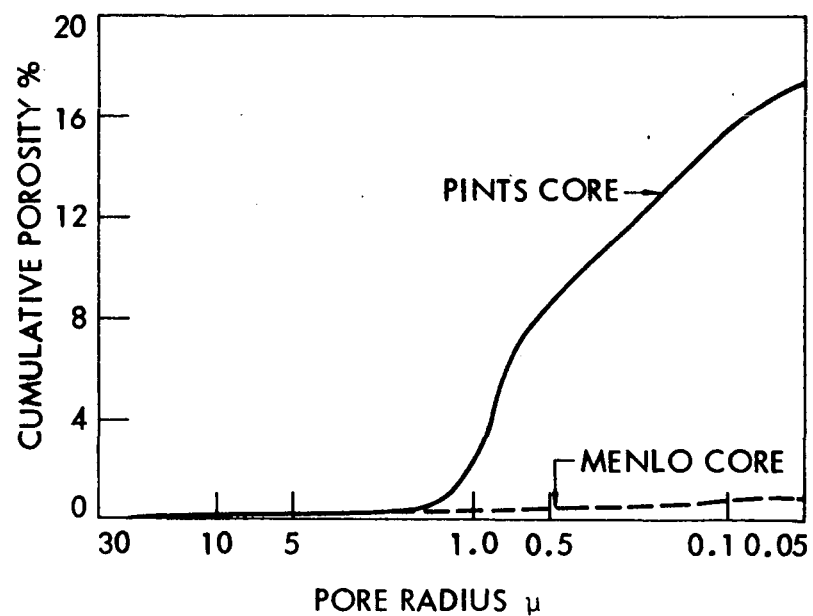


Fig. 44. Cumulative porosity distribution (Menlo vs Pints cores)

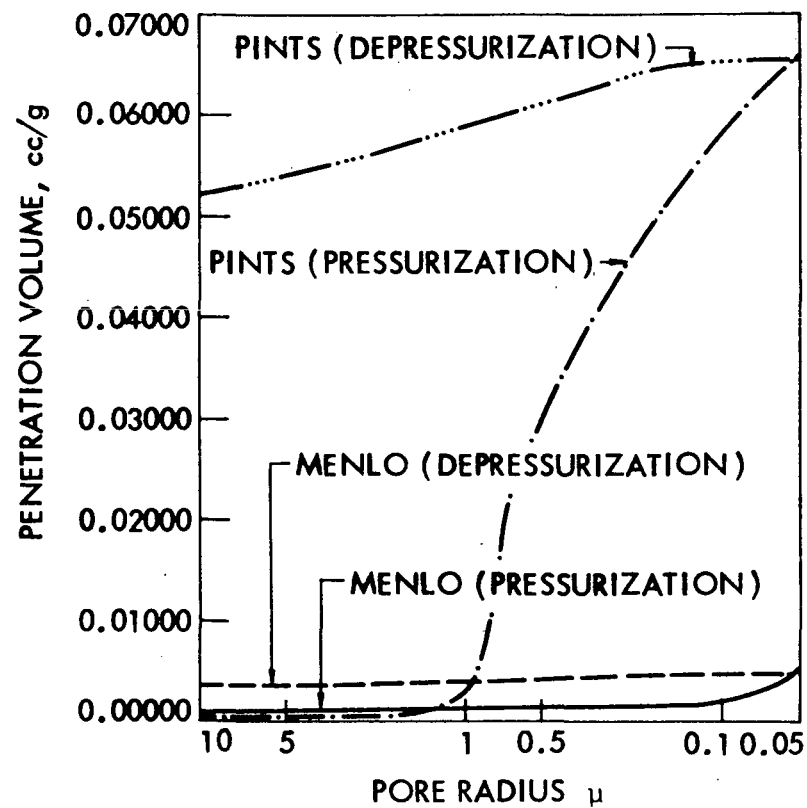


Fig. 45. Hysteresis in mercury porosimetry (Menlo vs Pints cores)



- Porosity in 0.7-0.05  $\mu$  size range has a direct effect on asphalt absorption. The relation is linear. Difference between absorption of Asphalt A and B gets larger as porosity in 0.7-0.05  $\mu$  range increases.
- Pore size in the 0.1-0.05  $\mu$  seems to determine the amount of water absorption.
- Effective porosity indicates a general trend of absorption of asphalt. Cores having more effective porosity (mercury intrusion) are likely to absorb more asphalt and vice-versa, provided the internal structure of the rock is not altered during mercury intrusion test.
- Percent mercury retained in the rock cores after depressurizing to 10 psi does not have any correlation with asphalt absorption (Table 24).

#### Asphalt Absorption by Photometer

Correlations between asphalt absorption by photo-colorimeter method and dye absorptions and asphalt absorption by immersion (Series C and D) are given in Table 28. Correlation coefficients between asphalt absorption and methylene blue absorption at 1 and 24 hr are 0.924 and 0.941, respectively, which are excellent (significant at 1% level), which also confirm the ranking table (Table 18) presented earlier. Correlation coefficients between asphalt absorption by the photometer method and the immersion method are from 0.652 to 0.817 (d.f. = 6).

Correlation coefficients between methylene blue absorption and asphalt absorption of corresponding laboratory crushed and fractioned aggregates of one minute immersion, 24 hr absorption and 60 min immersion, 24 hr

Table 28. Correlation between asphalt absorption by photocolormeter method (x) and other absorption properties (y)

No.	Property (y)	Correlation Coefficient (r)	Equation
1	Dye absorption, MB, 1 hr	0.924 <sup>a</sup>	$y = 0.0012 + 0.0001x$
2	Dye absorption, ST, 1 hr	0.295	$y = 0.0775 + 0.0005x$
3	Dye absorption, MB, 24 hr	0.941 <sup>a</sup>	$y = 0.0099 + 0.0002x$
4	Dye absorption, ST, 24 hr	0.652	$y = 0.2361 + 0.0011x$
5	Asphalt absorption, cores, 1 min immersion, 24 hr absorption	0.817 <sup>a</sup>	$y = -0.430 + 0.019x$
6	Asphalt absorption, cores, 60 min immersion, 24 hr absorption	0.672	$y = -0.882 + 0.036x$
7	Asphalt absorption, cores, + #4, 1 min immersion, 24 hr absorption	0.652	$y = -1.872 + 0.083x$
8	Asphalt absorption, cores, + #4, 60 min immersion, 24 hr absorption	0.709 <sup>a</sup>	$y = -1.689 + 0.096x$

<sup>a</sup>Significant at 5% level

Table 29. Linear correlation coefficients (r) between asphalt absorption by immersion

Absorp- tion	Cores						+ #4 fractions					
	1 min immersion			60 min immersion			1 min immersion			60 min immersion		
	2 hr (X <sub>15</sub> )	24 hr (X <sub>16</sub> )	2 wk (X <sub>17</sub> )	2 hr (X <sub>18</sub> )	24 hr (X <sub>19</sub> )	2 wk (X <sub>20</sub> )	2 hr (X <sub>21</sub> )	24 hr (X <sub>22</sub> )	2 wk (X <sub>23</sub> )	2 hr (X <sub>24</sub> )	24 hr (X <sub>25</sub> )	2 wk (X <sub>26</sub> )
X <sub>15</sub>	1.0000											
X <sub>16</sub>	0.9993	1.0000										
X <sub>17</sub>	0.9986		1.0000									
X <sub>18</sub>	0.9875			1.0000								
X <sub>19</sub>	0.9651			0.9998	1.0000							
X <sub>20</sub>	0.9618			0.9997		1.0000						
X <sub>21</sub>	0.9273			0.9790			1.0000					
X <sub>22</sub>	0.9271			0.9797			0.9999	1.0000				
X <sub>23</sub>	0.9324			0.9800			0.9991		1.0000			
X <sub>24</sub>	0.9340			0.9719			0.9949			1.0000		
X <sub>25</sub>	0.9335			0.9709			0.9945			0.9997	1.0000	
X <sub>26</sub>	0.9372			0.9716			0.9926			0.9997	0.9996	1.0000

absorption, are 0.730 and 0.773, respectively, both are significant at the 5% level.

It appears that the simple and rapid dye absorption test using methylene blue and photocolormeter can definitely be used to evaluate asphalt absorption.

#### Asphalt Absorption by Immersion Method

Correlation coefficients ( $r$ ) between 2 hr asphalt absorption results in Series C & D were calculated and given in Table 29. Even though  $r$  values are much higher for correlations within same series, cross-series correlations are also excellent (significant at 1% level). This means, when adequate data are available, absorption at one condition and time can be used to predict asphalt absorption at other conditions and time.

#### Field Study of Aggregate Absorption

As planned in the proposal, field study of absorption effects was to be conducted in the second phase of HR-142. It was proposed that four test sections of surface mixtures using absorptive aggregates of varied absorptive capacities (but without compensation of absorbed asphalts) would be laid as parts of regular construction projects during the 1968 construction season and the following parameters would be studied:

- Nature, occurrence, and frequency of cracks that may be observed at six-month intervals.
- The absorption history determined by the Rice method from point to pavement and at six-month intervals.
- Hardening and chemical changes in the asphalt at six-month intervals.

On August 6, 1968, Mr. Stephen E. Roberts, Research Engineer of the Iowa State Highway Commission, sent letters to nine county engineers (Butler, Decatur, Dubuque, Floyd, Mahaska, Sac, Wapello, Webster and Hardin Counties) asking for cooperation in the program. Subsequently, on September 11, 1968, letters were sent to the same county engineers by the principal investigator of Project HR-142, explaining the detailed field study program proposal. While some of the counties responded, none could participate in the program either because it was too late in the season or because no absorptive aggregates would be used in their paving projects. It was hoped that field study could be conducted during the 1970 construction season on either state or county paving projects. However, this again was not possible.

Nevertheless, absorption history has been studied on one asphalt surface project at Iowa State University laid on September 28, 1968. Aggregates used for the project were blends of 70% Cook's quarry 3/8-in. limestone and 30% concrete sand. Upon extraction, it was found that the asphalt content was 8.5% and the gradation of the aggregate was as shown in Table 30.

About 20 lb of the mixture was collected at the paver on September 28, 1968. Rice specific gravity of the mixture has been determined at regular intervals. Calculated asphalt absorption up to 1000 days is shown in Fig. 46, which clearly shows the increased asphalt absorption at a decreasing rate up to a year.

Table 30. Gradation of 1968 surface

Sieve	% Passing
3/8 in.	99.0
#4	77.9
#8	61.5
#30	29.9
#50	13.0
#100	6.9
#200	6.3
Bulk Specific Gravity	2.374

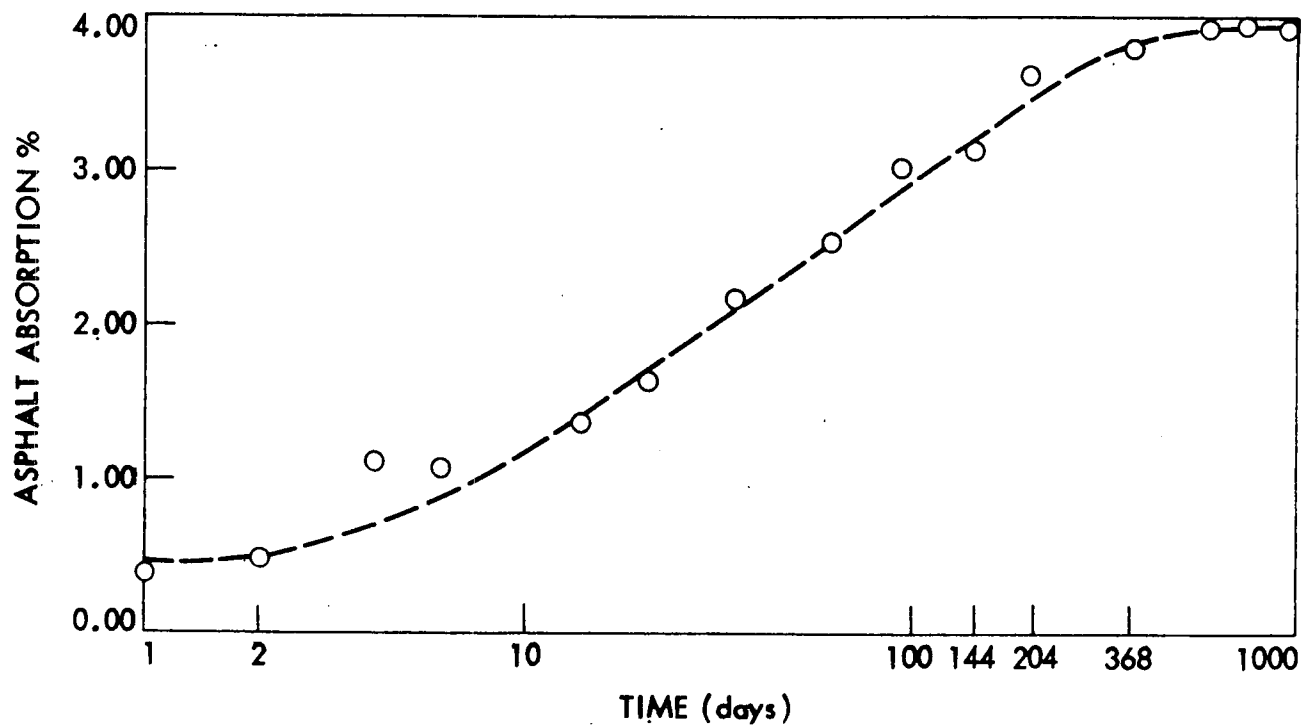


Fig. 46. Asphalt absorption vs time

## TREATMENT STUDIES

Summary

This chapter describes preliminary laboratory investigations undertaken to determine the most promising types of agents for absorptive aggregate treatment. The major objective at this time was to find what classes of chemicals will give the desired results. It is hoped that follow up work can be initiated to find agents most easily and economically applied, making the absorptive aggregates suitable for highway work. In this phase of work, practicability of application and economy were not controlling factors, although in later phases these considerations shall play a major role.

Five classes of agents were investigated in this project: (a) industrial wastes, (b) polymers, (c) synthetic resins, (d) inorganic chemicals, and (e) bituminous materials, each of which has advantages and disadvantages shown later in terms of effectiveness in water absorption reduction, asphalt absorption reduction, and relative costs. None of these fields has yet been exhausted. Efforts have been made, where possible, to suggest potential agents and references to related studies, especially soil stabilization studies, so further studies can be made.

Approach

One of the major objectives of this project was to investigate the possibility of utilizing absorptive but otherwise available and suitable aggregates. One approach in using absorptive aggregates in high-type asphalt paving mixtures is to treat the aggregate (prior to or during mixing with asphalt) with certain chemicals to reduce absorption, to

make binder content determination more reliable, and to avoid mixture deterioration due to excessive and selective absorption (adsorption).

The materials used in these treatments will achieve absorption reduction by: (a) changing the surface characteristics of the aggregate, (b) sealing the aggregate pores, (c) filling the aggregate pores, or (d) combining any of the above.

In order to serve this purpose, the chemicals or resulted end products of the treatments should be: (a) easily applied and no major health or other hazards, (b) effective in small quantities, (c) heat resistant to at least 200°C, (d) waterproof and water resistant, (e) resistant to freeze-thaw and volume change cycles, (f) resistant to chemical attack (inert), (g) good cementing agents and able to establish a strong bond with natural aggregates, and (h) readily coatable with bituminous materials. Certainly, cost of the chemical should be a major factor in determining the feasibility of using the chemical. However, it should be included in a total economic consideration of certain projects comparing availability of other quality aggregates, hauling costs of such aggregates, etc. Consequently, the cost was not a major consideration in selecting chemicals. Rather it was concerned with available chemicals and aggregates and how best to treat them.

Table 31 suggests some 40 chemicals that may have the potential of being used for aggregate treatment. About two-thirds of the listed chemicals were obtained and/or investigated in the study.

Not included in the table, but certainly having potential because of their uses in other film and coating applications, are polymers of all kinds such as polyethylene (10¢/lb), polypropylene (20¢/lb), styrene-butadiene rubber (SBR, 17¢/lb), various acrylic polymers, and PVC (polyvinyl chloride, 14¢/lb). Also deserving consideration are various thermosetting resins which



change irreversibly under the influence of heat from a fusible and soluble material into one which is infusible and insoluble through the formation of cross-linked, thermally stable network. These include phenolic resins (22¢/lb), amino resins (32¢/lb), epoxy resins (47¢/lb), and silicone resins, etc.

### Materials and Procedures

Three major series of chemical treatment experiments, all in laboratory scales, were conducted during this project. Materials and procedures involved in each series are as follows:

#### Series A

Two aggregates were used (Cook and Menlo), both graded (Grading A, Table 32) and core cylinders of 1 and 1/2 in., in conjunction with two asphalt cements (142-1 and 142-2) and four chemicals (aniline, furfural, Armac T, and methyl methacrylate). The properties of these chemicals are given in Tables 33 - 35. Not including screening and preliminary tests for mixing and curing conditions, a total of 16 treatments (2000 g mixtures) and 8 sets of treatment on cores, and 25 batches of asphalt concrete mixes made with treated aggregates, 20 lb each, were made. (See Ref. 94 for detailed procedures.) Treatments included 2:1 aniline furfural from 0 - 9% on graded aggregates and cores, Armac T (0 - 8%) on graded aggregates and cores, and impregnated methyl methacrylate treatment of cores by both thermal catalytic and gamma irradiation polymerizations.

Before the treatment of cylindrical rock cores with methyl methacrylate, preliminary investigations were made regarding impregnation and polymerization techniques.

Table 31. Potential materials for aggregate treatments

#	Material	Secondary Additives
1a	Acrylic polymer Rhoplex HA8	
1b	Acrylic polymer Rhoplex MC-4530	
1c	Acrylic Polymer Rhoplex E-330; E-460	
2	Acrylonitrile	
3a	Amsco Res 3001	
3b	Amsco Res 3004	
4	Aniline	Furfural
5	Armac T (Redicote E-44)	
6	Arquad 2HT (Redicote E-45)	
7a	Araplaz M- 95	
7b	Aroplaz 1254-M60	
7c	Aroplaz 1453 x 50	
8a	Asphalts emulsion	
8b	Asphalt cements	
8c	Asphalt cutbacks	
9	Calcium acrylate	P <sub>2</sub> O <sub>5</sub> Ammonium persulfate, sodium thiosulfate
10	Calcium chloride/sodium chloride	
11	Furfural	Aniline
12	Flyash	Lime
13a	Gantrez resins HY-0,L,M,H	
13b	Gantrez resins AN-139, 149	
14	Lignins (Lignosulfonate)	Sodium or potassium dichromate
15	Lime Ca(OH) <sub>2</sub> , CaO	
16	Methyl Methacrylate	TMPTMA, benzol peroxide
17	Methyl acrylate, ethyl acrylate	Benzol peroxide
18	NVX (Neutralized Vinsol resin)	
19	Polyacrylic acids	
20a	Polyvinyl alcohol (PVA) 52-22	
20b	Polyvinyl alcohol (PVA) 70-05	
20c	Polyvinyl alcohol (PVA) 71-30	
21	Polyvinyl acetate	
22	Phosphoric acid	Sodium fluosilicate
23	Phenol - formaldehyde resins (resionex)	Catalysts
24	Resorcinol - formaldehyde resins (amberite)	Catalysts
26	Resin 321 (gum resin - sodium rosinate - 3:1)	
26a	Rosins K-101 (a rosin modified phenolic)	
26b	Rosin K-1010 (phenolic)	
27	Rubber, latex (ammoniated)	
28	Superfloc	
29	Styrene (polystyrene)	TMPTMA + benzoyl peroxide
30	Stabinol (portland cement + complex resins - 3:1)	
31	Soilpak	
32	Silicones and related materials (e.g. silicone rubber)	
33	Sulfur	CaO, CaCl <sub>2</sub> , Mg Cl <sub>2</sub>
34	Silicates (sodium or potassium)	
35	Stabilizer AM-955 (AM-9)	Catalysts
36a	Siroc #1 (base)	Reactor and accelerator
36b	Siroc #2 (reactor)	
36c	Siroc #3 (accelerator)	
36d	Siroc #4 (accelerator)	
37	Tars	
38	Urea - formaldehyde resins (uformite)	
39	Vinyl acetate maleic acid (VAMA)	
40	Vinsol resin	
41	Sodium carbonate	
42	Shellac	
43	Epoxy resins	
44	Polyesters	

Table 31. Cont'd.

#	Cost	Source	Reference	Remark
1a	15¢/lb	Rohm and Haas Co.	58	Resin emulsions
1b	17¢/lb	Rohm and Haas Co.	58	Resin emulsions; cement modifiers
1c	17¢/lb	Rohm and Haas Co.	58	Resin emulsions; cement modifiers
2	\$2.20/kg		42,59,71	
3a	13¢/lb	Union Oil Co. of Calif.	84,86	Polyvinyl acetate emulsion
3b	12.5¢/lb	Union Oil Co. of Calif.		Polyvinyl acetate emulsion
4	\$8.00/gal	E.I. du Pont	49,50,81a	
5	31¢/lb	Armour Industrial Chemical	79	Amine acetate
6	26¢/lb	Armour Industrial Chemical	42,43,67	Quaternary ammonium chloride
7a	18¢/lb	Ashland Chemical Co.		Hammer resin
7b	21.1¢/lb	Ashland Chemical Co.		Architectural resin
7c	14.5¢/lb	Ashland Chemical Co.		Low cost enamels
			86-92	
			86-88	
			86-88	
9	\$19.50/kg	Borden Chemical	53,54,63,70,73,82,84	
			73,78	
11	\$4.00/kg		49,50	
			73,74	
13a	\$1.72/lb	G.A.F. Corp.		
13b	\$1.01/lb	G.A.F. Corp.		
14	6¢/lb	Scott Paper Co.	52,65,66,81	
			51,73,92	
16	45¢/lb		48	
17	\$2.20/lb	Borden Chemical	84,87	
18	10¢/lb	Hercules Inc.	56,73,75,81	
19	\$3.00/kg	Borden Chemical	41,42,43,67	
20a	55¢/lb	E.I. du Pont	41,42,44,72,81	
20b	51¢/lb	E.I. du Pont	41,42,44,72,81	
20c	45¢/lb	E.I. du Pont	41,42,44,72,81	
			41,42,80	
			68,77,84-92	
		Monsanto	49,56,73	
		Rohm and Haas Co.	56,73	
		Hercules Inc.	81,56,73,75,76	Salt of abietic acid
26a	25¢/lb	Lawter Chemicals Inc.		
26b	38.5¢/lb	Lawter Chemicals Inc.		
27	\$3.50/gal	Heveatex Co.	81	
		Fisher Chemical	41,42	
29	15¢/lb		42,48,86	
			56,73,75,81	
			56	
32	\$30/gal	Dow Chemicals	42,54,55,63,82	
33	2.6¢/lb	Stauffer Chemical Co.	63,81	
		Philadelphia Quartz	41,42,45,61,63,73,81,90,91	
35	60¢/lb	Am. Cyanamid Co.	62,63,64	Acrylamide
36a	33¢/gal	Raymond International Inc.		Modified sid. silicate
36b	\$1.60/gal	Raymond International Inc.		Amide
36c	\$6.50/cwt	Raymond International Inc.		Calcium chloride
36d	\$32/cwt	Raymond International Inc.		Sod. Alluminate
			49,56,73,82	
			41,42,46,47,69,71	
40	7.5¢/lb	Hercules Inc.	56,73,75,81	
			81	
			82	
			85,86,88	
			86,87	

Table 32. Chemical treatments grading A

Sieve size	% Passing
3/4 in.	100
1/2 in.	85
3/8 in.	63
#4	27
#8	0

Table 33. Physical constants of aniline

Properties	
Molecular weight	93.1
Color	Colorless to light yellow
Boiling point (760 mm)	184.2°C
Freezing point	-6.2°C
Specific gravity of liquid 20°/4°C	1.022
Density at 20°C	1.022
Viscosity at 77°F cP	4
Ignition temperature	770°C
Flash point (closed cup)	70.0°C
Flash point (open cup)	75.6°C
Solubility of aniline in water at 77°F	5.2 wt %
Solubility in organic solvent	Miscible with alcohol, benzene and most organic solvents

Table 34. Physical constants of furfural

Properties	
Molecular weight	96.08
Melting point	-36.5°C
Boiling point	161.7°C
Flash point (open cup)	56.8°C
Viscosity at 25°C	1.49 cP
Heat of combustion	560.1 kg cal/mol
Specific gravity at 20°/4°C	1.1598
Solubility in water (wt % at 20°C)	8.3
Solubility in al (wt % at 20°C)	infinite
Solubility in ether (wt % at 20°C)	infinite
Ignition temperature	393°C

Table 35. Physical constants of methyl methacrylate

Properties	
Color	colorless liquid
Boiling point	100°C
Density $d_4^{20}$	0.936
Index of refraction	1.413
Melting point	48°C
Specific heat	0.49 cal g/°C
Solubility in water at 30°C	1.5 wt %
Viscosity at 25°C	0.569 centistokes

Table 36. Chemical treatment grading B (sulfur series)

Sieve size	% Passing
3/4 in.	100
1/2 in.	90
3/8 in.	77
#4	59
#8	45
#30	24
#50	17
#100	11
#200	6

Impregnation treatment. To determine the condition required to obtain any desired degree of monomer loading in the rock cores, it is necessary to investigate the various parameters that alone or in combination give the best preparatory results. Monomer loading is defined as the weight percent increase of an untreated specimen.

Many factors influence monomer penetration. The main effort has been to obtain a maximum monomer loading in the samples, principally through removal of free water and air from the specimens by vacuum or thermal drying, the latter of which was found to be the most practicable for water removal because of its relative rapidity.

Another important parameter to be considered to obtain maximum monomer loading or to improve the efficiency of impregnation is evacuation of the specimens prior to soaking. Figures 47 and 48 show time-loading curves for the two rocks.

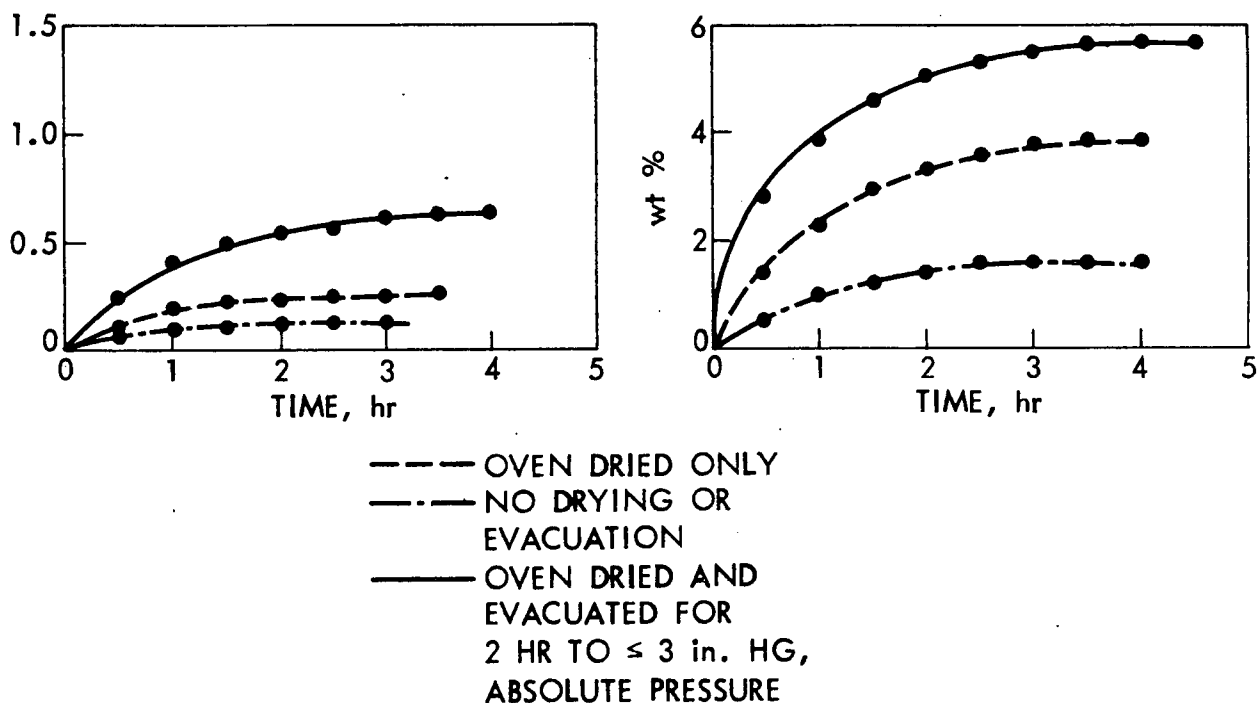


Fig. 47. Monomer loading vs time for Cook cylinders

Fig. 48. Monomer loading vs time for Menlo cylinders

Polymerization techniques. After impregnation of rock cores with liquid monomer consisting of 90 wt % of methyl methacrylate plus 10 wt % of trimethylolpropane trimethacrylate, it is polymerized by one of two methods: cobalt gamma radiation or thermal catalytic technique.

Preliminary tests to estimate maximum radiation dose requirement for complete polymerization of the monomer solution were conducted at the Ames Laboratory Research Reactor (ALRR) of the US Atomic Energy Commission. Dosages ranging from 0.2-4.5 megarads were used. Results show that in the case of methyl methacrylate plus 10% trimethylolpropane trimethacrylate, a radiation dosage of 1.0 megarad is necessary.

Thermal catalytic method of initiating the polymerization of monomer was also investigated. In this procedure, heat is used in conjunction with a free radical initiator such as benzoyl peroxide. In the present investigation, 1 wt % of benzoyl peroxide was added to the monomer solution and polymerized at a temperature of 185°F. It was found that polymerization was complete within 1 hr.

Treated aggregates were tested for water absorption, asphalt absorption by bulk-impregnated specific gravity method and Rice specific gravity method, and heat stability at 500°F. Asphalt concrete mixes of treated and untreated aggregates were compared on Marshall properties (stability, flow, voids and VMA), 24 hr Marshall immersion tests, and optimum asphalt contents.

#### Series B

In this series, sulfur (tire sulfur) was used to treat all six types of laboratory crushed and graded (both grades A and B, Tables 32 and 36) aggregates. Twenty-six mixes (2000 g each) were made with sulfur content varying from 0 - 9 wt % of aggregate. Seventeen of these sulfur treated



aggregates were also mixed asphalt, and asphalt absorption by the Rice method was determined at various time intervals up to 135 days.

### Series C

This was by far the most extensive, though not exhaustive, of the three series of treatment studies. A total of 148 batches of 1000 g mixtures were made with 30 chemicals. All aggregates were laboratory crushed (from block rock samples) and graded to meet either Grading A or Grading B. In several cases, due to limited quantities of laboratory crushed materials, single sized aggregates were used. They were either between 1/2 in. and 3/8 in. (+3/8 in.), between 3/8 in. and #4 (+#4) or passing #4 and retained on #8 (+#8). Aggregates were first batched and oven-dried before chemicals were added. In most cases, chemicals were maintained between 0.25 - 2.00 wt % of the aggregate. Chemicals were first diluted or dissolved in water or suitable solvent to a volume enough to cover all aggregate particles (calculated from water absorption data) and then added to the aggregates and hand mixed in a Hobart Kitchard mixer. Depending on type of chemical and solvent used, they were either air-cured or oven-cured (either 140 or 220°F) to constant weight before absorption tests were run. Absorption of treated and control samples were evaluated by the following manner: If the chemical is water soluble (such as PVA), the treated mix was mixed with asphalt cement (just enough to cover all particles) and asphalt absorption was determined at the end of one and two weeks. If the chemical involved is water insoluble, water absorption of the treated aggregate was first determined before mixing with asphalt for asphalt absorption determinations. Asphalt absorption in either case was determined by the Rice specific gravity method. For a summary of results of treatment in Series C, see Table 37.

Table 37. Series C aggregate treatment

Quarry	# treatment	# chemical	Gradings
Alden	12	10	A, B
Cook	11	11	A, +3/8 in.
Keota 1	11	8	A, B, + #4
Keota 2	14	11	A, B, +3/8 in.
Linwood	26	20	A, + #8
Menlo	21	18	A, +3/8 in.
Pints	39	23	A, B, + #4
X	14	10	A, + #8
Total	148	30	

### Results

#### Series A

#### Aniline Furfural Treatment

Treatment on graded crushed aggregate. The results of the tests conducted on the aggregates studied were encouraging. In Tables 38 - 40 water absorption and asphalt absorption for both untreated and treated aggregates are summarized.

While standard curing was done at 220-230°F for 5 days, curing curves for coarse-graded Cook and Menlo aggregates at 6% aniline-furfural were established for two other temperatures, 140 and 325°F. (Fig. 49). It can be seen that curing at 225 and 325°F can be considered complete after 24 hr, while curing at 140°F takes about 100-120 hr. The effectiveness of aniline furfural treatment was also dependent upon curing temperature, curing at lower temperature being more effective than these cured at higher temperatures (Fig. 50).

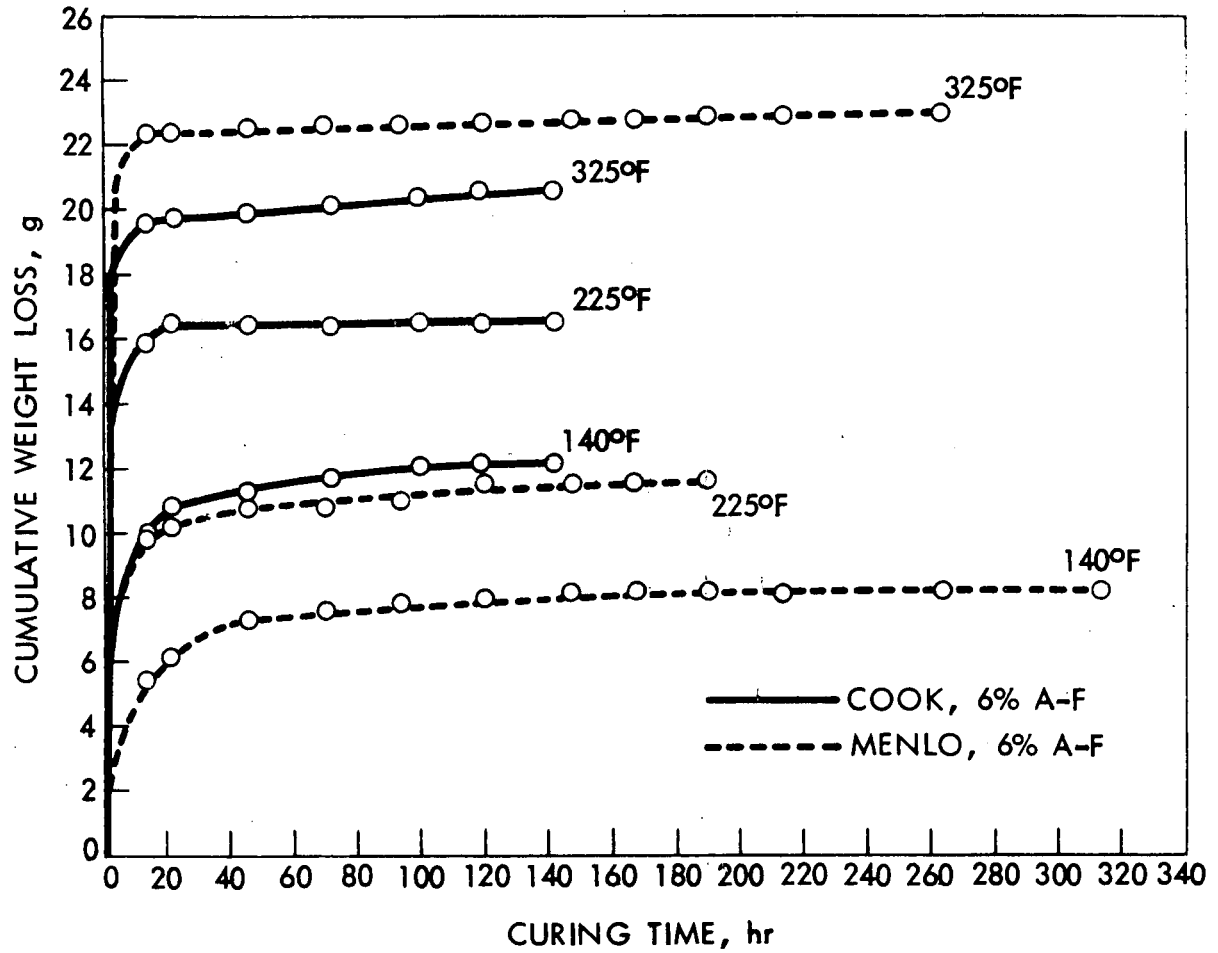


Fig. 49. Curing curves for aniline furfural treatments

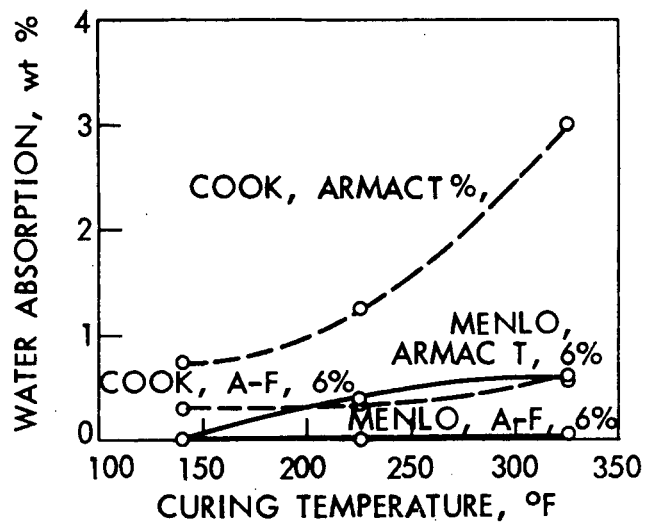


Fig. 50. Effects of curing temperature on water absorption

Effects of percent aniline furfural on water absorption of treated coarse graded aggregates are shown in Figs. 51 and 52. A sharp decrease was found in water absorption with 3% aniline furfural treatment. It was

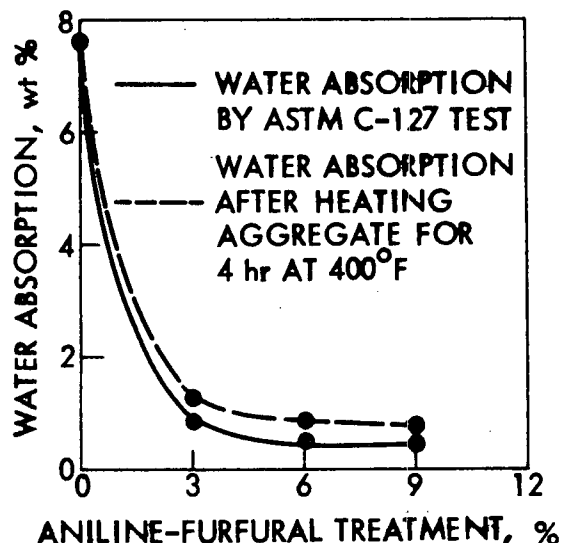


Fig. 51. Water absorption of Cook aggregate vs percent aniline furfural treatment

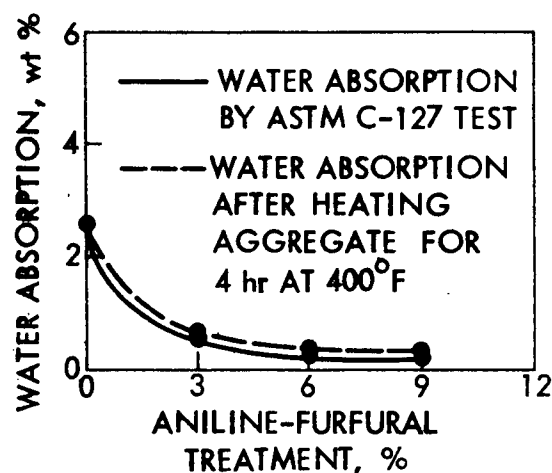


Fig. 52. Water absorption of Menlo aggregate vs percent aniline furfural treatment

also found that an increase in the percentage of aniline furfural beyond 6% resulted in very small decrease in water absorption.

In order to determine if heating at temperatures higher than the curing temperature of 220-230°F had any effect on the aggregates, both the untreated and treated aggregates were oven heated at a constant temperature of 400°F for 4 hr. Specific gravity and absorption tests were then conducted on these aggregates and their values are given in Table 39.

On heating the treated aggregates to 400°F for 4 hrs, a subsequent increase in water absorption over the unheated but treated aggregates was found. Treatments were still effective in reducing absorption. This change may be attributed to the burning of aniline furfural resin from the surface and pores of the aggregates.

Table 38. Specific gravity, water absorption, water permeable pores of graded crushed aggregates treated with aniline furfural

Aggregate	Treatment	Apparent specific gravity	Bulk specific gravity	Water absorption, wt %	Water permeable pores, %
Cook	Untreated	2.778	2.293	7.62	17.50
Cook	3% aniline furfural	2.360	2.314	0.86	2.00
Cook	6% aniline furfural	2.385	2.367	0.49	0.91
Cook	9% aniline furfural	2.400	2.380	0.44	0.90
Menlo	Untreated	2.663	2.392	2.57	6.42
Menlo	3% aniline furfural	2.598	2.565	0.50	1.27
Menlo	6% aniline furfural	2.537	2.521	0.26	0.65
Menlo	9% aniline furfural	2.519	2.506	0.20	0.52

Table 39. Heat stability of graded crushed aggregates treated with aniline furfural

Aggregate	Treatment	Apparent specific gravity	Bulk specific gravity	Water absorption, wt %	Water permeable pores, %
Cook	Untreated	2.778	2.293	7.62	17.5
Cook	3% aniline furfural	2.391	2.321	1.25	2.92
Cook	6% aniline furfural	2.425	2.375	0.85	2.03
Cook	9% aniline furfural	2.411	2.370	0.72	1.71
Menlo	Untreated	2.663	2.492	2.57	6.42
Menlo	3% aniline furfural	2.595	2.555	0.60	1.54
Menlo	6% aniline furfural	2.527	2.503	0.38	0.83
Menlo	9% aniline furfural	2.533	2.516	0.27	0.69

Asphalt absorption was determined by bulk impregnated specific gravity test (BISG). Two asphalts having penetrations of 92 and 127 were used. Results of asphalt absorption tests are summarized in Table 40.

Table 40. Asphalt absorption (wt %) of graded crushed aggregates treated with aniline furfural

Aggregate	Treatment	Asphalt	
		85-100 penetration	120-150 penetration
Cook	Untreated	4.28	3.82
Cook	3% aniline furfural	3.39	3.28
Cook	6% aniline furfural	1.66	1.56
Cook	9% aniline furfural	1.60	1.33
Menlo	Untreated	3.13	2.21
Menlo	3% aniline furfural	1.56	1.41
Menlo	6% aniline furfural	1.12	0.90
Menlo	9% aniline furfural	0.80	0.66

It was shown earlier that the reduction in water absorption was negligibly small beyond 6% aniline furfural treatment. Figures 53 and 54 show a similar trend of asphalt absorption for the two asphalts.

When the aggregates are mixed with 2:1 aniline furfural, the polar nature of the resin enables it to be easily absorbed both on the surface and within the interstices in the mass of the aggregates. The thin film of resin on the surface of these aggregates brings about certain changes in the surface properties of these aggregates, as a result of which they lose their affinity for water, becoming water repellent. This change in

Table 41. Specific gravity and water absorption of 1/2 in. cores treated with aniline furfural

Core	Treatment	Apparent specific gravity	Bulk specific gravity	Water absorption, %	Asphalt absorption, %	
					85-100 penetration	120-150 penetration
Cook	Untreated	2.72	2.48	3.61	0.68	0.65
Cook	2:1 aniline furfural	2.48	2.45	0.38	0.20	0.18
Menlo	Untreated	2.71	2.66	0.69	0.30	0.28
Menlo	2:1 aniline furfural	2.64	2.63	0.16	0.15	0.13

Table 42. Specific gravity, water absorption and permeable pores of Armac T treated crushed aggregates

Aggregate	Treatment	Apparent specific gravity	Bulk specific gravity	Water absorption, wt %	Permeable pores, %
Cook	Untreated	2.778	2.293	7.62	17.50
Cook	1/2% Armac T	—	—	3.46	—
Cook	1% Armac T	2.570	2.309	3.43	7.91
Cook	3% Armac T	2.442	2.324	2.08	4.83
Cook	6% Armac T	2.438	2.366	1.27	3.00
Cook	8% Armac T	—	—	0.77	—
Menlo	Untreated	2.663	2.492	2.57	6.42
Menlo	1/2% Armac T	—	—	1.16	—
Menlo	1% Armac T	2.608	2.528	1.21	3.7
Menlo	3% Armac T	2.574	2.519	0.85	2.13
Menlo	6% Armac T	2.505	2.481	0.39	0.96
Menlo	8% Armac T	—	—	0.40	—

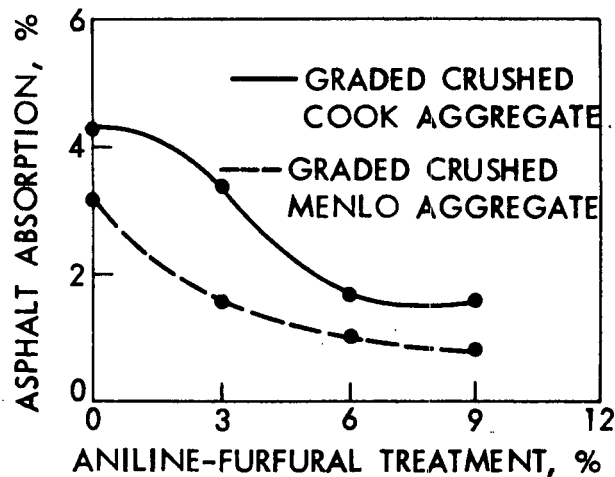


Fig. 53. Absorption of 85-100 penetration asphalt by graded crushed aggregates vs aniline furfural treatment.

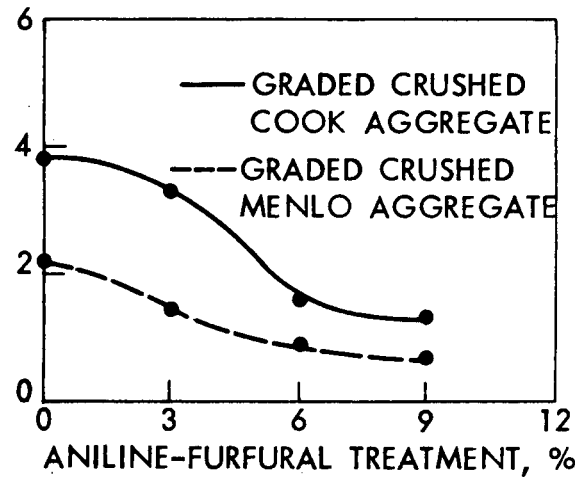


Fig. 54. Absorption of 120-150 penetration asphalt by graded crushed aggregates vs aniline furfural treatment

surface property is primarily responsible for the sharp decrease in water absorption characteristics of the aggregates. Decrease in asphalt absorption may be attributed to the plugging of the interstices as a result of resin formation inside.

Treatment on 1/2 in. cores. Results of tests conducted on 1/2 in. cores treated with 2:1 aniline furfural indicates that treatment on cylindrical cores are much more effective than on graded crushed aggregates. Table 41 gives the water and asphalt absorption of both untreated and treated cores from Cook and Menlo quarries.

On heating these treated cores to 400°F for 4 hrs, no change in specific gravity and water absorption was found. This indicates that 1 hr of soaking in the chemicals is a more effective method of treatment than the regular mixing procedure adopted for graded crushed aggregates.

Asphalt absorption of the treated cores was reduced to negligible value.



### Armac T. Treatment

Treatment on graded crushed aggregates. Similar tests were conducted on the aggregates treated with different percentages of Armac T. Results of specific gravity, water absorption and asphalt absorption are given in Tables 42 - 44. Results obtained by this treatment were also favorable but were not as effective as 2:1 aniline furfural treatment.

An appreciable reduction in water absorption was found (Fig. 55) with an increasing amount of Armac T. For 6% Armac T treatment, reduction in water absorption was of the order of 84% for Cook aggregate and 85% for Menlo aggregate.

On heating the treated aggregates to 400°F for 4 hr, it was found that the water absorption was further decreased. One possible explanation could be the presence of some unreacted Armac T which reacts at 400°F, thereby forming more resin both on the surface and within the porous medium of the aggregates.

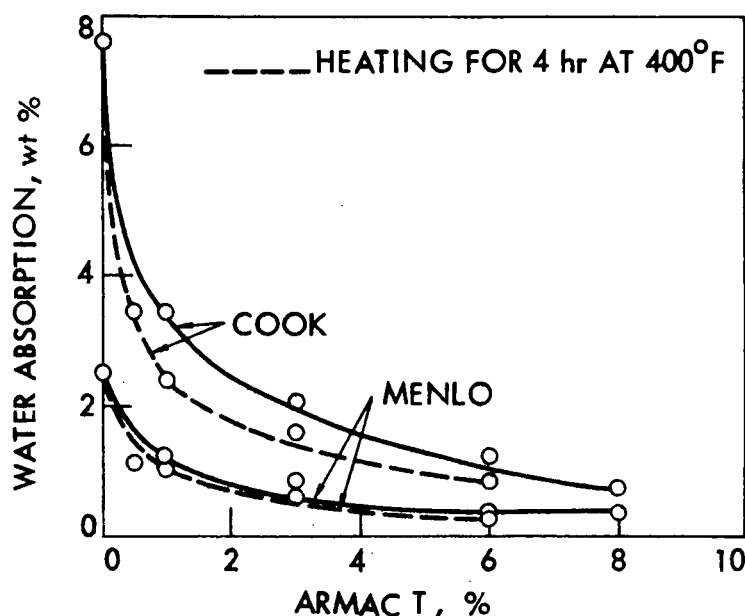


Fig. 55. Water absorption vs percent Armac T treatment

Table 43. Heat stability of graded crushed aggregates treated with Armac T

Aggregate	Treatment	Apparent specific gravity	Bulk specific gravity	Water absorption, wt %	Permeable pores, %
Cook	Untreated	2.778	2.293	7.62	17.50
Cook	1% Armac T	2.450	2.314	2.40	5.56
Cook	3% Armac T	2.417	2.324	1.63	3.78
Cook	6% Armac T	2.386	2.336	0.89	2.06
Menlo	Untreated	2.663	2.492	2.57	6.42
Menlo	1% Armac T	2.636	2.558	1.14	2.92
Menlo	3% Armac T	2.579	2.541	0.72	1.96
Menlo	6% Armac T	2.544	2.513	0.35	0.83

Asphalt absorption tests were carried out in both untreated and treated aggregates and fairly good results were obtained. Results of asphalt absorption by bulk impregnated specific gravity tests are given in Table 44.

Table 44. Asphalt absorption (wt %) of graded crushed aggregates treated with Armac T

Aggregate	Treatment	Asphalt	
		85-100 penetration	120-150 penetration
Cook	Untreated	4.28	3.82
Cook	1/2% Armac T	3.32	—
Cook	1% Armac T	3.25	3.36
Cook	3% Armac T	2.37	2.77
Cook	6% Armac T	1.78	1.89
Cook	8% Armac T	1.62	—
Menlo	Untreated	3.13	2.21
Menlo	1/2% Armac T	2.01	—
Menlo	1% Armac T	1.56	1.28
Menlo	3% Armac T	1.18	0.80
Menlo	6% Armac T	0.69	0.54
Menlo	8% Armac T	0.47	—

Like aniline furfural resins, Armac T has the ability to cause similar changes in the surface properties of the aggregates. With Armac T Treatment, reduction in asphalt absorption is not much compared to that for water absorption. Decrease in asphalt absorption could be due to the sealing of the pores of the aggregates by Armac T resins.

Curing curves for Armac T treated graded aggregates were determined for 6% Armac T at 140°F, 225°F and 325°F, and for 1/2% and 8% treatments at 225°F. The required curing time was dependent upon curing temperature, percent chemical and type of aggregate, and that, except for 140°F curing which required 100-120 hr, curing can be considered complete within 24 hr. The effects of curing temperature on the effectiveness of absorption reduction was the same as for aniline furfural treatment: higher curing temperature decreases the effectiveness (Fig. 50).

Graded aggregates were also treated by soaking in 1/2 and 3% Armac T water solution. The results indicated that it was not as effective as the mixing method.

Treatment of 1/2 in. cores. Half-inch cylindrical cores from Cook and Menlo quarries were also treated with Armac T solution. After proper curing, ASTM C-127 tests and asphalt absorption were conducted on these cores. Results of these tests are summarized in Table 45. Considerable reduction in water and asphalt absorption was observed.

#### Monomer Treatment

Treatment of 1 in. cores. The results of the tests conducted on Cook and Menlo cores indicate that monomer impregnation of the cylindrical rock cores to be the best method of reducing the absorptive capabilities of rock cores. The results of specific gravity, water absorption and asphalt

absorption for both the untreated and treated cylindrical cores have been summarized in Tables 46 and 47. Both thermal and radiation polymerization of the impregnated cores brought about the same degree of reduction in water and asphalt absorption.

Table 45. Specific gravity and absorption of 1/2 in. cores treated with Armac T

Cook	Treatment	Apparent specific gravity	Bulk specific gravity	Water absorption %	Asphalt absorption, %	
					85-100 penetration	120-150 penetration
Cook	Untreated	2.723	2.479	3.61	0.68	0.65
Cook	Armac T	2.487	2.460	0.47	0.26	0.25
Menlo	Untreated	2.712	2.662	0.69	0.30	0.28
Menlo	Armac T	2.685	2.620	0.19	0.18	0.18

Table 46. Specific gravity and absorption of cores impregnated with monomer

Core	Treatment	Apparent specific gravity	Bulk specific gravity	Water absorption, wt %	Permeable pores, %	Asphalt absorption, %
Cook	Untreated	2.723	2.479	3.61	8.97	0.68
Cook	Thermal polymerization	2.542	2.536	0.21	0.24	0.04
Cook	Radiation polymerization	2.551	2.534	0.57	0.67	0.07
Menlo	Untreated	2.712	2.662	0.69	1.85	0.30
Menlo	Thermal polymerization	2.673	2.673	0.00	0.00	0.00
Menlo	Radiation polymerization	2.671	2.668	0.00	0.11	0.05

Table 47. Specific gravity and absorption of graded crushed aggregates treated with monomer

Aggregate	Treatment	Apparent specific gravity	Bulk specific gravity	Water absorption wt %	Asphalt absorption %
Cook	Untreated	2.778	2.293	7.62	4.28
Cook	Thermal polarization	2.375	2.348	0.96	0.89
Menlo	Untreated	2.663	2.492	2.57	3.13
Menlo	Thermal polarization	2.590	2.564	0.85	0.78

On heating both thermal and radiation polymerized cylindrical cores to 400°F for 4 hr to determine their heat stability, values identical to the ones cited in Table 41 were obtained. This is a good indication of the heat stability of the impregnated polymer at temperatures as high as 400°F. This is mainly due to the cross-linking of the monomer with trimethylolpropane trimethacrylate, one of the functions of which is to increase the softening point of the monomer solution.

Treatment on graded crushed aggregates. Graded crushed aggregates from Cook and Menlo quarries were impregnated with the monomer solution, consisting of methyl methacrylate plus 10% trimethylolpropane-trimethacrylate plus 1% benzoyl peroxide, and then thermally polymerized at 185°F to compare the results of water and asphalt absorption of these aggregates with those of 1 in. cylindrical cores impregnated with the same monomer solution and thermally polymerized. Results of specific gravity, water and asphalt absorption of these impregnated aggregates are given in Table 47.

Reduction in water and asphalt absorption of graded crushed aggregates and cylindrical cores treated with the monomer solution was primarily due to the sealing of the pores as a result of polymerization of impregnated monomer solution. It was found that unlike aniline furfural and Armac T treatments, asphalt absorption values were lower than water absorption. This indicates that there was no change in the surface characteristics of the monomer treated aggregates.

### Asphalt Concrete Mixtures

In order to determine the performance of the chemically treated aggregates in asphalt paving mixtures, asphalt concrete mixtures using treated and untreated aggregates were prepared.

Untreated aggregates. Marshall specimens were prepared with untreated aggregates from Cook and Menlo quarries. In both cases, agricultural lime passing #8 sieve were added to the coarse Cook and Menlo fractions so that the combined gradation meet the Iowa Type A mix gradation. Four different percentages (6, 7, 8, and 9%) of 120-150 penetration asphalt cement were used in these mixes. From the values of Marshall Stability, flow, air void and voids in mineral aggregate (VMA), the optimum asphalt content of the asphalt paving mixes was determined. On the basis of these tests, it was found that 7.5 wt % asphalt mix was necessary for both aggregates (Figs. 56 and 57). In these figures, stability and flow values for Marshall Immersion Compression tests have also been plotted. It is found that for an asphalt content of 7.5%, the resistance of bituminous mixtures to the detrimental effect of water as expressed by percent retained strength are of the order of 74 and 77% for mixtures containing Cook and Menlo fraction, respectively. The US Army Corps of Engineers uses 75% retained strength as one of the criteria in bituminous mixture design. If this criterion is used in our mixture design, it is found that bituminous mixtures using Cook aggregate do not meet the requirement even at a high asphalt content of 7.5%.

### Treated aggregates

Aggregates from Cook and Menlo quarries and agricultural lime were treated with 6 wt % of 2:1 aniline furfural and Armac T. The selection of

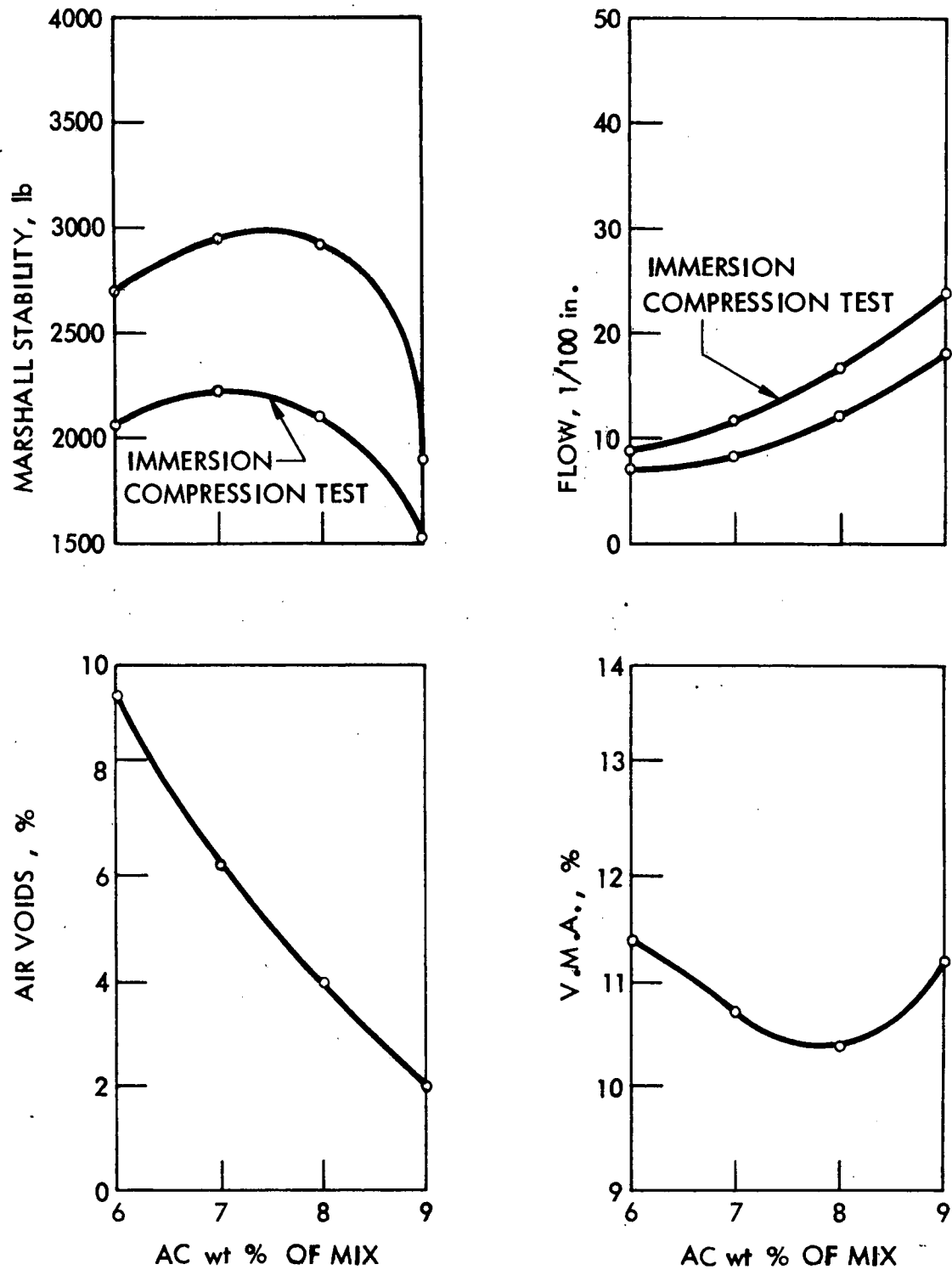


Fig. 56. Test property curves for mixes containing Cook aggregate and agricultural lime by the Marshall method

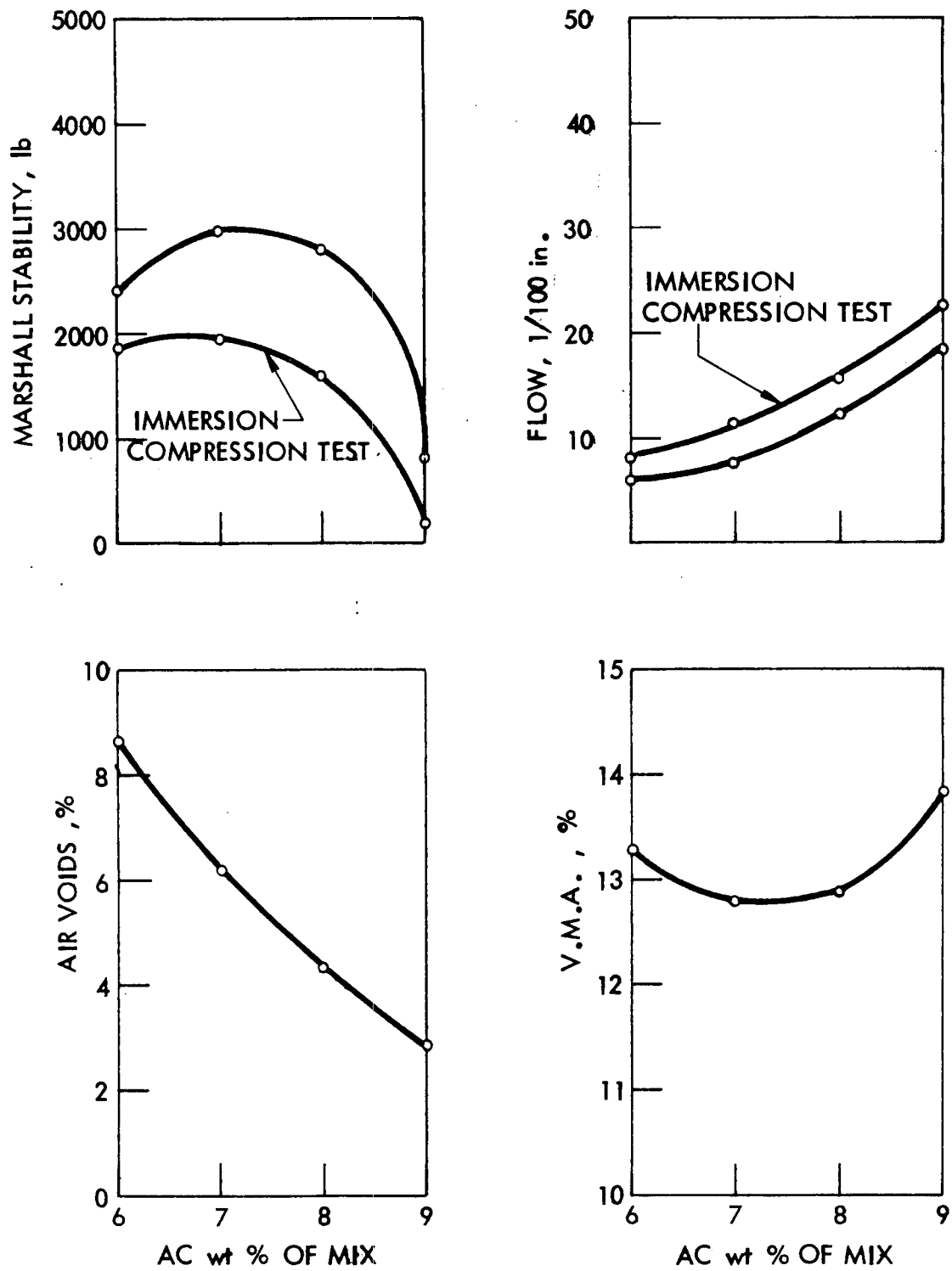


Fig. 57. Test property curves for mixes containing Menlo aggregate and agricultural lime by the Marshall method



6 wt % of these chemicals was based upon the results of tests on graded crushed aggregates treated with these chemicals.

Bituminous mixtures were made with aggregate treated with 2:1 aniline furfural using 120-150 penetration asphalt cement and Marshall specimens prepared. Figures 58 and 59 give the test property curves for mix design data by the Marshall method.

It was found that for aniline furfural treated aggregates, asphalt content for mixtures containing Cook aggregate was reduced to 5.5% and for those containing Menlo aggregate, 4.8%. The percent retained strength of the mixtures at optimum asphalt contents were 83 and 82%, respectively.

Bituminous mixtures were also prepared with Armac T treated aggregates. Results of the tests on these mixtures are summarized in Figs. 60 and 61. Optimum asphalt content for mixtures containing Cook aggregate was 5.6%; for those containing Menlo aggregate, 5%. The percent retained strength of the mixtures at optimum asphalt content were 81 and 84% respectively. The lowering of the optimum asphalt content and considerable increase in the percent retained strength of the chemically treated aggregate bituminous mixtures can be attributed to the effective chemical treatment of these aggregates.

Rice specific gravity tests were conducted on asphalt paving mixtures to determine the amount of asphalt absorbed by the treated aggregates in the mixtures. Results of these tests are given in Table 48. The absorption values are high even for these aggregates, due probably to incomplete coating of the particles. Thus the absorption indicated could be the combined absorption of both asphalt and some water. Nevertheless, considerable reduction in asphalt absorption of paving mixture was observed due to the treatments.

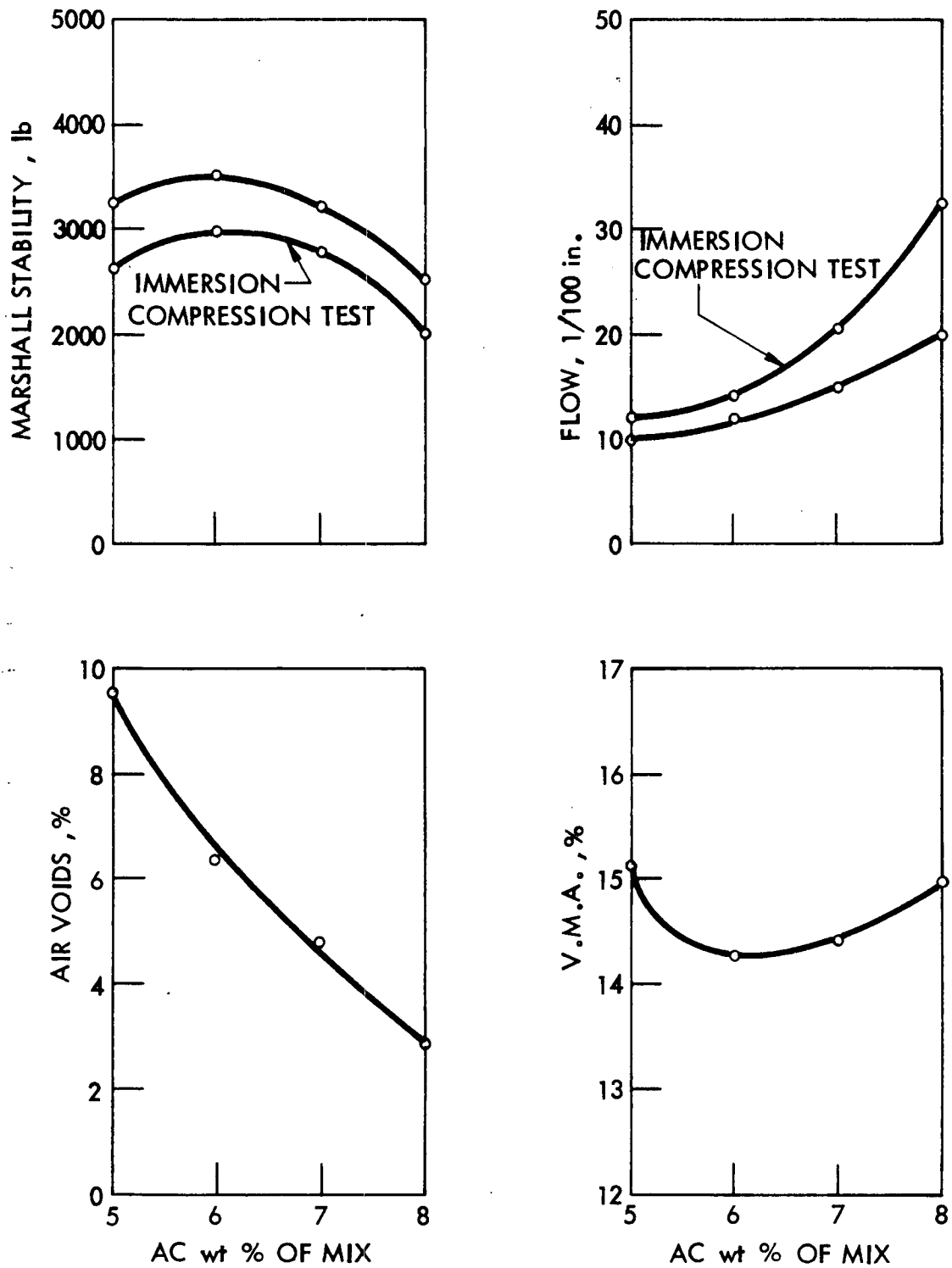


Fig. 58. Test property curves for mixes containing aniline furfural treated Cook aggregate and agricultural lime by the Marshall method

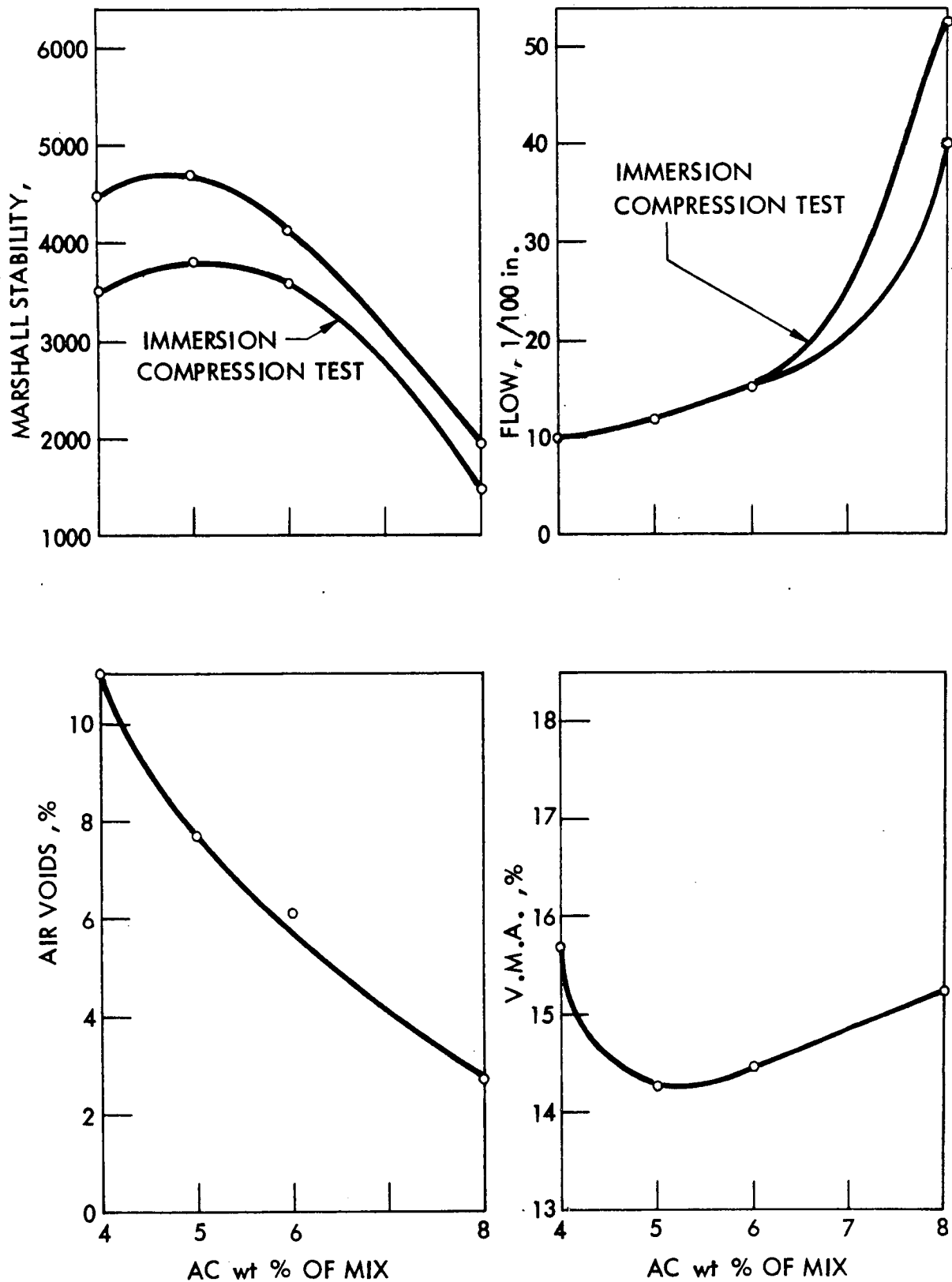


Fig. 59. Test property curves for mixes containing aniline furfural treated Menlo aggregate and agricultural lime by the Marshall method

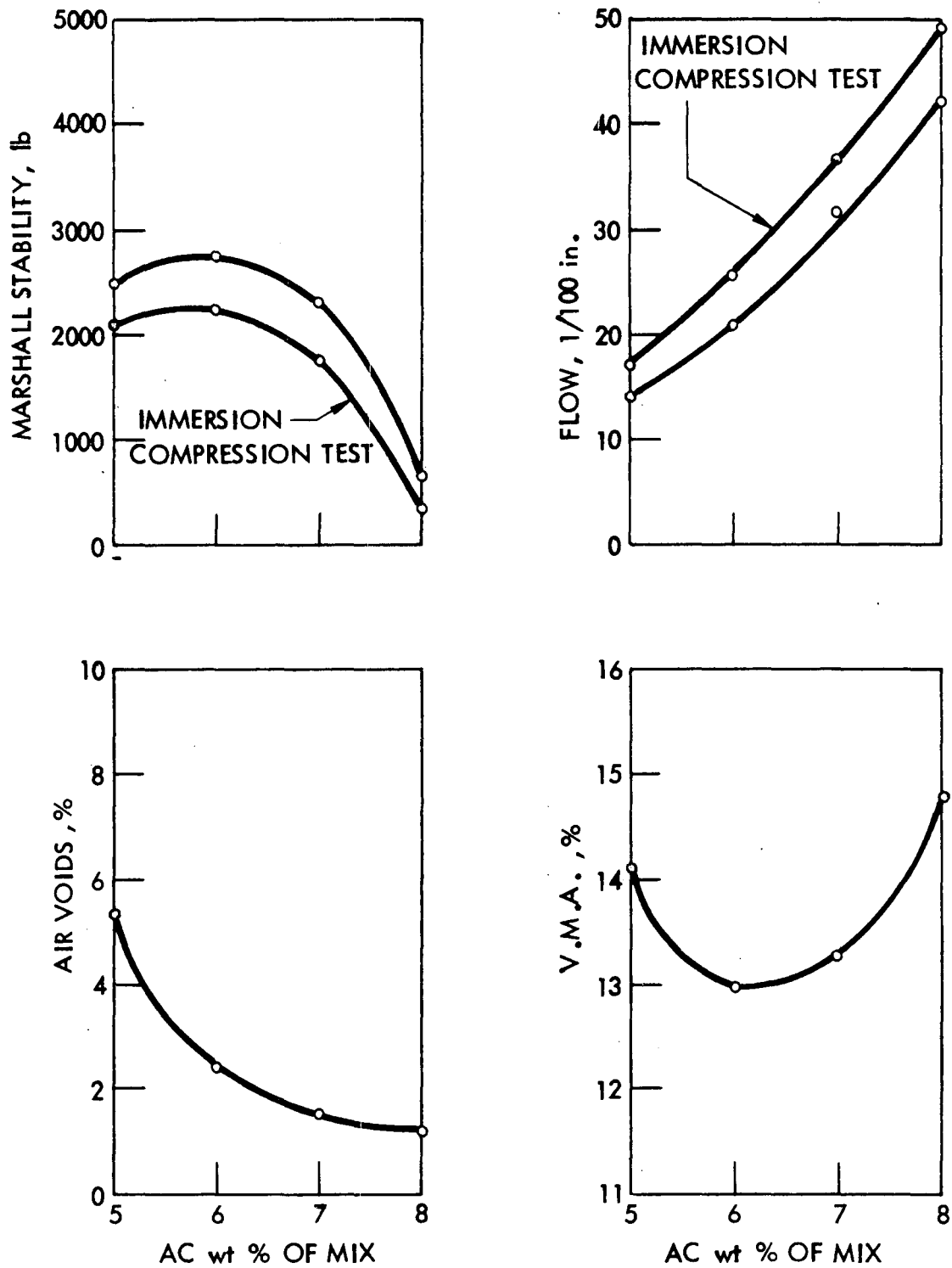


Fig. 60. Test property curve for mixes containing Armac T treated Cook aggregate and agricultural lime by the Marshall method

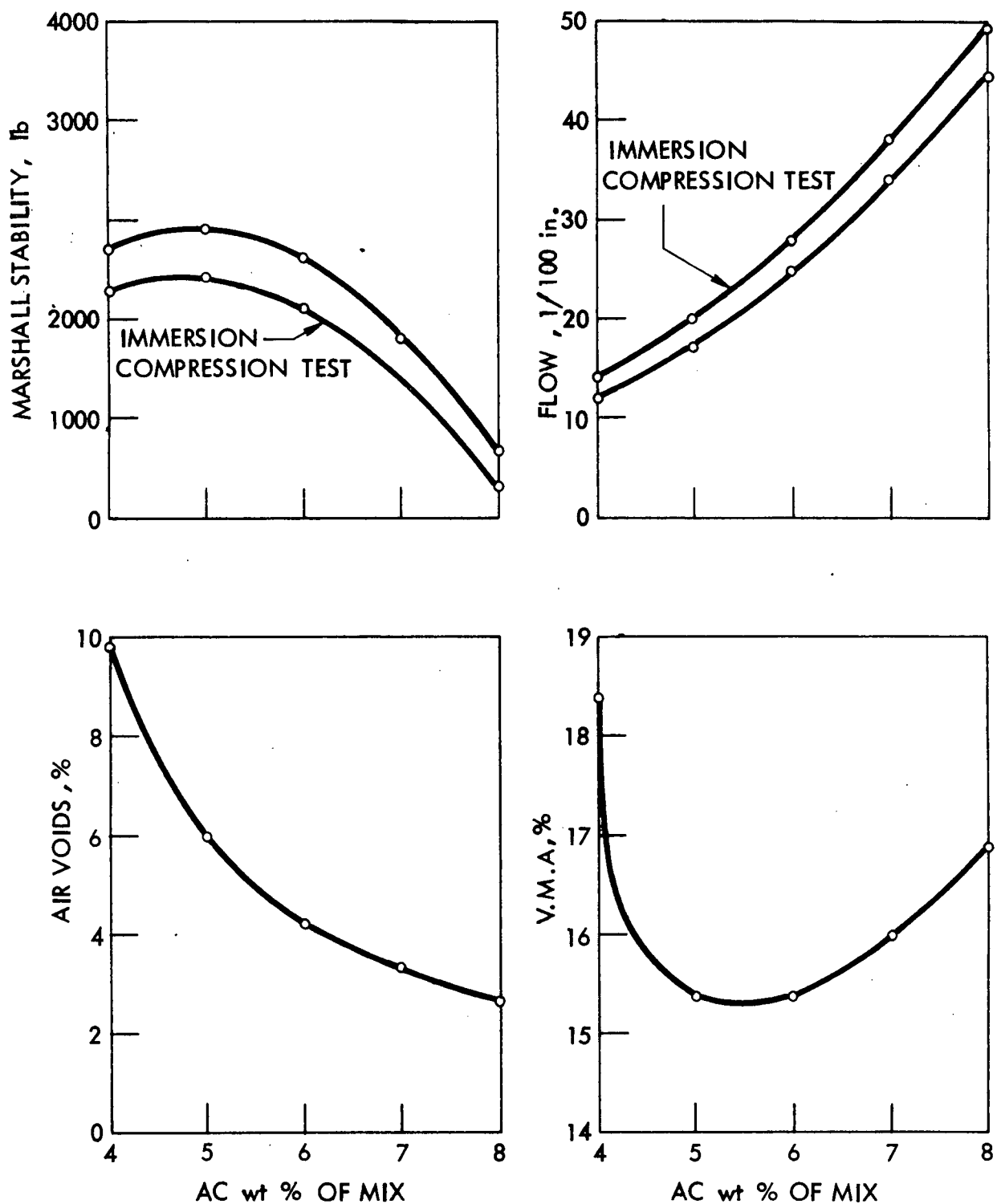


Fig. 61. Test property curves for mixes containing Armac T treated Menlo aggregate and agricultural lime by the Marshall method

Table 48. Asphalt absorption of bituminous mixes by Rice method

Aggregate	Treatment	A.C. wt % of mix	Asphalt absorption, wt %
Cook	Untreated	6	4.04
	Untreated	7	4.12
	Untreated	8	4.63
	Untreated	9	4.85
Menlo	Untreated	6	2.74
	Untreated	7	2.98
	Untreated	8	3.08
	Untreated	9	3.25
Cook	6% Aniline Furfural	5	2.04
	6% Aniline Furfural	6	2.19
	6% Aniline Furfural	7	2.45
	6% Aniline Furfural	8	2.56
Menlo	6% Aniline Furfural	4	1.72
	6% Aniline Furfural	5	2.12
	6% Aniline Furfural	6	2.46
	6% Aniline Furfural	8	2.56
Cook	6% Armac T	5	1.04
	6% Armac T	6	1.28
	6% Armac T	7	2.29
	6% Armac T	8	2.39
Menlo	6% Armac T	4	0.44
Menlo	6% Armac T	5	0.91
	6% Armac T	6	1.15
	6% Armac T	7	1.23
	6% Armac T	8	1.42

### Series B. Treatment of Absorptive Aggregates by Sulfur

Three sub-series of treatments by sulfur were made:

Sub-series A. In this series, one highly absorptive (Cook) and one moderately absorptive (Menlo) coarse-graded crushed limestone was treated with tire sulfur ranging from 1 - 9 wt % of aggregate. Water absorptions were determined and are given in Table 49 and plotted in Fig. 62. At 6% sulfur, absorption was reduced by 80% for Menlo and by 57% for Cook limestone.

Table 49. Water absorption of sulfur treated limestones<sup>a</sup>

Limestone <sup>b</sup>	Sulfur, <sup>c</sup> %	Water absorption, %
Menlo	0	2.57
"	1	0.97
"	3	0.64
"	6	0.53
Cook	0	7.62
"	1	6.35
"	3	5.08
"	6	3.29
"	9	1.94

<sup>a</sup>Aggregate temperature: 325°F;  
sulfur temperature: 75-77°F

<sup>b</sup>Coarse graded: 100% passing 3/4 in.,  
63% passing 3/8 in., 27% passing #4;  
0% passing #8 sieve

<sup>c</sup>Tire sulfur 21-4; wt % of aggregate

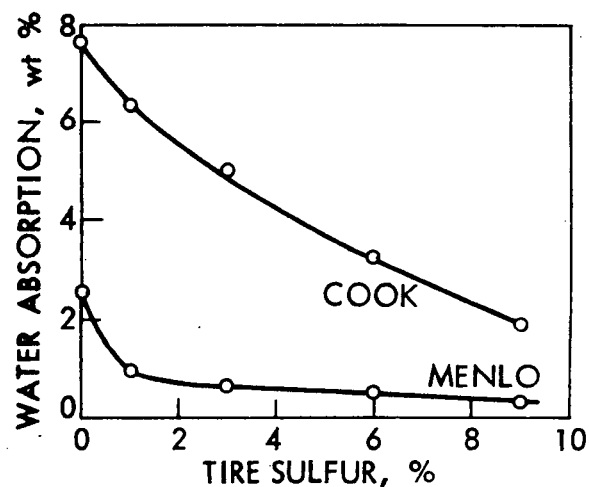


Fig. 62. Water absorption of sulfur treated limestones.

Sub-Series B Eight laboratory crushed and blended limestones were treated with 3 - 6% tire sulfur by weight of aggregate (2.71 and 5.07 wt % of total mixture) before being mixed with asphalt. Asphalt absorptions of these sulfur asphalt mixtures were determined at various time intervals up to 135 days. Results were compared with asphalt mixtures containing crushed limestones of identical gradation but without sulfur. The gradation of these mixtures are given in Table 33. The asphalt content, sulfur content and asphalt absorption after 1 day and after 100 days of the seventeen mixes are given in Table 50. The time-absorption curves of treated and untreated aggregates, are shown in Figs. 63 - 70. It can be noted that: (a) there are definite improvements in sulfur treated aggregate in reducing asphalt absorption, (b) the percent reduction varies with aggregates, (c) the differences in asphalt absorption between treated and untreated aggregates are greater at 100 days than at 1 day, i.e., there is a possible and significant advantage of reducing delayed absorption, and (d) the addition of sulfur beyond 6% resulted in little further improvement.

Sub-Series C. Asphalt absorption of sulfur treated and untreated Cook and Ferguson limestones were also determined during an investigation of effects of sulfur on mechanical properties of asphalt paving mixtures. The results are given in Table 51. It can be seen that sulfurized asphalt concrete reduced asphalt lost by absorption by 36% for Cook aggregate and by 56% for Ferguson aggregate, at optimum sulfur content of 5%.

#### Series C

A total of 148 batches (not including preliminary trial mixes) involving laboratory crushed and graded limestones from eight block sample (six quarries)



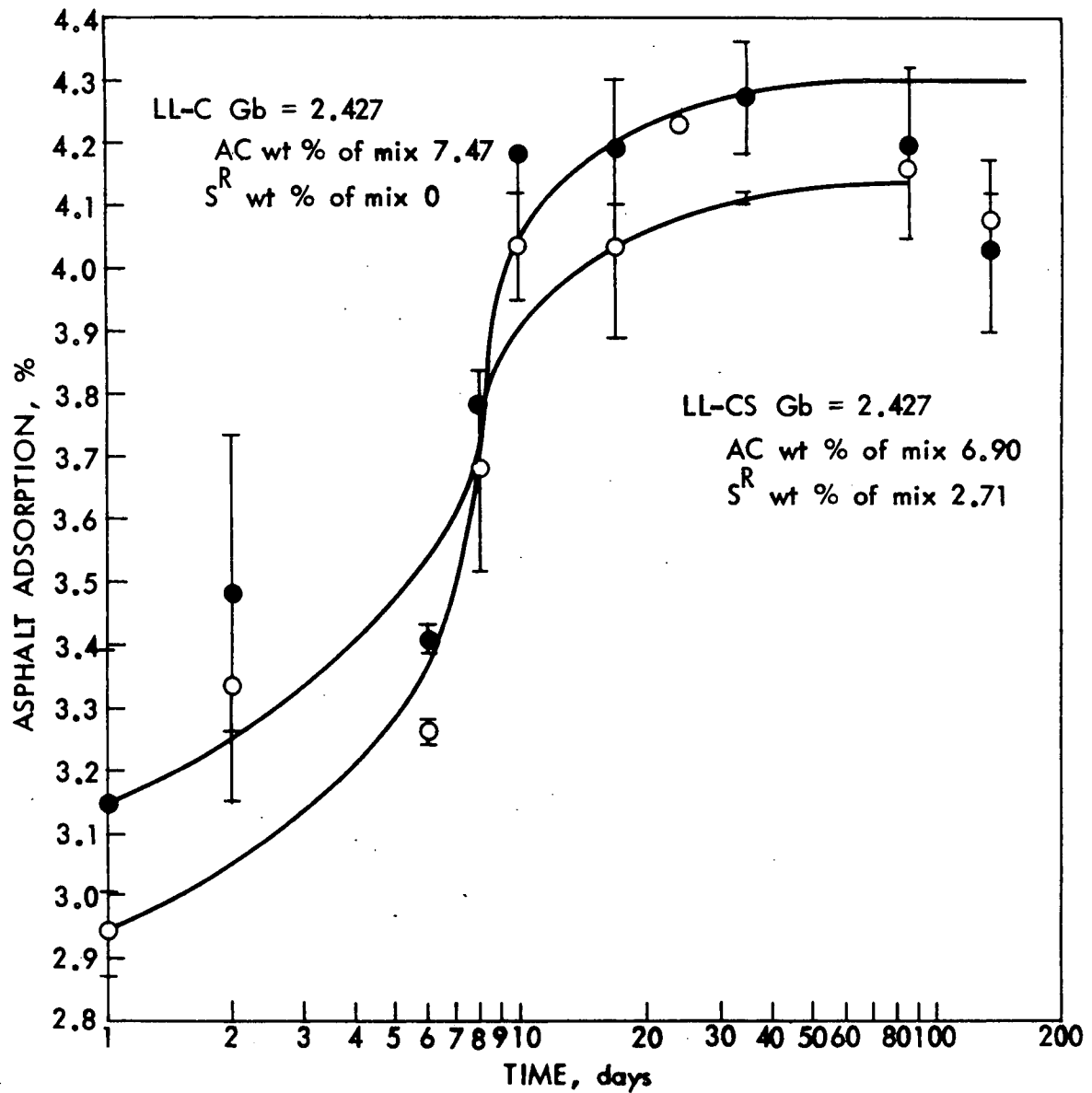


Fig. 63. Time-absorptive curves for treated and untreated Cook limestone

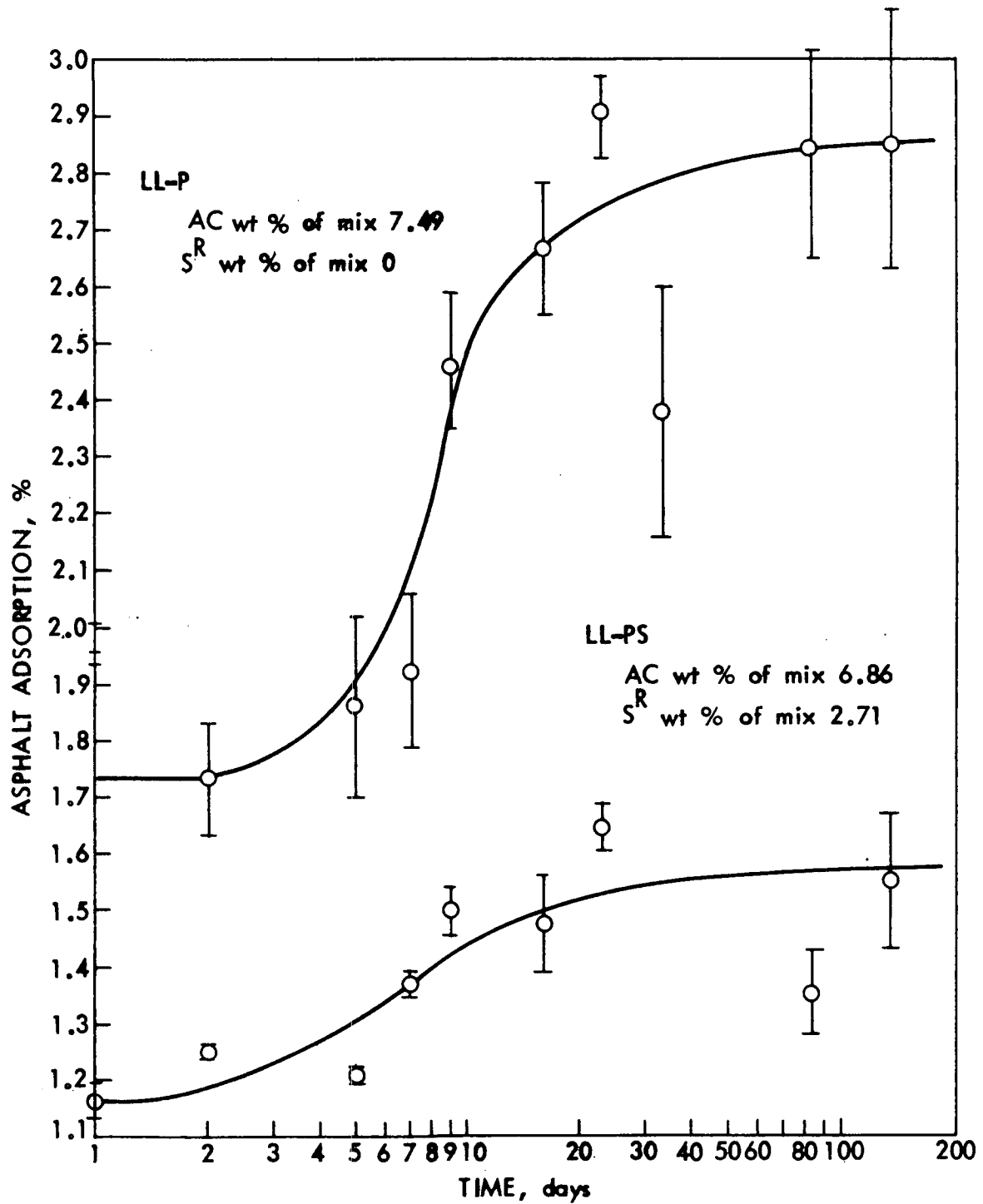


Fig. 64. Time-absorptive curves for treated and untreated Pints limestone

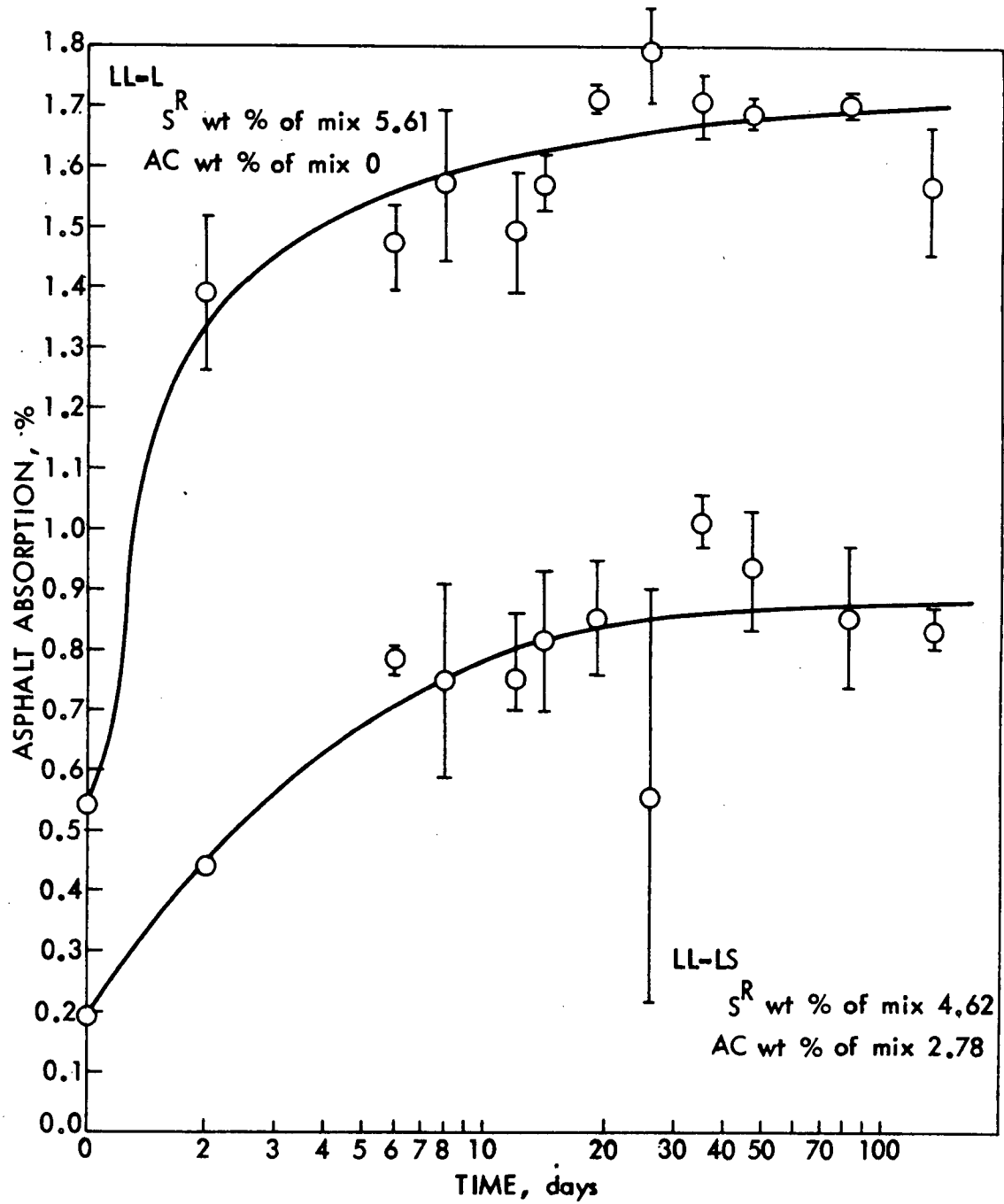


Fig. 65. Time-absorptive curves for treated and untreated Linwood limestone

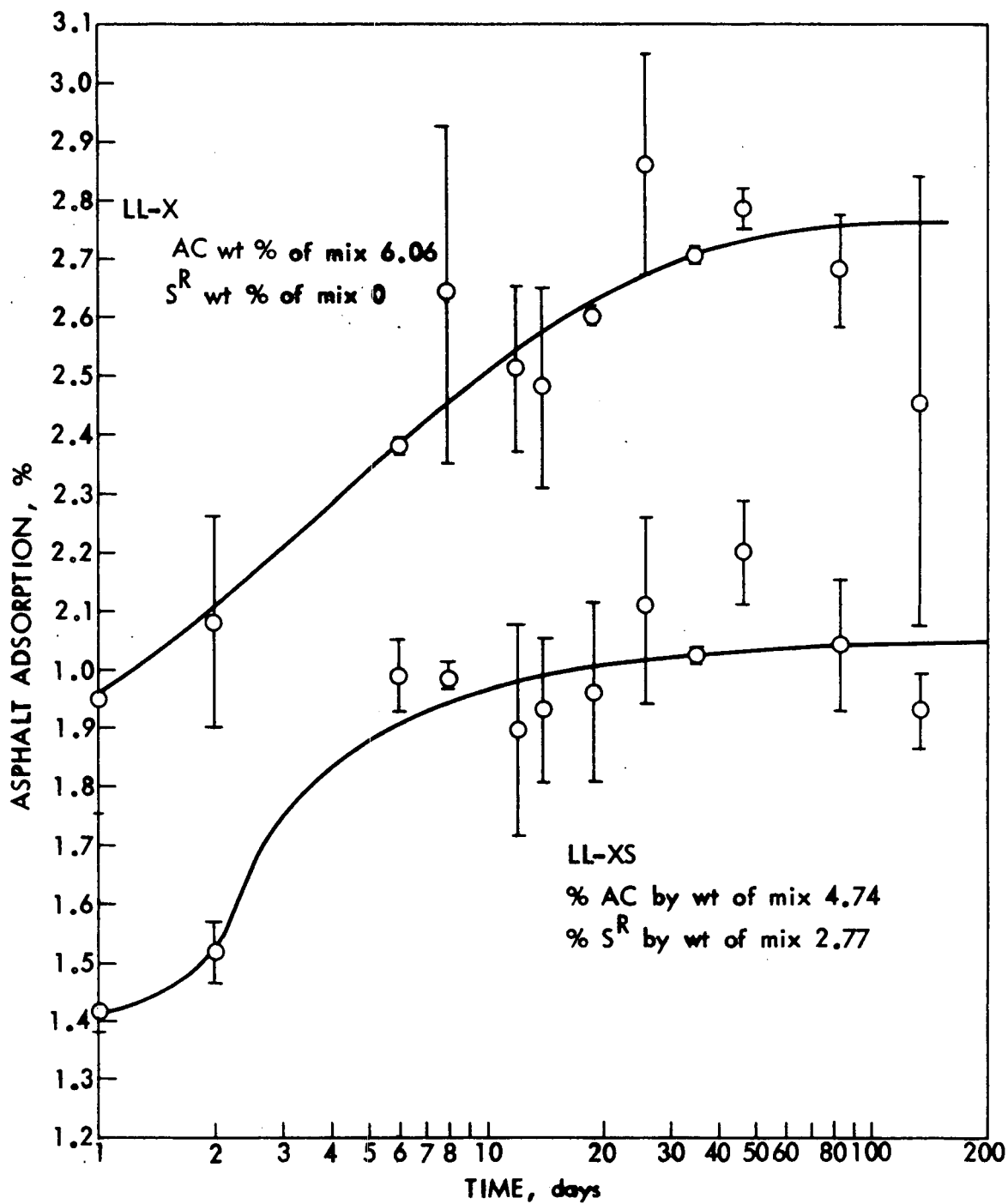


Fig. 66. Time absorptive curves for treated and untreated X (Alden II) limestone

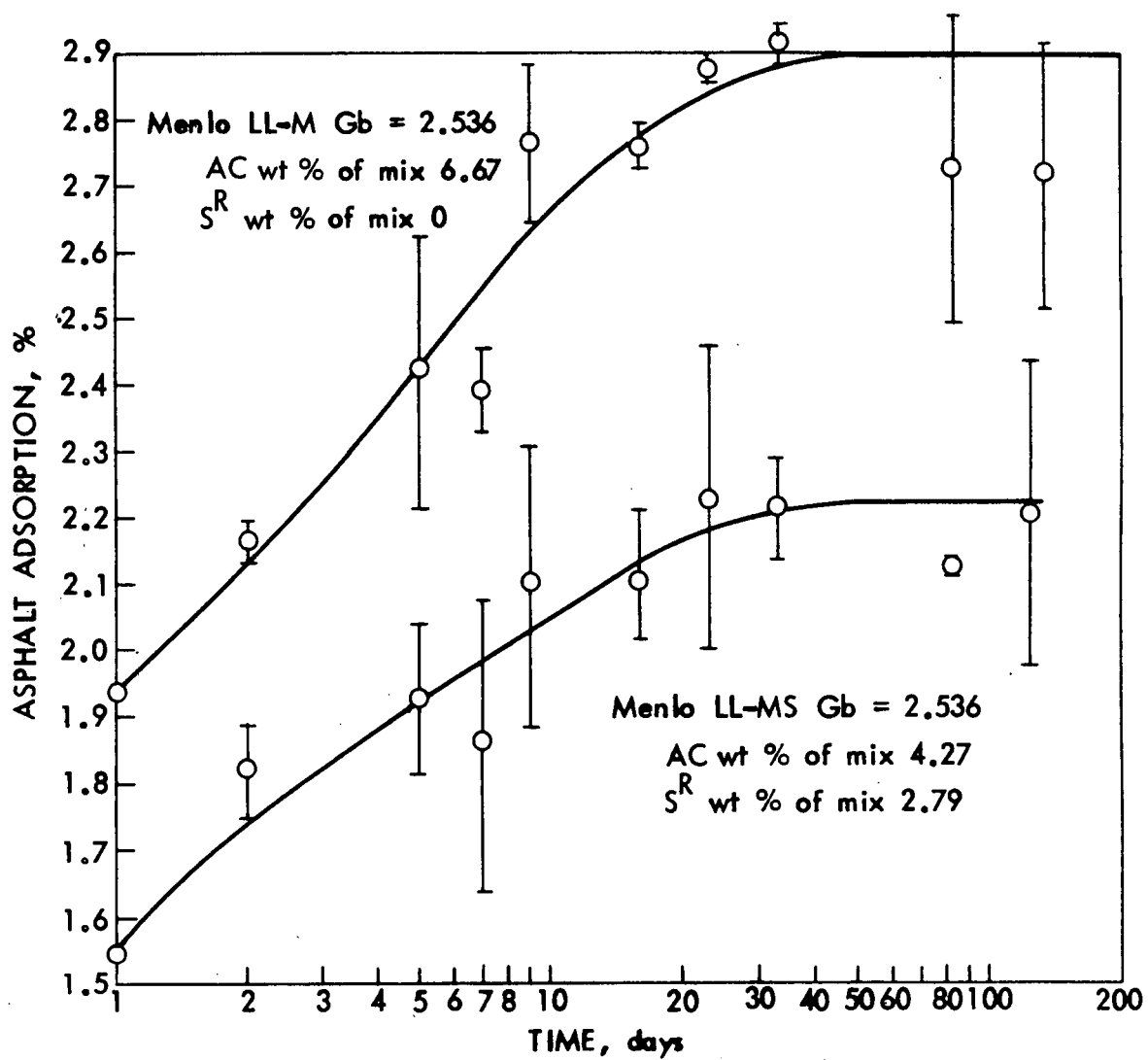


Fig. 67. Time-absorptive curves for treated and untreated Menlo limestone

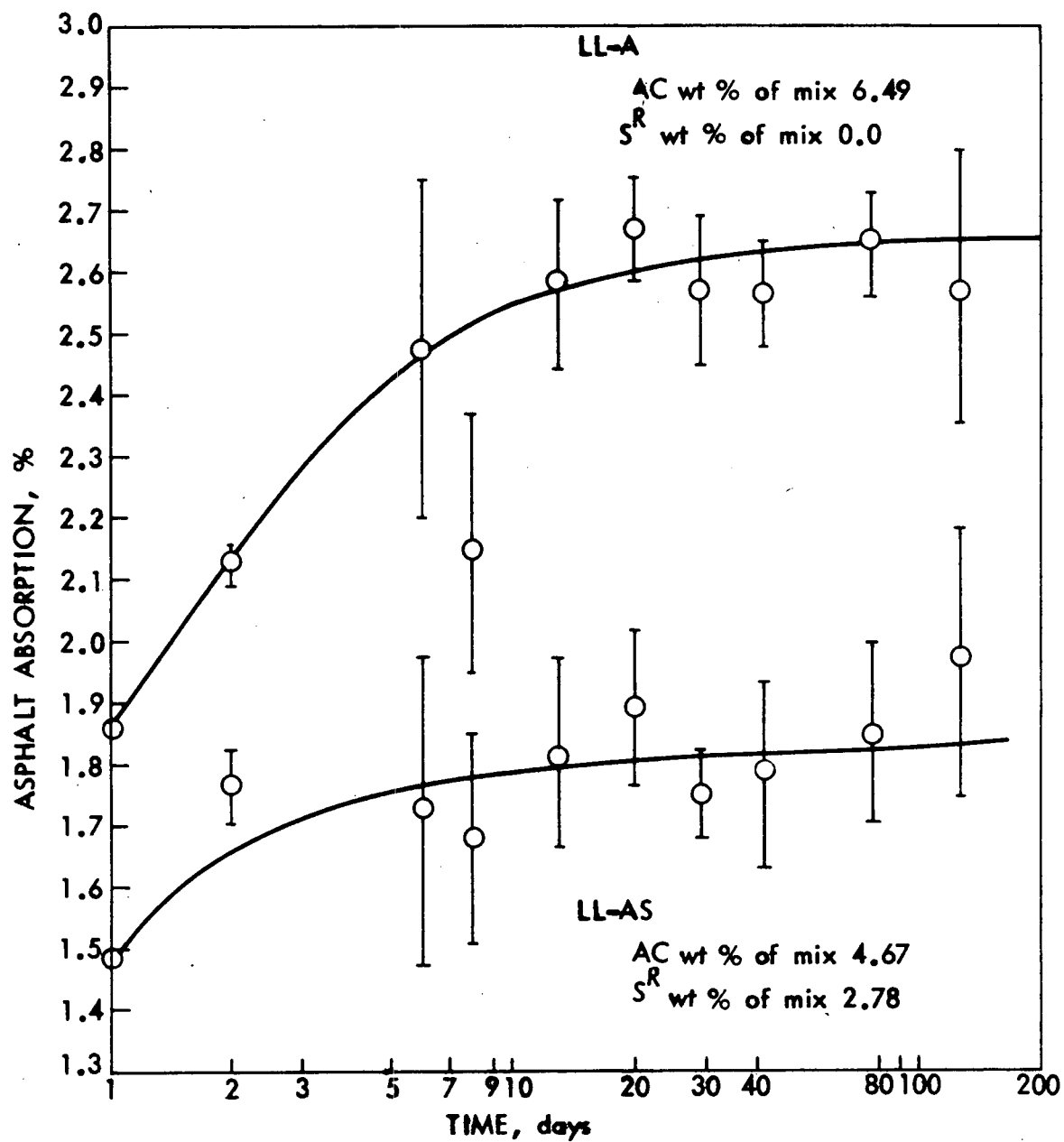


Fig. 68. Time-absorptive curves for treated and untreated Alden limestone

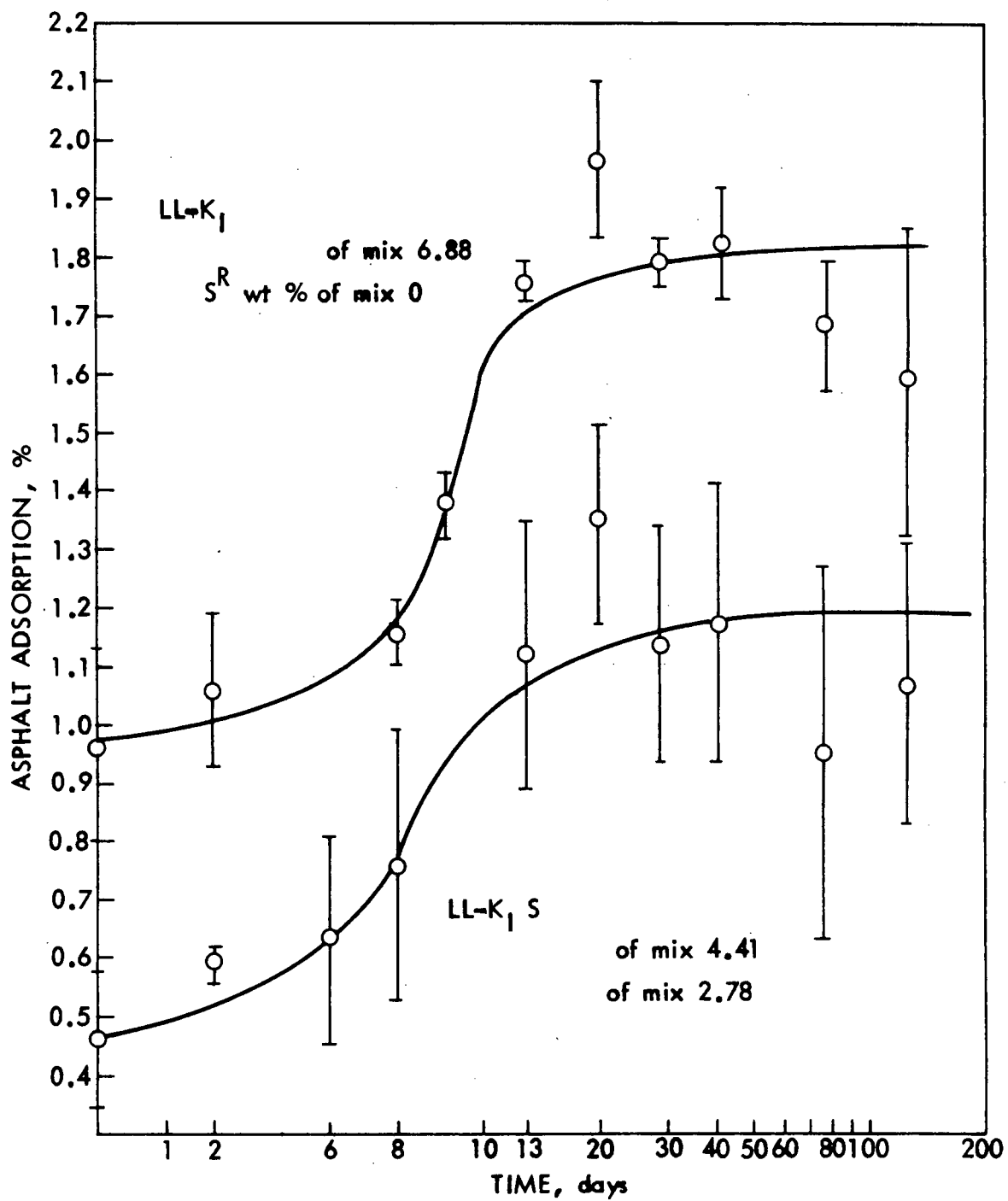


Fig. 69. Time-absorptive curves for treated and untreated Keota I limestone

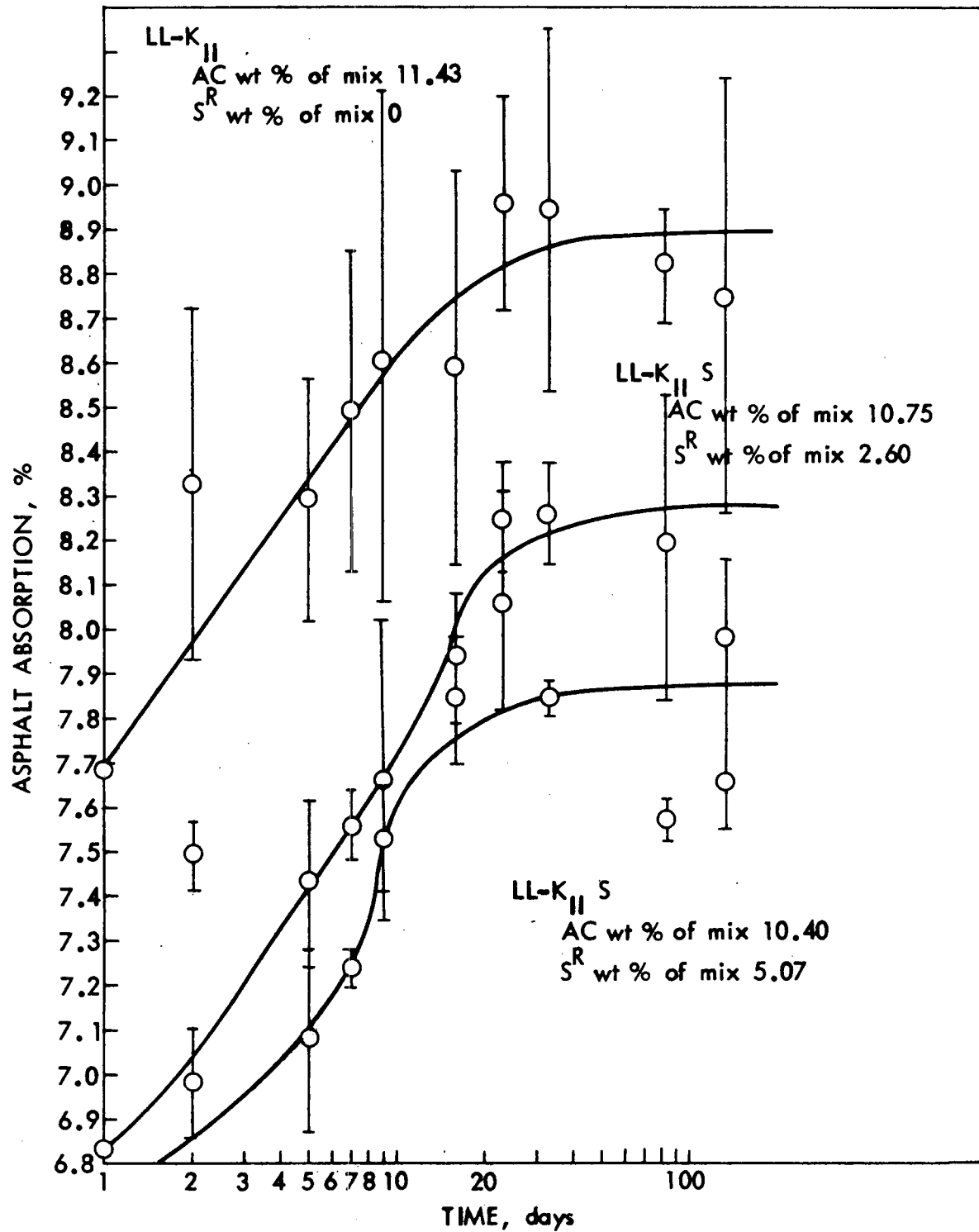


Fig. 70. Time-absorptive curves for treated and untreated Keota II limestone



Table 50. Asphalt absorption of sulfur treated limestones

Mix #	A.C. <sup>a</sup> ,%	Sulfur <sup>a</sup> ,%	Asphalt absorption, %	
			1 day	100 days
C	7.48	0	3.15	4.30
CS	6.91	2.71	2.94	4.14
P	7.49	0	1.73	2.85
PS	6.86	2.60	1.16	1.57
L	5.61	0	0.54	1.70
LS	4.62	2.71	0.19	0.88
X	6.06	0	1.94	2.75
XS	4.74	2.78	1.42	2.04
M	6.67	0	1.93	2.90
MS	4.28	2.77	1.54	2.23
A	6.49	0	1.86	2.65
AS	4.67	2.79	1.48	1.83
KI	6.88	0	0.98	1.80
KIS	4.41	2.78	0.49	1.13
KII	11.43	0	7.69	8.89
KIIS <sub>1</sub>	10.75	2.78	6.83	8.28
KIIS <sub>2</sub>	10.49	5.07	6.73	7.87

<sup>a</sup>By weight of mix

Table 51. Asphalt absorption<sup>a</sup> of sulfur treated limestone-series C & D

Limestone	Code	A.C. <sup>b</sup>	Sulfur <sup>c</sup>	Asphalt absorption <sup>b</sup>
Cook	C-1	7	0	4.4
"	C-2	7	3	3.6
"	C-3	7	6	2.8
"	C-4	7	9	2.4
Ferguson	D-1	5	0	1.6
"	D-2	5	1	1.6
"	D-3	5	3	1.1
"	D-4	5	6	0.7

<sup>a</sup>Determined by Rice method<sup>b</sup>wt % of aggregate<sup>c</sup>Tire sulfur; wt % of aggregate

and 30 chemicals were made in this series of treatment study. Asphalt and/or water absorption were determined on treated and control mixes. Results of water absorption by ASTM method and asphalt absorption by Rice method (after 1 week and 2 weeks), together with chemical type and concentration, are summarized in Tables 52 - 59. Nature of the chemicals, detailed treatment procedures, level of treatments, and qualitative observations of these chemical treatments are summarized in Appendix B. Because of the large number of chemicals, aggregate types and percent chemical involved, and limited observations per treatment conditions, quantitative evaluation on relative effectiveness of these chemicals is rather difficult and may be misleading. It seems, however, sufficient to state that: (a) Certain

agents, such as aniline-furfural, rapid curing cutbacks, crude tar, methyl methacrylate, PVA, resins K-101 and K-1010, could be used to reduce absorption effectively. Such treatments could thus make unsuitable or marginal aggregates useful in asphalt concrete mixtures; (b) Certain agents, such as rubber latex, lignin, acrylic polymers, while results were inconclusive, deserve further study for optimum conditions of treatments; and (c) Exploratory investigations should be expanded to other potential chemicals, especially polymers and industrial wastes.

### Conclusions

Aggregates of suitable quality for pavements of all types are in short supply in numerous areas of this country, including the southern part of Iowa.<sup>96-99</sup> According to a study by Witczak et al.<sup>98</sup> over one-third of the states in the US have "poor" to "very restricted" potential aggregate supply problems. The "realistic" (in contrast to "potential") appraisal of aggregate sources may show an even more unfavorable situation. The realistic appraisal of aggregate supply problems would include the problems of population distribution, area accessibility, urban development or changes in land uses, pollution control, increases in aggregate production costs and demands for better quality aggregates.

Several measures have been suggested and/or are being taken to cope with or compensate for the shortage of suitable aggregates for highway construction.<sup>97,98,35</sup> Among these are: (a) improved techniques for locating and identifying new aggregate sources; (b) use of natural materials such as shells and coral as substitutes of aggregates; (c) use of manufactured or synthetic aggregates; (d) improved handling and transportation of those

aggregates that are remote to the construction sites; and (e) development of novel materials and construction methods. However, by far the most promising and effective approach to alleviate the problem of aggregate shortage is better utilization of locally available aggregates, especially the "marginal" materials.

There is little question as to the impact that can be made on the aggregate supply problem by expanding the use of locally available materials of marginal quality.<sup>99</sup> Among the approaches that have proven merit (i.e., meet objectives of project HR-142) and/or justify research and evaluation are:

- (a) better materials characterization; (b) revision of material specifications;
- (c) benefaction, modification or upgrading otherwise unsuitable aggregates.

The work performed in this project on aggregate treatments is far from exhaustive. However, it is sufficient to show that there is a wide variety of additives and methods that may be used singly or in combination to improve the quality of selected aggregates.

One question of importance is cost. Justification of the costs of such improvements requires serious study and will be difficult especially while no other aggregate source alternatives are available. From the experiences of huge quantities of treated marginal materials used, very often successfully, in other construction areas (such as soil stabilization and anti-stripping additives for aggregates), there is little doubt as to the practicality and tensibility of upgrading absorptive aggregates for paving mixtures, especially when sufficient data and information regarding the selection and use of the additives for a given aggregate are available and the use of such treatments is dictated by necessity rather than by choice.

A case at hand similar to the treatment of absorptive aggregates is the use of precoated aggregates for surface treatments: Precoating of cold aggregates for surface treatment (dressing) has been widely practiced in Australia and New Zealand to improve adhesion between aggregate and binder and improve bonding and resistance to stripping, reduce moisture absorption by the aggregate, and eliminate the dusty aggregate problems during construction. Coating materials used for this purpose included low viscosity tars, diesel fuel oils, low viscosity cracked bitumens and asphalt emulsions. Of these, tar is the preferred coating material because of its lower costs and better wetting characteristics. Precoating machines were also designed.

As far as economic justification of precoating aggregate is concerned, it was estimated that "even if a surface dressing last only one year longer by using an improved aggregate it is justifiable to pay up to four times the cost for such an aggregate."<sup>100</sup>

As a matter of fact, it is considered a good practice in South Africa to precoat aggregate for use in all surface dressing construction.

The inevitable conclusion based on this aggregate treatment study and other evidences is that there is need for further research and evaluation on:

- More agents and detailed laboratory studies for the information on selection of additives.
- Effects of treatments other than absorption improvement.
- Field technical feasibility experiments.

Table 52. Absorption of chemically treated aggregate, Alden

Sample #	Chemical	Chemical wt % of aggregate	Grading	Water absorption, %	Asphalt absorption, %	
					1 week	2 week
8	Control	—	A	3.19	1.55	1.86
1	PVA 52-22	0.25	A	—	1.29	1.57
2	PVA 70-05	0.30	A	—	1.14	1.02
3	Styrene	0.75	A	2.70	1.10	1.67
4	Calcium acrylate	0.45	A	—	1.84	1.60
5	NVX	0.75	A	1.70	0.83	1.13
6	SS-1h	0.95	A	1.43	0.70	0.73
7	RC-70	1.25	A	1.34	0.00	0.81
9	Crude tar	2.30	A	1.04	0.00	0.39
10	RT-6	1.95	A	1.52	1.04	1.07
11	MC-30	1.50	A	1.50	0.89	0.86

Table 53. Absorption of chemically treated aggregates, Cook

Sample #	Chemical	Chemical wt % of aggregate	Grading	Water absorption, %	Asphalt absorption, %	
					1 week	2 week
9	Control	—	A	4.14	1.64	1.98
1	PVA 52-22	0.30	A	—	0.97	1.42
2	Styrene	0.95	A	3.24	1.38	1.68
3	Calcium acrylate	0.55	A	—	1.03	1.02
4	NVX	0.95	A	3.44	1.57	1.84
5	SS-1h	0.95	A	2.09	1.05	1.23
6	RC-70	1.30	A	2.21	1.21	1.18
7	Crude tar	1.95	A	2.42	1.05	1.11
8	MC-30	1.95	A	2.68	1.32	1.27
10	Calcium hydroxide	1.23	+3/8"	—	1.43	1.91
11	RT-6	2.15	+3/8"	1.94	0.96	1.04

Table 54. Absorption of chemically treated aggregates, Keota I

Sample #	Chemical	Chemical wt % of aggregate	Grading	Water absorption, %	Asphalt absorption, %	
					1 week	2 week
	Control	—	B	3.77	1.26	1.86
	RT-6	1.00	+#4	0.95	0.79	0.84
6	RT-6	1.50	A	1.32	0.61	0.71
1	PVA	0.30	A	—	0.78	0.76
	52-22					
2	Styrene	0.60	A	0.76	1.06	0.86
3	Calcium acrylate	0.35	A	—	0.88	0.74
4	NVX	0.60	A	2.84	1.06	1.36
5	SS-1h	0.95	A	1.15	0.87	0.83
7	RC-70	1.00	+#4	0.64	0.54	0.69
9	Crude tar	1.00	+#4	1.37	0.84	0.83
11	MC-30	1.00	+#4	0.62	0.96	1.06



Table 55. Absorption of chemically treated aggregates, Keota II

Sample #	Chemical	Chemical wt % of aggregate	Grading	Water absorption, %	Asphalt absorption, %	
					1 week	2 week
11	Control	—	A	13.70	8.33	8.62
5	SS-1h	0.90	A	9.55	5.65	5.60
101	SS-1h	0.90	B	6.50	3.83	4.28
10	Crude tar	5.65	+3/8"	4.09	2.06	2.42
7	Crude tar	7.45	A	3.89	2.21	2.54
1	PVA 52-22	0.85	A	—	7.42	7.59
2	Styrene	2.10	A	8.41	4.96	5.42
3	Calcium acrylate	1.25	A	—	5.75	5.88
4	NVX	2.10	A	3.76	2.71	3.02
6	RC-70	3.85	A	8.07	3.98	4.08
8	MC-30	4.85	A	5.13	3.98	4.13
9	PVA 70-05	0.85	+3/8"	—	6.24	5.15
102	MC-4530	2.00	B	—	6.04	6.90
103	HA-8	2.00	B	—	5.97	6.33

Table 56. Absorption of chemically treated aggregates, Linwood

Sample #	Chemical	Chemical wt % of aggregate	Grading	Water absorption, %	Asphalt absorption, %	
					1 week	2 weeks
10	Control	—	A	1.28	0.43	0.55
	Control	—	B	1.52	1.48	1.57
24	RC-70	1.00	+ #8	0.43	0.17	0.14
9	RC-70	1.10	A	0.85	0.37	0.30
19	Crude tar	1.00	A	0.66	0.19	0.28
25	Crude tar	1.00	+ #8	0.76	0.20	0.30
21	MC-30	1.00	A	1.04	0.53	0.35
26	MC-30	1.00	+ #8	0.92	0.34	0.15
1	PVA 52-22	0.15	A	—	0.50	0.54
22	PVA 52-22	0.20	+ #8	—	0.65	0.90
2	PVA 70-05	0.20	A	—	0.04	0.00
3	Styrene	0.45	A	1.09	0.48	0.65
4	Calcium acrylate	0.30	A	—	0.52	0.96
5	NVX	0.50	A	1.09	0.37	0.37
6	Polyvinyl acetate	0.40	A	1.65	0.44	0.62
7	Rubber latex	0.60	A	—	0.41	0.51
8	SS-1h.	0.95	A	0.70	0.04	0.40
11	K-101	0.62	A	1.11	0.42	0.37
12	AMSCO 3001	0.62	A	1.07	0.50	0.56
13	AN-139	0.25	A	—	0.52	0.40
14	CaCl <sub>2</sub>	0.65	A	—	0.47	0.43
15	Acrylonitrile	0.55	A	1.17	0.41	0.49
16	Ca(OH) <sub>2</sub>	1.00	A	—	0.52	0.50
17	HA-8	2.00	A	—	0.27	0.32
18	Methyl acrylate	1.00	A	1.25	0.64	0.54
20	RT-6	1.00	A	0.63	0.30	0.42

Table 57. Absorption of chemically treated aggregates, Menlo

Sample #	Chemical	Chemical wt % of aggregate	Grading	Water absorption, %	Asphalt absorption, %	
					1 week	2 weeks
9	Control	—	A	3.40	2.47	2.51
1	PVA 52-22	0.15	A	—	0.45	0.65
20	PVA 52-22	0.15	+3/8"	—	0.75	0.62
2	PVA 70-05	0.15	A	—	0.71	0.77
3	Styrene	0.45	A	1.39	1.00	1.09
4	Calcium acrylate	0.25	A	—	0.48	0.90
5	NVX	0.45	A	0.97	1.11	1.16
6	Rubber latex	0.55	A	—	0.68	0.80
7	SS-1h	0.95	A	0.69	0.49	0.58
8	RC-70	1.00	A	1.29	0.40	0.39
10	K-101	0.57	A	1.06	0.09	0.14
11	K-1010	0.40	A	1.36	0.69	0.77
12	AMSCO 3001	0.57	A	1.70	0.13	0.18
13	CaCl <sub>2</sub>	0.55	A	—	0.78	0.78
14	Acrylonitrile	0.45	A	1.40	0.80	0.87
15	Ca(OH) <sub>2</sub>	0.55	A	—	0.31	0.52
16	Crude tar	1.30	A	0.56	0.33	0.27
17	RT-6	1.00	A	0.80	0.47	0.51
18	MC-30	1.00	A	0.67	0.56	0.64
19	200-300 pen	1.00	A	0.40	0.39	0.55

Table 58. Absorption of chemically treated aggregates, Pints

Sample #	Chemical	Chemical wt % of aggregate	Grading	Water absorption, %	Asphalt absorption, %	
					1 week	2 week
1	Control	—	B	7.72	2.98	3.67
	PVA	0.35	A	—	2.01	3.01
2	52-22					
	PVA	0.35	A	—	2.37	2.06
	52-22					
3	PVA	0.35	A	—	2.43	2.00
	52-22					
5	Styrene	1.25	A	7.18	2.88	3.88
33	Styrene	1.25	+ #4	3.95	1.91	2.25
34	Calcium	0.30	+ #4	—	2.77	3.10
	acrylate					
6	Calcium	0.55	A	—	4.33	4.73
	acrylate					
8	Calcium	0.60	A	—	3.85	3.78
	acrylate					
7	Calcium	0.75	A	—	3.17	3.48
	acrylate					
35	SS-1h	0.50	+ #4	5.25	2.46	2.85
12	SS-1h	0.95	A	6.46	1.91	2.09
14	SS-1h	1.10	A	6.30	2.20	2.19
13	SS-1h	1.90	A	6.02	1.84	—
36	Crude tar	1.00	+ #4	3.09	0.74	0.78
25	Crude tar	1.95	A	4.66	1.75	1.72
26	Crude tar	2.95	A	4.04	1.52	1.64
28	MC-30	1.00	A	6.48	2.12	2.31
37	MC-30	1.45	+ #4	6.59	2.02	2.03
29	MC-30	2.00	A	5.77	2.53	2.25
30	MC-30	2.95	A	5.30	2.51	2.54
38	200-300	1.00	+ #4	1.24	0.89	1.11
	Pen					
31	200-300	2.00	A	4.52	0.96	1.18
	Pen					
4	PVA	0.35	A	—	3.63	3.65
	70-05					
9	NVX	1.30	A	5.08	2.08	2.66
10	Polyvinyl	1.15	A	7.42	3.18	3.29
	acetate					
11	Rubber	1.70	A	—	2.62	3.93
	latex					
15	RC-70	1.50	A	4.48	1.84	1.94
	Cut-back					
16	Methyl	1.00	A	7.15	2.90	2.91
	acrylate					
17	K-101	1.70	A	4.50	1.64	1.88
18	K-1010	1.20	A	3.42	1.27	1.23
19	AMSCO	1.70	A	7.29	2.68	2.21
	3001					
20	AN-139	0.60	A	—	2.94	3.10
21	Acrylonitrile	1.55	A	6.43	2.24	3.03
22	CaCl <sub>2</sub>	1.70	A	—	3.64	3.67
23	Ca(OH) <sub>2</sub>	1.00	A	—	2.97	2.75
24	E-330	1.90	A	—	1.52	0.72
27	RT-6	2.95	A	4.71	2.27	2.72
32	PVA	0.70	+ #4	—	2.61	2.99
	71-30					

Table 59. Absorption of chemically treated aggregates, X-Quarry

Sample #	Chemical	Chemical wt % of aggregate	Grading	Water absorption, %	Asphalt absorption, %	
					1 week	2 week
	Control	—	B	4.02	2.39	2.48
	Control	—	+ #8	5.55	3.68	4.02
8	Crude tar	2.00	A	0.77	0.03	0.01
13	Crude tar	2.45	+ #8	0.65	0.82	0.95
9	MC-30	1.95	A	0.82	0.26	1.54
14	MC-30	1.95	+ #8	1.76	0.85	1.18
1	PVA 52-22	0.25	A	—	0.55	0.51
2	PVA 71-30	0.55	A	—	1.06	1.13
3	Styrene	0.75	A	2.16	1.23	1.61
4	Calcium acrylate	0.50	A	—	0.89	1.00
5	NVX	0.80	A	0.75	0.41	0.67
6	SS-1h	0.95	A	0.94	0.69	0.64
7	RC-70	1.25	A	1.67	0.00	0.11
10	PVA 70-05	0.30	+ #8	—	1.11	1.28

## SUMMARY AND CONCLUSIONS

- Most aggregates absorb asphalt to some degree. The absorption of asphalt by aggregates may affect proper mixture design and pavement failure due to delayed absorption.
- No standard method is available to evaluate, describe and specify the absorptive characteristics of an aggregate with respect to asphalt. There is a need to establish such a test.
- Indirect prediction of asphalt absorption by water absorption, CKE or oil absorption is not always reliable.
- The bulk-impregnated specific gravity (Corps of Engineers) method can be used to determine the practical or realistic maximum asphalt absorption of an aggregate and is recommended for evaluating and comparing potential aggregate sources; the Rice specific gravity method can be used to determine the practical or realistic minimum asphalt absorption of an aggregate and is recommended for mixture design.
- The accurate determination of asphalt absorption in both methods depends upon the realistic and accurate determination of bulk specific gravity.
- Current ASTM methods for determination of bulk specific gravity of aggregate are inadequate and non-reproducible for use in the asphalt absorption tests recommended.
- Three methods for determination of bulk-specific gravity of aggregates (chemical indicator method, mercury pycnometer or penetration method and time-weight in water curve method) have been developed during this investigation. However, all three need more work and further refinement before formal adoption.

- Asphalt absorption is time dependent. Percent absorption increases with time at decreasing rate.
- Asphalt absorption is directly related to the porosity of an aggregate. The total porosity is a good indicator for absorption.
- Pore-size distribution of an aggregate has a direct effect on the nature and degree of asphalt absorption. Good correlation was found between percent porosity larger than  $1\ \mu$  and asphalt absorption for crushed aggregates and between percent porosity larger than  $0.1\ \mu$  and asphalt absorption for rock cores. In general, asphalt absorption increases as these coarse-pore porosities increase.
- Presence of ink-bottle pores of varying extent is indicated in all cores. The probable dimensions of the pore throats and internal cavities vary from one core to another and seem to affect the asphalt absorption.
- The photo-colorimetric technique can be used to evaluate the asphalt absorption of aggregates of all sizes and gradings.
- Chemical treatments of absorptive yet locally available aggregates is the most promising and effective approach to alleviate the problem of quality aggregate shortage which one-third of the US are facing. Such treatments not only make unsuitable or "marginal" aggregates useful but also reduces required optimum asphalt content, increase water resistance and decrease the possibility of pavement failure through reduction of effective binder content by delayed absorption.
- Among approximately 30 chemicals investigated, aniline-furfural, rapid curing cutbacks, crude tar, methyl methacrylate, PVA, synthetic resins K-101 and K-1010 were found to be effective in reducing asphalt absorption. Others such as rubber latex, lignin, acrylic polymers,

while results were inconclusive, deserve further study for optimum conditions of treatments.



## RECOMMENDATIONS

Since the start of this project in 1968, no less than three important studies concerning highway aggregates have been reported, all of which have reinforced the importance and urgency of this research and correctness of the approach and direction taken in this project.

The study by Witczak et al.<sup>97</sup> has shown that aggregates are potentially in short supply over about one-third of the United States, i.e., these areas have "limited to severe problem" ratings. Southern Iowa is included in these areas. Gallaway<sup>98</sup> reviewed the critical aggregate problems for the 1970s and suggested better utilization of locally available aggregates, expanded use of marginal materials (including better material evaluation and specifications), selective use of solid wastes and benefaction of otherwise unsuitable materials. A study by Walker et al.<sup>101</sup> has recommended in high priority a research entitled "The Influence of Asphalt Absorption Rate, Nature, and Amount by Aggregate Particles on Bituminous Mix Design and Performance."

In essence, these have been the philosophy, approach, and ultimate goals of HR-142. In this project, the nature and extent of asphalt absorption of limestone, of various chemical compositions have been studied; the factors affecting asphalt absorption have been identified; the characterization methods for asphalt absorption have been established and the possibility and potentials of upgrading highly absorptive or marginal aggregate have been explored. However, in order to establish tolerance levels of asphalt absorption rate and amount for specification and material evaluation purposes, and to treat absorptive and marginal aggregates economically and intelligently for use in asphalt paving mixtures, further research is needed. The following programs are recommended:

- Field study of effects of asphalt absorption by aggregate, especially in the areas of absorption history, influences on physical properties of the mixture, such as voids and stability, asphalt hardening and low temperature cracking of asphalt films due to absorption.
- Continued laboratory investigation of the feasibility (remedies and methods) of utilizing absorptive aggregates for asphalt paving mixtures.
- Field verification of laboratory developed concepts of mix design using absorptive aggregates, modification of plant mixing operations, construction standards, and specifications on aggregates and asphalts.
- Identification and establishment of data file on a regional basis, on aggregate types and sources that have high or detrimental asphalt absorption characteristics.
- Expand the treatment or upgrading poor aggregate phase of research, with experiences gained in HR-142, for the purposes of improving other marginal aggregates in terms of soundness, stripping, and hardness of the aggregates.

## ACKNOWLEDGMENTS

This report is the result of a study under Project HR-142, sponsored by the Iowa Highway Research Board and the Iowa State Highway Commission. The author is indebted to the Board for its support of this study and to the engineers of the Iowa Highway Commission, Mr. Steve E. Roberts in particular, for their interest and co-operation.

The author wishes to thank Dr. John Lemish, Professor of Geology Department, for making available the mercury porosimeter used in this study; to Dr. Adolf Voight, Ames Laboratory, for his permission to use the Gamma Irradiation Facility; and to Mr. Joseph Crudele, Ames Laboratory, for helping with radiation dosimetry work.

Acknowledgment is made to the Armour Industrial Chemical Company, Box 1805, Chicago, Illinois 60650; E. I. du Pont Nemours and Company, Wilmington, Delaware 19898; the Quaker Oats Company, Chemical Division, Merchandise Mart Plaza, Chicago, Illinois 60654; Hercules Incorporated, Wilmington, Delaware 19899; Heveatex Corporation, Melrose, Massachusetts 02176; Rohm and Haas Company, Philadelphia, Pennsylvania 19105; GAF Corporation, Chemical Company, Minneapolis, Minnesota 55420; Diamond Shamrock Corporation, Cleveland, Ohio 44115; Scott Paper Company, Oconto Falls, Wisconsin 54154; Philadelphia Quartz Company, Primos, Pennsylvania 19018; Union Oil Company of California, Palatine, Illinois 60067; Lawter Chemicals Company, Chicago, Illinois 60645; and Stauffer Chemical Company, New York, New York 10017 for their generous donation of chemicals used in this investigation.

The following individuals contributed, in various capacities at various times, to this investigation: Prithvi S. Kandhal, Rathindra N. Dutt,

Laticia A. Davis, William B. Cook, Gary Zimmerman, Karen S. Ogbourne,  
Denny V. Caslavka, Dale K. Vander Schaaf, and Larry W. Volkening.

This work was supported, in part, by funds of the Engineering Research  
Institute, Iowa State University. The scanning electron microscope used  
in this work was purchased through National Science Foundation Grant GK26423.

## REFERENCES

1. Bisque, R. E., J. Sed. Petro. 31, 113 (1961).
2. Pettijohn, F. J., Sedimentary Rocks, 2nd Ed., Harper and Row: N.Y. (1957).
3. Lee, Dah-yinn, Assoc. Asphalt Paving Tech. Proc. 38, 242 (1969).
4. Dinkle, R. E., MS thesis, University of Maryland (1966).
5. Scheidegger, A. E., The Physics of Flow through Porous Media, Macmillan: N.Y. (1957).
6. Dolch, W. L., ASTM, STP 169-A, 443 (1966).
7. Washburn, E. W., and Bunting, E. N., Am. Cer. Soc. J. 5, 112 (1922).
8. Beeson, C. M., Am. Inst. Mining Met. Petro. Eng. 189, 313 (1950).
9. Sweet, H. S., ASTM Proc. 48, 988 (1948).
10. Dolch, W. L., ASTM Proc. 59, 1204 (1959).
11. Washburn, E. W., and Bunting, E. N., Am. Cer. Soc. J. 5, 527 (1922).
12. Brunauer, S., Emmett, P. H., and Teller, E., Am. Chem. Soc. J. 60, 309 (1938).
13. Carman, P. C., Flow of Gases through Porous Media, Academic Press: N.Y. (1956).
14. Dallman, R. S., MS thesis, Iowa State University (1966).
15. Ritter, H. L., and Erich, L. C., Anal. Chem. 20, 7, 665 (July 1948).
16. Washburn, E. W., Nat. Acad. Sci. Proc. 7, 115 (1921).
17. Ritter, H. L., and Drake, L. C., Ind. Eng. Chem. Anal. Ed. 17, 782 (1945).
18. Purcell, W. R., AIME Trans. 186, 39 (1949).
19. Drake, L. C., Ind. Eng. Chem. 41, 780 (April 1949).
20. Hiltrop, C. L., and Lemish, J., HRB Bull. 239, 1 (1960).
21. Lohn, R. N., Assoc. Asphalt Paving Tech. Proc. 15, 188 (1943).
22. Kandhal, P. S., MS thesis, Iowa State University (1969).

23. Howard, E. L., Proc. Am. Concrete Inst. 54, 1215 (1958).
24. Pearson, J. C., Rock Prod. 32, 64 (1929).
25. Martin, J. Rogers, Assoc. Asphalt Paving Tech. Proc. 19, 41 (1950).
26. Saxer, E. L., Rock Prod. 87, 77 (1956).
27. Hughes, B. P., and B. Bahramian, Mat. Res. Standards, 18-23 (1967).
28. Kandhal, P. S., and D.Y. Lee, HRR, 307, 44 (1970).
29. Hveem, F. N., Assoc. Asphalt Paving Tech. Proc. 13, 9 (1942).
30. Donaldson, J. A., Loomis, R. J., and Krchma, L. C., Assoc. Asphalt Paving Tech. Proc. 16, 353 (1947).
31. Nevitt, H. G., and Krchma, L. C., Assoc. Asphalt Paving Tech. Proc. 13, 52068 (1942).
32. Lettier, J. A., Fink, D. F., Wilson, N. B., and Fraley, F. F., Assoc. Asphalt Paving Tech. Proc. 18, 278 (1949).
33. Goshorn, J. H., and Williams, F. M., Assoc. Asphalt Paving Tech. Proc. 13, 41 (1942).
34. Rice, J. M., ASTM STP 191, 43 (1956).
35. U.S. Corps of Engineers Waterways Experiment Station, Misc. Paper 4-88 (1954).
36. McLeod, N. W., Proc. HRB 36, 282 (1957).
37. Lee, Dah-yinn, "Study of absorptive aggregates in asphalt paving mixtures," Engineering Research Institute, Iowa State University Research Report HR-127 (1968).
38. Materials Manual, California Division of Highways (1966).
39. Ricketts, W. C., Sprague, J. C., Tabb, D. D., and McRae, J. L., ASTM Proc. 54, 1246 (1954).
40. Zube, E., and Cechetini, J., HRR, 104, 141 (1965).
41. Blavia, Moldenhauer & Law, Soil Science Soc. Am. Proc. 35, 119 (1971).
42. Blavia, F. J., MS thesis, Iowa State University (1970).
43. Davidson, D. T., et al., Iowa Eng. Exp. Sta. Bull. 193 (1960).
44. Williams, B. G., et al., Australian J. Soil Res. 5, 85 (1967).

45. Dutt, A. K., Soil Sci. Soc. Am. Proc. 12, 497 (1948).
46. Emerson, W. W., J. Soil Sci. 47, 117 (1956).
47. Martin, W. P., Soil Sci. Soc. Am. Proc. 17, 1 (1953).
48. Dikeou, J. K., et al., ACI J. 829 (Oct. 1969).
49. Winterkorn, H. F., CAA Tech. Note No. 43 (1947).
50. Sheeler, J. B., Proc. HRB 36, 755 (1957).
51. Andrews, A. C., and Noble, G. G., Proc. HRB 29, 496 (1949).
52. Smith, J. C., Proc. Conf. Soil Stab. MIT, 81 (1952).
53. Lambe, W. T., J. Boston Soc. Civil Engr. 38, 127 (1951).
54. Hauser, E. A., HRB Bull. 108, 58 (1955).
55. \_\_\_\_\_, Proc. HRB. 27, 431 (1947).
56. Mainfort, R. C., CAA Tech. Development Rep. 136 (1951).
57. Clare, K. E., J. Soc. Chem. Ind. 68, 69 (1949).
58. Fungaroli, A. A., and Prager, S. R., Indr. Ind. Chem. Res. Dev. 8, 4, 450 (1969).
59. Manowitz, B., et al., Paper presented at the IAEA Symposium on Utilization of Large Radiation Sources and Accelerators in Industrial Processing, Munich, Germany (1969).
60. Weldes, H. H., and Lange, K. R., Properties of Soluble Silicates, Ind. Engr. Chem. 61, 31 (1969).
61. Ellis, H. B., PhD thesis, Iowa State University (1956).
62. Afflack, J. G., Ind. Eng. Chem. 47, 2232 (1955).
63. Lambe, T. W., Ind. Eng. Chem. 47, 2234 (1955).
64. Lauritzen, C. W., Ind. Eng. Chem. 47, 2245 (1955).
65. Demirel, T., and Davidson, D. T., Iowa Acad. Sci. Proc. 67, 290 (1960).
66. Sinha, S. P., Davidson, D. T., and Hoover, J. M., Iowa Acad. Sci. Proc. 64, 314 (1957).
67. Nicholls, R. L., and Davidson, D. T., Iowa Acad. Sci. Proc. 64, 349 (1957).

68. Demirel, T., Roegiers, J. V., and Davidson, D. T., Iowa Acad. Sci. Proc. 65, 311 (1958).
69. Grossi, F. X., and Woolsay, J. L., Ind. Eng. Chem. 47, 2253 (1955).
70. Hopkins, R. P., Ind. Eng. Chem. 47, 2258 (1955).
71. Laws, W. D., Soil Sci. Soc. Am. Proc. 18, 378 (1954).
72. Theng, B. K. G., Australian J. Soil Res. 5, 69 (1967).
73. Mainfort, R. C., HRB Bull. 108, 112 (1955).
74. Chu, T. Y. et al., HRB Bull. 108, 122 (1955).
75. U.S. Waterways Exp. Station Tech. Memo 217-1 (1946).
76. McAlpin, G. W. et al., CAA Tech. Dept. Development Report No. 35 (1944).
77. HRB Bull. 318 (1962).
78. Wang, J. W. H., and Kremmydas, A. H., HRB Record 315, 8 (1970).
79. Davidson, D. T., Iowa Engr. Expt. Station Report No. 4 (1951).
80. Dobbs, J. B., and Hitchcock, M., Waterway Experiment Station, Contract Report 3-174 (1967).
81. MIT, Waterway Experiment Station, Contract Report 3-2, Phase 1 (1948).
82. Ibid. Phase 2 (1950).
83. Ibid. Phase 3 (1951).
84. Ibid. Phase 4 (1952).
85. Ibid. Phase 5 (1953).
86. Ibid. Phase 6 (1954).
87. Ibid. Phase 7 (1955).
88. Ibid. Phase 8 (1956).
89. Ibid. Phase 9 (1957).
90. Ibid. Phase 10 (1958).
91. Ibid. Phase 11 (1959).
92. Ibid. Phase 12 (1960).



93. Ibid. Phase 13 (1961).
94. Dutt, R. N., MS thesis, Iowa State University (1970).
95. Lee, D. Y., "Modification of Asphalt and Asphalt Paving Mixtures by Sulfur Additives," Engineering Research Institute Interim Report, Iowa State University, Ames (1971).
96. American Road Builders' Association, Research Report M-17 (1969).
97. Fondriest, F. F., and Snyder, M. J., NCHRP Report No. 8 (1964).
98. Witczak, M. W., Lovell, C. W., and Yoder, E. J., Paper presented at the 50th Annual Meeting of the Highway Research Board (1971).
99. Gallaway, B. M., Paper presented at the Annual Meeting of the Association of Asphalt Paving Technologists (1971).
100. Marais, C. P., National Institute for Road Research, South African Internal Report RB/AO/68 (1968).
101. Walker, R. D., Larson, T. D. and Cady, P. D., National Cooperative Highway Research Program Report 100 (1970).

# TECHNICAL APPENDIX

## APPENDIX A

Theses and Publications Resulting from HR-127 and HR-142

- Lee, Dah-yinn, "Study of Absorptive Aggregates in Asphalt Mixtures," Iowa State Highway Commission Research Report, HR-127 (1968).
- Lee, Dah-yinn, "The Relationship between Physical and Chemical Properties of Aggregates and their Asphalt Absorption". Proc. AAPT, 38, 242-275 (1969).
- Kandhal, Prithvi S., "Asphalt Absorption as Related to Pore Characteristics of Aggregates", M.S. Thesis, Iowa State University (1969).
- Lee, Dah-yinn, "Absorption of Asphalt by Aggregate", Iowa State Highway Commission Progress Report No. 1 (1970).
- Kandhal, P. S. and Lee, D. Y., "An Evaluation of the Bulk Specific Gravity for Granular Materials", Highway Research Records, 307, 44-55 (1970).
- Dutt, R. N., "Upgrading Absorptive Aggregates by Chemical Treatments", M.S. Thesis, Iowa State University (1970).
- Dutt, R. N. and Lee, D. Y., "Upgrading Absorptive Aggregates by Chemical Treatments". Highway Research Records 353:43 (1971).
- Kandhal, P. S. and Lee, D. Y., "Asphalt Absorption as Related to Pore Characteristics of Aggregates". Paper to be presented at the 1972 Annual Meeting of the Highway Research Board.

## APPENDIX B

Summary of Materials Studied as Possible Agents forAbsorptive Aggregate Treatments

## Aniline-Furfural

Description

Aniline-furfural was the cheapest synthetic bonding agent considered for soil stabilization. Aniline is a colorless to light yellow liquid, soluble in water (5.2 dry wt %), alcohol, benzene and most organic solvents, and is a primary aromatic amine to which all other compounds in this organic family are related. Furfural is a colorless to red-brown liquid manufactured from agricultural residues such as oat hulls, corncobs, cottonseed hulls, etc. and is soluble in water (8.3 dry wt %), alcohol and ether. Furfural polymerizes with aniline to a water-insoluble hard, dark red resin. Aniline is toxic but toxicity ceases after polymerizes with furfural. The polymerization mechanism is not known; however, it has been found that a mole ratio of 2 parts aniline and 1 part furfural is most effective. In this experiment, 0-9 wt % of aniline-furfural with 2:1 molar ratio were used in crushed and cored aggregates, oven cured at 140 °F for 3 days.

Aggregates Treated

Cook and Menlo, both crushed-graded and 1/2 in. cylindrical cores.

Tests

Water absorption (W)

Asphalt absorption by immersion method (AI)

Asphalt absorption by Rice method (AR)

Marshall stability (M)

Heat stability at 400 °F

Remarks

- Aniline and furfural are both liquids and do not need water dilution.
- Aniline is toxic before polymerization.
- Treatment by these chemical combinations is promising

Acrylic PolymersDescription

In addition to Methyl methacrylate and calcium acrylate, five more acrylic polymers were studied: acrylonitrile, methyl acrylate and three acrylic polymers from Rohm and Haas Co. (Rhoplex HA-8, E-330, and MC-4530). The former two polymers were tried at MIT for soil stabilization (Ref. 84, 87 ), HA-8 is a milky-white nonionic self-crosslinking acrylic polymer emulsion used in textile industry for fabric finishing and adhesives; E-330 and MC-4530, also milky-white emulsions, are portland cement mortar modifiers. Acrylonitrile was added as 2% acetone solution to aggregate in percentages from 0.5-1.5. Methyl acrylate was dissolved in methanol and added to aggregate at 1% level. Rhoplex HA-8, E-330 and MC-4530 were diluted with water and added to aggregates at 2% level. Acrylonitrile-treated aggregates were air-cured and the other mixed were oven-cured at 140 °F until constant weight.

Aggregates Tested

Laboratory crushed and graded Linwood, Menlo, and Pints.

Tests

W and AR

Remarks

- Acrylonitrile was effective only on Menlo aggregate, possibly due to incomplete polymerization. Polymerization may improve by use of a redox system such as ammonium persulfate plus sodium sulfite or sodium metabisulfite.

- Methyl acrylate was ineffective, possibly due to failure of removing of inhibitor before polymerization and use of catalyst in the treatments.

- Rhoplex polymers, especially E-330, were effective and easy to apply. They should be further investigated.

---

### Armac T

#### Description

Armac T is a water soluble amine acetate made from long-chained amines obtained from fatty acids. A characteristic of Armac T which has been used industrially is its ability to cause certain hydrophilic surfaces to become water repellent. In this investigation, Armac T was first diluted with water and then added to aggregates at percentages between 1/2-8 wt % of aggregate. Treated aggregates were cured at 230°F for five days.

#### Aggregates Treated

Cook and Menlo, both crushed, graded, and cores.

#### Tests

W, AI, AR, M, and H.

#### Remarks

Effective at 6% by "pore-plugging" mechanism. Lower (e.g. 1/2%) dosage should be possible if "surface changing" mechanism is utilized.

---

## Bituminous Materials

### Description

Six bituminous materials were tested as aggregate treatment agents. They included one asphalt cement (200-300 pen.), a rapid-curing cutback (RC-70), a medium-curing cutback (MC-30), a slow-setting asphalt emulsion (SS-1h), a road tar (RT-6), and a crude tar. Asphalt cement was added at 1 and 2 wt % of aggregate (Menlo and Pints). Both asphalt and aggregate were heated to 300 °F prior to mixing. The MC-30 was used to pretreat all aggregates studied at varying cutback content of 1.00-4.85% (asphalt residue content of 0.55 to 2.66%). Mixing was done at room temperature. Treated aggregates were air-cured for four days and oven-cured at 140 °F for two days. The RC-70 was also added and mixed at room temperature. Range of percent cutback was from 1.00-3.85% (asphalt residue content of 0.62-2.39%). The SS-1h was added to all aggregates at a concentration of 1% emulsion or 0.65% asphalt residue. Emulsion was first diluted with distilled water to volume sufficient to cover all aggregate particles and then mixed at room temperature and cured at 140 °F to constant weight. The crude tar and road tar RT-6 were obtained from U.S. Steel. The crude tar was tested on all aggregates at percentages between 1.0-7.5 wt % of aggregate. Aggregates were treated at room temperature and cured at 220 °F until constant weights were attained. The RT-6 was also tested on all aggregates at concentrations between 1-3 wt % of aggregate. Both mixing and curing were carried out at 220 °F.

### Aggregates Treated

All laboratory crushed and graded including both gradings A and B. Total number of treated samples: 57.

### Tests

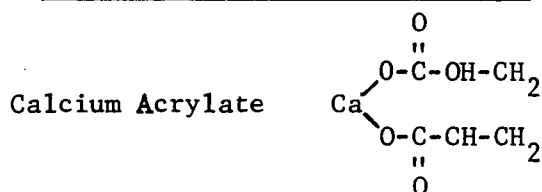
W, AR.

### Remarks

- With 1% agent, absorption can be reduced by 50-80%.
- Most effective: RC-70 and crude tar.
- Pretreatment with bituminous materials at 1% level seemed to retard delayed asphalt absorption.

• The relative effectiveness and the effective ranking of the six bituminous varied for different aggregates. It is suggested that they are related to pore shape and pore size distribution of respective aggregates. Further study in this area as well as mechanisms of absorption reduction should be pursued.

• Treatments with this group of materials can be adopted conveniently as "two-shot" mixing method or aggregate precoating method, and should be experimented on a large scale in the field.



#### Description

Calcium acrylate is a white powder, water soluble monomer (40-45% solubility), polymerized when ammonium persulfate and sodium thiosulfate, both water soluble, are used as catalyst and activator, respectively. Polymerization rate depends on catalyst concentration, monomer concentration, and curing temperature. In this investigation calcium acrylate was added in 8% solution with 1% ammonium persulfate and 1% sodium thiosulfate. Percent monomer ranged from 0.25-1.25%. All treated samples were air cured.

#### Aggregates Treated

All laboratory crushed and graded (grading A) samples.

#### Tests

AR

#### Remarks

- Soluble in water and can be polymerized in water solution.
- Polymer also soluble in water.



- Moderately effective at the range of percent chemical experimented.
- Expensive.

---

Inorganic Materials (Sodium silicate, hydrated lime,  
calcium chloride and Siroc 132 system)

#### Description

Four chemicals in this category were tested, all of them were used at some time as cementing and/or grouting agents for soil stabilization. Sodium silicate alone or with inorganic salt such as calcium chloride has been used successfully for soil stabilization and chemical grouts. Various types of sodium silicates (different  $\text{Na}_2\text{O}/\text{SiO}_2$  ratios) were tried with and without calcium chloride to treat aggregates by either vacuum soaking or mixing. However, limited results failed to show improvements. Siroc grout system 132 (Siroc No. 1 is a modified sodium silicate, Siroc No. 2 is a formamide reactant, and Siroc No. 3 is a dry crystalline accelerator) was also tested on several aggregate samples and was unsuccessful. Calcium chloride and hydrated lime were added to aggregate in water solution at average concentration of 1 wt %. Treated aggregates were oven cured at 220 °F to constant weights and then mixed with asphalt for absorption by the Rice method.

#### Aggregates Treated

Laboratory crushed and graded Menlo, Linwood, Pints, and Cook.

#### Tests

AR

#### Remarks

• Silicate treatments were not effective. However, in view of the proven success of sodium silicate in soil stabilization it is possible that the negative results in these series of trials may be due to lack of proper conditions of treatment (concentration of sodium silicate,

soda-silicate ratio, concentration of calcium ions, method of mixing or penetration, temperature of mixing and curing, etc.) rather than chemical itself. Further studies should be made.

- Calcium chloride and calcium hydroxide were effective in reducing asphalt absorption only on Menlo aggregate.

---

### Lignin

#### Description

Waste sulfite liquor (lignosulfonate) from the paper industry has been used on roads as cementing agent, but being water-soluble it must be periodically replenished. An alternative is to chemically polymerize the calcium lignosulfonate to produce a water-insoluble resin. Chromium ions introduced as sodium or potassium dichromate react with the lignosulfonate to form a dark, water-insoluble gel-like mass.

#### Aggregates Treated

Crushed and graded Menlo and Cook.

#### Tests

W and AR

#### Remarks

- Ineffective without chromium ions (water soluble).
  - Water absorption reduced by 50% when 3% lignin and 1% potassium dichromate was used in solution and cured at 220 °F for 24 hours.
  - Promising, due to lignin's low cost.
-

## Methyl Methacrylate

### Description

Methyl Methacrylate polymers have been used in industry for airplane windows, light fixtures, dental fillings, reflectors, and automobile tail lights. The methyl ester of methacrylic acid is a clear, colorless liquid that reacts with numerous reagents and polymerizes into a clear, colorless, transparent, water-insoluble plastic (Polymethyl methacrylate) with softening point, impact strength and weatherability better than most thermoplastics. Rock cores were first vacuum impregnated with a liquid monomer consisting of 90 wt % of methyl methacrylate plus 10 wt % of trimethylolpropane trimethacrylate; they were then polymerized by one of two methods: cobalt gamma radiation or thermal catalytic technique. Both of these methods have been tried. As far as reduction in water and asphalt absorption properties of the rock cores are concerned, same degree of improvement was obtained in both cases. One percent benzoyl peroxide was used as a free radical initiator in thermal polymerization (at 185 °F for 1 hour). Total dosage of 1 megarads was used in radiation treatment.

### Aggregates Treated

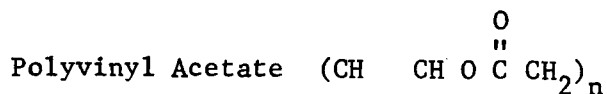
Cook and Menlo rock cores and crushed-graded.

### Tests

W, AI, and AR

### Remarks

- Expensive (\$0.45/lb.), but very effective.
  - Techniques should be developed for radiation polymerization in field plant operation.
-



### Description

Polyvinyl acetate is used in the production of water-based emulsion paints or adhesives. Emulsions can be diluted with water. Pure PVA can be applied in organic solvent such as acetone or alcohol or mixtures of the two it forms strong film if plasticizers are used. In this investigation PVA was added as solution in methanol (14%).

### Aggregates Treated

Laboratory crushed Linwood and Pints (Grading A).

### Tests

W and AR

### Remarks

• Not effective.

OH

PVA (Polyvinyl Alcohol)  $(\text{CCH}_2\text{CH})_n$

### Description

PVA is a white, soluble polymer. It dissolves slowly in cold water, but more rapidly at elevated temperatures, and can be dissolved completely above 90 °C. The aqueous solutions are unstable and can undergo a complex series of gelation reactions (both reversible and irreversible). Three series of treatments were made using different grades of PVA and in different concentrations (7% for 52-22 and 70-65, and 1.4% for 71-30) with percent chemical ranging from 0.15% to 0.85%. All treatments were oven cured at 220°F to constant weight.

Aggregates Treated

All laboratory crushed and graded aggregates.

Tests

AR

Remarks

- Dry polymer film is water soluble.
- Effective for most aggregates.
- Unstable at temperatures above 200 °C.
- Requires no organic solvent.

---

Rubber Latex

Description

An ammoniated natural latex from Heveatex Co. was used in the study. This latex, known also as S-4 latex, contains 61% dry rubber. Rubber was added to aggregates as mixtures of 1 part latex to 6 parts water. Latex content of treated aggregates ranged from 0.6-1.7%.

Aggregates Treated

Laboratory crushed Linwood, Menlo, and Pints meeting gradation A.

Tests

Asphalt absorption by Rice method.

Remarks

- Results of three aggregates inconsistent.
- Could have dual functions of modifying both aggregate and asphalt.
- Deserves further study.

---

Natural and Synthetic ResinsDescription

Five resinous materials were investigated for the purpose of reducing aggregate absorption. They were: (a) Vinsol NVX, a neutralized Vinsol resin that was used to impart water-repellent characteristics in soil stabilization; (b) Synthetic resins Krumbhaar K-101 (a resin modified phenolic), and K-1010 (a pure phenolic resin), both from Lawter Chemical Co.; (c) Armsco Resin 3001 from American Mineral Spirits Co.; and (d) Gantrez Resin AN-139, a medium molecular weight grade poly (methyl vinyl ether/maleic anhydride) from GAF Corp., used, among other things, as film former (adhesives and coatings), soil conditioner, emulsifier, flocculant, binder, air-entraining agent and stabilizer. The powdered NVX was added to aggregates in 13% acetone solution ranging from 0.45-2.10 wt % of aggregate. The treated aggregates were air cured for 3 days followed by oven curing at 220 °F for two days before water absorption and asphalt absorption determinations were made. Resin K-101 was added at concentration between 0.57-1.70 wt % of aggregate in 18% acetone solution. Resin K-1010 was added at concentrations of 0.49%-1.46% in 17% methanol solution. Both mixing and curing were done at room temperature. Armsco Resin 3001 (emulsion) was mixed with aggregate in 18% ethanol solution. Percent resin ranged from 0.57-1.70%. Both mixing and curing were done at room temperature. Grantrez Resin AN-139 was added to aggregate in 7% water solution at percentage from 0.2-0.6 wt % of aggregate. Mixtures were air cured for 3 days and oven cured to constant weight before absorption tests were run.

Aggregates Treated

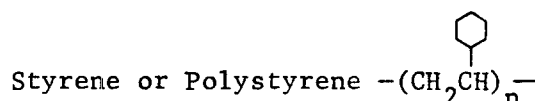
All aggregates.

Tests

Water absorption and asphalt absorption by Rice method.

Remarks

- Resins K-101 and K-1010 were very effective in reducing both water and asphalt absorption.
- Vinsol NVX was reasonably effective.
- Resins Amsco 3001 and AN-139 were not effective.

Description

Styrene is a colorless liquid monomer soluble in aromatic hydrocarbons and acetone. It can be polymerized (usually with a peroxide initiator) in solution, suspension or in bulk. Polystyrene is a thermoplastic, with reasonably good mechanical and thermal properties. In this investigation styrene was added to aggregates as 14% solution in acetone. Percent chemical in treated aggregates were between 0.45-2.10%. All treated aggregates were cured at 140 °F until constant weight.

Aggregate Treated

All laboratory crushed and graded (A) samples.

Tests

W and AR

Remarks

- Water insoluble; acetone as solvent is expensive and toxic.

- Moderately effective. Effectiveness may improve if initiator (benzoyl peroxide) were used.
- Softens at 100 °C.



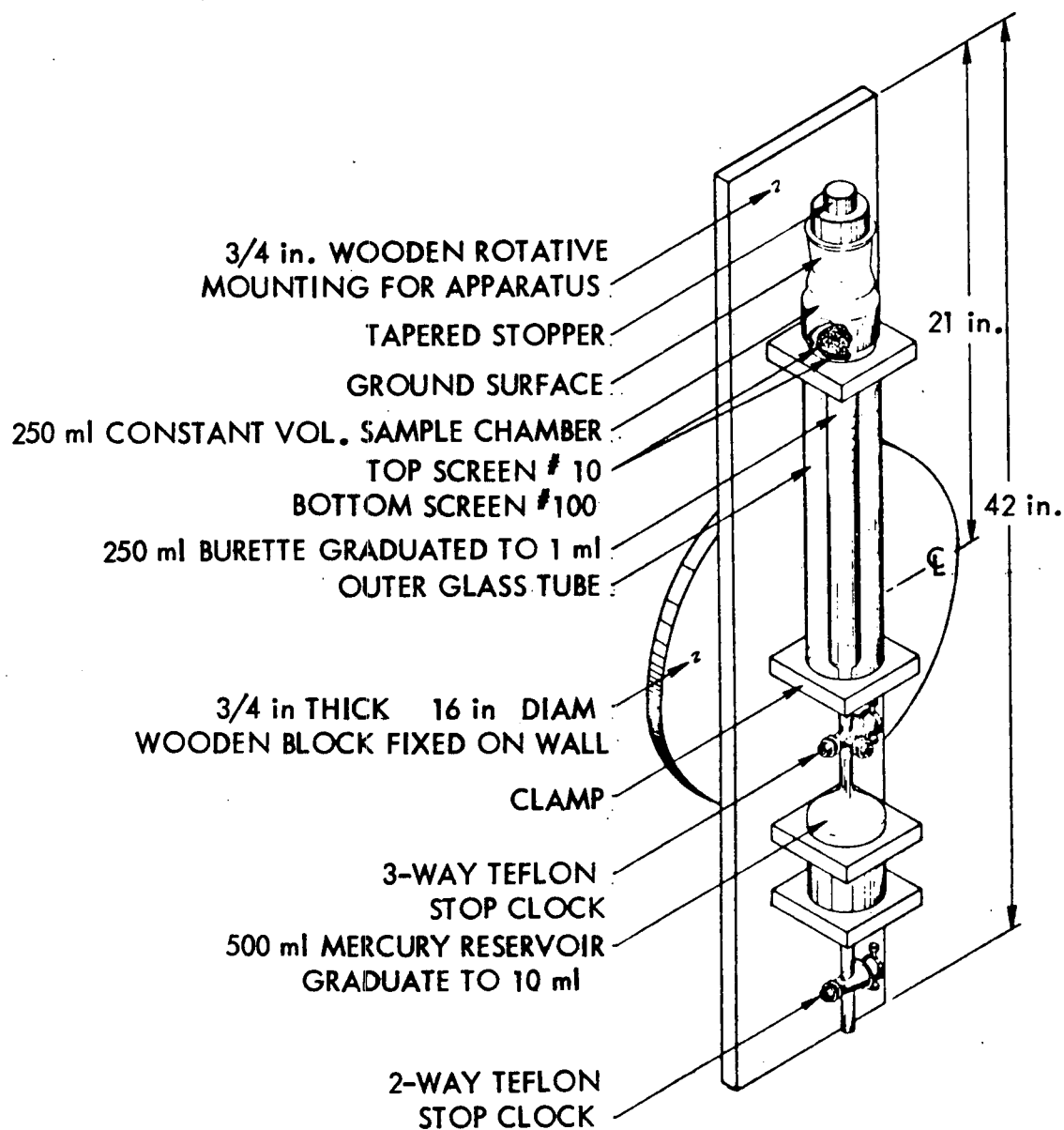
## APPENDIX C

Determination of Bulk Specific Gravity of Aggregates

## Mercury Pycnometer Method

Description

A sketch of the apparatus is shown in the figure below.



The apparatus consists of: (a) 250 ml constant volume sample chamber, (b) 250 ml burette, (c) 500 ml mercury reservoir. The apparatus is mounted on wood which rotates on a pivot.

### Procedure

Mercury is poured into the reservoir with the apparatus in an inverted position (with 3-way stop-cock closed). The apparatus is then set in the normal position. The following steps comprise a normal determination:

1. Apply vacuum grease and insert and secure the stopper by clamps (or springs).
2. Apply the 27 in. vacuum and evacuate the apparatus for 10 min.
3. Invert the apparatus and record the Hg level in the burette (A, cc) at 1 atm.
4. Close the stop-cock and again evacuate the apparatus. Return the apparatus to its normal position.
5. Open the 3-way stop-cock to atmosphere. Open the stopper and put the previously weighed (W, gms) aggregate in the sample chamber. Replace the stopper and secure it to the apparatus.
6. Evacuate the apparatus for 10 min.
7. Rotate and invert the apparatus; record the displaced Hg level in the burette (B, cc) at atmospheric pressure.
8. Close the two-way stop-cock, evacuate the apparatus for 10 min., then bring it to its normal position.

$$\text{Bulk specific gravity} = \frac{W}{B - A}$$

9. The mercury should be cleaned occasionally. This can be done by putting mercury in a container, covering it with a layer of 10% nitric acid, then blowing air through it by applying a vacuum for 3-4 hr, and then washing it with water and drying with blotting paper.

Data

A preliminary test was conducted on 1/2-in. rock cores, and the following results were obtained:

Rock core	Bulk specific gravity	
	By pycnometer	By ASTM
Menlo	2.710	2.637
Pints	2.312	2.271
Linwood	2.694	2.636
Cook	2.622	2.565
Keota	2.549	2.489

Samples were weighed to 0.0001 gm and volume observed to 1/4 cc.

Improvements of Procedure

1. Have the burette read to the nearest 1/10 ml instead of 1/4 ml as on the present apparatus.
2. The orifice at the bottom of the sample chamber (below the screens) could be widened to have a bore equal to that of the burette. This is necessary since the present apparatus has to be rotated back and forth to eliminate residual air bubbles trapped between the orifice and fine screen.
3. Good stop-cocks to withstand the vacuum; the present ones, though teflon coated, have to be coated with vacuum grease.
4. Contamination of the mercury by grease in the stopper of the sample chamber and stop-cocks should be avoided.
5. Use a more effective clamp to insure no movement of the stopper.

## Chemical Indicator Methods

Cobalt Chloride (CoCl<sub>2</sub>) Method

The procedure is the same as for ASTM C-127 and C-128 test except for the following points:

1. Immerse the sample in a 5% solution of cobalt chloride instead of plain water for 24 hr.
2. Remove the sample from the solution and put on a white surface such as a table or enameled tray. The aggregate may not seem colored, but the visible water films on the aggregate will be pinkish in color.
3. Spread the sample in such a fashion that a layer of individual particles are exposed to a gently moving current of warm air. Stir frequently to secure uniform drying. Some of the solution sticking to the porcelain will appear to be pink.
4. As drying proceeds, the aggregate attains bluish color which helps in adjusting the warm air. Frequently turn aggregate over by gentle hand action. If there is still some moisture left on the surface of the aggregate, the bluish color on the porcelain will change back to pink. Keep turning the sample, while exposing it to warm air, until all the aggregate is bluish in color and the bluish spots on the white porcelain no longer turn pink. This is assumed to be saturated surface-dry condition.
5. The saturated surface-dry coarse aggregate is immediately weighed in air and water as outlined in the ASTM C-127 test, while the fine aggregate is introduced into the Chapman's flask, filled with water to the 200 ml mark.

#### Fluorescein Di-Sodium Salt (FSS) Method

The procedure is essentially the same as the  $\text{CoCl}_2$  method. In this case a 0.5% solution of fluorescein di-sodium salt is used.

The sample is dried in the same manner as in the previous test. The sample acquires a yellowish color when taken from the solution after 24 hr immersion. On drying, an orange color appears on the aggregate, the porcelain also changes to a distinct orange. This is assumed to be the saturated surface-dry condition and the sample is further treated as per ASTM C-127 and C-128 tests' procedure.

The  $\text{CoCl}_2$  method is suitable for whitish to light grey colored aggregate. For dark aggregate, a 10% solution of  $\text{CoCl}_2$  can be employed or FSS can be used.

Before removing the samples from the solution, the latter should be agitated by turning over the aggregate.

Because a bluish color acquired by the saturated surface-dry aggregate fades with time, indicating possible adsorption of moisture from air or drawing moisture from within through capillaries, the sample should be weighed immediately.

## APPENDIX D

Determination of Asphalt Absorption

## Immersion Method

Procedure:

The following procedure was adopted: the bulk specific gravity and water absorption of the aggregates were determined in accordance with ASTM C-127. Weighing was done to the nearest 0.1 gram.

The aggregates were heated to 300°-325 °F and suspended, by means of a tared wire basket, in asphalt at 300 °F for one hour. The basket was then removed from the asphalt and suspended in the oven at 300 °F for 10 minutes to drain off the excess asphalt. The basket with coated aggregate was cooled to room temperature and weighed in air and in water at 77 °F.

Calculation:

From the above procedure, the following data were derived:

1. Weight of basket in air, gm.
2. Oven dry weight of cores + basket in air, gm.
3. Weight of coated aggregate + basket in air, gm.
4. Weight of coated aggregate + basket in water, gm.
5. Weight of basket in water, gm.
6. Weight of coated aggregate in water = 4-5
7. Weight of oven-dried aggregated in air = 2-1
8. Bulk volume of aggregate =  $\frac{7}{\text{Bulk sp. gr.}}$
9. Weight of asphalt = 3-2
10. Weight of coated aggregate in air = 3-1

11. Weight of asphalt on the surface of the aggregate =  
(10-6) - 8 × ga, where ga = specific gravity of asphalt
12. Weight of asphalt absorbed = 9-11
13. Percent asphalt absorbed by weight of dry aggregate =  
12/7 × 100

### Bulk Impregnated Specific Gravity of Aggregates

#### Procedure:

1. Dry aggregates weighing 1000 g to a constant weight at 230 °F, cool to room temperature and weigh to the nearest 0.1 gram.
2. Heat asphalt to 280° ± 5 °F, and pour sufficient amount into a 1 gal pail to fill it to about one third its depth. Insert a metal stirrer and allow bitumen to cool to 77° ± 2 °F.
3. Weigh pail plus bitumen and stirrer in air at room temperature and in water at 77° ± 2 °F.
4. Place the pail of asphalt with stirrer and the sample of aggregate in oven at 280° ± 5 °F and leave both until temperatures are equalized (a minimum of 4 hr is usually required).
5. Remove aggregate and bitumen from oven and add aggregate to bitumen, stirring thoroughly as aggregate is gradually added to the hot bitumen; continue stirring until entrapped air has been removed. During the cooling period, flame surface to remove air bubbles if such are present. Cool to 77° ± 2 °F (should cool overnight).
6. Weigh pail plus stirrer plus aggregate plus bitumen in air at room temperature and in water at 77° ± 2 °F.

#### Calculation:

$$\text{Bulk impregnated specific gravity (Gbi)} = \frac{W}{(D-E) - (B-C)}$$

where

W = weight of oven-dry aggregates in grams,

B = weight of pail plus stirrer plus asphalt in air, grams,

- C = weight of pail plus stirrer plus asphalt in water, grams,  
 D = weight of pail plus stirrer plus asphalt plus aggregates in air, grams,  
 E = weight of pail plus stirrer plus asphalt plus aggregates in water.

Asphalt absorption is calculated:

$$A + \left( \frac{1}{G_b} - \frac{1}{G_{bi}} \right) \times g_a \times 100$$

where

- A = asphalt absorption by weight of aggregates, percent,  
 G<sub>b</sub> = bulk specific gravity of aggregates (as per ASTM C-127),  
 G<sub>bi</sub> = bulk impregnated specific gravity of aggregate, and  
 g<sub>a</sub> = specific gravity of asphalt.

#### Modified Rice Method

1. About 500 g of the bituminous mixture is weighed to the nearest 0.1 g (A) and introduced into the pycnometer.
2. The pycnometer is filled with 0.01% aerosol solution to cover the sample.
3. The entrapped air in the sample is removed by agitation and applying vacuum (25 in. Hg) to the pycnometer with an aspirator for 15 min.
4. The pycnometer is completely filled with aerosol solution and brought to a temperature of 77 °F in a water bath and weighed to the nearest 0.1 g (B).
5. The pycnometer is completely filled with aerosol solution above and brought to 77 °F and weighed to the nearest 0.1 g (C).
6. The maximum specific gravity of the mixture

$$D_m = \frac{A}{A + C - B}$$

7. The effective specific gravity of the aggregate

$$G_e = \frac{100 - W_a}{100/D_m - W_a/g_a}$$



where

Wa = percentage asphalt (by weight of mixture), and

ga = specific gravity of asphalt.

8. Asphalt absorption

$$Aac = \left( \frac{G_e - G_b}{G_e \times G_b} \right) \times g_a \times 100$$

where

Gb = bulk specific gravity of aggregates.